

ZEBRAFISH TOOLS TO COMBAT ACUTE MYELOID LEUKAEMIA – THE
NUCLEOPORIN 98 KILODALTON—HOMEBOX A9 (NUP98-HOXA9) FUSION
ONCOGENE DRIVES MYELOPROLIFERATION BY UPREGULATING *DNA*
(CYTOSINE-5-)-METHYLTRANSFERASE 1 (DNMT1)

by

Alexander Michael Forrester

Submitted in partial fulfilment of the requirements
for the degree of Doctor of Philosophy

at

Dalhousie University
Halifax, Nova Scotia
July 2012

© Copyright by Alexander Michael Forrester, 2012

DALHOUSIE UNIVERSITY
DEPARTMENT OF MICROBIOLOGY & IMMUNOLOGY

The undersigned hereby certify that they have read and recommend to the Faculty of Graduate Studies for acceptance a thesis entitled “ZEBRAFISH TOOLS TO COMBAT ACUTE MYELOID LEUKAEMIA – THE *NUCLEOPORIN 98 KILODALTON—HOMEODOMAIN A9 (NUP98-HOXA9)* FUSION ONCOGENE DRIVES MYELOPROLIFERATION BY UPREGULATING *DNA (CYTOSINE-5-)-METHYLTRANSFERASE 1 (DNMT1)*” by Alexander Michael Forrester in partial fulfillment of the requirements for the degree of Doctor of Philosophy.

Dated: July 9, 2012

External Examiner: _____

Research Co-Supervisor: _____

Research Co-Supervisor: _____

Examining Committee: _____

Departmental Representative: _____

DALHOUSIE UNIVERSITY

DATE: July 9, 2012

AUTHOR: Alexander Michael Forrester

TITLE: Zebrafish Tools To Combat Acute Myeloid Leukaemia – The *Nucleoporin 98 kiloDalton—Homeobox A9 (NUP98-HOXA9)* Fusion Oncogene Drives Myeloproliferation By Upregulating *DNA (Cytosine-5-)-Methyltransferase 1 (dnmt1)*

DEPARTMENT OR SCHOOL: Department of Microbiology & Immunology

DEGREE: PhD CONVOCATION: October YEAR: 2012

Permission is herewith granted to Dalhousie University to circulate and to have copied for non-commercial purposes, at its discretion, the above title upon the request of individuals or institutions. I understand that my thesis will be electronically available to the public.

The author reserves other publication rights, and neither the thesis nor extensive extracts from it may be printed or otherwise reproduced without the author's written permission.

The author attests that permission has been obtained for the use of any copyrighted material appearing in the thesis (other than the brief excerpts requiring only proper acknowledgement in scholarly writing), and that all such use is clearly acknowledged.

Signature of Author

DEDICATION PAGE

For Liane.

I hope you dance.

TABLE OF CONTENTS

LIST OF TABLES	xiv
LIST OF FIGURES	xv
ABSTRACT	xviii
LIST OF ABBREVIATIONS & SYMBOLS USED.....	xix
ACKNOWLEDGEMENTS.....	xxiv
CHAPTER 1 INTRODUCTION.....	1
1.1 PREAMBLE.....	1
1.2 ACUTE MYELOID LEUKAEMIA (AML).....	3
1.2.1 High-Risk Versus Low-Risk Disease & Need For Targeted Agents.....	3
1.2.2 <i>HOXA9</i> & <i>MEIS1</i>	4
1.3 'PLATEAU' OF HUMAN CLINICAL STUDIES & LIMITATIONS OF TRADITIONAL ANIMAL MODELS	6
1.4 THE ZEBRAFISH AS A MODEL SYSTEM & RESEARCH TOOL.....	7
1.4.1 Conserved Genetics & Cell Biology Of Zebrafish Haematopoiesis.....	8
1.4.2 Antagonistic Relationship Between SPI1 And GATA1	10
1.4.3 Transgenic Zebrafish Tools For Studying Myelopoiesis.....	10
1.5 THE <i>HOX</i> FAMILY OF DEVELOPMENTAL TRANSCRIPTION FACTORS & THE <i>CDX-HOX</i> NETWORK IN BLOOD DEVELOPMENT.....	13
1.5.1 Homeobox Transcription Factors In Zebrafish Haematopoiesis.....	14
1.6 THE POTENTIAL OF ZEBRAFISH FOR AML RESEARCH.....	16

1.6.1	Genetic & Chemical Modifier Screens In Zebrafish	17
1.7	THE T(7;11P15;p15) <i>NUP98-HOXA9</i> MUTATION IN AML.....	18
1.7.1	<i>NHA9</i> Versus <i>HOXA9</i> In AML.....	19
1.8	RATIONALE OF STUDIES & HYPOTHESES	21
CHAPTER 2	MATERIALS & METHODS.....	31
2.1	ZEBRAFISH HUSBANDRY, EMBRYO COLLECTION & EMBRYO STAGING.....	31
2.2	CREATION OF TRANSGENIC ZEBRAFISH LINES	32
2.2.1	Bacterial Cloning	32
2.2.2	<i>NUP98-HOXA9 (NHA9)</i>	32
2.2.3	Gateway® Cloning	33
2.2.4	<i>ctnnb1-b*</i> [β -catenin(S/T→A)] & <i>Meis1</i>	34
2.3	ACTIVATION OF TRANSGENES	35
2.4	GENOTYPING	36
2.5	PCS2+ VECTOR CONSTRUCTION & MRNA SYNTHESIS.....	36
2.6	MORPHOLINO OLIGONUCLEOTIDE (MO)	36
2.7	RNA EXTRACTION & CDNA SYNTHESIS	37
2.7.1	RNeasy Method.....	37
2.7.2	TRIzol® + RNeasy Method	37
2.8	QUANTITATIVE REVERSE TRANSCRIPTION POLYMERASE CHAIN REACTION (QRT-PCR).....	38
2.8.1	Primer Design.....	38
2.8.2	Reagents, Thermocycler Conditions, Controls & Analysis	38
2.9	MICROARRAY.....	39

2.9.1	Identifying Mammalian Homologues For Zebrafish Genes	40
2.10	FLUORESCENCE-ACTIVATED CELL SORTING (FACS) & CYTOSPINS.....	40
2.10.1	Whole Kidney Marrow (WKM)	40
2.10.2	Whole Embryo Suspensions.....	41
2.10.3	Cytospins.....	42
2.11	WHOLE MOUNT RNA <i>IN SITU</i> HYBRIDIZATION (WISH)	42
2.11.1	RNA Probe Synthesis	42
2.11.2	Embryo Preparation (Optional Bleach & Methanol Storage).....	43
2.11.3	WISH Protocol	43
2.12	ANTIBODIES	44
2.13	WESTERN BLOTTING	44
2.14	5-BROMO-2-DEOXYURIDINE (BrdU) INCORPORATION ASSAY.....	45
2.15	IONIZING RADIATION (IR), ACRIDINE ORANGE (AO) STAINING & IMMUNOFLUORESCENCE (IF).....	46
2.16	TISSUE SECTIONING, HISTOLOGY & IMMUNOHISTOCHEMISTRY (IHC).....	47
2.16.1	<i>In Situ</i> Hybridization (ISH)	48
2.17	CHEMICAL COMPOUNDS	49
2.17.1	<i>dnmt1</i> Studies.....	49
2.17.2	β -catenin Studies.....	50
2.17.3	Prodigiosene Studies	50
2.18	TISSUE CULTURE & CELL LABELLING.....	51
2.19	XENOTRANSPLANTATION OF HUMAN LEUKAEMIA CELLS INTO ZEBRAFISH EMBRYOS, DISSOCIATION, & IMMUNOFLUORESCENCE.....	51

2.20	IMAGING & IMAGEJ ANALYSIS OF Z-STACK PROJECTIONS	52
2.20.1	Embryo Immunofluorescence	53
2.21	STATISTICS	53
CHAPTER 3 NUP98-HOXA9-TRANSGENIC ZEBRAFISH DEVELOP A MYELOPROLIFERATIVE NEOPLASM		65
3.1	BACKGROUND.....	65
3.1.1	Designing A Zebrafish Model Of <i>NUP98-HOXA9</i> Expression	65
3.2	EXPERIMENTAL FINDINGS	66
3.2.1	Transgenic Zebrafish Express Human <i>NHA9</i> In A Cre/ <i>lox</i> -Inducible Manner.....	66
3.2.2	<i>NHA9</i> -Transgenic Zebrafish Develop Malignant Myeloid Infiltrates.....	68
3.2.3	Difficulties Labelling Transgenic Myeloid Cells In Adult Zebrafish Tissue Sections By IHC Or ISH.....	69
3.2.4	A Role For <i>tp53</i> Mutation On MPN In <i>NHA9</i> Adult Zebrafish?.....	71
3.3	DISCUSSION.....	72
3.3.1	Transgenic Zebrafish Models Of Myeloid Disease.....	72
CHAPTER 4 NUP98-HOXA9 ZEBRAFISH EMBRYOS DISPLAY DEFECTS IN HAEMATOPOIESIS & CELLULAR APOPTOSIS		88
4.1	BACKGROUND.....	88
4.1.1	Using Transgenic Zebrafish As A Tool By Focusing On Leukaemia Phenotypes in Embryos	88
4.1.2	<i>NHA9</i> & <i>MEIS1</i>	89
4.2	EXPERIMENTAL FINDINGS	90

4.2.1	<i>NHA9</i> Inhibits Primitive Macrophage Differentiation And Perturbs Haematopoiesis To Promote Myeloid And Suppress Erythroid Fates.....	90
4.2.2	Knockdown Of <i>meis1</i> Eliminates Myeloid Cells From The Posterior Blood Island And HSCs From The Dorsal Aorta, And Inhibits <i>NHA9</i>	93
4.2.3	<i>NHA9</i> Suppresses Cell Cycle Arrest And Apoptosis In The Presence Of DNA Damage.....	94
4.2.4	FACS Isolation Of Myeloid Cells Undergoing Apoptosis	96
4.2.5	Modulating The Zebrafish <i>bcl2</i> Family	96
4.3	DISCUSSION.....	97
4.3.1	Similar And Distinct Findings For <i>NHA9</i> In Fish Versus Mammals.....	98
4.3.2	The Role Of <i>meis1</i> And <i>cdx-hox</i> In Definitive Haematopoiesis	98
4.3.3	Interplay Of <i>cdx-hox</i> And <i>tal1/scl</i> In <i>NHA9</i> Embryos	99
4.3.4	<i>NHA9</i> Dysregulates Cellular Homeostasis	101
CHAPTER 5 MICROARRAY IDENTIFIES DNMT1 AS NOVEL GENETIC COLLABORATOR OF NUP98-HOXA9		117
5.1	BACKGROUND.....	117
5.1.1	Using Zebrafish Embryos As An <i>In Vivo</i> Tool To Study Epigenetic Mechanisms In AML	117
5.1.2	Identifying Genetic Collaborators Of <i>NUP98-HOXA9</i>	118
5.2	EXPERIMENTAL FINDINGS	119
5.2.1	Microarray Analysis Of <i>NHA9</i> -Trangenic Zebrafish Embryos	119

5.2.2	<i>NHA9</i> -Transgenic Zebrafish Embryos Upregulate <i>dnmt1</i>	119
5.2.3	Knockdown of Zebrafish <i>dnmt1</i> Inhibits Myeloproliferation In <i>NHA9</i> Embryos	120
5.2.4	Inhibiting Zebrafish <i>dnmt1</i> Enzyme Activity Blocks Myeloproliferation In <i>NHA9</i> Embryos	120
5.3	DISCUSSION.....	121
5.3.1	Potential Mechanism For Epigenetic Dysregulation By <i>NHA9</i>	122
5.3.2	Targeting Epigenetic Regulation In Clinical Myeloid Disease.....	124
CHAPTER 6 MANIPULATING THE <i>NUP98-HOXA9</i> MYELOPROLIFERATION PHENOTYPE BY TARGETING WNT/β-CATENIN.....		132
6.1	BACKGROUND.....	132
6.1.1	Human <i>NUP98-HOXA9</i> Microarrays Identify Prostaglandin Signalling, Which Promotes Haematopoiesis Via Wnt/ β -catenin.....	132
6.1.2	The Canonical Wnt/ β -catenin Pathway Promotes Self-Renewal Of Cells ('Stemness')	133
6.1.3	AML Initiating Cells Require Wnt/ β -catenin.....	134
6.1.4	Using <i>NHA9</i> Zebrafish Embryos To Study Wnt/ β -catenin	136
6.2	EXPERIMENTAL FINDINGS	137
6.2.1	Direct Investigation Of The Wnt/ β -catenin Pathway In <i>NHA9</i> -Transgenic Zebrafish Embryos Reveals Upregulation Of <i>ptgs2</i> Isoforms.....	137
6.2.2	Inhibiting Wnt/ β -catenin In <i>NHA9</i> Embryos Blocks Myeloproliferation, But Stimulating Wnt/ β -catenin Has Unexpected Effect.....	138

6.2.3	Inhibiting Wnt/ β -catenin In <i>NHA9</i> Embryos Does Not Rescue Erythroid Cells.....	139
6.3	DISCUSSION.....	140
6.3.1	Reconciling Diverse Findings For Prostaglandin Signalling	141
CHAPTER 7	<i>IN VIVO</i> ANTI-LEUKAEMIA ACTIVITY OF NOVEL PRODIGIOSENES IN A ZEBRAFISH XENOGRAFT MODEL	152
7.1	BACKGROUND.....	152
7.1.1	A Pressing Need For Novel Anti-Leukaemia Agents	152
7.1.2	A Zebrafish Xenotransplantation Model To Investigate Genetics And Drug Responses Of Human Myeloid Leukaemia Cells.....	152
7.1.3	Prodigiosin & Its Derivatives Have Anti-Cancer Activity	154
7.2	EXPERIMENTAL FINDINGS	156
7.2.1	Synthesis Of C-Ring Modified Prodigiosenes	156
7.2.2	C-Ring Modified Prodigiosenes 8a-d Show Novel Anti-Leukaemia Activity <i>In Vitro</i>	156
7.2.3	<i>In Vivo</i> Anti-Leukaemia Activity Of Novel C-Ring Modified Prodigiosenes 8a-d In A Zebrafish Xenograft Model	157
7.2.4	Difficulties Quantifying Anti-Leukaemia Effects Of Prodigiosenes	159
7.2.5	Attempts To Assess Activity Of Prodigiosenes on <i>NHA9</i> -Transgenic Embryos	159
7.3	DISCUSSION.....	160
7.3.1	Potential Pitfalls Of Zebrafish Xenotransplantation	161

**CHAPTER 8 CONCLUSIONS & RECOMMENDATIONS
FOR STUDYING FUTURE PHENOTYPES & MODIFIERS 170**

8.1	SUMMARY OF FINDINGS.....	170
8.2	<i>NHA9</i> & MYELOID DISEASE.....	170
8.2.1	Challenges To Modelling Myeloid Disease In Transgenic Zebrafish	170
8.2.2	Future Directions – New Transgenic Tools.....	175
8.3	<i>NHA9</i> & <i>MEIS1</i>	176
8.3.1	Future Directions – Modulating <i>meis1</i> In <i>NHA9</i> Embryos	176
8.3.2	Future Directions – Microarray Analyses For <i>NHA9</i> & <i>meis1</i>	177
8.4	<i>NHA9</i> & <i>DNMT1</i>	178
8.4.1	Future Directions – Zebrafish <i>dnmt1</i> In <i>NHA9</i> Embryos	178
8.5	<i>NHA9</i> & WNT/ β -CATENIN	181
8.5.1	Wnt/ β -Catenin Regulates The <i>CDX-HOX</i> Network	181
8.5.2	Future Directions – Zebrafish Wnt/ β -catenin In <i>NHA9</i> Embryos.....	182
8.6	A POSSIBLE ROLE FOR RETINOIC ACID IN <i>NHA9</i> EMBRYOS.....	184
8.6.1	Retinoic Acid Signalling & <i>hox</i> -Independent Activity of <i>cdx</i>	184
8.6.2	Future Directions – Possible Interplay of Wnt/ β -Catenin And Retinoic Acid In <i>NHA9</i> Embryos.....	185
8.7	FUTURE DIRECTIONS – A SYNTHESIS OF <i>DNMT1</i> , WNT/ β -CATENIN, <i>CDX-HOX</i> , AND RA	186
8.8	FUTURE INVESTIGATIONS WITH XENOTRANSPLANTATION	187

8.9	<i>NHA9</i> -TRANSGENIC ZEBRAFISH PRESENT AN ATTRACTIVE <i>IN VIVO</i> MODEL FOR HIGH-THROUGHPUT DRUG DISCOVERY IN MYELOID DISEASE	188
8.10	CLOSING REMARKS.....	191
	BIBLIOGRAPHY	195
	APPENDIX A COPYRIGHT AND PERMISSIONS – DEVELOPMENTAL BIOLOGY (ELSEVIER)	228
	APPENDIX B COPYRIGHT AND PERMISSIONS – ADVANCES IN HEMATOLOGY (HINDAWI PUBLISHING CORPORATION).....	229
	APPENDIX C COPYRIGHT AND PERMISSIONS – BRITISH JOURNAL OF HAEMATOLOGY (WILEY-BLACKWELL)	230
	APPENDIX D ETHICS APPROVAL	231

LIST OF TABLES

Table 1.1. Description of AML fusion oncogenes (in order of mention in body text).....	23
Table 1.2. Common karyotype abnormalities in AML and their associated risk.....	23
Table 2.1. Primer sequences for pCS2+ vector construction.	54
Table 2.2. MO sequences for blocking gene expression.	54
Table 2.3. Primer sequences for genotyping and qRT-PCR.	55
Table 2.4. ProK permeabilization of zebrafish embryos at various developmental stages.	56
Table 2.5. SDS-PAGE recipes for Western blotting (all solutions prepared [w/v]).	57
Table 3.1. Incidence of <i>NHA9</i> -induced haematopathology in zebrafish.....	76
Table 7.1. Mean <i>in vitro</i> activity ^a of Prodigiosin (1) and prodigiosenes 8a-d over 60 cancer cell lines.	163

LIST OF FIGURES

Figure 1.1 (<i>next page</i>). Model of human <i>NHA9</i> oncogenic activity in embryonic zebrafish haematopoiesis.....	24
Figure 1.2. Overview of zebrafish developmental myelopoiesis and currently used transgenic lines.....	26
Figure 1.3. <i>HOXA9</i> is a central regulator in AML.....	27
Figure 1.4. Model depicting ‘waves’ of haematopoiesis in the zebrafish embryo.....	28
Figure 1.5. Relevant landmarks in a 28 to 30 hpf zebrafish embryo.....	29
Figure 1.6. The t(7;11)(p15;p15) translocation, yielding fusion oncogene <i>NHA9</i>	30
Figure 2.1 (<i>next four pages</i>). Timeline of zebrafish developmental stages.....	58
Figure 2.2. Schematic of vector assembly using Gateway® (Invitrogen) cloning technology.....	63
Figure 2.3. Assignment of blood cell gates on FACSARIA™ I.....	64
Figure 3.1 (<i>next page</i>). Schematic and visualization of Cre/ <i>lox</i> -inducible transgenic zebrafish that express <i>EGFP</i> and human <i>NHA9</i> under the control of the 9.1 kb zebrafish <i>spil</i> promoter.....	77
Figure 3.2. Extended timeline of transgenic expression in <i>NHA9</i> embryos.....	79
Figure 3.3 (<i>next page</i>). Cre/ <i>lox</i> recombination and expression of human <i>NHA9</i> fusion oncoprotein in <i>Tg(spil::lgl::NHA9)</i> transgenic zebrafish embryos.....	80
Figure 3.4 (<i>next page</i>). Activated <i>NHA9</i> -transgenic zebrafish develop disease similar to MPN.....	82
Figure 3.5 (<i>next page</i>). Additional histopathology analysis of <i>NHA9</i> (+ <i>Cre</i>) adult zebrafish with and without MPN.....	84
Figure 3.6 (<i>next page</i>). Evidence to suggest that loss-of-function <i>tp53</i> ^{M214K} mutation may collaborate with <i>NHA9</i> to induce myeloproliferative pathology.....	86
Figure 4.1 (<i>next page</i>). Schematic representing the impact of the <i>cdx-hox</i> transcriptional network and <i>spil-gata1a</i> antagonism on zebrafish primitive haematopoiesis.....	103
Figure 4.2 (<i>next page</i>). <i>NHA9</i> inhibits primitive macrophage differentiation, as well as promotes myeloid and suppresses erythroid gene expression.....	105

Figure 4.3. <i>NHA9</i> does not increase cellular proliferation.	107
Figure 4.4. <i>NHA9</i> transgenic embryos do not exhibit hyperactive cellular proliferation.	108
Figure 4.5 (<i>next page</i>). Knockdown of zebrafish <i>meis1</i> may limit <i>NHA9</i> effects on myeloid cells.	109
Figure 4.6. Knockdown of zebrafish <i>meis1</i> inhibits HSC development.	111
Figure 4.7 (<i>next page</i>). <i>NHA9</i> suppresses <i>tp53</i> -dependent cell cycle arrest and apoptosis.	112
Figure 4.8. Activation of <i>NHA9</i> by microinjection of <i>Cre</i> mRNA is sufficient to achieve suppression of <i>cas3</i>	114
Figure 4.9. FACS analysis on GFP+ myeloid cells from irradiated <i>NHA9</i> embryos.	115
Figure 4.10. Knockdown of <i>bcl2l1/bcl-xL</i> does not rescue apoptosis in <i>NHA9</i> transgenic embryos.	116
Figure 5.1. Schematic representing chromatin remodeling by DNMT1 and HDACs.	127
Figure 5.2. qRT-PCR from <i>NHA9</i> embryos depicting confirmation of microarray results and Wnt/ β -catenin investigations.	128
Figure 5.3. Knockdown of zebrafish <i>dnmt1</i> inhibits myeloproliferation by <i>NHA9</i>	129
Figure 5.4 (<i>next page</i>). Pharmacologic inhibition of zebrafish <i>dnmt1</i> enzyme activity with Decitabine inhibits myeloproliferation by <i>NHA9</i>	130
Figure 6.1. The canonical Wnt/ β -catenin signalling pathway.	143
Figure 6.2 (<i>next page</i>). Granulocytic and monocytic lineages, markers in myeloid differentiation, and impact of fusion oncoproteins.	144
Figure 6.3. qRT-PCR from <i>NHA9</i> embryos depicting Wnt/ β -catenin investigations.	146
Figure 6.4 (<i>next two pages</i>). The Wnt/ β -catenin pathway may play a limited role on the myeloproliferative phenotype in <i>NHA9</i> embryos.	147
Figure 6.5 (<i>next page</i>). Inhibition of the Wnt/ β -catenin pathway weakly rescues erythroid development in <i>NHA9</i> embryos.	150

Figure 7.1. Schematic of <i>in vivo</i> cell proliferation assay in xenotransplanted zebrafish embryos.....	164
Figure 7.2. Prodigiosin (1), analogue (2) and prodigiosene core structure (3).....	164
Figure 7.3. Novel anti-leukaemia activity of C-ring modified prodigiosenes.....	165
Figure 7.4. Baseline activity (24 hpi) of xenotransplanted K562 leukaemia cells in zebrafish embryo.	165
Figure 7.5 (<i>next two pages</i>). Anti-leukaemia activity of prodigiosenes 8a-d <i>in vivo</i> against K562 human leukaemia cells injected into <i>casper</i> zebrafish.	166
Figure 7.6. Comparison of casp3 immunofluorescence in <i>Cre</i> embryos treated with IR only versus IR + prodigiosene.....	169
Figure 8.1. Mating strategy to obtain <i>NHA9</i> + β -catenin(S/T \rightarrow A) zebrafish.	192
Figure 8.2. Schematic representing the impact of the <i>cdx4-raldh2</i> regulatory loop on zebrafish primitive haematopoiesis.	193
Figure 8.3. Screening for drugs that block <i>NHA9</i>	194

ABSTRACT

We need to better understand the genetic mechanisms that transform normal blood cells into acute myeloid leukaemia (AML). Overall survival is improving for children and adults with AML, but traditional therapies can be very toxic and high-risk forms of disease remain fatal for 2 out of 5 patients. One high-risk indicator is *homeobox A9 (HOXA9)*, a gene necessary for normal blood development. *HOXA9* is overexpressed in 80% of AML cases, especially as part of the *NUP98-HOXA9 (NHA9)* mutation. Our research goal is to improve survival for human AML caused by *NHA9*, by identifying new contributing genes and less toxic drugs.

To do this, a new animal model of disease is required. The zebrafish, *Danio rerio*, was chosen as a reliable *in vivo* tool to study leukaemia, thanks to its conserved genetics and cell biology. Compared to mice, zebrafish also support rapid chemical and genetic screening, which is a tremendous asset.

We created mutant zebrafish carrying the human *NHA9* mutation. We found that 23% of *NHA9* adult fish developed a myeloproliferative neoplasm (MPN) by 19 to 23 months of life, which highlights the role of mutant *HOXA9* in myeloid disease. In addition, ~80% of *NHA9* embryos displayed defects in early blood development. *NHA9* decreased *gata1a* erythroid expression and increased *spi1* myeloid expression, which matches the myeloproliferation in adult fish. Of note, the HOX co-factor, *MEIS1*, is also overexpressed in human AML, and zebrafish *meis1* gene knockdown inhibited myeloproliferation in *NHA9* embryos.

I then leveraged this myeloproliferation phenotype in *NHA9* embryos to examine new contributing genes and drugs. Microarray analysis identified high levels of zebrafish *dnmt1*, a gene that regulates blood cell maturation via epigenetic DNA methylation. Our preliminary evidence suggests that *NHA9* is inhibited by *dnmt1* gene knockdown or treatment with Decitabine, a demethylating agent. We also looked at the Wnt/ β -catenin pathway, which is often hijacked to promote AML. We blocked myeloproliferation in *NHA9* embryos by targeting Wnt/ β -catenin with Indomethacin, a COX inhibitor.

Finally, I transplanted human leukaemia cells into zebrafish for testing new drugs, called prodigiosenes. These drugs reduced the proliferation of leukaemia cells, and were reasonably non-toxic to embryos.

LIST OF ABBREVIATIONS & SYMBOLS USED

Gene & protein symbol conventions, as represented by “*DNA (cytosine-5)-methyltransferase 1*” gene.

Species	Gene symbol	Protein symbol
<i>Homo sapiens</i> (human), <i>Gallus gallus</i> (chicken)	<i>DNMT1</i> (UPPERCASE ITALICS)	DNMT1 (UPPERCASE)
<i>Mus musculus</i> (mouse), <i>Rattus norvegicus</i> (rat)	<i>Dnmt1</i> (Sentence case italics)	Dnmt1 (Sentence case)
<i>Danio rerio</i> (zebrafish), <i>Xenopus</i> spp. (frog)	<i>dnmt1</i> (lowercase italics)	dnmt1 (lowercase)

Adapted from Wikipedia, http://en.wikipedia.org/wiki/Gene_nomenclature

Units

bp	base pairs
dpf	days post-fertilization
f_	femto_ (10^{-15})
g	gram
x g	gravitational acceleration (centrifugation unit)
Gy	Gray (SI unit of absorbed radiation; 1 Gy = 1 Joule per kg)
hpf	hours post-fertilization
hpi	hours post-injection
k_	kilo_ (10^3)
kb	kilo base pairs
kDa	kilo Dalton (atomic mass unit; 1 kDa = $1.660\ 538\ 782(83) \times 10^{-24}$ g)
L	litre
M	molarity (1 M = 1 mole per liter)
m_	milli_ (10^{-3})
μ_	micro_ (10^{-6})
n_	nano_ (10^{-9})
nt	nucleotide(s)
p_	pico_ (10^{-12})
%	percentage concentration of solution; solid in solvent (1% = 1 g per 100 mL [w/v]), or liquid in solvent (1 mL per 100 mL [v/v])
rpm	revolutions per minute
U	enzyme catalysis units (1 U = 1 μmole of substrate consumed per minute)
v/v	volume by volume percentage solution
w/v	mass by volume percentage solution

Abbreviations & Symbols

1°	primary
2°	secondary
7-AAD	7-aminoactinomycin D
<i>AB</i>	‘wild-type’ zebrafish strain, genotype designation
AGM	aorta-gonad-mesonephros
(B/T)-ALL	(B-cell / T-cell) acute lymphoblastic leukaemia
ALPM	anterior lateral plate mesoderm
AML	acute myeloid leukaemia
<i>AML1-ETO</i>	<i>acute myeloid leukaemia 1—eight twenty-one</i> (fusion oncogene) Officially known as: <i>RUNX1-MTG8 runt-related transcription factor 1—myeloid transforming gene on chromosome 8</i> ; or, <i>RUNX1-RUNX1T1 (RUNX1— runt-related transcription factor 1; translocated to, 1)</i>
APL	acute promyelocytic leukaemia
AO	acridine orange
As ₂ O ₃	arsenic trioxide
AZA	Azacitidine (5-azacytidine; 5-azaC)
<i>actb1</i>	<i>actin, beta 1</i>
<i>bbc3 / puma</i>	<i>bcl2 binding component 3 / p53 upregulated mediator of apoptosis</i>
<i>bcl2</i>	<i>B-cell lymphoma 2</i>
<i>bcl2l1</i>	<i>bcl2-like 1</i>
<i>BCR-ABL1</i>	<i>breakpoint cluster region—v-abl Abelson murine leukaemia viral oncogene homologue 1</i> (fusion oncogene)
BH3	Bcl2 homology domain 3
BrdU	5-Bromo-2-deoxyuridine
casp3	activated caspase-3
CD(nn)	cluster of differentiation marker (number)
<i>cdkn1a</i>	<i>cyclin-dependent kinase inhibitor 1a</i>
<i>CDX</i>	<i>caudal type homeobox transcription factor</i>
CHT	caudal haematopoietic tissue
<i>clo</i>	<i>cloche</i>
CM-DiI	chloromethylbenzamido-1,1'-dioctadecyl-3,3,3'-tetramethyl-indocarbocyanine perchlorate
CML	chronic myelogenous leukaemia
CNS	central nervous system
COX	cyclooxygenase
<i>Cre</i>	<i>Cre</i> molecular recombinase (<i>Causes recombination</i>)
C _t	cycle threshold
<i>ctnnb</i>	<i>catenin (cadherin-associated protein), beta</i>
DAC	Decitabine (5-aza-2'-deoxycytidine; 5-azadC)
DIG	digoxigenin
DMSO	dimethyl sulphoxide
(c)DNA	(copy) deoxyribonucleic acid
<i>DNMT1</i>	<i>DNA (cytosine-5-)-methyltransferase 1</i>
<i>ef1a</i>	<i>elongation factor 1 alpha</i>

<i>EGFP</i>	<i>enhanced green fluorescent protein</i>
<i>egr2b</i>	<i>early growth response 2b</i> (also known as: <i>krox20</i>)
EMP	erythro-myeloid progenitor
<i>eng2</i>	<i>engrailed 2</i>
FACS	fluorescence-activated cell sorting
FBS	fetal bovine serum
FITC	fluorescein isothiocyanate
<i>fli1a</i>	<i>friend leukaemia integration 1a</i>
FSC	forward scatter (FACS)
G2 phase	growth/gap phase 2 of cell cycle
<i>gata1a</i>	<i>GATA-binding factor 1a</i>
GMP	granulocyte/monocyte progenitor
(mq)H ₂ O	(milli-Q) water
<i>hbbe3</i>	<i>hemoglobin beta embryonic-3</i>
HDAC	histone deacetylase complex
H/E	haematoxylin/eosin
<i>HOXA9</i>	<i>homeobox A9</i>
hs	heat-shock
HSC	haematopoietic stem cell
<i>hsp70</i>	<i>heat shock protein 70</i>
<i>kdrl / flk1a</i>	<i>kinase insert domain protein receptor like / fetal liver kinase 1a</i>
<i>kgg</i>	<i>kugleig (cdx4^{-/-})</i>
ICM / PLPM	intermediate cell mass / posterior lateral plate mesoderm
IF	immunofluorescence
IHC	immunohistochemistry
IgG	immunoglobulin G
IM	imatinib mesylate (also known as: Gleevec®)
Indo	Indomethacin (1-[4-Chlorobenzoyl]-5-methoxy-2-methyl-3-indoleacetic acid)
IR	ionizing radiation
<i>lcp1</i>	<i>lymphocyte cytosolic protein 1</i> (also known as: <i>l-plastin</i>)
<i>IGl</i>	<i>loxP-EGFP-loxP</i>
LIC	leukaemia-initiating cell
<i>lmo2</i>	<i>LIM domain only 2 (rhombotin-like 1)</i>
<i>loxP</i>	<i>locus of X-over bacteriophage P1</i>
LPM	lateral plate mesoderm
<i>lyz</i>	<i>lysozyme</i>
M phase	mitosis phase of cell cycle
MAB(-T)	maleic acid buffer (- Tween 20)
MDS	myelodysplastic syndrome
<i>MEIS1</i>	<i>myeloid ecotropic integration site 1</i>
<i>MLL-AF9</i>	<i>mixed lineage leukaemia—ALL1-fused gene from chromosome 9</i> (fusion oncogene) Officially known as: <i>MLL-MLLT3</i> (<i>mixed lineage leukaemia—myeloid/lymphoid or mixed-lineage leukaemia (trithorax homologue, Drosophila)</i> ; translocated to, 3)

<i>MLL-ENL</i>	<i>mixed lineage leukaemia—eleven nineteen leukaemia</i> (fusion oncogene) Officially known as: <i>MLL-MLLT1</i> (<i>mixed lineage leukaemia—myeloid/lymphoid or mixed-lineage leukaemia (trithorax homologue, Drosophila)</i>); <i>translocated to, 1</i>)
MO	morpholino oligonucleotide
<i>mon</i>	<i>moonshine</i> (<i>trim33 / tif1$\gamma^{-/-}$</i>)
<i>MOZ-TIF2</i>	<i>monocytic leukaemia zinc finger protein—transcriptional intermediary factor 2</i> (fusion oncogene) Officially known as: <i>MYST3-NCOA2</i> (<i>MYST histone acetyltransferase [monocytic leukaemia] 3—nuclear receptor coactivator 2</i>)
MPN	myeloproliferative neoplasm
<i>mpx</i>	<i>myeloperoxidase</i>
MTD	maximum tolerated dose
<i>c-myb</i>	<i>v-myb myeloblastosis viral oncogene homologue (avian)</i>
<i>Myc</i>	<i>v-myc myelocytomatosis viral oncogene homologue (avian)</i>
<i>NHA9</i>	<i>NUP98-HOXA9</i> (fusion oncogene)
NS-398	<i>N</i> -[2-(Cyclohexyloxy)-4-nitrophenyl]methanesulphonamide
(d)NTP	(deoxy)nucleotide triphosphate
<i>NUP98</i>	<i>nucleoporin 98 kDa</i>
p(N)	plasmid (Name)
PAS	periodic acid-Schiff
PBI	posterior blood island
PBS(-T)	phosphate buffered saline (- Tween 20)
<i>PBX</i>	<i>pre-B-cell leukaemia homeobox</i>
(qRT-)PCR	(quantitative reverse transcription) polymerase chain reaction
PFA	paraformaldehyde
(dm)PGE ₂	(16,16-dimethyl) prostaglandin E ₂
pH3	phosphorylated histone-H3
PLPM	posterior lateral plate mesoderm
<i>PML-RARA</i>	<i>promyelocytic leukaemia—retinoic acid receptor alpha</i> (fusion oncogene)
ProK	proteinase K
<i>ptger</i>	<i>prostaglandin E receptor</i>
<i>ptgs</i>	<i>prostaglandin-endoperoxide synthase (prostaglandin G/H synthase and cyclooxygenase)</i>
PTU	<i>N</i> -phenylthiourea
(AT)RA	(all- <i>trans</i>) retinoic acid
<i>rag2</i>	<i>recombination activating gene 2</i>
<i>RARA</i>	<i>retinoic acid receptor alpha</i>
<i>K-RAS</i>	<i>v-Ki-ras2 Kirsten rat sarcoma viral oncogene homologue</i>
(m)RNA	(messenger) ribonucleic acid
<i>runx1</i>	<i>runt-related transcription factor 1</i>
S phase	DNA synthesis phase of cell cycle
SDS	sodium dodecyl sulphate
<i>spi1 / pu.1</i>	<i>spleen focus forming virus (SFFV) proviral integration oncogene / purine-rich (PU)-box factor 1</i>

SSC	side scatter (FACS)
SSC-T	saline sodium citrate buffer - Tween 20
<i>tal1 / scl</i>	<i>T-cell acute lymphocytic leukaemia protein 1 / stem cell leukaemia</i>
TBS(-T)	Tris buffered saline (- Tween 20)
<i>TEL-AML1</i>	<i>translocation-ETS-leukaemia—acute myeloid leukaemia 1</i> (fusion oncogene) Officially known as: <i>ETV6-RUNX1</i> (<i>ets variant 6—runt-related transcription factor 1</i>)
<i>TEL-JAK2</i>	<i>translocation-ETS-leukaemia—janus kinase 2</i> (fusion oncogene) Officially known as: <i>ETV6-JAK2</i> (<i>ets variant 6—janus kinase 2a</i>)
<i>Tg</i>	transgene
<i>tp53</i>	<i>tumour protein 53</i>
<i>trim33 / tif1γ</i>	<i>tripartite motif-containing 33 / transcriptional intermediary factor 1 gamma</i>
<i>vlt</i>	<i>vlad tepes (gata1a^{-/-})</i>
WISH	whole-mount RNA <i>in situ</i> hybridization
WKM	whole kidney marrow
Wnt	wingless (Wg)-related mouse mammary tumour virus (MMTV) integration site (Int)

ACKNOWLEDGEMENTS

Firstly, I thank those who have directly contributed to, or supported this work: my thesis committee, Gerry Johnston, David Waisman, Roy Duncan, Graham Dellaire, and Mark Nachtigal for their tremendous guidance; Honours and graduate students, Andrew Coombs, Märta Vigerstad, Ellen Boyd, Fui-Boon Kai, and Adam Deveau for their enthusiasm and dedication; the Berman lab, Tuğçe Balci, Dale Corkery, Lauren Klein, Angela Young, Chansey Veinotte, Lindsay MacDonald, Babak Razaghi, Eve Teh, Tristan Dobson, Jake Seibert, Jocelyn Jaques, and lab managers, Sahar Da'as and Ameer Jarrar for their unwavering support, good food, and stimulating discussion; Eileen McBride and Sandy Edgar for their patience in teaching me pathology and FACS; the Chemistry lab, Deborah Smithen, Estelle Marchal, and Alison Thompson, as well as Rob Liwski and Aarnoud van der Spoel for their unique perspectives and enthusiasm for collaboration; Ian Chute, Daniel Leger, and Stephen Lewis (ACRI) for microarrays; Laura Reaume and Andrew Waskiewicz (UAlberta) for collaboration; Clemens Grabher, Evisa Gjini, Elspeth Payne, and Thomas Look (Dana-Farber) for fish lines and critical insight.

Secondly, I thank those who have enhanced my skills: David Traver and Julien Bertrand for haematopoiesis and FACS; Cicely Jette and Seth Carbonneau for apoptosis; David Langenau, Chi-Bin Chien, Kristen Kwan, Nathan Lawson, Steven Leach, and Elayne Provost for transgenics; Ujwal Pyati, Laura Gillis, and Craig McCormick for qRT-PCR; Cary Isenor and Mike Melanson for histology; and Randy Petersen, Len Zon, and Gary Gilliland for drug screens and many critical insights.

Thirdly, my mentors: Drs. David Malkin and Adam Durbin for setting me on my research path; and my supervisor, Dr. Jason Berman, for making me a part of his team, and for his enthusiasm, support, and guidance through this significant time.

Finally, to my friends and family – your support through hard times has meant the world to me. Above all, love to Mom, Dad, and Sue. From helping me to achieve my goals to keeping me sane – without you, none of this would have been possible.

This work was funded by a Nova Scotia Health Research Foundation (NSHRF) Operating Grant and Dalhousie Clinical Research Scholar Award; and Graduate Awards from the Canadian Institutes of Health Research (CIHR) and The Canadian Cancer Society, in conjunction with The Beatrice Hunter Cancer Research Institute.

CHAPTER 1 INTRODUCTION

1.1 PREAMBLE

Acute myeloid leukaemia (AML) results from multiple genetic abnormalities that alter white blood cell development, leading to a block in differentiation/maturation (Gilliland and Tallman 2002). AML continues to pose treatment challenges, with cure rates of less than 60%. Research efforts to expose the underlying genetic and molecular pathways will enable the development of therapies that target the specific abnormality in a leukaemia cell. We have focused on the gene, *homeobox A9* (*HOXA9*), a member of the highly conserved *HOX* family of transcription factors (CHAPTER 1). *HOXA9* is overexpressed in 80% of human AML (Golub *et al.* 1999), and is a partner in the *NUP98-HOXA9* (*NHA9*) translocation (Borrow *et al.* 1996; Nakamura *et al.* 1996b) (Table 1.1). Despite more than a decade of study into *HOXA9*- and *NHA9*-induced AML, there has been a relative lack of *in vivo* studies and there exists no platform for drug discovery.

Animal models of disease are needed to link *in vitro* studies with the use of new agents in clinical trials. The zebrafish, *Danio rerio*, reliably models human leukaemia (CHAPTER 1), and its advantage over mouse models is the capacity to perform genetic and chemical screens (Yeh and Munson 2010). We therefore created a transgenic zebrafish expressing the human *NHA9* oncogene in blood cells. My research shows that 23% of *NHA9*-transgenic zebrafish develop a myeloproliferative neoplasm (MPN) between 19 to 23 months of life (CHAPTER 3) (Forrester *et al.* 2011). Additionally, *NHA9* expression in transgenic zebrafish embryos disrupts early blood development, with an abundance of myeloid cells (expressing *spil*) at the expense of the erythroid population (expressing *gata1a*). In the presence of DNA damage, *NHA9* also suppresses cell cycle arrest and apoptosis by increasing expression of *bcl2* (CHAPTER 4).

Given the benefits of zebrafish as a screening tool, our *NHA9* transgenic fish is poised to examine the impact of collaborating genes and to discover new drugs that combat high-risk AML. We considered the *HOX* co-factor, *MEIS1*, because it is also upregulated in human AML, and because co-overexpression of mouse *Meis1* cooperates with mouse *Hoxa9* and human *NHA9* to produce AML in mice (Kroon *et al.* 2001; Thorsteinsdottir *et al.* 2001). I found that gene knockdown of zebrafish *meis1* inhibited

the myeloproliferative phenotype in *NHA9* embryos (**CHAPTER 4**). However, since this relationship was known, we performed microarray analysis to investigate novel gene collaborators. We found that *NHA9* embryos show increased expression of *DNA (cytosine-5-)-methyltransferase 1 (dnmt1)* (**CHAPTER 5**). In a process known as ‘epigenetics’, the methylating activity of DNMT1 protein helps to ‘close’ the chromatin, which leads to widespread loss of gene expression (Sauntharajah *et al.* 2012). *DNMT1* represses genes that are needed for terminal differentiation of blood cells and thus keeps blood cells trapped in an immature state, which is a defining feature of AML. We blocked myeloproliferation in *NHA9* zebrafish embryos by gene knockdown of *dnmt1* or by pharmacologic treatment with Decitabine, a demethylating agent that is used to treat some forms of myeloid disease (Pan *et al.* 2010).

Furthermore, there may be a critical role for the Wnt/ β -catenin pathway in AML, because it is activated by a number of oncogenes. Wnt/ β -catenin hyperactivity blocks blood cell maturation – a hallmark of AML – and produces leukaemia-initiating cells (LICs). I hypothesized that Wnt/ β -catenin would be activated in *NHA9* embryos, and indeed we showed upregulation of *ptgs2a*, a COX2 isoform that activates Wnt/ β -catenin in blood cells (**CHAPTER 6**). Myeloproliferation in *NHA9* embryos could be blocked by pharmacologic treatment with a COX inhibitor, Indomethacin, similar to other mouse and zebrafish models of myeloid disease (Wang Y *et al.* 2010; Yeh *et al.* 2009).

Our lab has also injected human leukaemia cells into zebrafish embryos to evaluate drug responses *in vivo* (Corkery *et al.* 2011). I applied this zebrafish xenograft system to test new synthetic drugs, called prodigiosenes (**CHAPTER 7**). I found that prodigiosenes inhibited the growth of the injected leukaemia cells and that some posed less toxic side effects to the animal. These experiments lay the groundwork for using zebrafish xenotransplantation to test novel drugs on human *NHA9* leukaemia cells.

The combined effects of *NHA9* activity in zebrafish are summarized in **Figure 1.1**. Future investigations (**CHAPTER 8**) will leverage the phenotypes in *NHA9*-transgenic zebrafish for performing a chemical modifier screen to identify potential therapeutic compounds targeted for high risk AML. These findings will provide further insight into the genes that promote disease pathogenesis and reveal promising new agents to treat this aggressive disease.

1.2 ACUTE MYELOID LEUKAEMIA (AML)

1.2.1 High-Risk Versus Low-Risk Disease & Need For Targeted Agents

AML is characterized by hyperproliferation and failure of cellular differentiation in the myeloid cell lineage (Gilliland and Tallman 2002). Despite the use of aggressive treatment regimens, there is a low overall survival rate of less than 60% for all AML cases (Table 1.2). In part, this is due to a major discrepancy in the clinical efficacy of current therapeutics on different genetic lesions (Giles *et al.* 2002). The most frequent mutation in human AML is the t(8;21)(q22;q22) translocation, yielding the fusion oncogene, *AML1-ETO* (Table 1.1). The *AML1-ETO* fusion gene is found in ~15% of all AML cases (Fazi *et al.* 2007) and is classified as a core binding factor (CBF) leukaemia, together with the inversion of chromosome 16 (inv[16][p13;q22]) mutation, yielding *CBFB-MYH11* (Table 1.1). CBF leukaemias generally respond well to conventional therapy and do not often require the use of targeted agents. By contrast, gene mechanism studies and the development of targeted agents have improved survival dramatically for patients carrying the t(15;17)(q22;q21) translocation, which yields the *PML-RARA* fusion oncogene (Table 1.1). This mutation is found in ~10% of all AML cases and in more than 90% of cases classified as acute promyelocytic leukaemia [APL], which is a distinct subtype of AML. For *PML-RARA*-induced disease, combination therapy with two targeted agents, all-*trans* retinoic acid (RA) and arsenic trioxide (As₂O₃), have produced an overwhelmingly positive response. Like adult patients with CBF AML, patients with *PML-RARA* can anticipate a 5-year survival of ~70%, and a relatively low relapse rate of 33% (Fanning *et al.* 2009; Grimwade *et al.* 1998) (Table 1.2).

Unfortunately, the strong majority of human AML cases (~80%) show upregulation of the gene, *homeobox A9* (*HOXA9*), which is the single most important predictor of treatment failure by conventional chemotherapy and radiation (Borrow *et al.* 1996; Golemovic *et al.* 2006; Golub *et al.* 1999). Adult human patients harbouring a karyotypic abnormality or mutation that leads to upregulation of *HOXA9* can anticipate a 5-year survival rate of between 15 to 48%, with a relapse rate of between 50 to 78% (Fanning *et al.* 2009; Grimwade *et al.* 1998). No targeted therapies exist to combat human *HOXA9*, which again highlights a major discrepancy in current therapeutics.

1.2.2 HOXA9 & MEIS1

The *HOX* genes are well-conserved transcription factors that play critical roles in normal embryonic development and differentiation in organisms extending from *Drosophila* to humans (Amores *et al.* 1998). In particular, human *HOXA9* is a homologue of *Drosophila* Abdominal B (AbdB) that is expressed in the posterior of the developing embryo. In mammals, *HOXA9* is essential for normal haematopoiesis (Kawagoe *et al.* 1999; Lawrence *et al.* 1997; Lawrence *et al.* 2005), which is defined as the creation of all mature blood cell types, passing through defined intermediate stages, arising from stem cells and early progenitors (general schematic in **Figure 1.2**, and myeloid-specific schematic presented later in **Figure 6.2**). Enforced expression of *HOXA9* in leukaemia models suppresses myeloid differentiation and maintains survival of blood cell precursors (Calvo *et al.* 2000; Calvo *et al.* 2001; Faber *et al.* 2009). The frequency of *HOXA9* overexpression in human AML may stem from its role as a downstream ‘hub’ in convergent signalling pathways that control haematopoiesis. For example, the *mixed lineage leukaemia* (*MLL*) (Jin *et al.* 2010), *retinoic acid receptor alpha* (*RARA*), and *runt-related transcription factor 1* (*RUNX1*, also known as *AML1*) pathways all activate *HOXA9*, and mutations in these pathways are common initiating events in human AML (discussed in Bansal *et al.* 2006 and Dorsam *et al.* 2004) (**Figure 1.3**). Notably, mutant mice that lack the essential HSC gene, *Runx1/Aml1*, exhibit a myeloproliferative phenotype (Growney *et al.* 2005). Such a model posits *HOXA9* as a central regulator of normal haematopoiesis and AML pathogenesis.

In human AML, *HOXA9* is frequently co-overexpressed with its co-factor, *myeloid ecotropic integration site 1* (*MEIS1*) (Lawrence *et al.* 1999), and together they form a trimeric protein complex with *pre-B-cell leukaemia homeobox* (*PBX*) that binds target DNA sites that carry an (A/G)TGATT(T/A)A(T/C)GG(C/G) consensus sequence (**bold underline** denotes preferred nucleotides at shared positions) (Shen *et al.* 1999). *In vitro* studies in mouse cell culture also show that co-overexpression of the native mouse genes, *Hoxa9* and *Meis1*, promotes immortalization, long-term proliferation, and impaired differentiation of committed myeloid progenitors and haematopoietic stem cells (HSCs) (Calvo *et al.* 2000; Calvo *et al.* 2001; Golemovic *et al.* 2006; Takeda *et al.* 2006; Thorsteinsdottir *et al.* 2002). Enforced expression of mouse *Hoxa9* alone rarely produces

myeloid disease in mice except after a long latency. Co-overexpression with mouse *Meis1*, however, promotes strong penetrance of AML after a latency phase (Kroon *et al.* 1998; Thorsteinsdottir *et al.* 2001), which suggests that *Hoxa9*-induced AML requires collaborating mutations.

The expression of human *MEIS1* helps to differentiate low-risk and high-risk cases of AML. Human patients harbouring the lower-risk *AML1-ETO* and *PML-RARA* mutations exhibit decreased expression of *MEIS1* (Lasa *et al.* 2004). By contrast, high expression of *MEIS1* (Wang QF *et al.* 2011) and *HOXA9* (Faber *et al.* 2009) is observed in primary human leukaemia cells harbouring higher-risk *MLL*-rearrangements (between 4 to 10% of all AML cases [Eklund, 2007; Seiter and Harris, 2011]) – such as the t(9;11)(p22;q23) translocation, yielding *MLL-AF9*, or the t(11;19)(q23;p13.3) translocation, yielding *MLL-ENL* (Table 1.1). In mammals, the native MLL protein helps to regulate the expression of homeobox genes, such as by binding the promoters of *HOXA7*, *HOXA9*, and *HOXA10* (reviewed in Eklund, 2007). This is consistent with evidence that places *HOXA9* and its partner *MEIS1* in the middle of a signalling loop that integrates *MLL* and *C-MYB* in the regulation of HSC self-renewal and differentiation in mammals (Jin *et al.* 2010). Part of the mechanism by which expression of *MEIS1* is increased by high-risk *MLL*-rearrangements and decreased by low-risk *AML1-ETO* and *PML-RARA* mutations may be in their different expression levels of *spleen focus forming virus (SFFV) proviral integration oncogene (SPII*; can be more commonly known as *purine-rich [PU]-box factor 1 [PU.1]*), a master regulator of myeloid development. A recent abstract in human cell culture shows that *SPII* activates *MEIS1* expression (Zhou *et al.* 2011) and *AML1-ETO* and *PML-RARA* mutations exhibit decreased expression of *SPII* (Cook *et al.* 2004; Mueller BU *et al.* 2006; Vangala *et al.* 2003). By contrast, *SPII* expression is elevated in *MLL*-rearranged cells, and knockdown of *SPII* led to decreased *MEIS1* and decreased cell proliferation and survival (Zhou *et al.* 2011).

The frequency of *HOXA9* and *MEIS1* upregulation in human AML by a variety of fusion oncogenes, and their association with high-risk, poor prognosis leukaemia (such as *MLL*-rearrangements) highlights a pressing need for research into the mechanisms of pathogenesis by *HOXA9*. Such research may identify conserved drugable targets that could be exploited to combat a majority or large plurality of AML cases.

1.3 'PLATEAU' OF HUMAN CLINICAL STUDIES & LIMITATIONS OF TRADITIONAL ANIMAL MODELS

Myeloid leukaemias represent a heterogeneous group of diseases that remain fatal for 40% of patients, both due to refractory disease and toxicity from traditional therapeutic agents (Marcucci *et al.* 2011; Roboz 2011). Some experts believe that AML treatment has reached a 'plateau' in efficacy (Lowenberg *et al.* 2011). AML is the most common acute leukaemia in adults and accounts for nearly 20% of childhood leukaemia. While paediatric clinical trials over the past decades have made significant improvements to overall survival of patients, cure rates have peaked in the 60% range – significantly inferior to the 90% cure rates in childhood acute lymphoblastic leukaemia (ALL) (Woods 2006). The need for new anti-leukaemia agents is pressing, particularly ones that avoid overlapping toxicities with current chemotherapies, such as Cytarabine (arabino-furanosyl cytidine, Ara-C) and anthracyclines (Attar *et al.* 2008; Walter *et al.* 2010).

Given the high incidence of *HOXA9* dysregulation in human AML, this would be a worthy focus for the pursuit of drugable targets. Transcription factors themselves are challenging to target with small molecules, although the modified peptide, SAHM1, has proven successful in targeting the Mastermind-like protein 1 (MAML1) transcription factor in order to inhibit the hyperactive Notch pathway of T-cell ALL (Moellering *et al.* 2009). Yet targeting the mammalian *HOXA9* protein directly may prove detrimental to normal haematopoiesis, and so it would be helpful to identify collaborating genes or molecular pathways that are better-suited for pharmacologic inhibition.

However, despite more than a decade of study into *HOXA9*-induced AML in mammals, there has been a relative paucity of *in vivo* mechanistic studies and lack of a suitable platform for novel drug discovery. Limitations of current cell culture and mouse models include the large genetic redundancy of vertebrate *HOX* genes (Amores *et al.* 1998), discrepancies between the transformation of cultured cells *in vivo* and their corresponding disease formation *in vivo* (Calvo *et al.* 2000; Calvo *et al.* 2001), and the relatively long latency of mouse *Hoxa9*- and human *NHA9*-induced myeloid disease in mice (3 and 8 months, respectively, compared to less than 1 month for *MLL-AF9*-induced disease in mice [Wang Y *et al.* 2010]). Therefore, we desire a new animal model of *HOXA9*- or *NHA9*-induced myeloid disease that can address some of these limitations.

1.4 THE ZEBRAFISH AS A MODEL SYSTEM & RESEARCH TOOL

The zebrafish (*Danio rerio*) is a small bony fish of the teleost family, discovered in the Ganges of India. It was first made popular as a vertebrate model system for studying biological development by investigators in Oregon in the 1960s (Grunwald and Eisen 2002). The zebrafish has been firmly established as a reliable *in vivo* approach for modeling human leukaemia (Langenau *et al.* 2003; Sabaawy *et al.* 2006; Yeh and Munson 2010), thanks to conserved genetics and cell biology, as well as its relative ease of husbandry, fecundity, genetic manipulation, and inherent capacity for high-throughput chemical screens compared to traditional murine models. Remarkably, these common tropical fish have similar blood cells to humans, and also rely on the same genes for the growth of their cells. They reproduce weekly and we can easily watch the growth of embryos, which are major advantages compared to using mice for gene research.

Many of the oncogenes and tumour suppressor genes in leukaemia and other human malignancies have zebrafish homologues, and the pathways regulating cell growth, proliferation, apoptosis, and cell differentiation appear well conserved (Feitsma and Cuppen 2008; Yang HW *et al.* 2004). Technological advances over the past two decades have allowed researchers to develop a number of relevant zebrafish cancer models, which produce tumours that resemble human malignancies, both histologically and genetically (Liu S and Leach 2011). At its inception as a cancer model, proliferation and angiogenesis were proposed as phenotypic attributes as readouts relevant to cancer pathogenesis (Amatruda and Zon 1999). However, the study that revolutionized the use of zebrafish as a cancer disease model was the generation of a transgenic zebrafish expressing the mouse *Myc* oncogene under the control of the *recombination activating gene 2* (*rag2*) promoter that went on to develop T-cell acute lymphoblastic leukaemia (ALL) (Langenau *et al.* 2003; Feng H *et al.* 2007). In the past 10 years, many models of oncogene induced cancer have been generated in zebrafish, including: *tp53*-induced malignant peripheral neural sheath tumours (zMPNST) (Berghmans *et al.* 2005), *B-RAF*-induced melanoma (Patton *et al.* 2005), *TEL-AML1*-induced pre-B-ALL (Sabaawy *et al.* 2006), *K-RAS*-induced rhabdomyosarcoma (Langenau *et al.* 2007), *MYCN*-induced neuroblastoma (Zhu *et al.* 2012), and *EWS-FLII*-induced Ewing's sarcoma (Leacock *et al.* 2012). Zebrafish studies complement leukaemia research in cell lines and mouse

models because a zebrafish model of AML can be used to rapidly screen for drugs that ameliorate the leukaemia in an *in vivo* system (Berman *et al.* 2003). Novel insights into the conservation of haematopoietic lineages, and improvements in our capacity to identify, isolate, and culture such haematopoietic cells continue to enhance our ability to use this simple organism to address disease biology.

1.4.1 Conserved Genetics & Cell Biology Of Zebrafish Haematopoiesis

The zebrafish is a highly efficient model system for studying blood cell development (Amatruda and Zon 1999; Bahary and Zon 1998; Gregory and Jagadeeswaran 2002) and leukaemogenesis (Langenau *et al.* 2003; Langenau *et al.* 2005a; Langenau *et al.* 2005b; Sabaawy *et al.* 2006). All of the major haematopoietic cellular lineages have zebrafish counterparts and the fundamental genetic mechanisms that control haematopoiesis are well conserved (Berman *et al.* 2003; Berman *et al.* 2005) (Figure 1.2). Zebrafish myelopoiesis parallels that in mammals with a number of studies detailing neutrophil and macrophage development (Bennett *et al.* 2001; Berman *et al.* 2005; Herbomel and Levraud 2005; Lieschke *et al.* 2001). Our laboratory was the first to identify a zebrafish mast cell lineage, which demonstrates conserved cell biology and function with their mammalian counterparts (Da'as *et al.* 2011; Dobson *et al.* 2008). These findings have helped justify modeling human myeloid diseases in the zebrafish.

Zebrafish haematopoiesis occurs in four 'waves', each defined by spatiotemporal foci and cell specification (Bertrand *et al.* 2007) (Figure 1.4). Primitive haematopoiesis influences the morphology of the developing embryo (Baumann and Dragon 2005; Hove *et al.* 2003) and produces circulating erythrocytes that facilitate tissue oxygenation during periods of rapid embryonic growth (Orkin and Zon 2008). In mammals, primitive haematopoiesis initiates with erythroid cells that arise in the blood islands of the placental yolk sac. By contrast, in zebrafish, primitive erythroid cells develop inside the animal body. Erythropoiesis begins as bilateral stripes in the posterior lateral plate mesoderm (PLPM) around 12 hours post-fertilization (hpf), which fuse between 16 to 18 hpf to form the intermediate cell mass (ICM). Erythroid cells express *GATA-binding factor 1a* (*gata1a*) in early progenitors, and mature to express *haemoglobin alpha embryonic-1* (*hbae1*), *hbae3*, and *hbbe3/βe3-globin*. Erythroid cells enter circulation by ~24 hpf.

Primitive macrophages remodel early tissues: they shape architecture, assist tissue vascularization, and eliminate apoptotic cells. Embryonic macrophages arise by day E7.5 in mice (Bertrand *et al.* 2005) and starting at 12 hpf in the anterior lateral plate mesoderm (ALPM) of zebrafish (Bennett *et al.* 2001; Herbomel *et al.* 1999; Warga *et al.* 2009). In the zebrafish, primitive macrophages almost immediately begin migrating over the yolk sac and spreading throughout the embryos. Transcriptional regulation of myeloid development is conserved between humans and zebrafish. Zebrafish myeloid cells express *spi1* (Herbomel *et al.* 1999; Herbomel and Levraud 2005; Le Guyader *et al.* 2008; Mathias *et al.* 2009), *lysozyme (lyz)* (Hall *et al.* 2007; Liu F and Wen 2002), and *myeloperoxidase (mpx)* (Bennett *et al.* 2001, Lieschke *et al.* 2001). All of these key myeloid genes perform analogous roles to their mammalian counterparts. Whereas *lcp1* and *lyz* were previously considered to specify monocytic and granulocytic differentiation, respectively, subsequent data has revealed that these genes show a pan-myeloid expression pattern in zebrafish embryos and may continue to mark progenitor cells through 48 hpf (Hall *et al.* 2007; Le Guyader *et al.* 2008). Primitive macrophages differentiate directly from mesenchymal progenitor cells (Hume 2006), since the multipotent haematopoietic stem cells (HSCs) do not arise until day E10 in mice (Boisset *et al.* 2010) and 24-36 hours in zebrafish (Bertrand *et al.* 2008; Bertrand *et al.* 2010).

Following these primitive waves, the first wave of definitive haematopoiesis occurs between 24 to 32 hpf in the posterior blood island (PBI) (**Figure 1.5**), with the emergence of dual-potential erythro-myeloid progenitor (EMP), which are marked in their undifferentiated state by combined expression of *gata1a* and *LIM domain only 2 (lmo2)* (Bertrand *et al.* 2007). This wave of haematopoiesis gives rise to a new crop of erythrocytes and multiple myeloid lineages. EMPs produce macrophages, neutrophils, and have recently been shown to produce early mast cells (expressing *cpa5*) (Da'as *et al.* 2012). Finally, definitive haematopoietic stem cells (HSCs), which can give rise to all haematopoietic lineages, are produced starting around 24 to 36hpf and uniquely express *integrin, alpha 2b (platelet glycoprotein IIb of IIb/IIIa complex, antigen CD41B (itga2b), v-myb myeloblastosis viral oncogene homologue (avian) (c-myb), and runx1*. HSCs arise directly from *kdrl/flk1a*-expressing haemogenic endothelium in the ventral wall of the dorsal aorta (Bertrand *et al.* 2010; Kissa and Herbomel 2010), and this region is

equivalent to the aorta-gonad-mesonephros (AGM) region in mammals. HSCs then migrate to the caudal haematopoietic tissue (CHT) where they seed and divide giving rise to all lineages of adult blood cells. Eventually, HSCs migrate to their final residence in the kidney and thymus, which are the adult organs of haematopoiesis in zebrafish.

1.4.2 Antagonistic Relationship Between SPI1 And GATA1

GATA1 encodes a zinc finger transcription factor that specifies erythroid cell fate. By contrast, *SPI1* is an ETS family transcription factor that is responsible for specifying myeloid cell fate (Anderson KL *et al.* 1998; McKercher *et al.* 1996; Scott *et al.* 1994; Zhang DE *et al.* 1996). *GATA1* and *SPI1* proteins physically interact to inhibit transcription of target genes, and therefore compete to specify erythroid or myeloid cell fate, respectively (Nerlov *et al.* 2000; Rekhtman *et al.* 1999; Stopka *et al.* 2005; Zhang P *et al.* 1999; Zhang P *et al.* 2000). Overexpressing *GATA1* in mammalian myeloid cells inhibits myeloid differentiation, and induces a switch to megakaryocyte-erythroid cell fate (Iwasaki H *et al.* 2003). Zebrafish also exhibit the classic antagonism between *SPI1* and *GATA1* transcription factors. Zebrafish *vlad tepes* (*vlt^{m651}; gata1a^{-/-}*) mutant and *gata1a*-morphant embryos display reduced numbers of erythrocytes, and expanded populations of granulocytic neutrophils and macrophages (Galloway *et al.* 2005; Lyons *et al.* 2002; Rhodes *et al.* 2005) indicating that *gata1a* represses myeloid differentiation. In fact, the absence of *gata1a* permits these expanded myeloid populations to encroach into the posterior ICM. In a reciprocal fashion, *spi1*-morphant zebrafish embryos exhibit ectopic *gata1a* expression in the ALPM (Rhodes *et al.* 2005).

1.4.3 Transgenic Zebrafish Tools For Studying Myelopoiesis

Unfortunately, cross-reactive antibodies to zebrafish proteins are lacking. This limitation means that the detailed lineage and differentiation status analysis of haematopoiesis, so elegantly understood in the murine system, is currently challenging to undertake in the zebrafish. Thus a major endeavour has been the generation of transgenic tools for analysis of the haematopoietic system, which has brought a much broader

understanding of myeloid lineage development in zebrafish. A summary of transgenic lines and markers for myeloid populations is shown in **Figure 1.2**.

The first transgenics for early myeloid cells expressed *enhanced green fluorescent protein (EGFP)* from the major myeloid transcription factor, *spi1* (Hsu *et al.* 2004), and my supervisor, Dr. Jason Berman, participated in its development. Zebrafish harbouring *Tg(spi1::EGFP)* display GFP in primitive myeloid cells, first visible at 12 hours post fertilization (hpf) in the ALPM, and can be traced over the ensuing 12 hours as they migrate. New GFP production is then observed in definitive myeloid cells around 24 hpf in the PBI. The expression of zebrafish *spi1* does get downregulated around 2 days post-fertilization (dpf) (Ward *et al.* 2003; Hsu *et al.* 2004), but is renewed again in adult haematopoietic tissues. These experiments suggested the *spi1* promoter was a good candidate for use in developing a transgenic line to study AML, particularly because it provided opportunity for development of myeloid disease later in the animal's life.

To visualize neutrophil granulocytes later in development, various laboratories have generated several transgenic lines. These include the *Tg(lyz::dsRed)* and *Tg(lyz::EGFP)* lines (Hall *et al.* 2007) as well as *Tg(mpx::EGFP)* (Renshaw *et al.* 2006; Mathias *et al.* 2009) and *Tg(myd88::EGFP)* (Hall *et al.* 2009) (*myd88* = *myeloid differentiation primary response gene 88*). While all of these lines label predominantly neutrophil granulocytes, it is notable that the overlap in expression of the endogenous transcripts (by whole-mount *in situ* hybridization [WISH]) or protein (by antibody) as well as the reporter gene expression between transgenic lines is not fully concordant, suggesting that subtly different populations are labelled by each depending on the developmental time point of evaluation (Hall *et al.* 2007; Le Guyader *et al.* 2008).

Some of these subtleties in gene and protein expression have been addressed. Specifically, in some early studies, *lcp1* has been suggested to mark monocyte/macrophage lineage cells, but there is clear evidence that this protein is expressed (as in mammals) in all leukocytes (Le Guyader *et al.* 2008). The *Tg(lyz::EGFP)* fish expresses GFP from 22 hpf, initially in primitive macrophages arising from the ALPM. Expression of GFP increases and is notable in the CHT (likely labelling differentiating definitive myeloid cells) and the developing brain and retina (more likely to represent the on-going expression in a proportion of macrophages).

To clarify precisely which cells express the EGFP from the *Tg(lyz::EGFP)* transgene, Hall *et al.* performed anti-GFP staining along with fluorescent WISH for *mpx*, *lcp1*, and *colony stimulating factor 1 receptor (csf1r)*. Dual staining was observed for GFP with each of these myeloid transcripts, however there were some *Tg(lyz::EGFP)*-expressing cells that did not express *mpx*, some *csf1r*-expressing cells that did not express *Tg(lyz::EGFP)* and some *lcp1*-expressing cells that did not express *Tg(lyz::EGFP)*. Thus the *Tg(lyz::EGFP)* marks primitive macrophages and a majority of granulocytes, but does not label all *mpx* positive granulocytes or all *csf1r* expressing macrophages (Hall *et al.* 2007). It is possible that these subtleties may give us more detailed information about myeloid subpopulations, such as their stage of differentiation. More recently, transgenic lines using the *macrophage expressed gene 1 (mpeg1)* or *csf1r* promoters (Ellett *et al.* 2011; Gray *et al.* 2011) have been used to distinguish monocytic from granulocytic populations, further enhancing studies of the innate immune system. However, *csf1r* reporter animals exhibit expression in xanthophores as well as macrophages. By contrast, the *mpeg1* promoter appears exclusive to macrophages. The *major histocompatibility complex class II DAB gene (mhc2dab)* promoter was isolated to further delineate the expression pattern of macrophages and other mononuclear phagocytes in adult fish. In combination with *Tg(ptprc::dsRed)* (*ptprc* = *protein tyrosine phosphatase, receptor type, C* [also known as *cd45 antigen*]), which labels all leukocytes except B cells), the *Tg(mhc2dab::EGFP)* transgenic line has now allowed identification of macrophages and dendritic cells, as well as B lymphocytes in adult zebrafish tissues (Wittamer *et al.* 2011).

Several recent studies have also delineated additional granulocytic subpopulations. Zebrafish mast cells can be identified by expression of the *cpa5* transcript. Like their mammalian counterparts, zebrafish mast cells stain positively for Toluidine blue, express mast cell-specific proteins, such as tryptase and kit/cd117 (Dobson *et al.* 2008). Zebrafish mast cells also express Toll-like receptor (TLR) pathway components, as evidenced by co-expression of *cpa5* and *EGFP* in the *Tg(myd88::EGFP)* line (Da'as *et al.* 2011). These cells have also been isolated post-fixation by flow cytometry of Fast Red-stained WISH for *cpa5* (Dobson *et al.* 2009). The distinction of zebrafish mast cells from zebrafish eosinophils has also been addressed using a *Tg(gata2a::EGFP)* fish line. This study confirmed the presence of, and described in

detail the characteristics of zebrafish eosinophils. In adult *Tg(gata2a::EGFP)* fish, eosinophils express high levels of GFP and have high forward scatter (FSC) and side scatter (SSC) characteristics by flow cytometry. These cells were also demonstrated to be functionally orthologous to human eosinophils (Balla *et al.* 2010).

As well as facilitating assessment of the ontogeny and spectrum of zebrafish haematopoietic and immune systems, the utility of this array of transgenic animals extends to more functional analysis of zebrafish haematopoiesis, which will be particularly useful in zebrafish disease models. Once again utilizing cell sorting by flow cytometry, Stachura *et al.* have established an assay system by which to assess the clonogenic myelo-erythroid capability of subpopulations of haematopoietic cells (Stachura *et al.* 2011). This recent study utilized traditional clonogenic techniques, commonly used for mammalian haematopoietic cell analysis in methylcellulose, facilitated by recombinant zebrafish growth factors, erythropoietin (epo) and granulocyte colony-stimulating factor (g-csf/csf3) and serum derived from carp. Such studies are in their infancy but should lead the way to further capability to assess clonogenic and lineage potential of zebrafish blood precursors. Critically, this will allow more detailed biological analysis of haematopoietic populations, which are currently lacking.

1.5 THE *HOX* FAMILY OF DEVELOPMENTAL TRANSCRIPTION FACTORS & THE *CDX-HOX* NETWORK IN BLOOD DEVELOPMENT

In animals, from flies to humans, mutations that affect *HOX* gene expression or activity give rise to defects in anterior-posterior patterning, such as homeotic transformation of body segment identity (*i.e.* legs in place of eyes). Mammalian *HOX* genes, especially those expressed in the posterior of the developing embryo (*HOXB7*, *HOXA9*, *HOXA10*, *HOXD9*) are essential for normal haematopoiesis (Kawagoe *et al.* 1999; Lawrence *et al.* 1997; Lawrence *et al.* 2005) and have been implicated in acute myeloid leukaemia (AML) pathogenesis (Golub *et al.* 1999; Kroon *et al.* 1998; Kroon *et al.* 2001; Nakamura *et al.* 1996a; Pineault *et al.* 2003; Slape and Aplan 2004).

The DNA-binding specificity of mammalian *HOX* proteins is achieved through its interaction with other DNA-binding co-factors. Such co-factors include the Three Amino acid Loop Extension (TALE)-class homeodomain transcription factors, PBX and MEIS1,

which form heterodimeric and heterotrimeric protein complexes with HOXB7, HOXA9, HOXA10 and HOXD9 to regulate DNA-binding affinity and specificity (Chang *et al.* 1995; Chang *et al.* 1997; Ebner *et al.* 2005; Knoepfler *et al.* 1996; Mann *et al.* 2009; Sarno *et al.* 2005; Shen *et al.* 1999). Together, these trimeric HOX complexes can act as transcriptional activators (Bei *et al.* 2005) or transcriptional repressors (Kasper *et al.* 1999; Mann *et al.* 2009), because MEIS1 can control the availability of histone deacetylase complexes (HDACs) and cyclic AMP response element-binding (CREB)-binding protein (CREBBP) at HOX-regulated promoters (Choe *et al.* 2009).

In vertebrates, PBX and MEIS1 proteins also bind together in the absence of HOX proteins (Chang *et al.* 1997; Rieckhof *et al.* 1997), and even in the absence of DNA (Knoepfler *et al.* 1996). For example, human MEIS1 normally localizes to the cytoplasm, but PBX-MEIS1 complexes are actively transported into the nucleus (Abu-Shaar *et al.* 1999; Jaw *et al.* 2000; Mercader *et al.* 1999). MEIS1 and PBX proteins also stabilize each other (Stevens and Mann 2007), which is dependent upon conserved N-terminal motifs (MH domain of MEIS1, and PBC domains of PBX4) (Longobardi and Blasi 2003; Waskiewicz *et al.* 2001). Overexpressing zebrafish *pbx4* generates a post-transcriptional increase in *meis1* protein levels, and vice versa (Waskiewicz *et al.* 2001), and *pbx* is required for nuclear import of *meis1* *in vivo* (Pillay *et al.* 2010).

There are 39 *Hox* genes in mice and 47 identified *hox* homologues in zebrafish – the greater number in fish is due, in part, to whole genome duplication that occurred in teleost evolution (Amores *et al.* 1998). Zebrafish possess two *HOXA9* homologues, *hoxa9a* and *hoxa9b*, with *hoxa9a* possessing the conserved role in haematopoiesis. The co-factors, *meis1*, *pbx2*, and *pbx4* are similarly conserved in zebrafish (Pillay *et al.* 2010; Waskiewicz *et al.* 2001). The regulation of anterior-posterior segment identity by HOX proteins and their co-factors programs undifferentiated cells in the early embryo to adopt a specialized fate. It is therefore important to understand the role of these factors in normal haematopoiesis, and how transcriptional dysregulation leads to pathogenesis.

1.5.1 Homeobox Transcription Factors In Zebrafish Haematopoiesis

Mouse studies highlight the role of mammalian *HOX* factors as master regulators of haematopoietic cell fate decisions (Abramovich *et al.* 2005). Overexpression of

posterior *Hox* genes in the mouse induces hyperproliferation of haematopoietic stem cells (HSCs) and predominant myelopoiesis, culminating in acute myeloid leukaemia (AML). Targeted deletions have also been made to several mouse *Hox* genes, including *Hoxb3*, *Hoxb4*, *Hoxb6*, *Hoxa7*, *Hoxc8*, and *Hoxa9*, respectively, which possess defects in the development of blood cells, and an inability of HSCs to repopulate blood lineages (Bjornsson *et al.* 2003; Brun *et al.* 2004; Izon *et al.* 1998; Kappen 2000; Ko *et al.* 2007; Lawrence *et al.* 1997; Magnusson *et al.* 2007; Shimamoto *et al.* 1999; So *et al.* 2004). Mammalian HOX proteins perform overlapping functions in haematopoiesis, which can be seen by the fact that triple mutant mice lacking *Hoxb3*, *Hoxb4*, and *Hoxa9* display more severe defects than single mutant mice lacking *Hoxa9* alone.

Functional redundancy (Amores *et al.* 1998) has made global analysis of HOX gene function challenging, especially *in vivo*, but was achieved in zebrafish *kugleig* (*kgg^{tv205}*) mutants harbouring a null mutation in *caudal type homeobox transcription factor 4* (*cdx4*). Mouse and zebrafish studies stress the critical importance of a CDX-HOX signalling axis in haematopoiesis, which may also occupy a central role in AML pathogenesis (Bansal *et al.* 2006; Davidson *et al.* 2003; Davidson and Zon 2006; Frohling *et al.* 2007; Koo *et al.* 2010; Magnusson *et al.* 2007). *CDX4* controls HOX expression, and ectopic expression of mouse *Cdx4* dysregulates a host of *Hox* factors involved in adult mouse haematopoiesis (Frohling *et al.* 2007; Bansal *et al.* 2006). Zebrafish *kgg^{tv205}* (*cdx4^{-/-}*) mutants downregulate *hoxb6b*, *hoxb7a*, *hoxb8b*, and *hoxa9a*, which inhibits HSC formation (Davidson *et al.* 2003; Davidson and Zon 2006; Shimizu *et al.* 2006). Mutant *kgg^{tv205}* embryos also show severe defects in primitive haematopoiesis, such as loss of *gata1a* and *hbae3* erythroid expression. Overexpressing *hoxb7a* or *hoxa9a* partially rescues *gata1a* expression in *kgg^{tv205}* mutant embryos (Davidson and Zon 2006), indicating that these posteriorly expressed *hox* genes act with *cdx* upstream of *gata1a* to regulate erythropoiesis.

In mice, the Hox co-factors, *Pbx* and *Meis1*, have an important role in embryonic haematopoiesis (Di Rosa *et al.* 2007). *Pbx1*-knockout mice display a lethal reduction in definitive multi-potent blood progenitors, leading to severe embryonic anemia (DiMartino *et al.* 2001). *Meis1*-deficient mice display a severe reduction in myelo-erythroid colony-forming cells (likely common myeloid progenitors CMPs) (Azcoitia *et al.* 2005; Hisa *et*

al. 2004). Similar to the loss of *cdx*, zebrafish embryos lacking the hox co-factors, *pbx* and *meis1*, also display phenotypes that are consistent with a total lack of zebrafish *hox* function. For example, embryos that have severe knockdown in the zebrafish *pbx* genes demonstrate hindbrains in which rhombomeres 2-6 take on the identity of rhombomere 1 (Erickson *et al.* 2007; Maves *et al.* 2007; Popperl *et al.* 2000; Waskiewicz *et al.* 2002). A nearly identical phenotype results from gene knockdown of *hoxa1*, *hoxb1*, and *hoxd1* in *Xenopus* (McNulty *et al.* 2005). During primitive haematopoiesis, zebrafish *pbx2*, *pbx4*, and *meis1* are expressed in the posterior lateral-plate mesoderm (PLPM) and intermediate cell mass (ICM) (Maves *et al.* 2007; Minehata *et al.* 2008; Popperl *et al.* 2000; Waskiewicz *et al.* 2002). Embryos that lack either *pbx* or *meis1* show similar anemia and decreased *gata1a* and *hbae3* erythroid gene expression in the bilateral stripes of the PLPM (Pillay *et al.* 2010), and the combined loss of *pbx* and *meis1* together produces a more severe defect. Zebrafish studies strongly suggest that the posterior hox proteins, *hoxa9a* and *hoxb7a*, require the *meis1* co-factor to activate *gata1a* erythroid gene expression (Davidson and Zon 2006; Pillay *et al.* 2010). This is similar to evidence in mammals that MEIS1 binds posterior HOX proteins, such as HOXA10 (Shanmugam *et al.* 1999), and this pair directly binds the GATA1 promoter (Magnusson *et al.* 2007). These findings are consistent with a positive role for HOX and MEIS1 proteins in haematopoiesis.

1.6 THE POTENTIAL OF ZEBRAFISH FOR AML RESEARCH

Zebrafish are being used more and more to study the molecular mechanisms of cancer. Human and mouse oncogenes, or mutations to zebrafish tumour-suppressor genes are being introduced into the fish from early embryonic stages to investigate primary gene collaborators and the stepwise progression to acute transformation, which is a difficult undertaking in traditional mouse models. The establishment of a clinically-identifiable tumour has historically been a desired goal in the zebrafish cancer community. However, the focus on zebrafish as a valuable research tool seems has gained greater favour in recent years. In this sense, many important findings into the underlying mechanisms of transformation have come from work at the embryonic and larval stages, regardless of whether disease phenotypes are observed in adult fish.

The chief advantage of this focus on reproducible defects in the early zebrafish embryo is the ability to then leverage these phenotypes to perform high-throughput genetic and chemical modifier screens. Screens are prohibitively expensive and time-consuming in traditional mouse models, but can be accomplished relatively easily using zebrafish embryos, sometimes within the timespan of a few months.

1.6.1 Genetic & Chemical Modifier Screens In Zebrafish

Zebrafish have an advantage over *Drosophila* and *C. elegans* in their status as vertebrates, with extra-uterine fertilization providing simplicity in the observation and manipulation of embryonic processes not easily performed in mammals (Streisinger *et al.* 1981; Detrich *et al.* 1999). Furthermore, studies in zebrafish – as a cost-effective *in vivo* model – complement research in cell lines and mouse models because of the facility with which genetic and chemical modifier screens can be performed.

Indeed, the foundation for conducting research using zebrafish (as a faithful model of haematopoietic development) was established in some of the first forward genetic screens. These large-scale mutagenesis screens identified a number of mutant lines with bloodless phenotypes – with such colourful names as *riesling*, *merlot*, *cabernet*, and *shiraz* (Ransom *et al.* 1996). Many of these, including *kugleig* (*kgg^{lv205}*; *cdx4^{-/-}*) (Davidson *et al.* 2003; Davidson and Zon 2006; de Jong *et al.* 2010), *moonshine* (*mon^{tg234}*; *trim33/tif1^{-/-}*) (Bai *et al.* 2010; Monteiro *et al.* 2011; Ransom *et al.* 2004), *cloche* (*clo^{m39}*; gene candidate *lycat*) (Stainier *et al.* 1995; Dooley *et al.* 2005; Liang *et al.* 2012), and *vlad tepes* (*vlt^{m651}*; *gata1a^{-/-}*) (Lyons *et al.* 2002), have contributed greatly to our understanding of transcription factor networks in vertebrate haematopoiesis, including posteriorly-expressed *HOX* genes and their master regulator *CDX*.

Frazer *et al.* demonstrated the feasibility of using zebrafish in a phenotype-driven forward genetic screen for lymphoid leukaemia (Frazer *et al.* 2009). The group induced point mutations in a transgenic line that expresses GFP from the *rag2* early lymphocyte promoter. Several mutant fish lines with clonal and heritable predisposition to T-cell malignancies emerged, although the specific genetic alterations were not identified. Rudner *et al.* subsequently used these fish lines as well as the original *Myc*-induced T-ALL model to perform array comparative genomic hybridization (aCGH) (Rudner *et al.*

2011). They showed that zebrafish and human T-ALL have a similar gene expression signature, highlighting the conservation of molecular processes that produce leukaemia.

The first drug discovery screen in zebrafish identified effective compounds that restored normal vascular development in a zebrafish model of aortic coarctation (Peterson *et al.* 2004), while subsequent screens have identified behaviour modifying neurochemicals (Kokel *et al.* 2010) and novel retinoic acid (RA)-like compounds affecting embryogenesis (Das *et al.* 2010). Moreover, two recent chemical screens (North *et al.* 2007; Yeh *et al.* 2009) both identified PTGS/COX (prostaglandin-endoperoxide synthase (prostaglandin G/H synthase and cyclooxygenase) inhibitors, such as Indomethacin (Indo) and NS-398, as pharmacological modifiers of haematopoietic differentiation. These studies highlight the power of zebrafish as *in vivo* tool for rapid discovery of genetic collaborators and chemical modifiers of haematopoiesis, and therefore leukaemogenesis, through the leveraging of robust embryonic phenotypes.

1.7 THE T(7;11P15;P15) NUP98-HOXA9 MUTATION IN AML

The overexpression of *HOXA9* in human AML can be the result of *MLL*-rearrangements (Golub *et al.* 1999), or can occur as part of the t(7;11)(p15;p15) translocation, yielding the *NUP98-HOXA9* (*NHA9*) fusion oncogene (Table 1.1). This abnormality fuses the 5' region of *nucleoporin 98 kiloDalton* (*NUP98*) on chromosome 11p15 in frame to the 3' coding sequence of *HOXA9* on chromosome 7p15 (Borrow *et al.* 1996; Nakamura *et al.* 1996b) (Figure 1.6). The expression of *HOXA9* is tightly regulated in space and time during embryo, tissue, and cell development, but the *NHA9* fusion event links the *HOXA9* gene to the ubiquitously-active *NUP98* promoter (the function of *NUP98* protein is described below). In effect, this leads to the overexpression of *HOXA9*. In humans, the *NHA9* translocation is a rare, but recurrent event (as high as 2% of all cases [Chou WC *et al.* 2009]). *NHA9* confers inferior prognosis for affected patients with *de novo* and treatment-related AML, and in myelodysplastic syndrome (MDS) (Moore MA *et al.* 2007), and results in progression of chronic myelogenous leukaemia (CML) to blast crisis (Ahuja *et al.* 2001; Dash *et al.* 2002). In humans, *NHA9* alone has long latent transforming activity, and often first presents as MDS (Hatano *et al.* 1999). In blast crisis CML, *NHA9* induces terminal differentiation arrest, which

cooperates with clonal hyperplasia induced by the fusion oncogene, *BCR-ABL1* (the product of the t[9;22][q34;q11] translocation) (Dash *et al.* 2002; Mayotte *et al.* 2002) (Table 1.1). Given the central role of *HOXA9* in mammalian haematopoiesis and leukaemogenesis, as well as its overexpression resulting from the *NHA9* fusion event, elucidating the activity of *NHA9* has the potential to reveal universal mechanisms of AML leukaemogenesis.

1.7.1 *NHA9* Versus *HOXA9* In AML

In mammals, *HOXA9* functions both as a transcriptional activator (Bei *et al.* 2005) and repressor (Kasper *et al.* 1999) in the maintenance of haematopoietic stem cells and other blood precursors. The *NHA9* fusion event eliminates the N-terminal domain of human *HOXA9*, which eliminates transcriptional repression activity (Kasper *et al.* 1999). Furthermore, phenylalanine-glycine (FG)-rich domains on the human NUP98 peptide promote the interaction of *NHA9* with chromatin remodeling proteins, such as cyclic AMP response element-binding (CREB)-binding protein (CREBBP) and E1A binding protein p300 (EP300) (see Figure 1.6). This has led to the suggestion that whereas the native human *HOXA9* protein does perform transcriptional repression, the *NHA9* fusion oncoprotein functions predominantly as a transcriptional activator. In its native form, human NUP98 protein is a member of the nuclear pore complex (NPC) and functions in transportation of mRNA out of the nucleus (Griffis *et al.* 2004). However, NUP98 protein also associates with nuclear bodies that are transcriptionally active, and binding to RNA polymerase II is dependent on various domains in the N-terminus of NUP98. This may help to explain the unique transcriptional activity of *NHA9* compared to native human *HOXA9*. Recently, an abstract suggested that native zebrafish *nup98* plays a role in haematopoiesis, and that injection of *nup98* MO into zebrafish embryos leads to upregulated *spi1* and *tall/scl* (Fung *et al.* 2010). However, a detailed analysis of the mechanism by which zebrafish *nup98* contributes to haematopoiesis was not provided.

In primary mouse bone marrow, overexpression of the native mouse *Hoxa9* gene alone immortalized a late myelomonocyte progenitor cell *in vitro*, which then failed to undergo terminal differentiation to granulocytes or monocytes in the presence of granulocyte-monocyte colony-stimulating factor (GM-CSF/CSF2) or interleukin 3 (IL-3),

respectively (Calvo *et al.* 2000). This finding is in keeping with a plethora of evidence in the last decade, using multiple oncogenes, that postulates the cell-of-origin in AML (or leukaemia-initiating cell [LIC]) as a lineage-committed progenitor cell (Cozzio *et al.* 2003; Guibal *et al.* 2009; Huntly *et al.* 2004; Jamieson *et al.* 2004; Krivtsov *et al.* 2006; Minami *et al.* 2008; Muller-Tidow *et al.* 2004; Neering *et al.* 2007; Wang Y *et al.* 2010; Wojiski *et al.* 2009). Mouse bone marrow transformed by overexpression of mouse *Hoxa9* does retain the ability to differentiate. These *Hoxa9*-transformed mouse cells respond to granulocyte CSF (G-CSF/CSF3) to form neutrophils, macrophage CSF (M-CSF/CSF1) to form macrophages, and ATRA to form either monocytic or mixed monocytic and neutrophilic populations. These phenotypes in *Hoxa9*-transformed mouse cells do not require the co-overexpression of native mouse *Meis1*, and can even be achieved using a truncated *Hoxa9* coding sequence after deletion of the ANWL Pbx-interaction motif (Calvo *et al.* 2000). This suggests that *Hoxa9* alone is capable of transforming cells *in vitro*.

However, in bone marrow reconstitution experiments into live mice, only the co-overexpression of native *Hoxa9* and *Meis1* mouse genes can generate overt AML (*i.e.* appearance of AML blast cells and/or 25% myeloblasts in marrow). In mice, overexpression of mouse *Meis1* alone does not cause disease, and overexpression of mouse *Hoxa9* alone only rarely produces AML after an 8 month latency (Iwasaki M *et al.* 2005; Kroon *et al.* 1998; Kroon *et al.* 2001; Thorsteinsdottir *et al.* 2001). This either highlights independent contributions from *Meis1*, or a dosage effect where overexpression of *Meis1* bolsters the molecular changes begun by *Hoxa9*. Indeed, mouse bone marrow transformed with *Hoxa9* alone exhibited cell death in the presence of stem cell factor (SCF), but co-overexpression of *Meis1* allowed the mouse cells to proliferate in response to SCF (Calvo *et al.* 2001). Furthermore, mouse bone marrow that has been co-transformed with mouse *Hoxa9;Meis1* became refractory to granulocytic differentiation by G-CSF/CSF3. It is interesting that overexpression of mouse *Hoxa9* does not upregulate endogenous *Meis1* mRNA transcripts in the mouse (Calvo *et al.* 2000), given that the majority of human AML shows upregulation of both *HOXA9* and *MEIS1* (Golub *et al.* 1999). These findings suggest that the expression of *MEIS1* may be controlled separately and has unique contributions to the formation of *HOXA9*-induced

myeloid disease. This is supported by the role of MEIS proteins in controlling the availability of HDACs and CREBBP at HOX-regulated promoters (Choe *et al.* 2009).

The mouse bone marrow cell phenotypes using expression of the human *NHA9* fusion oncogene were similar to the co-overexpression of native mouse *Hoxa9* and *Meis1* (Calvo *et al.* 2001). *NHA9*-transformed mouse bone marrow immortalized myeloid progenitors and prevented differentiation in response to GM-CSF/CSF2, IL-3, and G-CSF/CSF3 (Calvo *et al.* 2002). *NHA9* permitted proliferation in SCF, the ligand for KIT receptor, which is a receptor expressed on all HSCs and early progenitors, and typically lost upon lineage differentiation (Edling and Hallberg 2007). *NHA9* also upregulated the endogenous *Hoxa7*, *Hoxa9*, *Hoxa10*, and *Meis1* transcripts in the mouse (Calvo *et al.* 2002). It is interesting that human *NHA9* was able to immortalize cells in *Hoxa9*^{-/-} mutant mouse bone marrow, because it suggests that *NHA9* is a dominant mutation that replaces native *Hoxa9*.

In mice, overexpression of human *NHA9* produces disease, but passes through a longer latency phase than co-overexpression of mouse *Hoxa9* and *Meis1*. Another distinct feature of *NHA9*-transformed mice is that they show an initial presentation of a myeloproliferative neoplasm (MPN), a pre-leukaemia condition characterized by increased numbers of myeloid cells that have mature or semi-mature morphologies (*i.e.* they do not resemble AML blast cells). Both retrovirally-transduced and germline transgenic *NHA9* mice develop MPN as late as 8 to 15 months, which progressed to overt AML following a latency period of at least 4 months (Kroon *et al.* 2001; Iwasaki M *et al.* 2005). Co-overexpression of mouse *Meis1* with human *NHA9* in transgenic mice accelerates the onset of overt AML, but maintains the MPN latent stage with roughly the same timing as *NHA9* alone (Kroon *et al.* 2001).

1.8 RATIONALE OF STUDIES & HYPOTHESES

We wanted to enlist the advantages of the zebrafish to address our research goal of improving survival for high-risk forms of human AML. Specifically, research efforts that can identify new contributing genes and molecular pathways will enable the development of less toxic drug therapies that selectively target the specific abnormality in a leukaemia cell. These approaches have already been successful in significantly

improving the outcome in some subtypes of leukaemia including imatinib mesylate (IM; Gleevec®) in CML, as well as ATRA and As₂O₃ in APL.

As mentioned above, our research has focused on the paradigm of high-risk AML caused by *HOXA9*, which is overexpressed in 80% of human AML (Golub *et al.* 1999), including the *NHA9* translocation. We therefore endeavoured to create a stable transgenic zebrafish line that expresses the human *NHA9* mutation under the control of the 9.1 kb zebrafish *spil* myeloid promoter. Furthermore, we set out to characterize robust and reproducible phenotypes in our *NHA9* zebrafish embryos, which would enable us to interrogate genetic collaborators and chemical modifiers that impact the development of high-risk myeloid disease. As a graduate candidate for a Doctor of Philosophy (PhD) degree, I have used our *NHA9*-transgenic zebrafish to explore the following hypotheses.

In **CHAPTER 3**, I hypothesized that we could employ the advantages of the zebrafish animal model to create a model of *NHA9* myeloid leukaemogenesis, which would recapitulate critical aspects of human high-risk AML.

In **CHAPTER 4**, I used our *NHA9*-transgenic zebrafish embryos to explore defects in early haematopoiesis and cellular survival. In this chapter, I also investigated the relationship between *NHA9* and *MEIS1*, with the hypothesis that zebrafish *meis1* will impact myeloid development in zebrafish embryos, and will cooperate with *NHA9* in the causation of haematopoietic defects.

In **CHAPTER 5** and **CHAPTER 6**, I sought to leverage the haematopoiesis defect in *NHA9* embryos in order to identify novel collaborating genes and to test therapeutic agents *in vivo*.

Finally, in **CHAPTER 7**, we used an innovative xenotransplantation platform to inject human leukaemia cells into zebrafish embryos in order to characterize novel chemotherapy agents.

The zebrafish has tremendous potential to characterize gene mutations that lead to leukaemia and to identify new drugs to combat human disease. The *NHA9* zebrafish model of high-risk myeloid disease in our lab, as well as possibilities afforded by the xenotransplantation platform will help in the identification of newer, better, and safer drugs to treat AML in human cancer patients. Our lab ultimately aims to make a significant clinical impact in improving survival for both childhood and adult AML.

Table 1.1. Description of AML fusion oncogenes (in order of mention in body text).

Chromosome translocation	Fusion gene symbol	Fusion gene name	Frequency in AML
t(7;11)(p15;p15)	<i>NUP98-HOXA9</i>	<i>nucleoporin 98 kiloDalton—homeobox A9</i>	up to 2%
t(8;21)(q22;q22)	<i>AML1-ETO*</i>	<i>acute myeloid leukaemia 1—eight twenty-one*</i>	15%
inv(16)(p13;q22)	<i>CBFB-MYH11</i>	<i>core-binding factor, beta subunit—myosin, heavy chain 11, smooth muscle</i>	up to 25%
t(15;17)(q22;q21)	<i>PML-RARA</i>	<i>promyelocytic leukaemia—retinoic acid receptor alpha</i>	10%
t(9;11)(p22;q23)	<i>MLL-AF9*</i>	<i>mixed lineage leukaemia—acute lymphoid leukaemia (ALL)1-fused gene from chromosome 9*</i>	up to 10%
t(11;19)(q23;p13.3)	<i>MLL-ENL*</i>	<i>mixed lineage leukaemia—eleven nineteen leukaemia*</i>	
t(9;22)(q34;q11)	<i>BCR-ABL1</i>	<i>breakpoint cluster region—v-abl Abelson murine leukaemia viral oncogene homologue 1</i>	95% of all CML cases
inv(8)(p11;q13)	<i>MOZ-TIF2*</i>	<i>monocytic leukaemia zinc finger protein—transcriptional intermediary factor 2*</i>	rare
t(9;12)(p24;p13)	<i>TEL-JAK2</i>	<i>translocation-ETS-leukaemia—janus kinase 2</i>	rare (atypical CML)

* for official GenBank gene symbols and names, refer to **LIST OF ABBREVIATIONS**

Table 1.2. Common karyotype abnormalities in AML and their associated risk.

Risk Category	Abnormality	5-year survival	Relapse rate
Good	t(8;21), t(15;17), inv(16)	70%	33%
Intermediate	Normal, +8, +21, +22, del(7q), del(9q), abnormal 11q23, t(9;11)	48%	50%
Poor	-5, -7, del(5q), abnormal 3q, t(11;19); complex cytogenetics	15%	78%

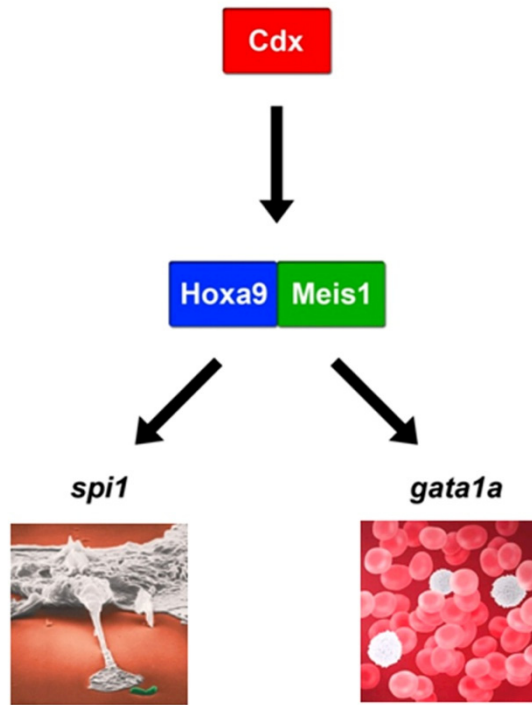
Adapted from [Fanning et al. 2009](#); [Grimwade et al. 1998](#); [Eklund, 2007](#).

Figure 1.1 (next page). Model of human *NHA9* oncogenic activity in embryonic zebrafish haematopoiesis.

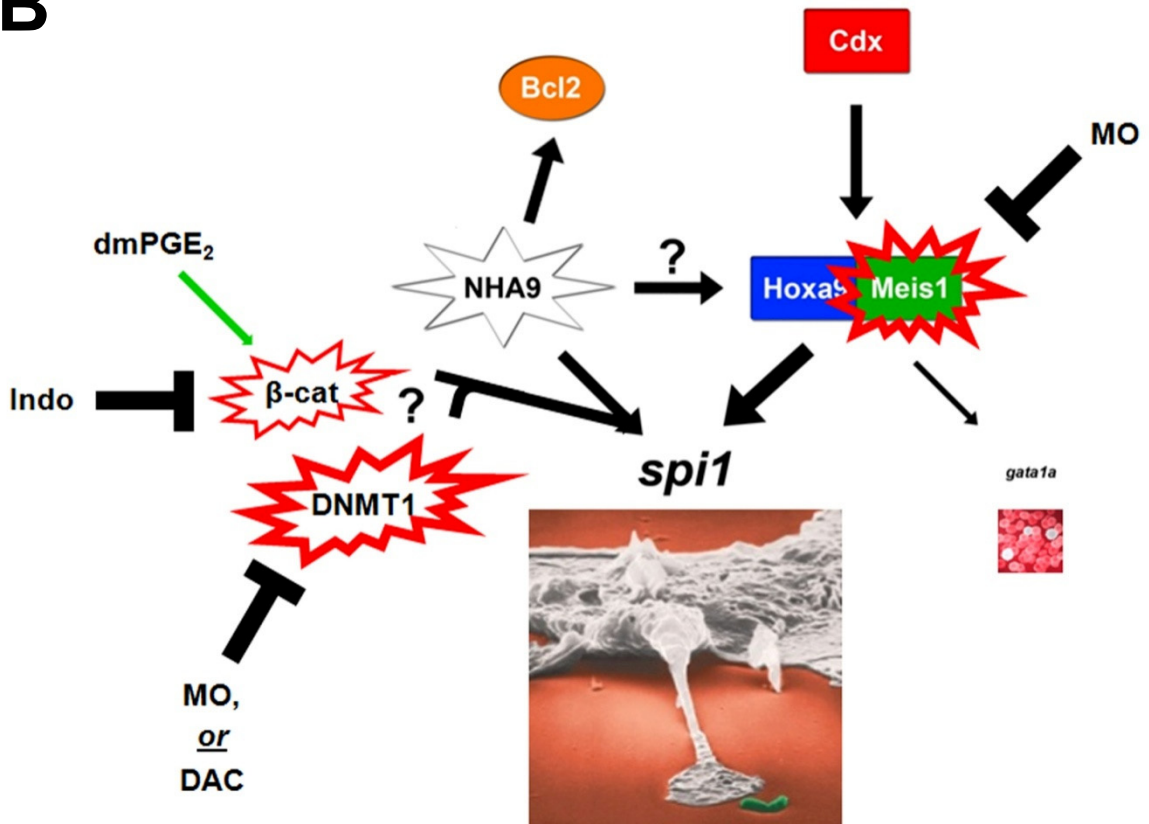
The current paradigm posits a Cdx-Hox transcriptional network in the initiation of haematopoiesis. (A) In wild-type zebrafish haematopoiesis, the *Hoxa9* protein and its cofactor, *Meis1*, regulate the balance of myeloid (*spi1*) and erythroid (*gata1a*) gene expression and fate determination. (B) The human *NHA9* fusion oncoprotein perturbs native *Hoxa9* activity in the zebrafish, especially given recruitment of CREBBP and EP300 by *NHA9*. With regards to zebrafish blood development, the human *NHA9* fusion oncoprotein may thus skew the balance towards myeloid gene expression (with partial inhibition of differentiation), at the expense of erythroid fates. The activity of human *NHA9* in embryos may be supported by activation of zebrafish factors, such as *Meis1* (inhibited by MO), DNMT1 (inhibited by MO or DAC), and/or the Wnt/ β -cat pathway (stimulated by dmPGE₂, inhibited by Indo). *NHA9* also promotes cellular survival signalling in zebrafish embryos likely through upregulation of *Bcl2*. Taken together, a burgeoned myeloid population with increased capacity for survival may ultimately lead to the development of zebrafish MPN. Representative symbols: size of font reflects relative gene expression levels, and line thickness of action bubble or arrow reflects relative contribution to activity of human *NHA9*. Adapted from Forrester *et al.* 2011.

New abbreviations used: β -cat = β -catenin; *Bcl2* = B-cell lymphoma 2; CREBBP = cyclic AMP response element-binding (CREB)-binding protein; DAC = Decitabine; dmPGE₂ = 16,16-dimethyl prostaglandin E₂; DNMT1 = DNA (Cytosine-5-)-methyltransferase 1; EP300 = E1A binding protein p300; *gata1a* = *GATA binding factor 1a*; *Hoxa9* = homeobox A9; *Meis1* = myeloid ecotropic integration site; Indo = Indomethacin; MO = morpholino oligonucleotide; *NHA9* = NUP98-HOXA9; NUP98 = nucleoporin 98 kiloDalton; *spi1* = *spleen focus forming virus (SFFV) proviral integration oncogene*.

A



B



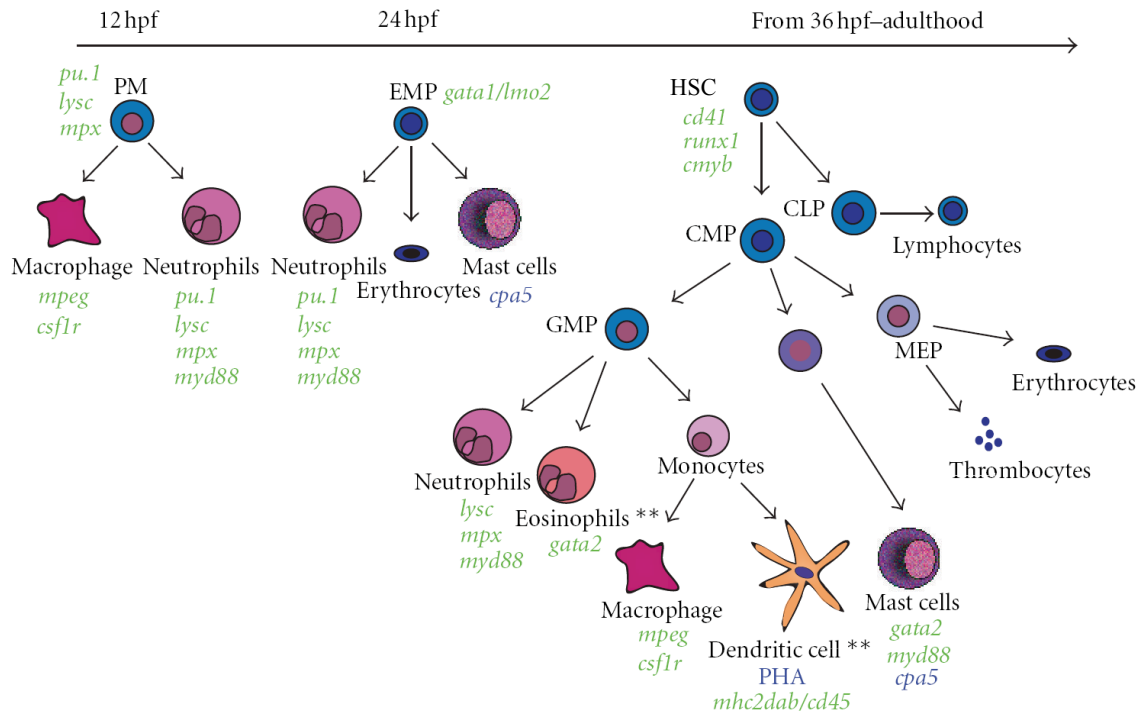


Figure 1.2. Overview of zebrafish developmental myelopoiesis and currently used transgenic lines.

Key transgenic lines and lineage identification tools labelling myeloid cell populations during developmental haematopoiesis (transgenic lines are shown in green, other specific lineage identifiers are in blue). Lineage intermediates are shown for clarity but are yet to be isolated as distinct populations in zebrafish. Representative symbols: ** = lineages only demonstrated in adult zebrafish. Excerpted from [Forrester et al. 2012](#).

New abbreviations used: CMP = common myeloid progenitor; CLP = common lymphoid progenitor; EMP = erythro-myeloid progenitor; HSC = haematopoietic stem cell; MEP = megakaryocyte/erythroid progenitor; GMP = granulocyte/monocyte progenitor; PHA = peanut haemagglutinin; PM = primitive myelopoiesis.

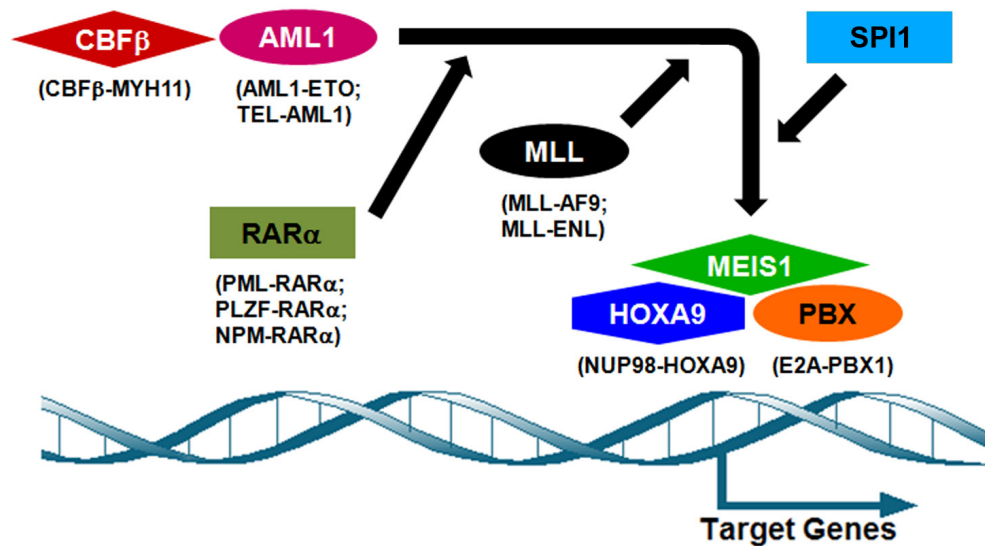


Figure 1.3. *HOXA9* is a central regulator in AML.

HOXA9 is a critical transcription factor in vertebrate haematopoiesis, and is a downstream target of several proto-oncogenes in myeloid leukaemia.

Chromosomal translocations that promote leukaemia noted in parentheses.

New abbreviations used: AML1 = acute myeloid leukaemia 1; CBFβ = core binding factor beta; MLL = mixed lineage leukaemia; PBX = pre-B-cell leukaemia homeobox; RARα = retinoic acid receptor alpha.

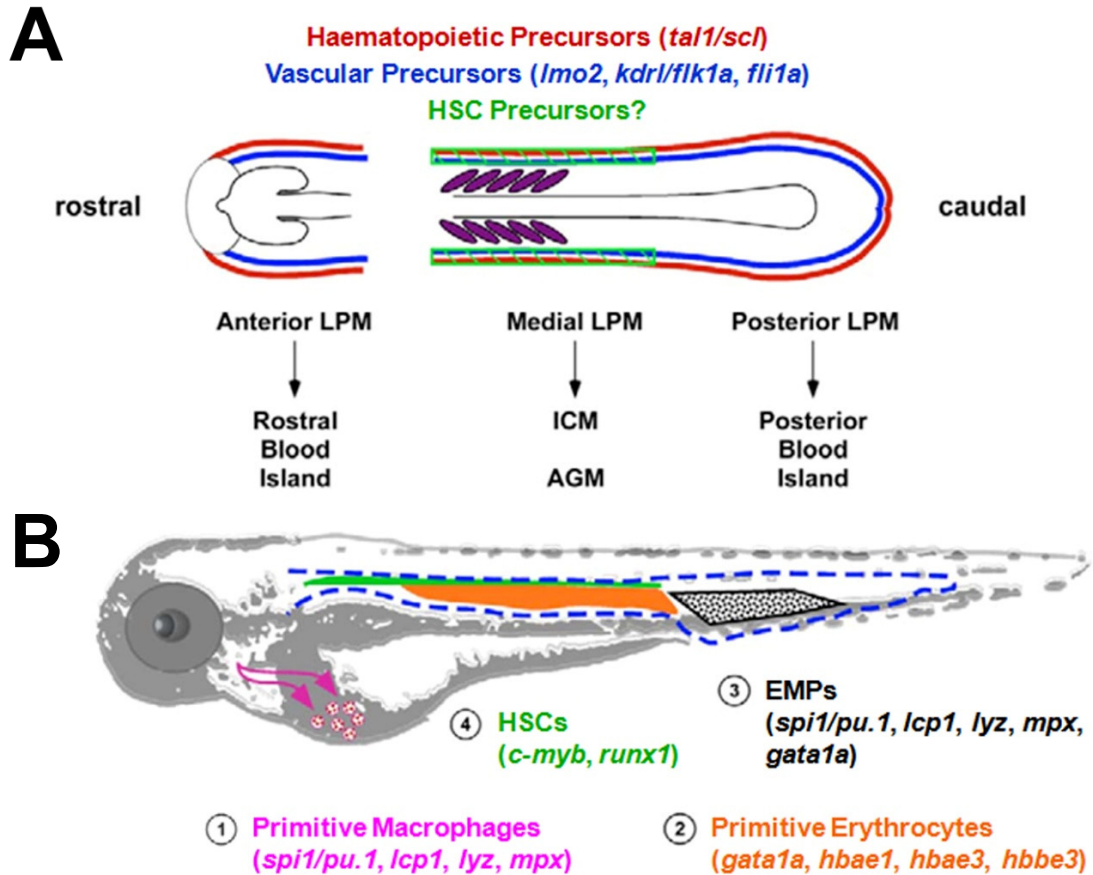


Figure 1.4. Model depicting ‘waves’ of haematopoiesis in the zebrafish embryo. Gene markers of cell populations noted in parentheses. (A) Lateral plate mesoderm (LPM) gives rise to anatomically distinct regions of blood cell precursors. Drawing depicts a flat-mount dorsal view of a five-somite-stage embryo (approximately 12 hpf). The bilateral stripes of LPM are highlighted in red (haematopoietic) and blue (vascular). (B) Embryonic haematopoiesis occurs through four independent waves of precursor production (described in text). Each wave is numbered by temporal appearance of functional cells from each subset. Adapted from [Bertrand *et al.* 2007](#).

New abbreviations used: AGM = aorta-gonad-mesonephros; ICM = intermediate cell mass; LPM = lateral plate mesoderm.

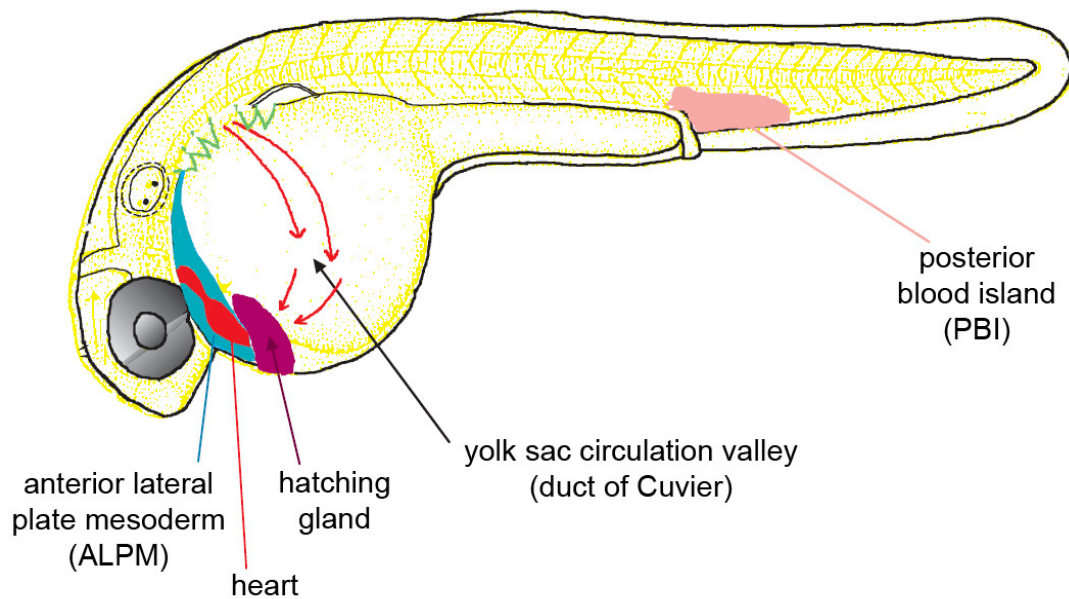


Figure 1.5. Relevant landmarks in a 28 to 30 hpf zebrafish embryo.

Lateral view showing anterior to the left. The ALPM (light blue), heart (red), hatching gland (purple) and PBI (pink) are visible. Red arrows on the yolk sac indicate venous blood flow in a depression of the yolk surface designated here as the ‘yolk sac circulation valley’ (duct of Cuvier).

Adapted from [Herbomel et al. 1999](#).

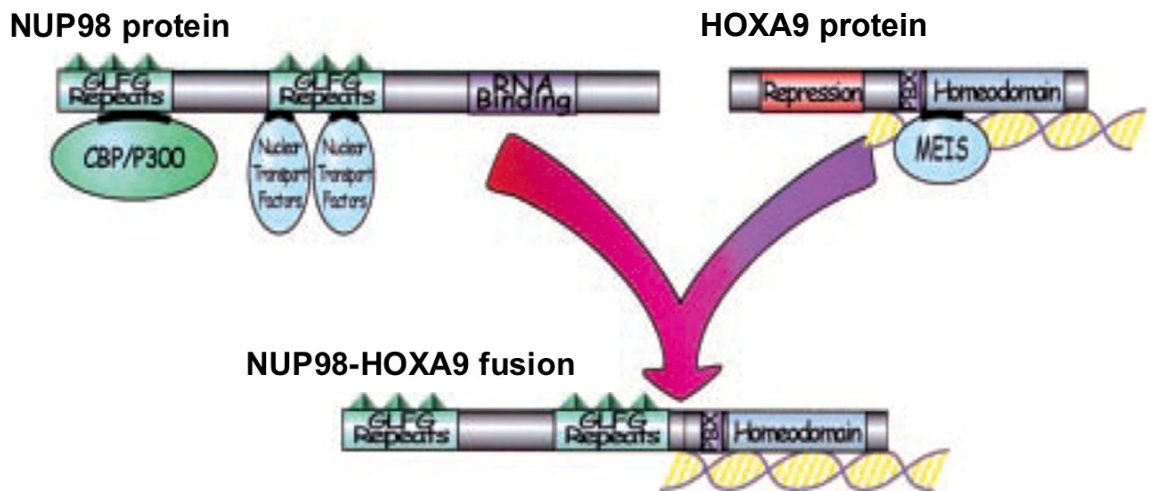


Figure 1.6. The t(7;11)(p15;p15) translocation, yielding fusion oncogene *NHA9*.
 The 5' region of *NUP98* on chromosome 11p15 is fused in frame to the 3' coding sequence of *HOXA9* on chromosome 7p15. The human *NHA9* fusion oncoprotein possesses the DNA-binding homeodomain of the *HOXA9* peptide, but lacks its N-terminal transcriptional repression domain. In fact, *HOXA9* gains novel transcriptional activation domains from the N-terminus of the *NUP98* peptide, due to its interactions with CREBBP/CBP and EP300. *NHA9* transcriptional activity is discussed in the text. Adapted from Scandura *et al.* 2002.

CHAPTER 2 MATERIALS & METHODS

2.1 ZEBRAFISH HUSBANDRY, EMBRYO COLLECTION & EMBRYO STAGING

Use of zebrafish in this study was approved by the Dalhousie University Animal Care Committee (protocol no. 11-129; see **APPENDIX D ETHICS APPROVAL**). Zebrafish were maintained according to standard protocol ([Westerfield 2000](#)). Fish were maintained at 28.5°C on a 14 hour light/10 hour dark cycle. Fish water consisted of reverse osmosis water supplemented with sodium bicarbonate (Aquatic Eco-Systems, Inc., Apopka, FL, USA) and Instant Ocean® sea salt (Spectrum Brands, Inc., Madison WI, USA) to maintain a pH of 6.8 to 7.5. Adult zebrafish were fed twice daily with cultured brine shrimp, *Artemia* spp. (INVE Aquaculture Nutrition, Salt Lake City, UT, USA). Up to 4 weeks of age, juvenile fish were fed crushed brine shrimp and Zeigler® zebrafish feed (Aquatic Eco-Systems).

Embryos were collected and grown in E3 embryo medium (5 mM NaCl, 0.17 mM KCl, 0.4 mM CaCl₂, and 0.16 mM MgSO₄, pH 7.5, supplemented with 1 x 10⁻⁵% Methylene Blue [v/v]) at 28.5°C. Embryos lacking pigmentation were obtained through incubation of living embryos in E3 medium containing 0.003% (w/v) 1-phenyl-2-thiourea (PTU; Sigma-Aldrich, St. Louis, MO, USA). Alternatively, embryos completely lacking melanocytes, xanthophores, and iridophores were obtained through use of *casper* (*roy orbison*^{-/-}; *nacre*^{-/-}) double mutant zebrafish line ([White et al. 2008](#)).

Embryos were dechorionated using 10mg/mL stock solution of Pronase (Roche Applied Science, Laval, PQ, Canada). Briefly, E3 medium was drained from Petri dish until embryo chorions crested the water level, 150-170 µL of stock Pronase was added, and embryos were incubated for 15-30 minutes at 28.5°C with swirling/agitation every 10 minutes. Upon dechoriation, embryos were washed thoroughly 5 times with E3 medium to remove residual enzyme. Embryos were allowed to rest at least 30 minutes at 28.5°C. Embryos remaining in their chorions were manually removed using needles.

Embryos were developmentally staged according to [Kimmel et al. 1995](#). (**Figure 2.1**). For certain indicated experiments, embryonic development was delayed by incubation overnight (19-21 hours) at 22°C. In terms of normal staging, this would produce embryos that were developmentally matched to embryos at the '12 hpf' stage.

2.2 CREATION OF TRANSGENIC ZEBRAFISH LINES

2.2.1 Bacterial Cloning

To propagate all plasmids and cloning vectors, DH5 α TM and OneShot[®] TOP10 (Invitrogen Corporation, Carlsbad, CA, USA) strains of chemically-competent *Escherichia coli* (*E. coli*) were used for transformation, plating, and culturing. Transformation used 1-5 μ L of suspended plasmid with 35-50 μ L of *E. coli* for 10 minutes on ice, then transferring to 42°C for 45 seconds. Transformed bacteria were then supplied with 250 μ L Super Optimal broth with Catabolite repression(SOC), liquid culture was grown at 37°C for 1 hour with agitation, 50-250 μ L of culture was spread-plated on Lysogeny/Luria broth (LB) agar supplemented with antibiotic (either 50 μ g/mL kanamycin, or 100 μ g/mL ampicillin), plates were inverted, and incubated at 37°C overnight. Selected bacterial colonies were then cultured in a 15 mL conical bottom tube containing 3-5 mL of LB liquid medium supplemented with appropriate antibiotic, and incubated at 37°C overnight with agitation. Liquid cultures were then mini-prepped using GenEluteTM Plasmid Mini-prep Kit (Sigma-Aldrich) according to manufacturer's instructions. Purified plasmids were stored at 4°C or -20°C.

Immediately prior to mini-prep, glycerol stocks of transformed bacteria were prepared with 0.5-1 mL of liquid culture in 100-200 μ L 80% (v/v) glycerol, and placed in long-term storage at -80°C. When more purified plasmid or cloning vector was required, a sterile pipet tip was used to extract a small quantity of glycerol stock, which was streak-plated on LB agar supplemented with appropriate antibiotic, and plate was inverted and incubated at 37°C overnight. Liquid cultures and mini-prep were performed as above. Purified plasmids were sent for sequencing (Robarts Research Institute, London, ON, Canada), with DNA primers (Integrated DNA Technologies, Coralville, IA, USA) designed using Vector NTI Advance[®] 11.5.1 software (Invitrogen).

2.2.2 *NUP98-HOXA9* (*NHA9*)

The human *NHA9* fusion oncogene, kindly provided by DG Gilliland, was cloned downstream of the 9.1 kb zebrafish *spil* promoter and a *loxP-EGFP-loxP* (*IGI*) 'strong STOP' cassette and assembled into a pISce mammalian expression vector (Grabher *et al.*

2004). Purified *Tg(spi1::IGL::NHA9)* pISce vector was suspended at a final concentration of 50 ng/μL with 0.5 U/μL I-Sce I meganuclease (New England BioLabs, Inc., Ipswich, MA, USA) in 0.1% (w/v) phenol red, and 100 pg of vector was injected into *AB* wild-type zebrafish embryos at the one-cell stage of development. Transgenic founder fish were screened by presence of GFP, outcrossed to *AB* wild-type zebrafish, and screened for germline transmission of GFP to create a heterozygous F₁ generation. The F₁ generation was inbred, screened for brightest transmission of GFP to create a homozygous F₂ generation.

2.2.3 Gateway® Cloning

A brief description follows on the method of cloning genes of interest using Gateway® (Invitrogen) technology (refer to schematic in **Figure 2.2**). Complete details are found at http://tools.invitrogen.com/content/sfs/manuals/multisite_gateway_man.pdf. A genetic sequence of interest is amplified by PCR with primers containing modified *attB* (*B* for ‘bacteria’) extension sequences of approximately 20-22 nt. The modifications of *att* sites are necessary to facilitate the directionality of recombination and identification of the genetic element of interest. For example, promoters are amplified with *attB4* forward and *attB1r* reverse primers; genes/ORFs with *attB1* forward and *attB2* reverse; and tags with *attB2r* forward and *attB3* reverse (**Figure 2.2**, ‘PCR fragments’).

A ‘BP reaction’ is performed, which recombines the *attB* PCR product with pDONR donor vector that contain *attP* (*P* for ‘phage’) sites (**Figure 2.2**, ‘pDONR Vectors’). Recombination is achieved using BP Clonase II®, a recombinant enzyme that is a modification of the Integrase (Int) protein expressed by phage λ. A ‘BP reaction’ produces an ‘entry clone’ and the process of recombination changes the identity of plasmid *att* sites to *attL* (*L* for ‘left’), thereby preventing the reaction from happening in reverse. Entry clones adopt designations based on the genetic sequence that has been inserted: promoters are housed in 5’ entry clones (p5E); genes/ORFs in middle entry clones (pME); tags in 3’ entry clones (p3E) (**Figure 2.2**, ‘Entry Clones’). The completed entry clone is then transformed and cultured into DH5α™ *E. coli* cells. The original pDONR vector carries a *ccdB* suicide cassette, which kills DH5α™ *E. coli*. The recombination event during a ‘BP reaction’ replaces the *ccdB* suicide cassette with the

PCR fragment. This allows for easy selection of successful recombinants in DH5 α TM *E. coli* cells, as unsuccessful recombinants will continue to carry the *ccdB* suicide cassette and will kill the bacteria. Successful recombinant entry clones are found by restriction digest and sequencing, and mini-preps of pure entry clone can then be prepared.

An ‘LR reaction’ is then performed to create an ‘expression vector’, which can be any desired combination of: (i) three elements (promoter + gene/ORF + tag) for labelled *in vivo* transgenic expression; (ii) two elements (promoter + tag; promoter + gene/ORF; gene/ORF + tag), respectively for *in vivo* lineage mapping, unlabelled *in vivo* transgenic expression, or labelled mRNA synthesis; or (iii) one element (gene/ORF) for unlabelled mRNA or anti-sense riboprobe synthesis. An ‘LR reaction’ assembles genetic elements in the proper direction based on their *attL* identities, and recombines the entire linear fragment into a pDEST destination vector (often pTol2 for transgenes, or pCS2+ for RNA synthesis) that contains *attR* (*R* for ‘right’) sites (**Figure 2.2**, ‘Destination Vector’). As with pDONR vectors, pDEST vectors also carry the *ccdB* suicide cassette. The recombination event during an ‘LR reaction’ replaces *ccdB* with fragments from the entry clones. Compared to the ‘BP reaction’, the ‘LR reaction’ must perform a greater number of recombination events to create a successful expression clone (**Figure 2.2**, ‘Expression Clone’). Thus, completed expression clones are transformed and cultured into OneShot[®] TOP10 *E. coli* cells, which are very sensitive to any *ccdB* suicide cassettes that have not been removed. This permits aggressive selection for successful recombinants.

2.2.4 *ctnnb1-b** [β -catenin(S/T \rightarrow A)] & *Meis1*

The *Xenopus* (frog)-derived, hyperactive β -catenin(S/T \rightarrow A) mutation (genetically referred to as “*ctnnb1-b**”) was kindly provided by SA Armstrong. Mouse *Meis1* was kindly provided by G Sauvageau. For isolation and cloning of full-length *ctnnb1-b** or *Meis1* cDNA, primers were designed with Gateway[®] (Invitrogen) *attB* extensions at the 5’ and 3’ sequence ends (underlined below) (refer to Gateway[®] schematic in **Figure 2.2**). Primer sequences were: *ctnnb1-b** *attB1-F*, GGG GAC AAG TTT GTA CAA AAA AGC AGG CTT ATC GAT CCT CCC TTT ATC C; *ctnnb1-b** *attB2-R-NOstop*, GGG GAC CAC TTT GTA CAA GAA AGC TGG GTA CTT GTC GTC GTC GTC CTT; *Meis1 attB1-F*, GGG GAC AAG TTT GTA CAA AAA AGC AGG CTT AAT CGA

ATT CCT GCA GCC C; *Meis1 attB2-R-NOstop*, GGG GAC CAC TTT GTA CAA GAA AGC TGG GTA CAT GTA GTG CCA CTG CCC. (NB: The reverse primer eliminated the STOP codon on cDNA to permit activity of the *PTV1-2A* viral linker sequence in the Gateway® 3' entry clone [p3E], described below.)

The 2.5 kb *ctnnb1-b** or the 1.3 kb *Meis1* cDNA with Gateway® *attB* extensions was gel extracted, and BP recombinations with 20-50 fmol cDNA and 150 ng/μL pDONR™ 221 (*attP1*→*attP2*) donor vector were performed overnight at room temperature using BP Clonase™ II enzyme. The resulting *ctnnb1-b** or *Meis1* middle entry clone (pME [*attL1*→*attL2*], Kanamycin-resistant) were transformed into DH5α™ *E. coli* (Invitrogen), plated on LB agar supplemented with 50 μg/mL kanamycin, cultured in LB liquid medium (50 μg/mL kanamycin), stored in glycerol stock, and mini-prepped.

For the creation of *ctnnb1-b** or *Meis1* transgenic zebrafish line, *Tol2* transposon-linked expression vectors were assembled to facilitate genomic integration (Kwan *et al.* 2007, Villefranc *et al.* 2007). LR recombination was performed overnight at room temperature using LR Clonase™ II enzyme, using 10 fmol *ctnnb1-b** or *Meis1* pME (*attL1*→*attL2*), 10 fmol zebrafish *hsp70* promoter 5' entry clone (p5E [*attL4*→*attL1*]), 10 fmol *PTV1-2A-mCherry* 3' entry clone (p3E [*attL2*→*attL3*]), and 20 fmol pTol2 DEST (*attR4*→*attR3*) destination vector (Ampicillin-resistant). The 66 bp *PTV1-2A* viral linker sequence permits stoichiometrically-equivalent protein expression from polycistronic mRNA transcripts, via co-translational cleavage of the polypeptide chain. Thus, equal amounts of protein are produced from the *ctnnb1-b** or *Meis1* cDNA and the *mCherry* red fluorescent reporter gene (Provost *et al.* 2007). The resulting pTol2 expression clones, *Tg(hsp70::ctnnb1-b*::2A-mCherry)*, or *Tg(hsp70::Meis1::2A-mCherry)*, were transformed into OneShot® TOP10 *E. coli*(Invitrogen), on LB agar supplemented with 100 μg/mL ampicillin, clear bacterial colonies (*Tol2kit* Wiki, http://chien.neuro.utah.edu/tol2kitwiki/index.php/Main_Page) were cultured in LB liquid medium supplemented with 100 μg/mL ampicillin, stored in glycerol stock, and mini-prepped as above.

2.3 ACTIVATION OF TRANSGENES

For *NHA9*-transgenic fish, excision of *IGI* 'strong STOP' cassette by Cre recombinase was achieved by outcross to the *Tg(heat shock protein 70[hsp70]::Cre)* line

and incubation of embryos at 37°C or 39°C for one hour (‘heat-shock’), which was performed at indicated timepoints (see schematic in **Figure 3.1A**). Alternatively, *Tg(spi1::lgl::NHA9)* fish were outcrossed with *AB* wild-type zebrafish and embryos were injected at the one-cell stage with 50 ng/μL *Cre* mRNA in 0.1% (w/v) phenol red.

2.4 GENOTYPING

Selected embryos were heat-shocked at 24 hpf and grown to 28 hpf, or whole adult zebrafish were anaesthetized with 0.090 mg/mL MS-222 (Tricaine; Sigma-Aldrich) and fin clips were taken. For genotyping, genomic DNA extraction from single embryos or fin clips and subsequent PCR detection was performed using REDExtract-N-Amp™ Tissue PCR Kit (Sigma-Aldrich), according to manufacturer’s instructions.

2.5 PCS2+ VECTOR CONSTRUCTION & MRNA SYNTHESIS

Gateway® primers were designed to clone full-length cDNA for human *NHA9*, frog *ctnbl-b**, and mouse *Meis1* (**Table 2.1**). (*NB*: Reverse primers include the STOP codon for the purposes of mRNA synthesis.) cDNAs were gel extracted, BP recombinations, bacterial transformation and mini-preps were performed as above.

For synthesis of mRNA, LR recombinations were performed as above, but using 10 fmol of the respective pMEs (*attL1*→*attL2*) with 20 fmol of the pCS2+ DEST (*attR1*→*attR2*) destination vector. The resulting *NHA9* + STOP, *ctnbl-b** + STOP, and *Meis1*+ STOP pCS2+ expression clones were transformed and mini-prepped as above. Vectors were then linearized, mRNA transcripts were synthesized using mMACHINE mMACHINE® Sp6 Kit, and mRNA cleaned up using NucAway™ Spin Columns (Applied Biosystems/Ambion, Inc., Austin, TX, USA).

2.6 MORPHOLINO OLIGONUCLEOTIDE (MO)

Gene-blocking MOs were purchased from GeneTools, LLC (Philomath, OR, USA) or Open Biosystems Products (Thermo Fisher Scientific, Huntsville, AL, USA). The MOs listed in **Table 2.2** suppress gene expression and protein translation by inhibiting ribosome binding (designated ‘atg/5’UTR’). MOs were suspended in 0.1%

(w/v) phenol red at final concentrations listed in **Table 2.2** and were injected into zebrafish embryos of indicated genotypes at the one- to four-cell stage of development.

2.7 RNA EXTRACTION & cDNA SYNTHESIS

RNA was extracted from at least 45-50 embryos per experimental group, according to the procedures below. RNA samples were quantified in 10 mM Tris-HCl, pH 7.5 and stored at -80°C. cDNA synthesis was performed using QuantiTect® Reverse Transcription Kit (QIAGEN, Mississauga, ON, Canada).

2.7.1 RNeasy Method

Live embryos were chilled on ice for 5-10 minutes, rinsed with mqH₂O, and then stabilized with RNAlater® (AB/Ambion). According to manufacturer's instructions, RNA was harvested using RNeasy™ Mini Kit (QIAGEN), 'Animal Tissues' protocol, including Step 12 where the eluate is reapplied to the column to improve RNA yield.

2.7.2 TRIzol® + RNeasy Method

Live embryos were chilled on ice for 5-10 minutes, rinsed with mqH₂O, transferred to a 5 mL conical bottom tube, and 1 ml of TRIzol® (Invitrogen) was added. Embryos were homogenized with a rotor-stator, transferred to an Eppendorf tube, incubated at room temperature for 5 minutes, then 200 µL chloroform (Sigma-Aldrich) was added in a fumehood, and sample was vortexed for 15 seconds. Sample was allowed to settle for 2-3 minutes, touch-vortexed, and then centrifuged at 12,000 x g for 15 minutes at 4°C. The top aqueous phase was carefully transferred to a fresh Eppendorf tube, 1 volume of 70% (v/v) ethanol/30% (v/v) DEPC mqH₂O was added, and sample was then loaded onto an RNeasy™ Mini Kit column (QIAGEN). RNeasy™ protocol was then followed from 'Animal Tissues – Step 5', according to manufacturer's instructions.

2.8 QUANTITATIVE REVERSE TRANSCRIPTION POLYMERASE CHAIN REACTION (QRT-PCR)

2.8.1 Primer Design

Primers (**Table 2.3**) for zebrafish transcripts were designed using Primer-BLAST software (<http://www.ncbi.nlm.nih.gov/tools/primer-blast/>, Rozen and Skaletsky 2000) with modified parameters (Dorak 2006):

- PCR product size: 70 – 150 bp;
- Primer must span an exon-exon junction (Exon at 5' side: 7, Exon at 3' side: 4);
 - **OR**, Primer must be separated by at least one intron (Min: 1000, Max: 1000000);
- Database: Refseq RNA;
- Misprimed product size deviation: 250 bp;
- Splice variant handling: YES;
- Primer GC content: 40 – 60%;
- GC clamp: 1;
- Max Poly-X: 4;
- Max 3' end complementarity: 2.0

2.8.2 Reagents, Thermocycler Conditions, Controls & Analysis

qRT-PCR was performed using QuantiFast™ SYBR® Green PCR Kit (QIAGEN) with a Stratagene Mx3000P™ QPCR thermocycler (Agilent Technologies, Inc., Santa Clara, CA, USA). Two-step thermocycler conditions were: 1) 1 cycle – 95°C, 5:00 to activate; 2) 40 cycles – 95°C, 0:10 to denature, 60°C, 0:30 combined annealing and extension, with collection of fluorescence data; 3) 1 cycle for melting curve analysis – 95°C, 1:00 to denature, 55°C, 0:30 climb to 95°C, 0:30, with collection of fluorescence data. Reverse-transcription was performed on 0.5 – 2 µg of RNA. Four-fold dilutions of cDNA were made. For each primer set, two dilutions per genotype were plated in triplicate; in effect, each primer set per genotype had six representations for each independent round of amplification. Negative controls for qRT-PCR were: 1) no template controls (NTC) for each primer set; 2) no RT for each independent RNA

extraction. Controls were plated in duplicate for each independent round of amplification. Cycle thresholds (C_t) for each control were negligible. C_t , reaction efficiency, and melting curve analysis were performed using MxPro – Mx3000P v3.20 build 340, Schema 74 (Agilent Technologies, Inc., Santa Clara, CA, USA).

Quantification was performed using the $2^{-\Delta\Delta C_t}$ method (Dorak 2006; AB/Ambion 2001; AB/Ambion 2005). In brief, for every gene in each biological sample, the C_t 's from each independent round of amplification were averaged. This was performed for all genes of interest and housekeeping genes (*actb1*, *ef1a*) (Table 2.3). The averaged C_t for each gene of interest was normalized/subtracted against the averaged C_t for the housekeeping gene to find a ΔC_t for that biological sample. Then, the ΔC_t for each gene of interest in sample (*i.e.* NHA9) cDNA was normalized against the ΔC_t for that gene in control (*i.e.* wild-type) cDNA to find a $\Delta\Delta C_t$. One unit of $\Delta\Delta C_t$ represents a 2-fold relative change in gene expression between samples. The relationship is a negative exponential ($2^{-\Delta\Delta C_t}$) because the expression of housekeeping genes is usually elevated compared to genes of interest. Thus, housekeeping genes have a lower C_t value (detected earlier). So, for example, a $\Delta\Delta C_t$ of -3 (an 8-fold relative change) reflects that the difference (or 'distance') between C_t 's in sample cDNA is less (or 'closer') than in control cDNA, thus expression of the gene of interest has *increased* compared to control.

2.9 MICROARRAY

Microarray studies employing Agilent oligo-arrays were performed in collaboration with Dr. Stephen Lewis at the Atlantic Cancer Research Institute in Moncton. Extraction of mRNA was performed using the Trizol + RNeasy method. In Dr. Lewis's laboratory, the purified mRNA was then reverse transcribed to generate cDNA that was differentially labeled with fluorescent dyes using the SuperScript Plus Direct cDNA Labeling System (Invitrogen). Specifically, groups of mRNA were labeled with Alexa Fluor® 555 (orange fluorescent dye, false-coloured green for analyses) or with Alexa Fluor® 647 (far-red fluorescent dye) (Invitrogen). Any samples with low concentrations of RNA were subjected to whole genome amplification (WGA) using Amino Allyl MessageAmp II aRNA Amplification Kit (AB/Ambion) with Alexa Fluor® 555 and Alexa Fluor® 647 reactive dye packs (Invitrogen). Equal amounts of labeled

cDNA were mixed and competitively hybridized to a zebrafish oligonucleotide genome array containing 43,803 probes (Agilent) using standard procedures. The hybridized array was scanned and analyzed using a GenePix 4200AL autoloader microarray scanner (Molecular Devices, Japan) and associated software (GenePix Pro 6.0, Acuity 4.0). The microarray experiments were performed at least three times for each sample pair. In addition, ‘dye-swap’ experiments, in which the fluorescent label for each sample is switched, were performed in triplicate to eliminate any variation due to labeling efficiency and/or dye properties. The mRNAs whose expression changed ≥ 2 -fold were considered significant.

2.9.1 Identifying Mammalian Homologues For Zebrafish Genes

Putative mammalian homologues of zebrafish mRNAs indicated by microarray were identified using sequences of unannotated gene identifiers (zgc), predicted loci (LOC), nucleotides (NM, XM, XR), expressed sequence tags (EST), and uncharacterized proteins. Homologues were predicted using default parameters of algorithm tools, such as: NCBI HomoloGene, Basic Local Alignment Search Tool (BLAST), and UniProt.

2.10 FLUORESCENCE-ACTIVATED CELL SORTING (FACS) & CYTOSPINS

Prior to preparation of cell suspensions, 5 mL conical bottom tubes were pre-coated with 0.9X phosphate buffered saline (PBS) supplemented with 5% (v/v) heat-inactivated fetal bovine serum (FBS) for at least 45 minutes on ice.

2.10.1 Whole Kidney Marrow (WKM)

Adult zebrafish were euthanized with 2 mg/mL Tricaine (Sigma-Aldrich). Incisions were made – without cardiac puncture – to form an open dermal flap for exposure of internal organs: starting from the anus, a straight cut was made along ventral side up to the operculum; two cross-wise cuts were made from the ventral side up to the dorsal side, one from the anus and one across the gills. Kidney tissue along the dorsal body cavity, which is associated with pigmented cells, was dissected and placed into ice-cold 0.9X PBS/5% (v/v) FBS in pre-coated tubes. Whole kidney marrow (WKM) was

gently disaggregated with a P1000 pipetman and strained to a single-cell suspension through a 40 μ M filter into ice-cold 0.9X PBS/5% (v/v) FBS in pre-coated tubes. WKMs were centrifuged at 350 x g for 10 minutes at 4°C and re-suspended in 0.9X PBS/5% (v/v) FBS. WKMs were treated with 10 μ g/mL 7-aminoactinomycin D (7-AAD; Sigma-Aldrich) for live cell exclusion and sorted on a FACSAria™ I (BD Biosciences, San Jose, CA, USA) at. WKMs were gated by FSC and SSC and interrogated by Coherent® Sapphire™ solid state 488 nm laser with dual band pass filter for FITC (515-545nm) and Fast Red (600-620 nm) emission. WKM was interrogated for lowest 7-AAD (647 nm) emission and 7-AAD^{LO} live cells were gated by FSC and SSC into ‘myelomonocyte’ (FSC^{MID-to-HI}, SSC^{MID}), ‘precursor’ (FSC^{MID-to-HI}, SSC^{LO}), and ‘lymphocyte’ (FSC^{LO}, SSC^{LO}) populations (Traver *et al.* 2003). WKM from *gata1a::EGFP*, *gata2a::EGFP*, and *mpx::EGFP* transgenic zebrafish lines were also interrogated in the ‘FITC’ channel (Figure 2.3). Gated cells were sorted into 0.9X PBS/5% (v/v) FBS. Unfortunately, *gata1a*-expressing erythroid cells cannot be reliably interrogated by the FACSAria™ I because they scatter unevenly (Traver D, personal communication) (Figure 2.3A). We thus could not account for erythroid populations when quantifying WKM cellularity.

2.10.2 Whole Embryo Suspensions

At 28 hpf, 30-40 live embryos were euthanized with 2 mg/mL Tricaine (Sigma-Aldrich) and dissociated to a single cell suspension, as described in Covassin *et al.* 2009. Briefly, 1.2 mL per well of Protease solution (0.25% [w/v] trypsin, 1 mM EDTA, pH 8.0 in 1X PBS) was transferred into a 12-well plate or Eppendorf tube, and warmed for 10 minutes at 28.5°C. Dechorionated embryos were washed twice in Calcium-free Ringer’s solution (116 mM NaCl, 2.6 mM KCl, 5 mM HEPES, pH 7.0), and either chilled on ice for 15 minutes or euthanized with 2 mg/mL Tricaine. Embryos were then transferred to warm Protease solution, 27 μ L of 100 mg/mL collagenase in Hank’s Balanced Salt Solution (HBSS) was added, and incubated for 15 minutes at 28.5°C, with gentle homogenization every 5 minutes with a P1000. To stop trypsin digestion, 200 μ L of 6X Stop solution (30% [v/v] FBS, 6 mM CaCl₂ in 1X PBS) was added, digest solution was mixed and transferred to microcentrifuge tubes, and cells were centrifuged at 350 x g for

5 minutes at 4°C. Supernatant was discarded, pellets were washed and gently vortexed in 1 mL of chilled Suspension media (1% [v/v] FBS, 0.8 mM CaCl₂ in Dulbecco's Modification of Eagle's Medium [DMEM]), and then centrifuged at 350 x g for 5 minutes at 4°C. Supernatant was discarded, pellets were washed and gently vortexed in 700 µL of chilled Suspension media, and cells were passed through a 40 µm strainer into pre-coated 5 mL conical bottom tubes. Cell suspensions were sorted on a FACS Aria™ I at 4°C. GFP⁺ myeloid cells were gated by interrogation for FSC^{HI}, SSC^{HI} scatter and GFP^{HI} (509 nm), and sorted into 0.9X PBS/5% (v/v) FBS. For apoptosis assays on GFP⁺ myeloid cells, dissociated cells were supplemented with 1 µg/mL 7-AAD, gated for FSC^{HI}, SSC^{HI}, and GFP^{HI}, and interrogated for 7-AAD^{HI} dead cells.

2.10.3 Cytospins

FACS sorted cells were centrifuged at 350 x g for 5 minutes at 4°C. Supernatant was discarded, and cells were resuspended in 100-250 µL Suspension media or 0.9X PBS/5% (v/v) FBS, supplemented with 20 µL of 22% (w/v) BSA. Cytofunnels were assembled, filter cards were pre-wetted with 100 µL of 0.9X PBS/5% (v/v) FBS, and centrifuged at 200 rpm for 3 minutes at room temperature. Cells were loaded (100-150 µL) into cytofunnels and centrifuged at 200 rpm for 5 minutes. Slides were then treated with Wright-Giemsa stain at the IWK Histology, Pathology & Lab Medicine Service.

2.11 WHOLE MOUNT RNA *IN SITU* HYBRIDIZATION (WISH)

2.11.1 RNA Probe Synthesis

Digoxigenin (DIG)- or fluorescein isothiocyanate (FITC)-labelled anti-sense RNA probes for zebrafish *spi1/pu.1*, *lcp1*, *lyz*, *mpx*, *gata1a*, *bcl2*, and *bcl2l/bcl-x_L* were synthesized from cDNA templates, according to the published literature. Briefly, cDNA vectors were linearized and anti-sense RNA probes were synthesized using T3, T7, or Sp6 RNA polymerase with FITC or DIG RNA labeling kits, according to manufacturer's instructions (Roche). Template DNA was digested using TURBO™ DNase (AB/Ambion) and probes were cleaned using NucAway™ Spin Columns (AB/Ambion).

2.11.2 Embryo Preparation (Optional Bleach & Methanol Storage)

Embryos were heat-shocked and fixed at indicated timepoints in 4% (w/v) paraformaldehyde (PFA) overnight at 4°C. Embryos were then washed 3 x 5 minutes in 1X PBS-T, permeabilized with Proteinase K (ProK; Roche) (refer to **Table 2.4** for details), rinsed in 1X PBS-T, and re-fixed in 4% (w/v) PFA for 20 minutes. If necessary to remove pigmentation post-fixation, embryos were treated with 1mL 1X bleach solution (3% [v/v] H₂O₂, 1% [w/v] KOH) in a 15 mL tube at room temperature until embryos were clarified. Time of treatment ranged from 2-10 minutes depending on extent of pigmentation and batch strength variation of bleach. Embryos have tendency to float in bleach solution, so bleaching was terminated by filling the 15 mL tube with 1X PBS-T, rinsing thoroughly until embryos settled, and washing 4 x 5 minutes in 1X PBS-T. ProK treatment for half as long when embryo pigmentation was inhibited prior to fixation using E3 medium supplemented with 0.003% (w/v) PTU. Embryos could then be washed 3 x 5 minutes in chilled 100% methanol and placed into long-term storage at -20°C. When ready to stain, embryos were brought to room temperature, rehydrated in a graded methanol:PBS-T series of 75% (3:1), 50% (1:1), and 25% (1:3) for 5 minutes each (all solutions prepared [v/v]), and then thoroughly washed 5 x 5 minutes in 1X PBS-T.

2.11.3 WISH Protocol

WISH assays were adapted from standard protocol. Fixed embryos were washed in pre-hybridization buffer (Hyb⁻; 5X saline sodium citrate buffer with 0.1% (v/v) Tween 20 (SSC-T), 50% (v/v) formamide) for 15 minutes at 65°C, and then blocked in hybridization buffer (Hyb⁺; same formulation as Hyb⁻, supplemented with 5 mg/mL torula (yeast) RNA type IV, 50 µg/mL heparin) for 1 hour at 65°C. Embryos were incubated overnight at 65°C in labeled anti-sense RNA probes (1:100 to 1:200 dilution). Embryos were then washed 2 x 15 minutes in 2X SSC-T/50% (v/v) formamide, 1 x 15 minutes in 2X SSC-T, and 2 x 15 minutes in 0.2X SSC-T (all washes at 65°C). Next, embryos were washed 3 x 5 minutes in 1X maleic acid buffer (MAB-T; 100mM maleic acid, 150mM NaCl, 10% [w/v] Tris, 0.1% [v/v] Tween-20, pH 7.5) at room temperature, and incubated in WISH blocking solution (2% [w/v] blocking reagent [Roche], 10% [v/v]

heat-inactivated FBS in 1X MAB-T) at room temperature for 1 hour. Embryos were incubated overnight at 4°C in sheep anti-digoxigenin/-fluorescein-AP, Fab fragments (Roche) (2°) antibody (1:10,000). At room temperature, embryos were then washed 1 x 15 minutes in WISH blocking solution and 2 x 15 minutes in 1X MAB-T.

For chromogenic development with BCIP/NBT (Vector Laboratories, Inc., Burlingame, CA, USA), embryos were washed 4 x 5 minutes in 0.1M Tris, pH 9.5 staining buffer. Staining was performed according to manufacturer's instructions for 1 to 4 hours (length of time depending on specific probe) at room temperature in the dark. To stop the staining, embryos were washed in 1X PBS-T for 5 minutes. Embryos were then de-stained in 100% methanol for 5-10 minutes, and transferred back to 1X PBS-T for imaging. For long-term storage at 4°C, embryos were placed in 4% (w/v) PFA.

2.12 ANTIBODIES

Primary (1°) antibodies used were monoclonal rat anti-Nup98 (clone 2H10) IgG2c- κ , rabbit anti-p-Histone H3 (Ser10)-R IgG (Santa Cruz Biotechnology, Inc., Santa Cruz, CA, USA), rabbit anti- β -actin IgG (Cell Signalling Technology, Danvers, MA, USA), monoclonal mouse anti-BrdU (clone 3D4) IgG₁- κ , and rabbit anti-Caspase-3, Active Form (clone C92-605) IgG (BD Pharmingen, Mississauga ON, Canada). Secondary (2°) antibodies used were sheep anti-fluorescein/-digoxigenin-AP, Fab fragments (Roche), goat anti-rat/-rabbit IgG, HRP-linked (Cell Signalling), and Alexa Fluor® 565 goat anti-rabbit/-mouse IgG (Invitrogen).

2.13 WESTERN BLOTTING

At 28 hpf, embryo deyolking and protein extraction were performed (as described in [Sidi *et al.* 2008](#)). For each genotype, at least 40 embryos were chilled on ice for 60 min in E3 medium and rinsed twice in ice-cold Ringer's solution. Embryos were deyolked by gently with a P200 pipette tip, transferred to a chilled 2 mL microcentrifuge tube, and residual Ringer's solution was removed. Lysis buffer (50 mM Tris, pH 7.4-7.7, 100 mM NaCl, 1% [v/v] Nonidet P-40, 0.1% [v/v] sodium dodecyl sulphate [SDS], 10 mM EDTA, 50 mM NaF, 1 mM sodium orthovanadate, supplemented with Complete

Mini protein inhibitor cocktail [Roche; *NB*: 1 tablet/5 ml]) was added to each tube (1 μ l per embryo) and the embryos were homogenized with a pestle. Homogenate was transferred to a chilled 1.5 mL microcentrifuge tube, vortexed for 15 seconds, and centrifuged at 16,000 \times g for 10 minutes at 4°C. Supernatant was transferred to a fresh 1.5 mL tube, protein concentration was quantified, and stored at -80°C.

Western blotting was performed on protein extracts (as described in ref. 24). Protein extract (5-60 μ g) was added to 5X Laemmli sample buffer (300 mM Tris-HCl, pH 6.8, 10% [w/v] SDS, 50% [v/v] glycerol, 25% [v/v] β -mercaptoethanol, with bromophenol blue), and boiled at 95°C for 5 minutes. Samples were run on an 8-15% [w/v] SDS-PAGE (polyacrylamide gel electrophoresis) gel (recipes in **Table 2.5**) using a Mini-PROTEAN® apparatus (BioRad Life Science, Mississauga, ON, Canada) in 1X Running Buffer (25 mM Tris, 192 mM glycine, 3.5 mM SDS) at 200V for 1 hour. Protein was transferred to a polyvinylidene fluoride (PVDF) membrane (BioRad; activated in 100% methanol for 15 seconds, rinsed three times in mqH_2O , and washed in 1X Transfer Buffer [25 mM Tris, 192 mM glycine, 20% (v/v) methanol, pH 8.3]) using a Mini Trans-Blot® module (BioRad) submerged in 1X Transfer Buffer at 30 mA overnight at 4°C. Membranes were rinsed in 1X Tris-buffered saline (20 mM Tris, 500 mM NaCl, pH 7.6) with 0.1% (v/v) Tween-20 (TBS-T) and blocked with 5% (w/v) milk in 1X TBS-T for 1 hour at 4°C. Membranes were probed with 1° antibodies overnight at 4°C: monoclonal rat anti-Nup98 (clone 2H10) IgG2c- κ (1:100); rabbit anti- β -actin IgG (1:1000). Membranes were then washed 3 \times 5 minutes in 1X TBS-T and incubated with anti-rat/-rabbit IgG, HRP-linked (2°) antibodies (1:2000) in 5% (w/v) milk/1X TBS-T for 2 hours at room temperature. Membranes were washed 2 \times 5 minutes in 1X TBS-T, 2 \times 5 minutes in 1X TBS, and developed using Enhanced ChemiLuminescence (ECL) Plus™ (Amersham, GE Healthcare Bio-Sciences Corp., Piscataway, NJ, USA) and imaged on a Kodak ImageStation 4000MM (Mandel, Guelph, ON, Canada).

2.14 5-BROMO-2-DEOXYURIDINE (BRDU) INCORPORATION ASSAY

At 28 hpf, BrdU incorporation was performed, as described in ref. 25 with modifications. Briefly, dechorionated embryos were chilled on ice in E3 medium for 15

minutes. Embryos were then transferred to 1 mL of BrdU solution (10 mM BrdU [Sigma-Aldrich], 15% [v/v] dimethylsulphoxide [DMSO; Sigma-Aldrich] in E3 medium) and incubated for 20 minutes on ice. Embryos were then transferred to warm E3 medium, incubated for exactly 5 minutes at 28.5°C to label cells with BrdU, and immediately fixed in 4% (w/v) PFA for 2 hours at 4°C. Fixed embryos were then washed 3 x 5 minutes in chilled 100% methanol and placed for long-term storage at -20°C.

When ready to stain, embryos were brought to room temperature and rehydrated in a graded methanol:PBS-T series of 75% (3:1), 50% (1:1), and 25% (1:3) for 5 minutes each (all solutions prepared [v/v]). Embryos were washed 3 x 5 minutes in 1X PBS-T, permeabilized with 1-2 µg/mL of Proteinase K (ProK; Roche) for 10 minutes, rinsed in 1X PBS-T, and re-fixed in 4% (w/v) PFA for exactly 20 minutes. Embryos were then rinsed in 1X PBS-T, rinsed 3 times in mqH₂O, rinsed once in 2 N HCl, then incubated in 2 N HCl for 1 hour to expose the BrdU-labeled DNA. Embryos were rinsed twice, and washed 2 x 5 minutes in 1X PBS-T, then incubated for 30 minutes in BrdU blocking solution (0.2% [w/v] blocking reagent [Roche], 10% [v/v] heat-inactivated FBS, 1% [v/v] DMSO in 1X PBS-T). Monoclonal mouse anti-BrdU (1°) antibody was added at a dilution of 1:100 and embryos were incubated overnight at 4°C. Embryos were washed 3 x 5 minutes in 1X PBS-T and then incubated in 1:250 Alexa Fluor® 565 goat anti-mouse IgG (2°) antibody in BrdU blocking solution overnight at 4°C to achieve greater signal. Embryos were washed 3 x 5 minutes in 1X PBS-T and imaged within one week.

2.15 IONIZING RADIATION (IR), ACRIDINE ORANGE (AO) STAINING & IMMUNOFLUORESCENCE (IF)

DNA damage was induced by exposure to 16 Gy IR at 26 hpf, using a Gammacell GC3000 Irradiator (MDS Nordion, Ottawa, ON, Canada). At 28 hpf, living embryos were stained with 10 µg/mL AO (BioBasic Inc., Amherst, NY, USA) to label apoptotic cells. Fixed embryos were used to perform IF for phosphorylated histone-H3 (pH3) (as in [Shepard *et al.* 2004](#)) or activated caspase-3 (casp3) (as in [Jette *et al.* 2008](#)).

For pH3, fixed embryos were either permeabilized with chilled acetone for 7 minutes at -20°C, or 100% methanol for at least 2 hours, then rehydrated and

permeabilized with ProK (as above). Permeabilized embryos were then washed 3 x 5 minutes in 1X PBS-T and incubated in pH3 blocking solution (2% [w/v] blocking reagent [Roche], 10% [v/v] heat-inactivated FBS in 1X PBS-T) for 1 hour at room temperature. Rabbit anti-p-Histone H3 (Ser10)-R IgG (1°) antibody was added at a dilution of 1:250 and embryos were incubated overnight at 4°C. Embryos were washed 3 x 5 minutes in 1X PBS-T and then incubated in Alexa Fluor® 565 goat anti-mouse IgG (2°) antibody (1:500) in pH3 blocking solution for 2 hours at room temperature. Embryos were finally washed 3 x 5 minutes in 1X PBS-T and imaged within one week.

For casp3, fixed embryos were dehydrated in 100% methanol at -20°C for at least 2 hours. Embryos were rehydrated as above, and permeabilized with PDT (1X PBS-T, 1% [v/v] DMSO, 0.3% [v/v] Triton-X) for 20 minutes at room temperature. Permeabilized embryos were incubated in casp3 blocking solution (2% [w/v] blocking reagent [Roche], 10% [v/v] heat-inactivated FBS in PDT) for 1 hour at room temperature. Embryos were then incubated overnight at 4°C Rabbit anti-Caspase-3, Active Form (clone C92-605) IgG (1°) antibody (1:200). Embryos were washed 3 x 20 minutes in PDT, re-blocked for 30 minutes, and incubated in Alexa Fluor® 565 goat anti-mouse IgG (2°) antibody (1:250) in casp3 blocking solution for 2 hours at room temperature. Embryos were finally washed 3 x 5 minutes in 1X PBS-T and imaged within one week.

To obtain double stains of IF + WISH, embryos were first incubated with FITC-labelled *spi1/pu.1* or *lcp1* RNA probe overnight at 65°C, and then co-incubated with sheep anti-fluorescein-AP (2°), plus rabbit anti-p-Histone H3 (Ser10)-R (1°) antibodies in pH3 blocking solution overnight at 4°C. Embryos were incubated with Alexa Fluor® 565 goat anti-rabbit IgG (2°) and WISH label was developed with BCIP/NBT (Vector).

2.16 TISSUE SECTIONING, HISTOLOGY & IMMUNOHISTOCHEMISTRY (IHC)

Whole adult zebrafish were euthanized with 2 mg/mL Tricaine (Sigma-Aldrich) and fixed in 10% (w/v) neutral buffered formalin. Fixed fish were sent to the IWK Histology, Pathology & Laboratory Medicine Service for standard protocols, which include: embedding in paraffin, obtaining 5 µm serial sections, and staining with haematoxylin and eosin (H/E) or periodic acid-Schiff (PAS).

2.16.1 *In Situ* Hybridization (ISH)

ISH for genes expressed in myeloid cells, *lcp1* and *mpx*, was performed directly in the Berman lab. Paraffin-embedded tissue sections on slides were heated 30 minutes to 2 hours at 65°C in an empty slide holder ('chalet') to melt and drain paraffin. Dewaxing was performed in fume hood with chalets at room temperature, starting with xylene washes 3 x 10 minutes, followed by rehydration through graded alcohols – 100% ethanol, 3 x 10 minutes; 95% (v/v) ethanol, 2 minutes; 85% (v/v) ethanol/1% (w/v) NaCl, 2 minutes; 60% (v/v) ethanol/1% (w/v) NaCl, 2 minutes; 30% (v/v) ethanol/1% (w/v) NaCl, 1 minute – and finally, 3 rinses in mqH₂O. Slides were then washed in 1X PBS for 5 minutes, fixed in 4% PFA, 20 minutes at 4°C, rinsed once in 1X PBS and rinsed twice in mqH₂O. Slides were then permeabilized with 0.2 M HCl for 10 minutes at room temperature, rinsed twice in 1X PBS, rinsed twice in mqH₂O, and finally treated with 20 µg/mL ProK in 50 mM Tris-HCl, pH 7.4, with 5mM EDTA for 15 minutes at room temperature. Permeabilized slides were then rinsed twice in 1X PBS, re-fixed in 4% PFA for 5 minutes at 4°C, rinsed twice in 1X PBS, and washed in 1X PBS for 5 minutes. Slides were then rinsed in mqH₂O, dehydrated through graded alcohols – 30% (v/v) ethanol/1% (w/v) NaCl, 2 minutes; 60% (v/v) ethanol/1% (w/v) NaCl, 2 minutes; 85% (v/v) ethanol/1% (w/v) NaCl, 2 minutes; 95% (v/v) ethanol, 2 minutes; 100% ethanol, 2 x 2 minutes – and allowed to air dry for 30 minutes or more. A slide box or Petri dish was fitted with filter paper, saturated with Hyb- buffer (see recipe above), and overlaid with parafilm, onto which dehydrated slides were placed. Tissue sections were covered with 80 µL Hyb+ buffer (see recipe above) and incubated 30 minutes at 55°C.

Prior to labelling, 2 µL FITC- or DIG-labelled *lcp1* or *mpx* antisense RNA probe was denatured for 3 minutes at 95°C, added to 18 µL ice-cold Hyb+, and 20 µL probe solution was added to Hyb+ already on sections (1:50 final dilution of probe). Coverslips were added to slides, slide box or Petri dish was wrapped in parafilm to prevent evaporation, and samples were incubated overnight at 55°C. The next day, slides were washed at 55°C as follows: 5X SSC for 5 minutes to remove coverslip, 2X SSC/50% (v/v) formamide for 1 hour, and 1X SSC/50% (v/v) formamide for 30 minutes. To eliminate unbound probe, slides were washed in RNaseA buffer (10mM Tris-HCl, pH 7.5, 15 mM NaCl, 1 mM EDTA) for 2 x 5 minutes at 37°C, and then treated with 20

$\mu\text{g}/\text{mL}$ RNaseA for 30 minutes at 37°C . Slides were returned to 55°C and washed in 2X SSC for 1 hour, and 0.1X SSC for 2 x 1 hour. Slides were brought to room temperature and washed in 1X MAB for 2 x 5 minutes, incubated in ISH blocking solution (2% [w/v] blocking reagent [Roche], 10% [v/v] heat-inactivated FBS in 1X MAB) for 20 minutes, and exposed to sheep anti-digoxigenin/-fluorescein-AP, Fab fragments (Roche) (2°) antibody at a dilution of 1:400 overnight at 4°C . Coverslips were added to prevent evaporation. Slides were then washed at room temperature in 1X MAB for 3 x 20 minutes, and in 0.1X Tris, pH 9.5 for 2 x 5 minutes.

Slides were developed using BCIP/NBT (Vector Laboratories), supplemented with $400 \mu\text{g}/\text{mL}$ levamisole (to quench endogenous peroxidase activity) for 1-4 hours at room temperature in the dark. To stop the staining reaction, slides were washed in 0.1X Tris, pH 8.2, 10mM EDTA for 5-10 minutes at room temperature, rinsed in mqH_2O , rinsed twice in 1X PBS, and fixed in 4% PFA for 5 minutes at 4°C to preserve staining. Slides were brought to room temperature, rinsed twice in 1X PBS, and washed in 1X PBS for 5 minutes. Slides were finally counterstained by exposure to 1% (v/v) methyl green for 5 minutes, followed by rinse in mqH_2O , and quick dehydration through 95% ethanol (10 dips until sections turn green) and two changes of 100% ethanol (10 dips each). Completed slides were mounted with CytoSeal medium for imaging.

2.17 CHEMICAL COMPOUNDS

2.17.1 *dnmt1* Studies

The activity of *dnmt1* was inhibited using $75 \mu\text{M}$ Decitabine (5-aza- $2'$ -deoxycytidine, 5-azadC; Sigma-Aldrich) (Martin CC *et al.* 1999; Ceccaldi *et al.* 2011). To ensure long-term stability, chemicals were resuspended to 100 mM stock solution in DMSO, and aliquots were stored at -80°C (den Hartigh *et al.* 1989; Duriez *et al.* 2011; Eramo *et al.* 2005). Embryos staged at 24 hpf were dechorionated and arrayed into 6-well plates with 6 mL of pure E3 medium (Methylene Blue-free, PTU-free). Chemicals were added to E3 medium at indicated concentrations (0.3-0.5% [v/v] DMSO served as a vehicle control). Embryos were then heat-shocked and grown to 28 – 30 hpf bathed in the chemical.

2.17.2 β -catenin Studies

The activity of the Wnt/ β -catenin pathway was stimulated using 10 μ M 16,16-dimethyl-Prostaglandin E₂ (dmPGE₂; Santa Cruz) and was inhibited using 10 μ M Indomethacin (Indo; 1-[4-Chlorobenzoyl]-5-methoxy-2-methyl-3-indoleacetic acid; Sigma-Alrich). Embryos treated with 0.3-0.5% [v/v] DMSO served as a vehicle control.

For *in situs* at 28 – 30 hpf, embryos staged at 24 hpf were dechorionated and arrayed into 6-well plates with 6 mL of pure E3 medium (Methylene Blue-free, PTU-free). Chemicals were added to E3 medium at indicated concentrations. Embryos were then heat-shocked and grown to 28 – 30 hpf bathed in the chemical.

For *in situs* at 18 hpf, or 36 – 40 hpf, embryo development was delayed by incubation overnight at 22°C. Embryos staged at 12 hpf were heat-shocked and dechorionated, and arrayed into 6-well plates with 6 mL of pure E3 medium (Methylene Blue-free, PTU-free). Chemicals were resuspended in DMSO and added to E3 medium at indicated concentrations. Embryos were then grown to 18 hpf, or kept overnight to 36 – 40 hpf bathed in the chemicals.

2.17.3 Prodigiosene Studies

The *in vivo* activity of prodigiosenes were tested on pigment-free *casper* (*roy orbison*^{-/-}; *nacre*^{-/-}) double mutant embryos. Four derivatives, designated **8a-d**, were synthesized in the lab of Dr. Alison Thompson, Department of Chemistry, Dalhousie University, using a multi-step sequence beginning with simple pyrroles.

Mutant *casper* embryos were dechorionated at 24 hpf, grown to 48 hpf, and arrayed in 12-well plates with 1 mL of pure E3 medium (Methylene Blue-free, PTU-free). Chemicals were resuspended in 100% DMSO and added to E3 medium at indicated concentrations (0.3% DMSO [v/v] served as vehicle control). Toxicity curves of synthetic prodigiosenes were conducted by treating 48 hpf embryos for 72 hours at 35°C. The optimal dose was calculated as 50% of the maximum tolerated dose [MTD].

2.18 TISSUE CULTURE & CELL LABELLING

Human K562 cells (gift of Drs. D Small and R Arceci [Johns Hopkins School of Medicine]) were cultured in RPMI containing 10% (v/v) FBS with the addition of penicillin/streptomycin. For labelling, 5 million cells were pelleted by centrifugation for 5 minutes at 1200 rpm. The cell pellet was resuspended in PBS containing 5 µg/mL CM-DiI (Invitrogen) and incubated for 5 min at 37°C followed by an additional 20 min at 4°C. The suspension was centrifuged for 5 min at 1200 rpm and the pellet washed twice with PBS to remove excess dye. After the final wash the pellet was re-suspended in 500 µl of media to produce a final cell concentration of 10⁶ cells/mL.

2.19 XENOTRANSPLANTATION OF HUMAN LEUKAEMIA CELLS INTO ZEBRAFISH EMBRYOS, DISSOCIATION, & IMMUNOFLUORESCENCE

Mutant *casper* zebrafish embryos at 48 hpf were anaesthetized with 0.090 mg/mL Tricaine (Sigma-Aldrich) and placed in a Petri dish on their sides on a ramp comprised of 1.5% (w/v) agarose. The cell transplantation protocol was adapted from [Haldi *et al.* 2006](#) and described in [Corkery *et al.* 2011](#). Briefly, CM-DiI-labeled K562 cells were loaded into in pulled glass micropipette pulled by a P-97 Flaming/Brown micropipette puller (Sutter Instrument Co., Novato, CA). The needle was placed in a PLI-100 Pressure Injector (Harvard Apparatus, Holliston, MA) and 25-50 cells were delivered, as a single injection, into the yolk sac of each embryo (Injection conditions: 40ms pulse time, 4.6 psi positive pressure) while under observation using a Leica MZ16F modular stereomicroscope (Leica Microsystems GmbH, Wetzlar, Germany). Following injection embryos were allowed to recover at 28°C for 1 hour before transfer to 35°C where they remained for the rest of the experiment. At 24 hours post injection (hpi), only embryos with a uniform fluorescent cell mass at the site of injection were used for proliferation studies. Embryo xenotransplanted with human cancer cells were then maintained in groups of 15-20 within individual Petri dishes prior to drug treatment. At 24 hpi, prodigiosenes were added directly to the fish water, at indicated concentrations, and embryos were incubated for 72 hours until 96 hpi. Embryos treated with 0.3% (v/v) DMSO served as a negative control for drug efficacy. Embryos treated with 20 µM

imatinib mesylate (a targeted inhibitor for the human *BCR-ABL1* mutation in K562 cells) served as a positive control for drug efficacy (Corkery *et al.* 2011).

At 24 hpi and 72 hpi (with or without drug treatment), populations of embryos were dissociated (as above). Specifically, 15-20 embryos were incubated in 1.2 mL Protease solution with 27 μ L collagenase for 15-45 minutes at 35°C, and homogenized every 10 minutes with a Pasteur pipette. Dissociation was considered complete once eyes had fully detached from embryos and remaining embryo bodies were adhered together. Reaction was stopped and sample was centrifuged as usual. Only 0.9X PBS/5% (v/v) FBS was used to resuspend cells after centrifugation, at a volume of 10 μ L per embryo.

It was attempted to immunostain single-cell suspensions against the CD33, CD34, and CD45 cell surface marker to differentiate between human and zebrafish cells. Between washing and incubation steps, cells were pelleted using centrifugation at 350 x g for 5 minutes and supernatant was discarded. Single cell dissociations were fixed in 4% (w/v) PFA for at least 2 hours at 4°C. Cells were then washed 3 x 5 minutes in 1X PBS, and blocked in 1X PBS with 5% (v/v) donkey serum (Invitrogen) for 20 minutes at room temperature. Mouse anti-CD34 IgG (1°) antibodies (Cedarlane, Burlington, NC, USA), or a combination of anti-CD33 and CD45 IgG (1°) antibodies (Cedarlane) was added at a dilution of 1:250 and cells were incubated overnight at 4°C. Cells were washed 3 x 5 minutes in 1X PBS and then incubated in Alexa Fluor® 647 donkey anti-mouse IgG (2°) antibody (1:200; Invitrogen) in blocking solution for 2 hours in the dark at room temperature. Cells were washed 3 x 5 minutes in 1X PBS and imaged within one week.

2.20 IMAGING & IMAGEJ ANALYSIS OF Z-STACK PROJECTIONS

Cytological and histopathological analysis of zebrafish sections was performed on-site at the IWK Health Centre with the assistance of double-board-certified haematologist/haematopathologist, Dr. ER McBride. Tissue sections were imaged using an Olympus BX51 microscope (2X, 40X, and 100X objectives) with an Olympus DP25 color camera (Olympus America Inc., Center Valley, PA, USA). Microscopy images of embryos were captured on a Leica MZ16F microscope (5X objective) with a Leica DFC 490 camera running Leica Application Suite, Version 2.4.0 R1 [Build :795] (Leica). For

WISH assays, blood cell counts were performed by marking cells in Adobe Photoshop CS2. Z-stack projections were captured on an inverted Zeiss AxioObserver.Z1 microscope (5X and 10X objectives) equipped with a Colibri LED light source and a Zeiss AxioCam HRm camera running Zeiss AxioVision, Release 4.7.1 software (Carl Zeiss Microimaging GmbH, Gottingen, Germany). Where applicable, Z-stack acquisitions were performed with equal exposure time and Z-slice distance. All acquisitions were performed with a 'gamma' value of 1. Brightness and contrast of micrographs were adjusted using Adobe Photoshop CS2.

Fluorescence micrographs were processed using MacBiophotonics ImageJ, Version 1.43m (as in ref. 24 with modifications), a modification of NIH software (available at <http://www.macbiophotonics.ca/downloads.htm>).

2.20.1 Embryo Immunofluorescence

In keeping with other published reports (Jette *et al.* 2008; Sidi *et al.* 2008), embryo tails in each micrograph were aligned from the mid-yolk sac to the end of the yolk tube extension using Adobe Photoshop CS2. Background fluorescence was corrected using a rolling ball radius of 50.0. Four to five regions of interest (ROIs) were chosen along the aligned section of the mid-tail region only and applied equally to all embryos in an experiment. After thresholding, *Area Fraction* was calculated for each ROI to determine a mean fluorescence value per unit area for each embryo.

2.21 STATISTICS

Micrographs are representative of at least 2 independent trials with 15-20 embryos per genotype. Data from qRT-PCR is representative of at least 2 biological replicates, each with 45-50 embryos per genotype, and each round of amplification was performed in triplicate on two dilutions of cDNA. Data reported as mean values +/- SEM. Statistical analysis was performed using two-tailed student's *t*-tests.

Table 2.1. Primer sequences for pCS2+ vector construction.

Gene	Accession	Forward (fwd) primer sequence*	Reverse (rvs) primer sequence*	Amplicon size
<i>NHA9</i>	-	<u>GGG GAC AAG TTT GTA</u> <u>CAA AAA AGC AGG CTT</u> <u>ACC GAA GCG GCG GTC</u> GGT G [▲]	<u>GGG GAC CAC TTT GTA</u> <u>CAA GAA AGC TGG GTA</u> TCA CTC GTC TTT TGC TCG	1.9 kb
<i>ctnnb1-b</i> [β-catenin (S/T→A)]	NM_001090576.1	<u>GGG GAC AAG TTT GTA</u> <u>CAA AAA AGC AGG CTT</u> <u>ATC GAT CCT CCC TTT</u> ATC C	<u>GGG GAC CAC TTT GTA</u> <u>CAA GAA AGC TGG GTA</u> TTA CTT GTC GTC GTC GTC [†]	2.5 kb
<i>Hoxa9</i>	NM_010456.2	<u>GGG GAC AAG TTT GTA</u> <u>CAA AAA AGC AGG CTT</u> <u>ACC GAA GCG GCG GTC</u> GGT G [▲]	<u>GGG GAC CAC TTT GTA</u> <u>CAA GAA AGC TGG GTA</u>	1.0 kb
<i>Meis1</i>	NM_010789.2	<u>GGG GAC AAG TTT GTA</u> <u>CAA AAA AGC AGG CTT</u> <u>AAT CGA ATT CCT GCA</u> GCC C [▲]	<u>GGG GAC CAC TTT GTA</u> <u>CAA GAA AGC TGG GTA</u> TTA CAT GTA GTG CCA CTG	1.3 kb

* underlined sequences are *attB* extensions at the 5' and 3' ends

[▲] primer amplifies multiple cloning site (MCS) sequence at 5' end

[†] *ctnnb1-b** rvs primer amplifies repetitive sequence for 3' FLAG tags

Table 2.2. MO sequences for blocking gene expression.

Gene	Accession	Target site	MO sequence	Injected concentration
<i>bcl2l1</i> / <i>bcl-x_L</i> ¹	NM_131807.1	atg/5'UTR	CCAGTTCTCGGTTATAGTAAGACAT	1 mM
<i>dmnt1</i> ²	NM_131189	atg/5'UTR	ACAATGAGGTCTTGGTAGGCATTTC	0.75 mM
<i>meis1</i> ³	NM_131893.1	atg/5'UTR	GTATATCTTCGTACCTCTGCGCCAT	1 mM

¹ Jette C, Carbonneau S, personal communication

² Rai *et al.* 2006

³ Pillay *et al.* 2010

Table 2.3. Primer sequences for genotyping and qRT-PCR.

Gene target	Accession	Forward (fwd) primer sequence	Reverse (rvs) primer sequence	Amplicon size
<i>sp1::NHA9*</i>	-	TAC CCA CAC ACC CCA AAA AT	GAG GCC TCC AGT ATT GTT GC	2 kb (un-activated); 775 bp (Cre-activated)
<i>Cre*</i>	NC_005856.1	GCC TGC ATT ACC GGT CGA TGC CAA CGA	GTG GCA GAT GGC GCG GCA ACA CCA	720 bp
<i>efla*</i>	NM_131263.1	TCT GTT GAG ATG CAC CAC GA	TTG GAA CGG TGT GAT TGA GG	701 bp
<i>gata1a</i> ¹	NM_131234.1	GAG ACT GAC CTA CTG CCA TCG	TCC CAG AAT TGA CTG AGA TGA G	110 bp (amplicon crosses intron 2)
<i>actb1 / β-actin1</i> ^{†2}	NM_131031.1	TGC TGT TTT CCC CTC CAT TG	TTC TGT CCC ATG CCA ACC A	66 bp (amplicon does not cross intron)
<i>bbc3 / puma</i> ³	NM_001045472.2	ATG ATG CCT TCA GCT TGG AC	CCT CTG AGG AGC TCT GGT TG	132 bp (amplicon crosses intron 2)
<i>bcl2</i>	NM_001030253.2	TGT GCG TGG AAA GCG TCA ACC	GAA GGC ATC CCA ACC TCC ATT TTC	125 bp (rvs spans exon @ nt 607/608)
<i>bcl2l1 / bcl-xL</i>	NM_131807.1	TGT GTT ATG GGT ATG AGC CAT TGC	TGT TGC TCG TTC TCC GAT GTC	126 bp (fwd spans exons @ nt 102/103)
<i>ccnd1</i>	NM_131025.4	ACA GCA ACC TGT TGA ATG AC ⁴	GGC CAG ATC CCA CTT CAG TT ⁴	404 bp (amplicon crosses introns 1 and 2)
<i>cdkn1a</i> ⁵ / <i>p21</i> ^{waf1/cip1}	XM_001923789.2	AGC TGC ATT CGT CTC GTA GC	TGA GAA CTT ACT GGC AGC TTC A	399 bp (amplicon does not cross intron)
<i>dmnt1</i>	NM_131189	CAG CGC TCA AGA ACC ACA GG	TCT GAG ATG CCT GCT TGA TGG	107 bp (fwd span exons @ nt 3244/3245)
<i>efla</i> ^{†6}	NM_131263.1	CTG GAG GCC AGC TCA AAC AT	ATC AAG AAG AGT AGT ACC GCT AGC ATT AC	87 bp (fwd spans exons @ nt 695/696)
<i>meis1</i>	NM_131893.1	GCC AGC AGC ACA TGG GAA TCA G	TGG CAT GCT CTG TAG TCT TCC CC	141 bp (rvs spans exons @ nt 1606/1607)
<i>ptger1a</i>	NM_001166333.1	AGC AGG AGT CTG TTC GTC TCA GC	TCA GAC CGA AGA TCA GCA GAG GG	141 bp (rvs spans exons @ nt 927/928)
<i>ptgs1</i> ⁷	NM_153656.1	TAT GGC TTG GAG AAG CTG GT	CGA TTC AAC GAT GAC CCT CT	117 bp (amplicon crosses intron 9)
<i>ptgs2a</i> ⁷	NM_153657.1	CCAGACAGATGCGCT ATCAA	GAC CGT ACA GCT CCT TCA GC	126 bp (amplicon cross intron 8)

Table 2.3 (continued). Primer sequences for genotyping and qRT-PCR.

<i>ptgs2b</i> ⁷	NM_001025504.2	CAG GAA ACG CTT CAA CAT GA	CAG CAT AAA GCT CCA CAG CA	119 bp (amplicon crosses intron 9)
----------------------------	--------------------------------	-------------------------------	-------------------------------	--

* primers used for genotyping (all other sequences used for qRT-PCR)

[†] *actb1* / β -*actin1* and *ef1a* were selected as housekeeping genes for qRT-PCR (McCurley and Callard 2008; Tang *et al.* 2007)

¹ Pillay *et al.* 2010

² Rojo *et al.* 2007

³ Pyati U, personal communication

⁴ Duffy *et al.* 2005

⁵ Liu TX *et al.* 2003

⁶ Tang *et al.* 2007

⁷ Yeh *et al.* 2009

Table 2.4. ProK permeabilization of zebrafish embryos at various developmental stages.

Embryonic stage	Length of treatment (min) when using PTU E3 medium	Length of treatment (min) when using 1X bleach solution	ProK concentration (μg/mL)
24 hpf	10	5	1
30 hpf	20	10	1
36 hpf	30	15	1
48 hpf	45	22	1
55 hpf	60	30	1
60 hpf	25	12	10
72 hpf	30	15	10

Adapted from Talbot JC, <https://wiki.zfin.org/display/prot/Triple+Fluorescent+In+Situ>

Table 2.5. SDS-PAGE recipes for Western blotting (all solutions prepared [w/v]).

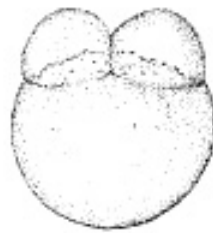
	Resolving				Stacking
	5%	10%	12%	15%	4%
MW range (kDa)	60 – 200	16 – 70	14 – 60	12 – 45	
mqH₂O	3.05 mL	2.42	2.18	1.8	1.59
40% (w/v) Acrylamide/Bis- Acrylamide (37.5:1)	625 µL	1.25 mL	1.5	1.875	250 µL
1.5 M Tris-HCl, pH 8.8	1.25 mL	1.25	1.25	1.25	-
0.5 M Tris-HCl, pH 6.8	-	-	-	-	625 µL
10% (w/v) SDS	50 µL	50	50	50	25
10% (w/v) ammonium persulphate (APS)	25 µL	25	25	25	10
Tetramethylethylene- diamine (TEMED)	3.33 µL	3.33	3.33	3.33	2
TOTAL	5 mL				2.5 mL

Figure 2.1 (next four pages). Timeline of zebrafish developmental stages.

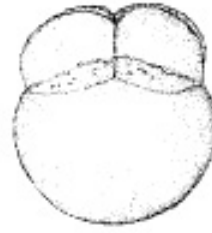
The following four pages depict camera lucida sketches of the embryo at selected stages of development. For the early stages ('1-cell' to '90% epiboly'), the animal pole (consisting of embryo cells) is oriented to the top and the vegetal pole (consisting of yolk sac containing maternally-deposited nutrients, RNAs, and proteins) is oriented to the bottom. For the later stages ('bud' and beyond), the anterior (head) end of the embryo is oriented to the top, the posterior (tail) end is oriented to the bottom, the ventral (front) side is oriented to the left, and the dorsal (back) side is oriented to the right. The only exception to these viewing conventions is for the 'germ-ring' and 'shield' stages during gastrulation, where two animal polar (AP) views are shown below their side view counterparts. 'Face-on' views are shown throughout cleavage and blastula stages; *i.e.* from '1-cell' to '50% epiboly', after which gastrulation begins. After 'shield' stage, the views are of the embryo's left side, but before 'shield' arises, one cannot reliably ascertain which side is which. Pigmentation is not shown. Arrowheads indicate the early appearance of some key diagnostic features at the following stages: '1k-cell' = yolk syncytial layer (YSL) nuclei; 'dome' = the doming yolk syncytium; 'germ ring' = germ ring; 'shield' = embryonic shield; '75% epiboly' = Brachet's cleft; '90% epiboly' = blastoderm margin closing over the yolk plug; 'bud' = polster; '3-somite' = third somite; '6-somite' = eye primordium (upper arrow), Kupffer's vesicle (lower); '10-somite' = otic placode; '21-somite' = lens primordium; 'prim-6' = primordium of the posterior lateral line (on the dorsal side), hatching gland (on the yolk ball); 'prim-16' = heart; 'high-pec' = pectoral fin bud. Scale bar = 250 μm . Adapted from [Kimmel *et al.* 1995](#)



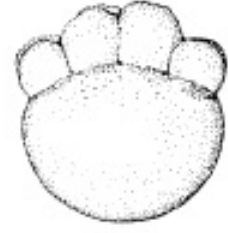
1-cell
0.2 h



2-cell
0.75 h



4-cell
1 h



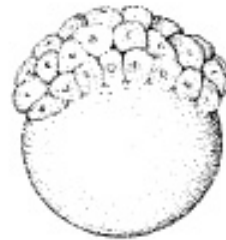
8-cell
1.25 h



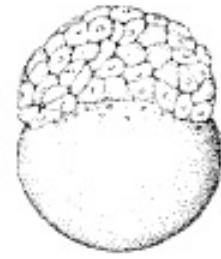
16-cell
1.5 h



32-cell
1.75 h



64-cell
2 h



128-cell
2.25 h



256-cell
2.5 h



512-cell
2.75 h



1k-cell
3 h



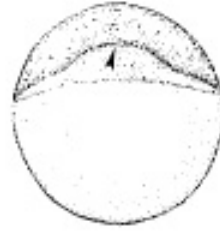
high
3.3 h



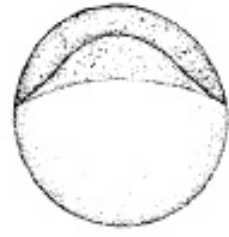
oblong
3.7 h



sphere
4 h



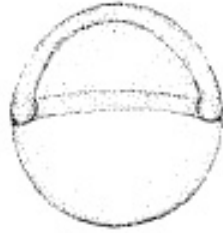
dome
4.3 h



30%-epiboly
4.7 h



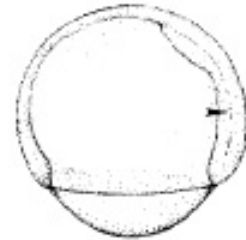
50%-epiboly
5.3 h



germ ring
5.7 h



shield
6 h



75%-epiboly
8 h



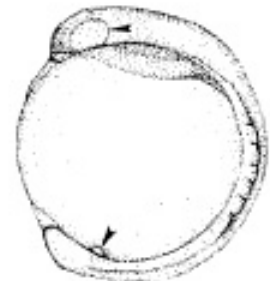
90%-epiboly
9 h



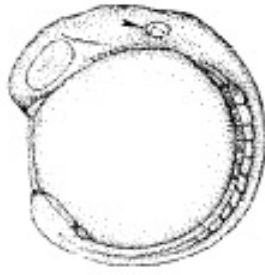
bud
10 h



3-somite
11 h



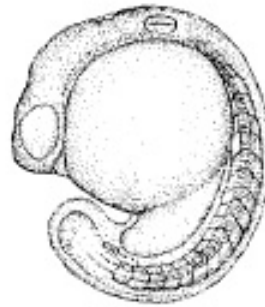
6-somite
12 h



10-somite
14 h



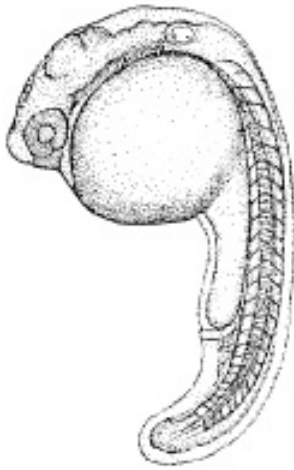
14-somite
16 h



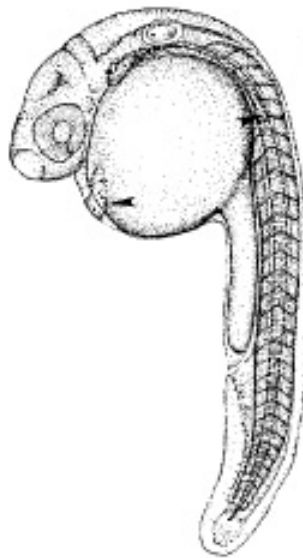
18-somite
18 h



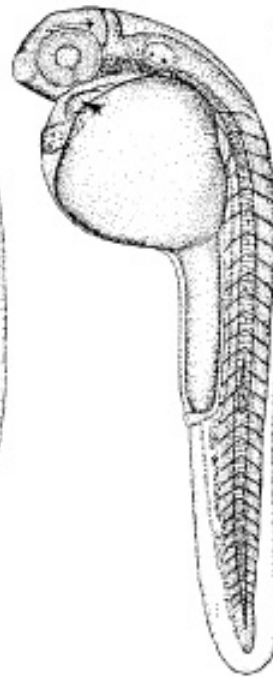
21-somite
19.5 h



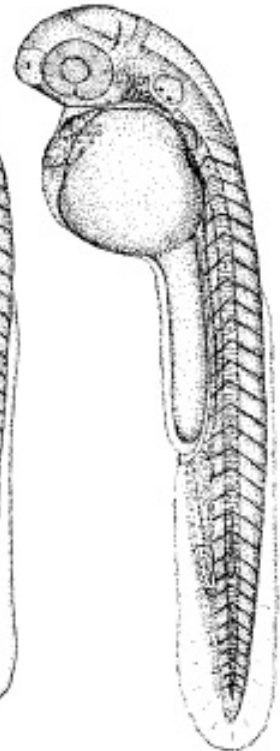
26-somite
22 h



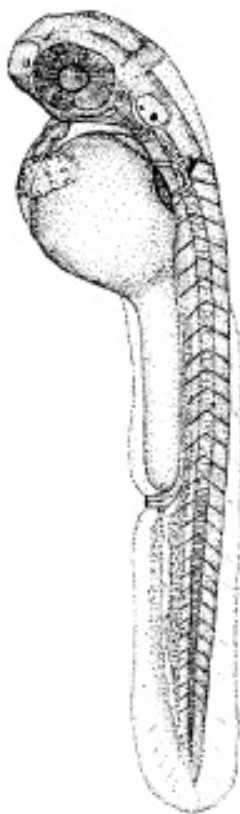
prim-6
25 h



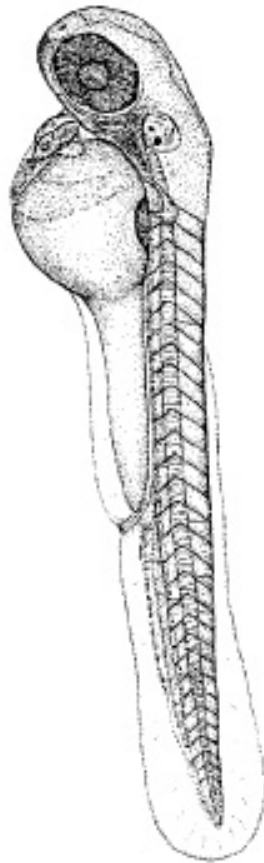
prim-16
31 h



prim-22
35 h



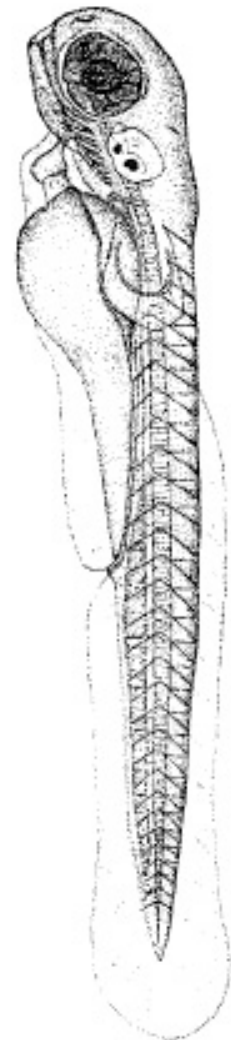
—
high pec
42 h



long pec
48 h



pec fin
60 h



protruding
mouth
72 h

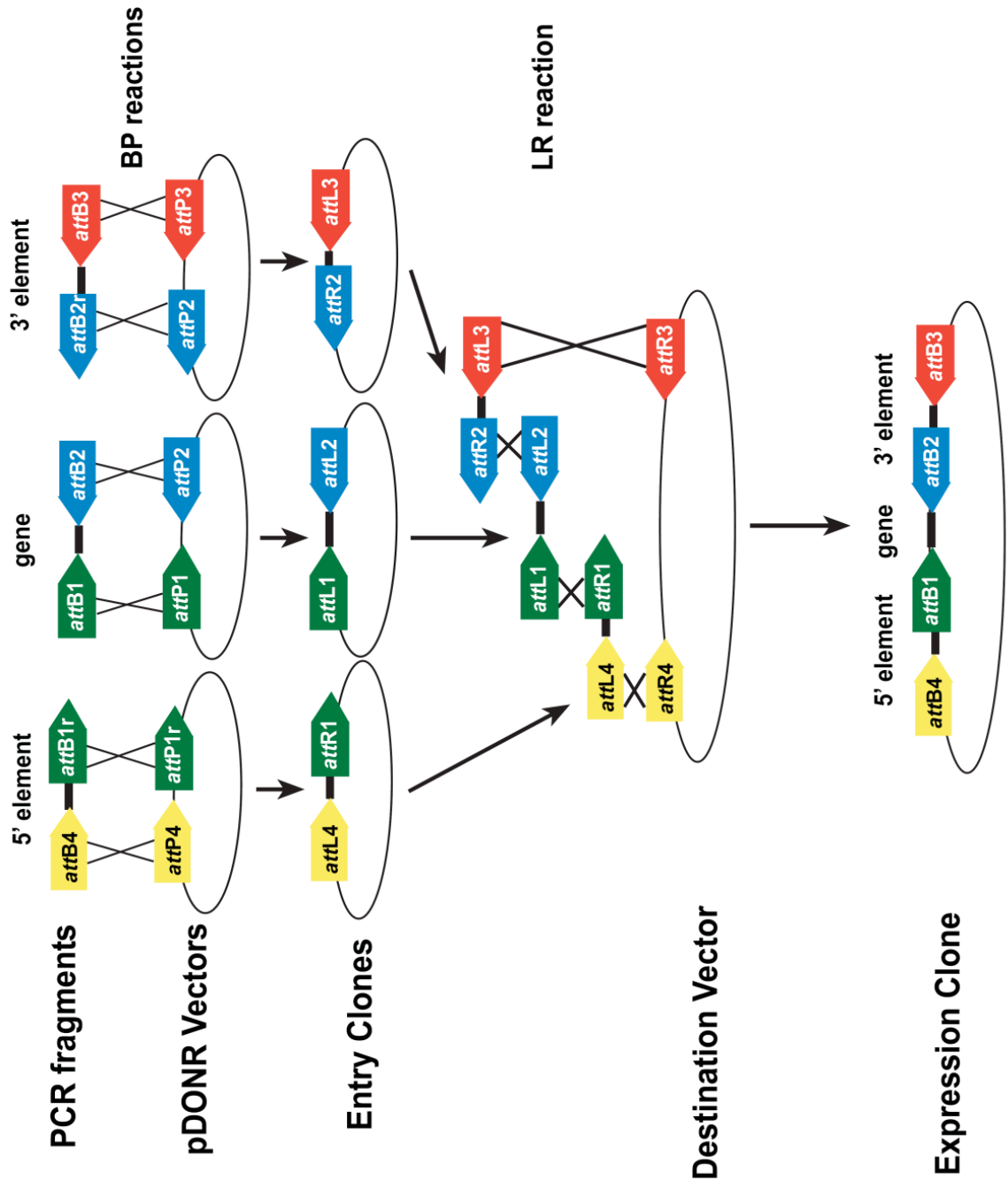


Figure 2.2. Schematic of vector assembly using Gateway® (Invitrogen) cloning technology.

Gateway® cloning permits a modular ‘mix-and-match’ of genetic elements (promoters, genes/ORFs, tags) to create novel expression vectors. Using site-specific recombination *in vitro*, desired genetic sequences are inserted into uniquely identifiable donor vectors (called ‘entry clones’), which are then recombined with proper directionality into a final destination vector (called ‘expression clones’). Site-specific recombination is achieved by the use of DNA *att* sequences, which are target sites for viral genome integration during bacteriophage λ infection of *E. coli* bacteria.

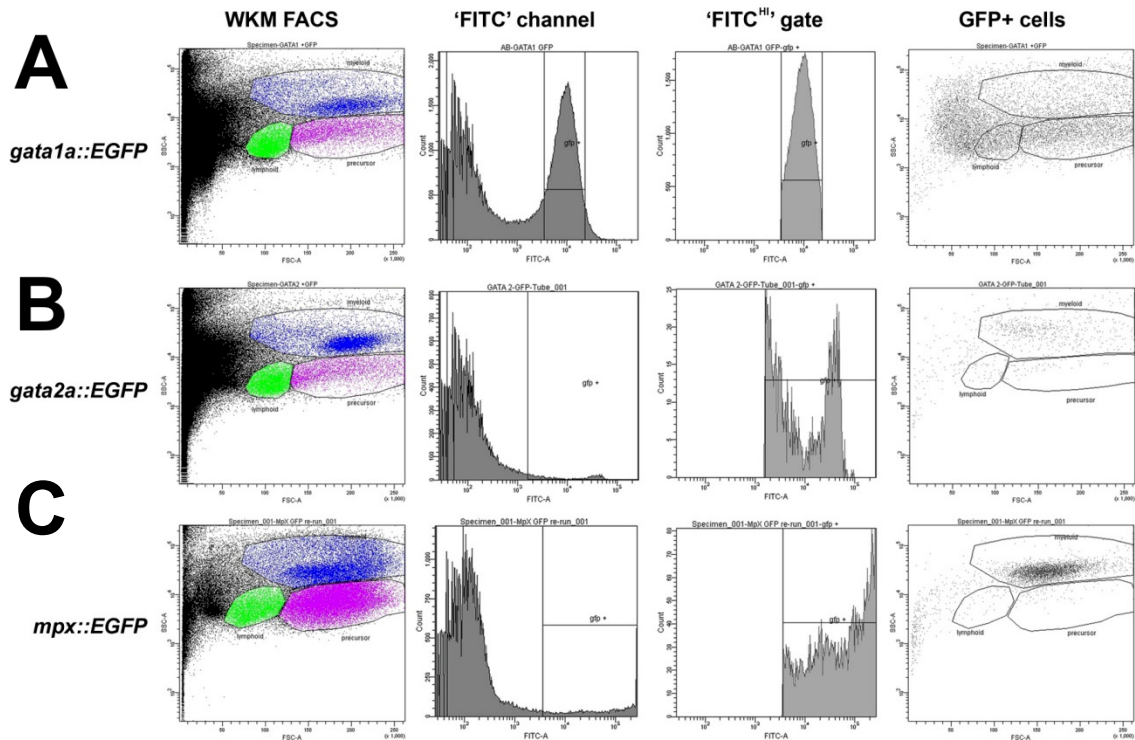


Figure 2.3. Assignment of blood cell gates on FACS Aria™ I.

WKM was collected from (A) *Tg(gata1a::EGFP)*, (B) *Tg(gata2a::EGFP)*, and (C) *Tg(mpx::EGFP)* transgenic adult zebrafish and analyzed by FACS (leftmost panels). WKMs were interrogated for fluorescence in the 'FITC' channel and gated by 'FITC^{HI}' (middlemost panels) to identify GFP+ cells. By FSC and SSC, GFP+ cells scattered to predicted plot locations (rightmost panels). Dot plots are representative of 2 independent trials.

(A) *Tg(gata1a::EGFP)* labels erythroid cells, which scatter unevenly.

(B) *Tg(gata2a::EGFP)* labels eosinophils, which scatter to SSC^{HI} within the 'myelomonocyte' gate.

(C) *Tg(mpx::EGFP)* labels neutrophils, which scatter to SSC^{MID} within the 'myelomonocyte' gate.

New abbreviations used: FITC = fluorescein isothiocyanate; FSC = forward scatter; *mpx* = myeloperoxidase; SSC = side scatter.

Acknowledgement: lab technician, Sandy Edgar, operated FACS Aria™ I and assisted analysis.

CHAPTER 3 ***NUP98-HOXA9*-TRANSGENIC ZEBRAFISH DEVELOP A MYELOPROLIFERATIVE NEOPLASM**

3.1 BACKGROUND

3.1.1 Designing A Zebrafish Model Of *NUP98-HOXA9* Expression

As discussed in **CHAPTER 1**, *homeobox A9 (HOXA9)* is upregulated in ~80% of human AML cases, often along with its transcriptional co-factor *myeloid ecotropic integration site 1 (MEIS1)* (Lawrence *et al.* 1999), and is considered a high-risk indicator. One way in which *HOXA9* can be overexpressed is through the t(7;11)(p15;p15) chromosomal translocation, yielding the *NUP98-HOXA9 (NHA9)* fusion oncogene (Borrow *et al.* 1996; Nakamura *et al.* 1996b). The molecular mechanism by which the *HOXA9* and *NHA9* oncogenes promotes the development and progression of high-risk AML remains largely unknown, despite studies in mammalian models, both *in vitro* (Calvo *et al.* 2000; Calvo *et al.* 2001; Calvo *et al.* 2002; Chung *et al.* 2006; Ghannam *et al.* 2004; Kasper *et al.* 1999; Takeda *et al.* 2006) and *in vivo* (Kroon *et al.* 1998; Kroon *et al.* 2001; Thorsteinsdottir *et al.* 2001; Thorsteinsdottir *et al.* 2002; Iwasaki M *et al.* 2005). The recent identification of a Wnt/ β -catenin mechanism underlying the production of AML in mice that co-overexpression mouse *Hoxa9* and *Meis1* (Wang Y *et al.* 2010) certainly helps to establish new research directions. However, the pathological kinetics and stages of AML are different when comparing mouse *Hoxa9;Meis1* co-overexpression with the human *NHA9* mutation. Co-overexpression of mouse *Hoxa9* and *Meis1* in reconstituted mouse bone marrow leads to the direct establishment of AML after a short latency phase of 3 months post injection (Wang Y *et al.* 2010). However, overexpression of human *NHA9* in mouse bone marrow produces disease that passes through a longer latency phase, with an initial presentation of MPN prior to overt AML (*i.e.* appearance of AML blast cells and/or 25% myeloblasts in marrow). Retrovirally-transduced *NHA9* chimeric mice develop MPN as late as 8 to 15 months post-bone marrow transplantation, which progressed to AML following a latency period of at least 4 months (Kroon *et al.* 2001). In another study, 22% of germline transgenic mice harbouring *Tg(Ctsg::*NUP98-HOXA9*)* developed MPN and subsequent AML by 15 months (Iwasaki M *et al.* 2005).

The development of new animal models that have the capacity to support high-throughput chemical and genetic modifier screens, such as the zebrafish, would be of great help to shed light on the elusive molecular mechanisms that are distinct to high-risk myeloid leukaemia in general, and to *NHA9*-induced AML in particular.

We hypothesized that we could employ the advantages of the zebrafish animal model to create a model of *NHA9* myeloid leukaemogenesis, which would recapitulate critical aspects of human high-risk AML. We established a germline, Cre/*lox*-inducible transgenic zebrafish harbouring the human *NHA9* fusion oncogene under the control of the zebrafish *spi1* myeloid promoter. We monitored *Tg(spi1::loxP-EGFP-loxP::NHA9)* adult fish for incidence of AML and assessed embryos for defects in early haematopoiesis (Calvo *et al.* 2002), cell cycle (Faber *et al.* 2009), and apoptosis (Wermuth and Buchberg 2005). Importantly, 23% of adult *NHA9* fish developed a myeloproliferative neoplasm (MPN) at 19 to 23 months of age.

3.2 EXPERIMENTAL FINDINGS

3.2.1 Transgenic Zebrafish Express Human *NHA9* In A Cre/*lox*-Inducible Manner

The human *NHA9* fusion oncogene was expressed under the control of the 9.1 kb zebrafish *spi1* early myeloid promoter (Hsu *et al.* 2004). In zebrafish, *spi1* labels embryonic myeloid cells at the mRNA level from 12 to 48 hours post fertilization (hpf), at the protein level until at least 5 days post fertilization (dpf) (Le Guyader *et al.* 2008), and is expressed at low levels in adult kidney marrow (Hsu *et al.* 2004), which corresponds to mammalian bone marrow. We cloned human *NHA9* downstream of zebrafish *spi1* promoter an *enhanced green fluorescent protein (EGFP)* cassette flanked by Cre/*lox* recombination sites (*loxP-EGFP-loxP*; shortened to '*lGI*') (Figure 3.1A). Thus, in order for *NHA9* to be expressed, this “floxed” *EGFP* cassette requires excision by the Cre molecular recombinase. This Cre/*lox*-inducible strategy allows expression of the human *NHA9* fusion oncogene after the essential processes of gastrulation are complete (Langenau *et al.* 2005a; Le *et al.* 2007).

Germline transmission of the *NHA9* transgene was monitored by fluorescence microscopy to observe expression of the floxed *EGFP* cassette. This can only be performed in the un-activated condition, given that Cre-mediated recombination removes this cassette and thus turns off expression of *EGFP*. In *NHA9*-transgenic embryos, *EGFP* expression could be observed as early as the two-cell stage of development (**Figure 3.1Bi**), suggesting that the transgene was being expressed ubiquitously. Furthermore, by 18 hpf and continuing to 28 hpf, *EGFP* expression was clearly observed in off-target tissues, such as the central nervous system (CNS) and musculature. This was in addition to *EGFP* expression in targeted myeloid cells, given that punctate GFP+ blood cells could be observed at the anterior lateral plate mesoderm (ALPM) in the head region, the intermediate cell mass (ICM) in the mid-body region, and the posterior blood island (PBI) in the tail region (**Figure 3.1Bi**, *white arrowheads*). A complete timeline of transgene expression is provided in **Figure 3.2**, which shows that ubiquitous transgene expression persists at variable levels until at least 7 dpf. This off-target expression pattern is consistent with the one previously observed with the zebrafish 9.1 kb *spi1* promoter (Hsu *et al.* 2004), and so we were not concerned by our findings. However, to solidly confirm that the *NHA9* transgene was being expressed within the haematopoietic compartment, we performed FACS analysis and cytospin of large, GFP+ cells from *NHA9*-transgenic embryos at 28 hpf. Analysis of cell and nucleus morphology by Wright-Giemsa stain confirmed that the *NHA9* transgene was being expressed in myeloid lineage at multiple stages of cell development, including immature precursors and mature neutrophils (**Figure 3.1Bii**).

To turn on the expression of *NHA9*, we outcrossed *Tg(spi1::IGL::NHA9)* fish to the *Tg(hsp70::Cre)* activator line, which controls the expression of *Cre* from the *heat shock protein 70* (*hsp70*) promoter. To activate *Cre* and therefore excise the *IGL* cassette, *NHA9;Cre* heterozygous embryos would be subjected to heat-shock (1 hour incubation at 37 to 39°C). Cre-mediated recombination of the transgene was monitored by PCR amplification of genomic DNA from embryos. Excision of the *IGL* cassette converts a 2 kb amplicon to a 775 bp amplicon, which was robustly observed in 28 hpf *NHA9;Cre* heterozygous embryos that were activated by heat-shock at 24 hpf (designated '*NHA9* [+*Cre*]'; **Figure 3.3A**, white arrow). Some expected minimal recombination was observed

in un-activated (*i.e.* not heat-shocked) *NHA9;Cre* heterozygotes (designated '*NHA9* [-*Cre*]'), due to known "leakiness" of the *Tg(hsp70::Cre)* zebrafish line (Le *et al.* 2007).

We further ventured to confirm expression of the *NHA9* transgene by performing Western blot on embryo protein lysates at 28 hpf, using an antibody against the N-terminal human NUP98 peptide. We were able to detect the human *NHA9* fusion oncoprotein (approximately 50 kDa [Kroon *et al.* 2001]) in *NHA9* (+ *Cre*) embryo lysates (**Figure 3.3B**, black arrow), but not in *AB* wild-type nor un-activated *IGF1::NHA9* embryo lysates, which had also been subjected to heat-shock. Historically, zebrafish studies have not often used Western blots to confirm expression of their gene of interest, which is due, in part, to the paucity of available antibodies that faithfully cross-react against the homologous zebrafish protein. For example, the 98 kDa native zebrafish *nup98* protein was not recognized on our blots by the chosen primary antibody. Thanks to the human origin of the *NHA9* transgene, we attempted our Western blot hoping to avoid these known difficulties. However, our anti-NUP98 antibody also appeared to recognize an unknown band of slightly higher molecular weight (**Figure 3.3B**, white arrow) above the suspected human *NHA9* band at 50 kDa. This unknown band was observed in all control lysates, and in at least three of our Western blot trials, so we have called it 'non-specific' ('n.s.'). It did not escape our notice that there appears to be a higher concentration of this non-specific band in the *NHA9* (+ *Cre*) embryo lysate. Similar blotting patterns were observed in all of our Western blots with the chosen anti-NUP98 antibody. Other trial runs of Western blots displayed a more equal loading of the non-specific band, but the representative Western blot in **Figure 3.3B** was chosen for its superior visual clarity of the suspected human *NHA9* band at 50 kDa. In the future, use of a mammalian NUP98 blocking peptide may help to confirm the identity of the 50 kDa band.

3.2.2 *NHA9*-Transgenic Zebrafish Develop Malignant Myeloid Infiltrates

At 24 hpf, *NHA9;Cre* heterozygous embryos were heat-shocked to excise the *IGF1* cassette, and these fish were then grown to adulthood. Between 19 to 23 months of life, many *NHA9* (+ *Cre*) zebrafish presented with abdominal masses (**Figure 3.4I, M**) and/or laboured swimming. On whole fish histological sections, we identified 6 out of 26 (23%) adult *NHA9* (+ *Cre*) fish with kidney hypertrophy (**Figure 3.4J, N**), which is the site of

definitive haematopoiesis in adult zebrafish. In affected kidneys, we found evidence of highly-disorganized, malignant infiltrates composed of pleiomorphic, mitotically-active cells that display characteristic myeloid morphologies (**Figure 3.4K, O** and insets). Mature neutrophils with horseshoe and multi-lobed nuclei were easily identified on H/E staining. Moreover, we confirmed that a portion of these infiltrating cells were myeloid, using PAS staining for eosinophils and mast cells (**Figure 3.4L, P**; black arrows and insets) (Dobson *et al.* 2008). Furthermore, these cells were intact (*i.e.* not degranulated), which suggests that these infiltrates were not the result of inflammation or infection. This myeloid pathology was not observed in age-matched *AB* wild-type fish (**Figure 3.4A – D**), nor in un-activated *IGL::NHA9* fish (**Figure 3.4E – H**). Normal kidney structures, such as glomeruli and tubules were nearly absent in affected *NHA9 (+ Cre)* fish compared to controls and unaffected *NHA9 (+ Cre)* animals (compare **Figure 3.4C, G, K, O** and **Figure 3.5A – D**), and any remaining structures were undergoing invasion or suffering stress due to the myeloid infiltrate (**Figure 3.5D** shows pyknotic nuclei of epithelial cells suggestive of apoptosis). Overall, this pathology is consistent with MPN, a pre-leukaemia condition characterized by increased numbers of mature or semi-mature myeloid cells. This phenotype was encouraging because it is reminiscent of mice that express human *NHA9*: these *NHA9* mice also develop a long latency, polyclonal MPN prior to onset of AML (Iwasaki M *et al.* 2005; Kroon *et al.* 2001). However, none of the *NHA9* zebrafish were found to display progression to overt AML (*i.e.* appearance of AML blast cells and/or 25% myeloblasts in marrow). However, three affected fish were identified with infiltration of liver, gastrointestinal tract, and/or pancreas (**Figure 3.5E – L**), which may represent more advanced stages of zebrafish MPN and perhaps the beginnings of clonal expansion.

3.2.3 Difficulties Labelling Transgenic Myeloid Cells In Adult Zebrafish Tissue Sections By IHC Or ISH

Reviewers of our work have raised questions about the morphology of MPN cells in our *NHA9* zebrafish and the markers that they express. They have requested myeloid-specific stains to confirm our interpretation of the pathology. I tried using both myeloperoxidase (MPO) stain to label granulocytes, Sudan Black B (Sigma-Aldrich)

stain to label granulocytes and monocytoïd cells, non-specific esterase (NSE) stain to label monocytes, and keratin counterstain for structural kidney tissue. However, these stains were unsuccessful in our paraffin-embedded fish tissues, even in positive controls. We reviewed the literature and discussed staining protocols with a number of our zebrafish haematology colleagues and these stains have not to date been successfully applied to adult zebrafish tissue sections (Lieschke G, Huttenlocher A, Langenau D, personal communication). PAS has been shown by our group and others to label subpopulations (eosinophil/basophil/mast cell lineages) within the zebrafish myeloid lineage (Balla *et al.* 2010; Da'as *et al.* 2011; Dobson *et al.* 2008). Though PAS does not universally stain all cells within the myeloid infiltrate in affected *NHA9* adult zebrafish kidney, we did observe a dramatic increase in the number of PAS+ cells compared to wild-type and unaffected *NHA9* controls. The results of these stains were included as panels in the final published versions of **Figure 3.4** and **Figure 3.5**. I also attempted to perform *in situ* hybridization (ISH) on our tissue sections using RNA probes for zebrafish *mpx* and *lcp1*. These were also unsuccessful, likely due the degradation of tissue RNA in paraffin-embedded tissues (Seibert J, Ellis L, personal communication). Cryostat freeze-fixed tissue sections respond better to ISH staining, but all of our affected fish specimens had already been fixed by paraffin-embedding prior to this knowledge.

Reviewers also requested that we interrogate the zebrafish MPN cells for GFP expression through IHC. However, anti-GFP antibody is also unlikely to be informative as the GFP cassette is excised in *NHA9*-transgenic fish upon Cre activation. While an adequate minimal GFP signal remains in embryos enabling the FACS-apoptosis studies outlined above, this would not persist to adulthood. Even in the original *Tg(spi1::EGFP)* fish line we described (Hsu *et al.* 2004) where GFP was not excised, anti-GFP antibodies in adult kidney marrow only labeled 0.1% of cells.

Thus, in summary I have considered and attempted a number of staining studies to further characterize the MPN lesions in our *NHA9* zebrafish. I believe the additional PAS panels in the pathology micrographs further characterize the myeloproliferative phenotype of these lesions and provide a more detailed analysis of the zebrafish MPNs to some degree.

3.2.4 A Role For *tp53* Mutation On MPN In *NHA9* Adult Zebrafish?

We observed that *NHA9*-transgenic zebrafish develop disease similar to MPN between 19-23 months of life, but its latency suggests a requirement for additional genetic ‘hits’. Mutations in the human *tumour protein 53* (*TP53*) tumour suppressor gene, like *NHA9*, are uncommon in *de novo* AML, but have been found in secondary AML and MDS (Pedersen-Bjergaard *et al.* 2006). The p53 protein regulates cell cycle arrest and apoptosis, and inhibition of zebrafish *tp53* decreased such responses to DNA damage in embryos (Berghmans *et al.* 2005; Vogelstein and Kinzler 2004).

The disruption of zebrafish *tp53*-dependent cell cycle and apoptosis in *NHA9* embryos prompted us to further explore collaboration of *NHA9* and the *tp53* tumour suppressor gene in adult transgenic zebrafish. We therefore hypothesized that we could encourage overt AML (*i.e.* appearance of AML blast cells and/or 25% myeloblasts in marrow) in zebrafish by outcrossing *Tg(spi1::lgl::NHA9)* with the *tp53*^{M214K} loss-of-function mutant fish (Berghmans *et al.* 2005), with activation of *NHA9* expression by embryonic microinjection of *Cre* mRNA (Table 3.1). Uninjected *lgl::NHA9;tp53*^{M214K} heterozygotes served as controls. Although we observed a promising trend towards a higher incidence of MPN in *Cre*-injected *NHA9;tp53*^{M214K} heterozygotes (58.3%) compared to *NHA9* (+ *Cre*) alone (23.1%), we performed a χ^2 statistical test (degree of freedom = 1) and could not reject the null hypothesis of no significant difference.

I then collected whole kidney marrow (WKM) from control *AB* (Figure 3.6A) and uninjected *lgl::NHA9;tp53*^{M214K} heterozygous (Figure 3.6B) adult zebrafish, as well as *Cre*-activated *NHA9;tp53*^{M214K} heterozygotes (Figure 3.6C) and analyzed by FACS to specifically assess haematopoietic cell number, distribution, and differentiation (Traver *et al.* 2003). Due to poor availability of fish, a *Cre*-activated *NHA9;tp53*⁺ control could not be included in the WKM comparison. WKM from activated *NHA9;tp53*^{M214K} fish appeared to display an increased number of total leukocytes compared to *AB* wild-type and uninjected *lgl::NHA9;tp53*^{M214K} fish, particularly in the ‘myelomonocyte’ and ‘precursor’ gates (Figure 3.6, middle panels, quantification in Figure 3.6D). However, inter-experimental variance and error bars were very large, so statistical analysis could not be performed. It is possible that this variance occurred because we did not standardize the weight of WKM that is used for FACS analysis. Such standardization

may be necessary to ensure that the number and distribution of cells per collected sample are similar, are so that the calculated blood cell numbers are not being skewed in favour of *NHA9* fish purely because of their enlarged kidney.

Additionally, cytopins from the ‘myelomonocyte’ and ‘precursor’ gates in Cre-activated, *NHA9;tp53*^{M214K} fish demonstrated a population of immature granulocytic cells with large cytoplasmic inclusions (arrowheads in **Figure 3.6C**, *rightmost panel*), which were not observed in cytopins from the un-activated controls. These inclusions are reminiscent of Auer rods, a pathognomic feature often seen in mammalian AML blast cells, which suggests that these fish exhibited an advanced stage of myeloid disease. Overall, these findings indicate a possible role for *tp53* mutations in the development of MPN in *NHA9* zebrafish. However, since we were unable to include a WKM sample from a Cre-activated, *NHA9;tp53*⁺ control fish, and also unable to perform rigorous statistical analysis on our FACS analysis, I suggest that these experiments should be repeated (with more controls and greater standardization) to confirm the interpretation.

3.3 DISCUSSION

3.3.1 Transgenic Zebrafish Models Of Myeloid Disease

Despite the paucity of specific cross reactive antibodies, to date, zebrafish myeloid tumours have been found to possess histological characteristics similar to those observed in humans and mice (Forrester *et al.* 2011; Le *et al.* 2007; Zhuravleva *et al.* 2008). Aged wild-type zebrafish (24+ months) develop neoplasms, such as malignant peripheral neural sheath tumours (zMPNST) with an incidence rate as low as 11% (Amsterdam *et al.* 2004), but rarely haematopoietic disease. The generation of transgenic zebrafish models of myeloid leukaemias has been facilitated greatly by *Tol2* transposon-mediated genomic integration and Gateway® (Invitrogen) cloning strategies (Kwan *et al.* 2007, Villefranc *et al.* 2007), and the continually evolving array of promoters to drive transgene expression.

Our *Tg(spil::loxP-EGFP-loxP::NHA9)* zebrafish line is one of five models of zebrafish myeloid oncogenesis, and only the second to show a specific, robust myeloid disease phenotype in adult fish. A report using the human *inv(8)(p11;q13)* fusion

oncogene, *MOZ-TIF2* (**Table 1.1**), driven by the zebrafish *spi1* myeloid promoter was the first to demonstrate overt AML in zebrafish at 14 to 26 months of life (<1% incidence) ([Zhuravleva et al. 2008](#)). *Tg(spi1::MOZ-TIF2-EGFP)* fish showed an accumulation of immature myelomonocytes in the kidney marrow and a reduction in haematopoietic cells within the spleen. Another model used Cre/*lox*-inducible activation of *Tg(actb1::loxP-EGFP-loxP[IGI)::K-RAS^{G12D})* zebrafish, which resulted in many tumour types, including MPN between 34-66 days of life (~2% incidence). *K-RAS^{G12D}* fish affected with MPN showed increased myelomonocytes and myeloid precursors in kidney marrow, and a significant loss of mature erythrocytes ([Le et al. 2007](#)). However, both *Tg(spi1::MOZ-TIF2-EGFP)* and activated *Tg(actb1::IGI::K-RAS^{G12D})* fish showed low penetrance of disease, and their underlying molecular mechanisms remain unexplored.

Other studies have provided more mechanistic insight into oncogenic activity in zebrafish myelopoiesis. In humans, *TEL-JAK2* was identified in a rare case of CML. A myeloid-specific *Tg(spi1::FLAG-tel-jak2a)* zebrafish was novel for its fusion oncogene created from zebrafish homologues, rather than use of human cDNA ([Onnebo et al. 2005](#)). In embryos, zebrafish *tel-jak2a* led to an accumulation of large myeloid cells in blood smears, induction of the cell cycle, and a gain in cells expressing myeloid markers *spi1* and *lcp1* at 24 hpf. Yet despite a loss of circulating mature erythrocytes by 48 hpf, *Tg(spi1::FLAG-tel-jak2a)* fish also showed expanded distribution of erythroid markers *gata1a* and *hbbe3/βe3-globin* at 24 and 48 hpf. This concurrent increase in erythroid and myeloid lineages could be related to the role of Janus kinase/signal transducer and activator of transcription (JAK/STAT) signalling in cell survival and proliferation. For example, activation of JAK/STAT leads to increased signalling through phosphoinositide 3-kinase/mammalian target of rapamycin (PI3K/mTOR) and MYC pathways, which are also active in myeloid disease ([Rawlings et al. 2004](#)). Subsequent studies corroborate the effects of JAK/STAT signalling on pan-haematopoiesis in zebrafish embryos. Mutant *chordin* (*chd^{tt250}*) zebrafish that overexpress *jak2a* also show upregulation of both erythroid and myeloid genetic markers, and this could be phenocopied in wild-type embryos by injection of constitutively-active *jak2a* mRNA ([Ma et al. 2007](#)). The phenotype in *chd^{tt250}* mutants could be rescued by injection of *jak2a* morpholino or pharmacological treatment with the Jak2 inhibitor, AG490. Downstream

phosphorylation of *stat5* is the likely culprit, as the injection of zebrafish *stat5* mRNA carrying a constitutively-active H298R/N714F mutation led to increases in erythroid, myeloid, and B cell numbers (Lewis *et al.* 2006). Similar findings were observed in a zebrafish model of the myeloproliferative disease, polycythemia vera (PCV) where erythroid dysregulation by injection of zebrafish *jak2a*^{V581F} mRNA could be rescued by co-injection of *stat5* morpholino (Ma *et al.* 2009). Despite these promising embryonic findings, however, none of the *Tg(spi1::FLAG-tel-jak2a)* transgenic embryos survived to adulthood to establish a stable germline.

Similarly, the *Tg(hsp70::AML1-ETO)* zebrafish line demonstrated an accumulation of large myeloid cells in blood smears, and a gain in cells expressing myeloid markers, such as *spi1* and *mpx* (Yeh *et al.* 2008). *Tg(hsp70::AML1-ETO)* fish also do not present with myeloid disease in adulthood, but have had great success as a research tool to rapidly study gene interactions and perform drug discovery (discussed in detail in **CHAPTER 4**).

Compared to the *MOZ-TIF2*, *K-RAS*^{G12D}, *tel-jak2a*, and *AML1-ETO* fish lines, the findings that we show here represent a comprehensive characterization of *NHA9*-induced myeloid disease in adult zebrafish, and also in embryos (see **CHAPTER 4**). We have developed a new germline transgenic zebrafish expressing the human *NHA9* fusion oncogene. We employed the *Cre/lox*-induction strategy (Feng H *et al.* 2007; Langenau *et al.* 2005a; Le *et al.* 2007), which confers a degree of experimental control that has become standard in cell culture systems and mouse models. Our study reports a 23% incidence of an MPN-like malignancy, with some cellular maturation, in *Cre*-activated, germline *Tg(spi1::lGf::NHA9)* zebrafish between 19 to 23 months of life. We were encouraged that this was a similar disease presentation and time frame found in both retroviral-transduced (Kroon *et al.* 2001) and germline transgenic mice (Iwasaki M *et al.* 2005). It is interesting, however, that *NHA9*-induced disease often presents first as MDS in humans (defined by differentiation arrest), yet in mice and now zebrafish it first manifests as MPN (defined by polyclonal hyperproliferation). This may therefore highlight important distinctions in AML pathogenesis between humans and animals. Alternatively, these findings may postulate a unique genetic background in humans that predisposes MDS. However, the experimental methodology may also contribute to this

discrepancy between humans and laboratory animals. In both mice and zebrafish, many cells carry the *NHA9* fusion oncogene, and each cell can contain multiple copies, and the oncogene is sometimes driven by blood-specific promoters. This likely does not reflect the human condition in which one or a very few cells suffers the initial mutation. Recent oncogenic strategies in mouse models have relied on homologous recombination to knockin just a single copy of the oncogene, such as human *PML-RARA* (Guibal *et al.* 2009; Wojiski *et al.* 2009). Using such a strategy with mouse models of *NHA9* might show a different sequence of events in the initiation of myeloid disease.

Despite evidence of myeloid proliferation and delayed cell maturation, none of our *NHA9*-transgenic zebrafish were identified with overt AML (*i.e.* appearance of AML blast cells and/or 25% myeloblasts in marrow). This may reflect the shortened life-span of fish compared to mice, or possible inadequacies of the chosen *spil* myeloid promoter (discussed in **CHAPTER 8**). It may also suggest a requirement for collaborating genetic lesions to achieve transformation to acute disease. These will be explored in the following three chapters.

Table 3.1. Incidence of *NHA9*-induced haematopathology in zebrafish.

Genotype	No. Affected / Total No.	% incidence	Median Age (months)	Pathology
<i>NHA9</i> (- <i>Cre</i>)	0 / 17	0.0	-	-
<i>NHA9</i> (+ <i>Cre</i>) *	6 / 26	23.1	20.8 +/- 1.3	Abdominal mass with kidney, liver infiltrates (intestinal infiltrates); pleiomorphic, mitotic, myeloid morphologies
<i>NHA9;tp53</i> ^{M214K} (- <i>Cre</i>) [▲]	0 / 30	0.0	-	-
<i>NHA9;tp53</i> ^{M214K} (+ <i>Cre</i>)	7 / 12	58.3	29.6 +/- 0.9 [†]	Abdominal mass; increased cellularity in kidney marrow (myelomonocyte and precursor); immature granulocytes harbor large cytoplasmic inclusions

* 2/26 developed orbital mass; preliminary pathology revealed possible retinoblastoma or rhabdomyosarcoma; not investigated further

[▲] 10/26 developed abdominal mass, some with pathology reminiscent of zebrafish malignant peripheral neural sheath tumour (zMPNST)

[†] affected zebrafish were identified late in disease progression

Figure 3.1 (next page). Schematic and visualization of Cre/lox-inducible transgenic zebrafish that express EGFP and human NHA9 under the control of the 9.1 kb zebrafish spil promoter.

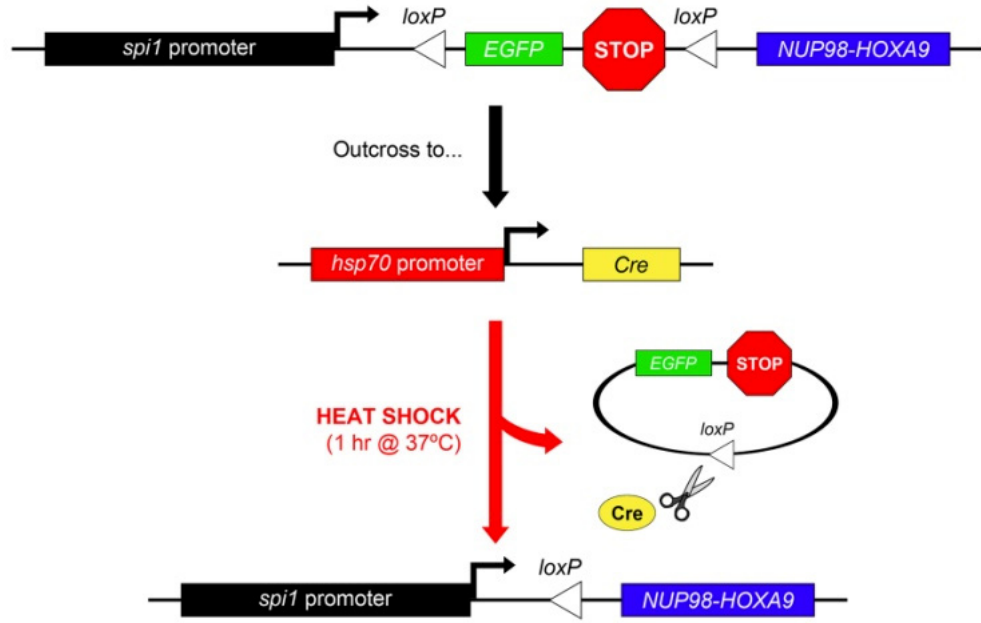
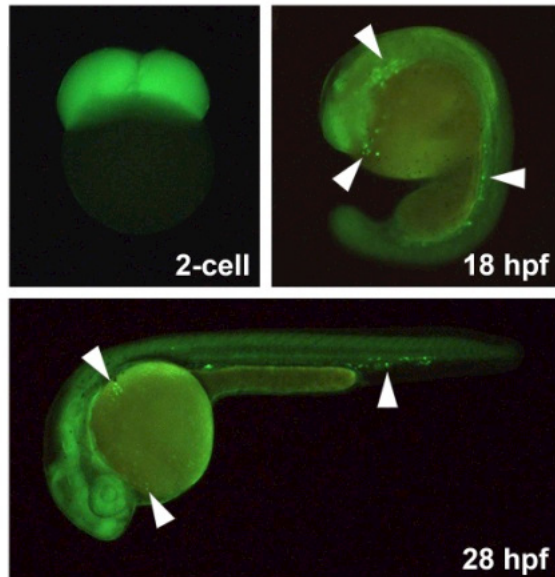
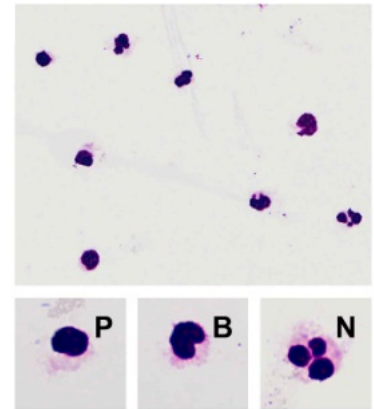
(A) Schematic representation of *Tg(spil::lgl::NHA9)* expression vector. Floxed *EGFP* inhibits expression of the human *NHA9* fusion oncogene. The *EGFP* cassette is removed by outcross to *Tg(hsp70::Cre)*, followed by ‘heat-shock’ for 1 hour at 37 to 39°C.

(B) (i) Fluorescence microscopy (509 nm) to observe *EGFP* expression in homozygous *Tg(spil::lgl::NHA9)* zebrafish embryos at indicated timepoints. Embryos displayed in side profile, animal pole to the top (2-cell) or anterior to the left (18+ hpf). Arrowheads point to GFP+ blood cells. **(ii)** Cytospin of FACS-sorted GFP+ cells (509 nm) from *NHA9*-transgenic embryos. Cell and nucleus morphology were assessed with Wright-Giemsa stain (*top*, 40X magnification; *bottom*, 100X).

Representative symbols: P = precursor; B = band form; N = neutrophil with segmented nucleus.

New abbreviations used: *EGFP* = enhanced green fluorescent protein; FACS = fluorescence-activated cell sorting; hpf = hours post-fertilization; *hsp* = heat-shock protein; *lgl* = loxP-EGFP-loxP; *NHA9* = NUP98-HOXA9; *spil* = spleen focus forming virus (SFFV) proviral integration oncogene

Acknowledgement: former colleague, C Grabher, performed vector construction and microinjection into zebrafish embryos and conducted early screening for generation of the *NHA9* transgenic zebrafish line; co-op student, F-B Kai, conducted screening and performed pilot experiments; lab technician, Sandy Edgar, operated FACSaria™ I for panel **Bii**; haematopathologist, Eileen McBride, reviewed Wright-Giemsa stain for panel **Bii**.

A**B i****ii**

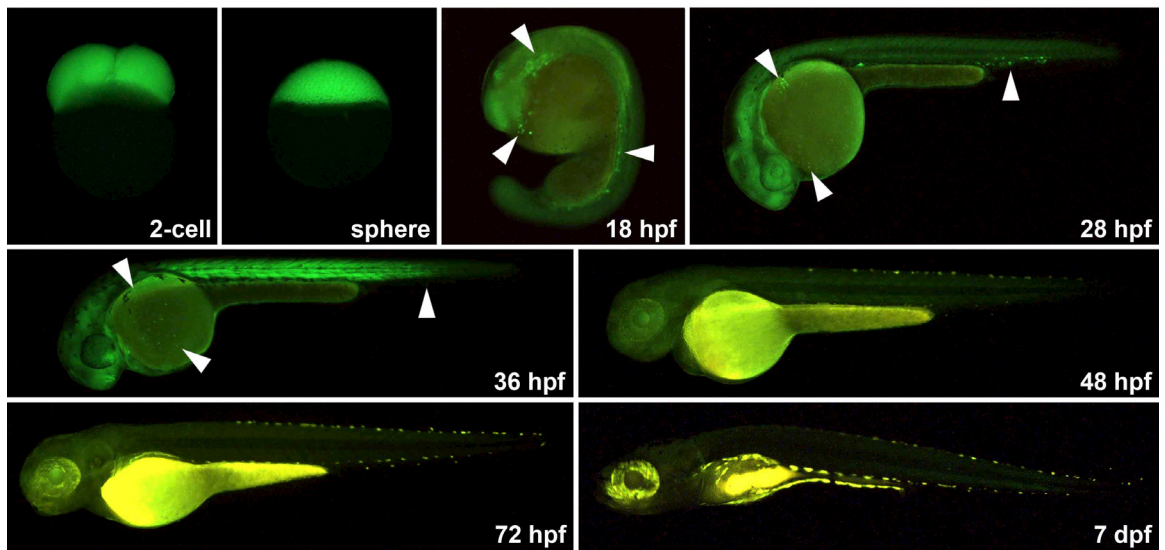


Figure 3.2. Extended timeline of transgenic expression in *NHA9* embryos. Fluorescence microscopy (509 nm) to observe *EGFP* expression at indicated timepoints in F₃ generation embryos harbouring *Tg(spi1::lgl::NHA9)*. Embryos displayed in side profile, animal pole to the top (2-cell) or anterior to the left (18+ hpf). Arrowheads point to GFP+ blood cells.
New abbreviations used: dpf = days post fertilization.

Figure 3.3 (next page). Cre/lox recombination and expression of human NHA9 fusion oncoprotein in *Tg(spi1::IGL::NHA9)* transgenic zebrafish embryos.

(A) Agarose electrophoresis following PCR of genomic DNA (gDNA) extracted from zebrafish embryos at 28 hpf. Leftmost lane carries 1 kb DNA ladder; rightmost lane carries 100 bp DNA ladder. A *spi1* forward primer and *NHA9* reverse primer (*'spi1::NHA9'*) were used to confirm presence of transgene and monitor excision of *IGL* cassette following Cre-mediated recombination. In un-activated, full-length conditions (*i.e.* not outcrossed to *Cre*, or not subjected to heat-shock), *Tg(spi1::IGL::NHA9)* transgene produces PCR amplicon size of 2 kb. In Cre-activated, excised conditions (*i.e.* outcrossed to *Cre* and subjected to heat-shock at 24 hpf), transgene produces with PCR amplicon sizes of 775 bp (white arrow). Primers for '*Cre*' amplicon (720 bp) were used as a PCR control to confirm successful outcross with *Tg(hsp70::Cre)* activator zebrafish line. Primers for '*efla*' amplicon (701 bp) were used as a PCR control to confirm successful extraction of gDNA from zebrafish samples. Samples from *left-right*: purified *Tg(spi1::IGL::NHA9)* pISce vector served as positive controls for '*spi1::NHA9*' primer amplification; '- pISce' and '- primers' served as negative controls for PCR amplification; *AB* wild-type gDNA served as negative zebrafish control; *Tg(hsp70::Cre)* gDNA served as positive zebrafish control for '*Cre*' amplicon; incrossed *NHA9* gDNA (*'IGL::NHA9'*) served as positive zebrafish control for embryos not crossed to *Cre*, but subjected to heat-shock; *NHA9* [- *Cre*] gDNA served as zebrafish control for embryos that were outcrossed to *Cre* but not subjected to heat-shock; *NHA9* [+ *Cre*] gDNA served as zebrafish experimental sample for embryos that were both outcrossed to *Cre* and subjected to heat-shock.

(B) Western blot for detection of human NHA9 fusion oncoprotein (black arrow; white arrow points to a non-specific band ['n.s.']) from zebrafish embryos at 28 hpf. Detection of β -actin protein served as protein loading control. Protein molecular weight ladder is not shown, but indicated left of the α -NUP98 portion of blot. All embryo groups were heat-shocked at 24 hpf. Samples, similar to panel (C), from *left-right*: *AB* wild-type protein, incrossed '*IGL::NHA9*' protein, and *NHA9* [+ *Cre*] protein.

New abbreviations used: *efla* = *elongation factor 1 alpha*; gDNA = genomic DNA.

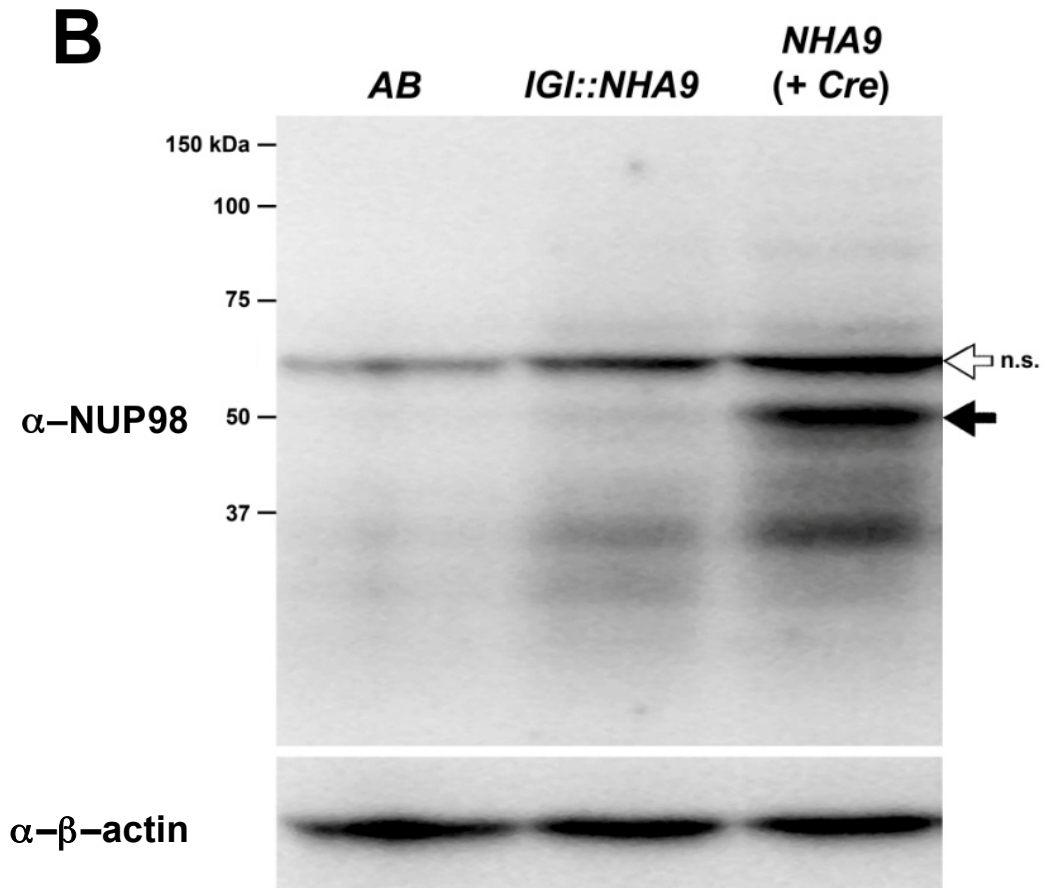
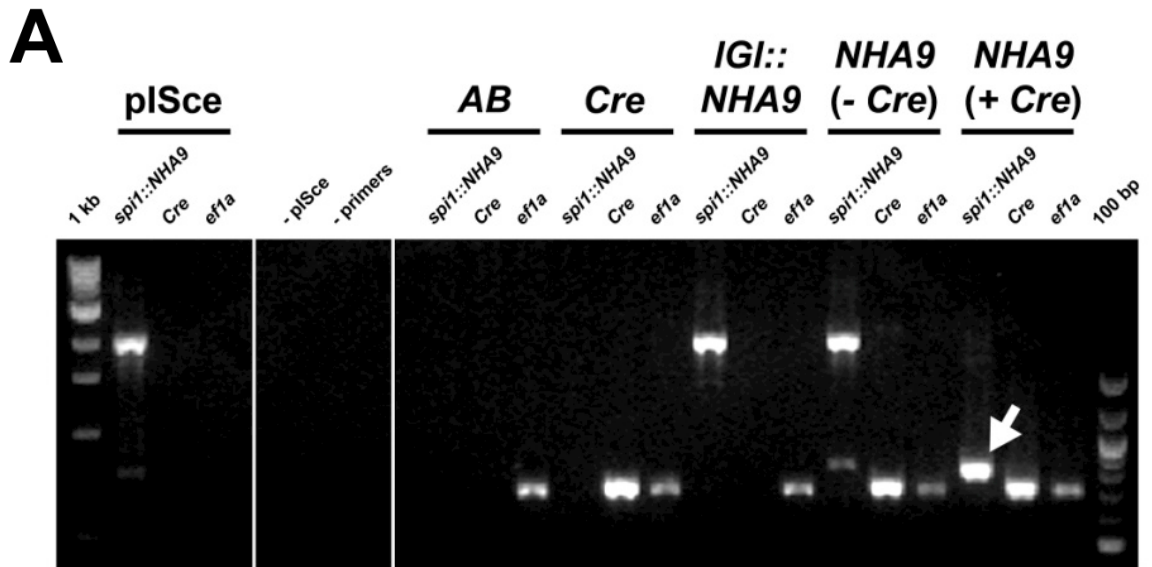


Figure 3.4 (next page). Activated *NHA9*-transgenic zebrafish develop disease similar to MPN.

At 24 hpf, *NHA9;Cre* heterozygous embryos were heat-shocked to excise the *IgI* cassette, and these fish were then grown to adulthood.

Gross anatomy and histopathology of (*A – D*) *AB* wild-type (n=4), (*E – H*) un-activated *IgI::NHA9* (aged 23 months) (n=4), and (*I – P*) two affected *NHA9 (+ Cre)* adult zebrafish (aged 23 and 22 months, respectively).

Panels *A, E, I, M* depict gross anatomy (0.71X magnification), with abdominal masses in *NHA9 (+ Cre)* fish (black arrowheads).

Panels *B, F, J, N* depict wide-field microscopy (2X; scale bar = 200 µm) of histological sectioning and H/E staining of zebrafish tissue. Representative symbols: white arrowheads = kidney; black arrowhead = liver.

Panels *C, G, K, O* depict high-power microscopy (100X; scale bar = 100 µm) of kidney tissue (G = glomerus; T = kidney tubule). Insets show artificially magnified views. Representative symbols: * = mitotically-active; black arrowhead = myelomonocytic precursor; white arrowhead = mature neutrophil.

Panels *D, H, L, P* depict high-power microscopy (100X; scale bar = 100 µm) of kidney tissue stained with PAS to identify granulocytic myeloid cells. Insets show artificially magnified views. Representative symbols: black arrows = PAS+ eosinophil or mast cell (note that some arrows may point to a grouping of multiple cells).

New abbreviations used: H/E = haematoxylin/eosin; PAS = periodic acid-Schiff.

Acknowledgement: haematopathologist, Eileen McBride, reviewed H/E and PAS stains and assisted analysis.

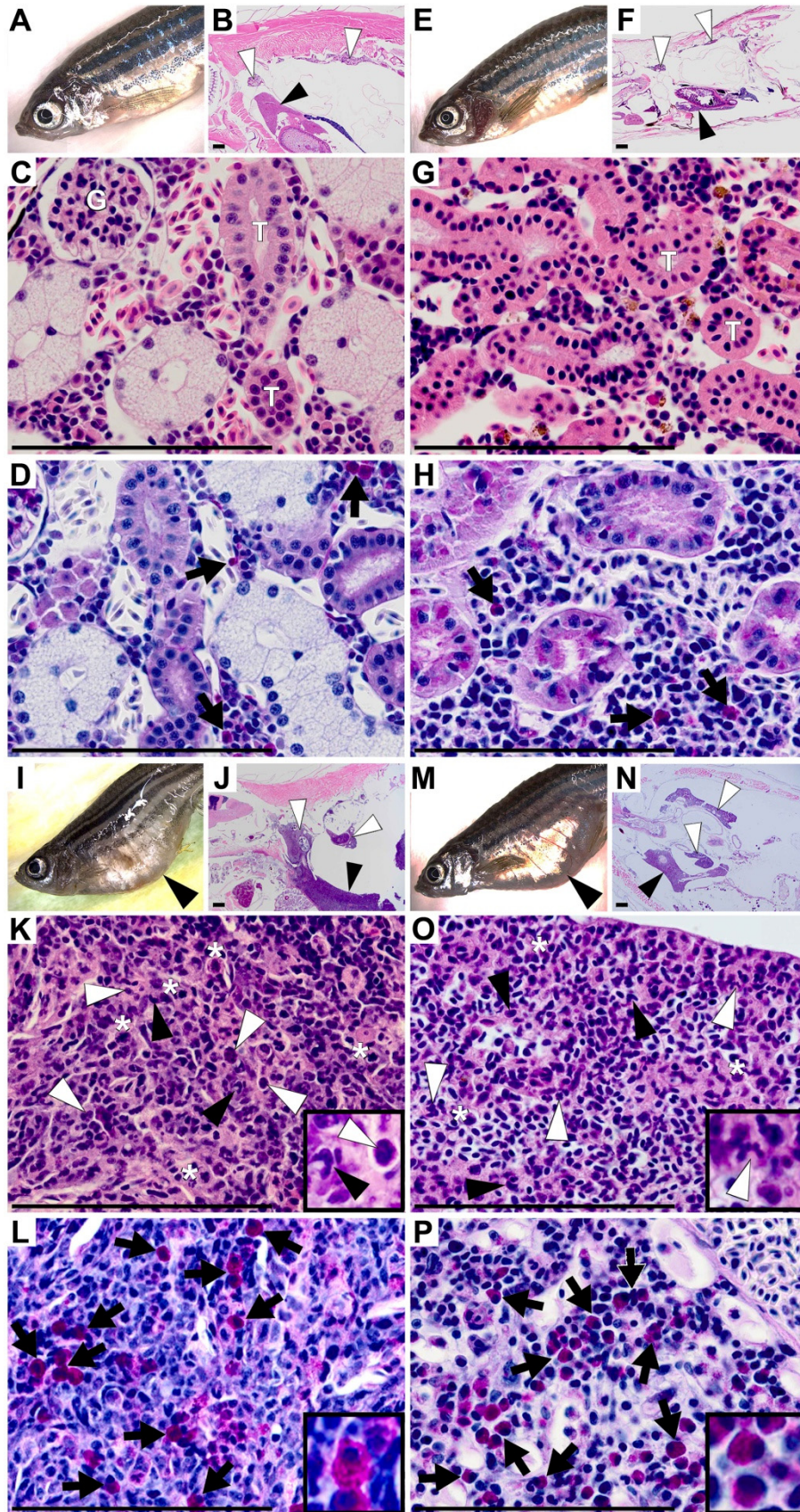


Figure 3.5 (next page). Additional histopathology analysis of *NHA9 (+ Cre)* adult zebrafish with and without MPN.

Histopathology of unaffected and affected *NHA9 (+ Cre)* adult zebrafish. At 24 hpf, *NHA9; Cre* heterozygous embryos were heat-shocked to excise the *IGI* cassette and these were then grown to adulthood. For all panels, scale bar = 100 μ m.

(A) Wide-field microscopy (2X magnification) of H/E staining of unaffected *NHA9 (+ Cre)* fish (aged 16 months). Representative symbols: white arrowheads = kidney; black arrowhead = liver;

(B) High-power microscopy (100X) of H/E staining in kidney of unaffected *NHA9 (+ Cre)* fish. Representative symbols: G = glomerus; T = kidney tubule.

(C) High-power microscopy (40X) of H/E staining in kidney of affected *NHA9 (+ Cre)* fish (aged 23 months). Representative symbols: white arrowheads = invading myeloid cells.

(D) High-power microscopy (40X) of H/E staining in kidney of affected *NHA9 (+ Cre)* fish. Representative symbols: white arrowhead = pyknotic nuclei of kidney tubule epithelial cells; MY = myeloid infiltrate.

(E) Wide-field microscopy (10X) and (F) high-power microscopy (40X) of H/E staining of affected *NHA9 (+ Cre)* fish. Representative symbols: L = liver; black arrow = intestine; MY = myeloid infiltrate.

(G) High-power microscopy (100X) of PAS staining in liver of affected *NHA9 (+ Cre)* fish (aged 23 months). Insets show artificially magnified views. Representative symbols: black arrowheads = PAS+ eosinophil or mast cell (note that some arrows may point to a grouping of multiple cells).

(H) High-power microscopy (100X) of PAS staining in liver of un-activated *IGI::NHA9* control fish.

(I) Wide-field microscopy (2X) of H/E staining in intestine of affected *NHA9 (+ Cre)* fish. Note the thickened intestinal muscularis in the black box area.

(J) High-power microscopy (40X) of the black box area in panel (I). Representative symbols: M = intestinal muscularis.

(K) High-power microscopy (40X) and (L) magnified view (100X) of H/E staining in pancreas of affected *NHA9 (+ Cre)* fish (aged 19 months). Representative symbols: black arrow = normal pancreas; white arrowheads = monomorphic granulated cells.

Acknowledgement: haematopathologist, Eileen McBride, reviewed H/E and PAS stains and assisted analysis.

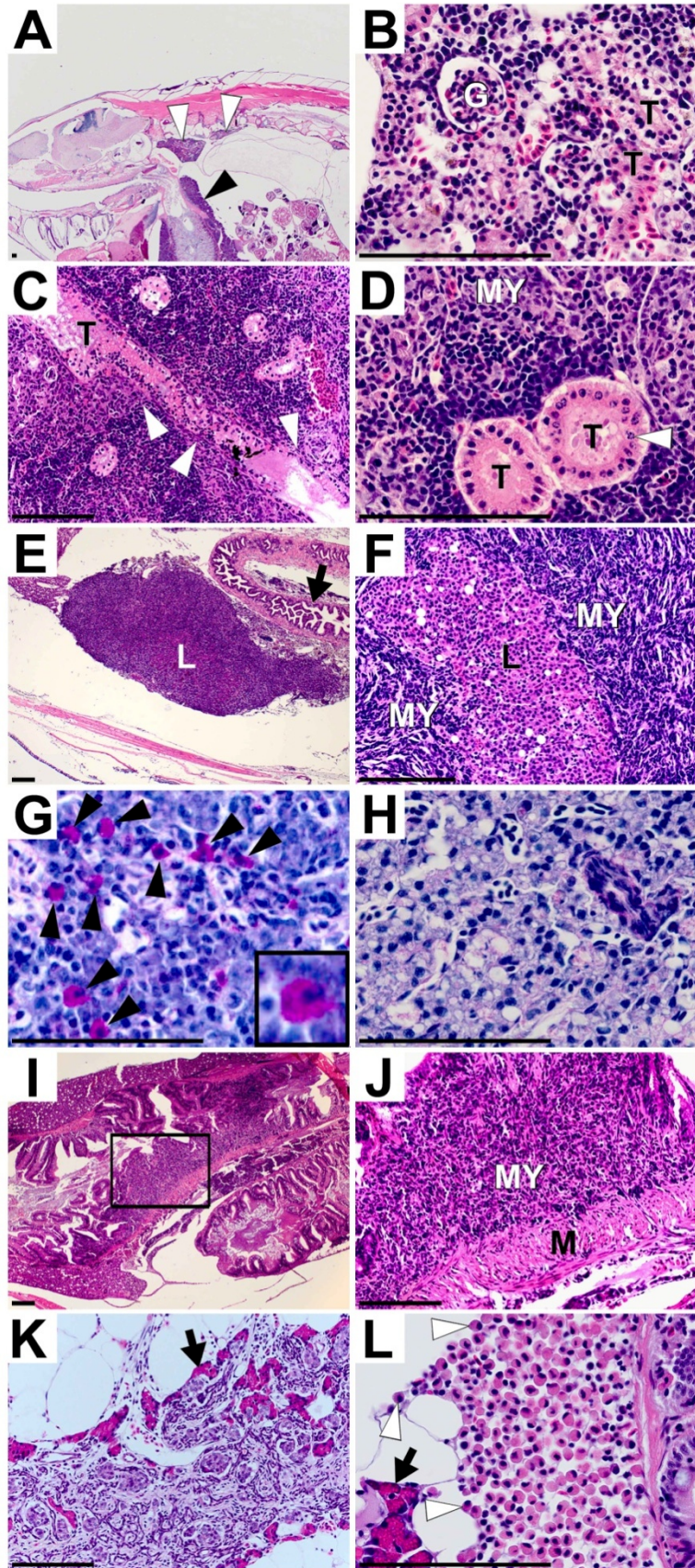


Figure 3.6 (next page). Evidence to suggest that loss-of-function $tp53^{M214K}$ mutation may collaborate with *NHA9* to induce myeloproliferative pathology.

Analysis of adult WKM is shown for (A) *AB* wild-type control fish, (B) uninjected (*i.e.* un-activated) *IGl::NHA9;tp53^{M214K}* heterozygote control fish, and (C) *Cre*-injected *NHA9;tp53^{M214K}* heterozygote fish.

Leftmost panels show gross anatomy (0.71X magnification).

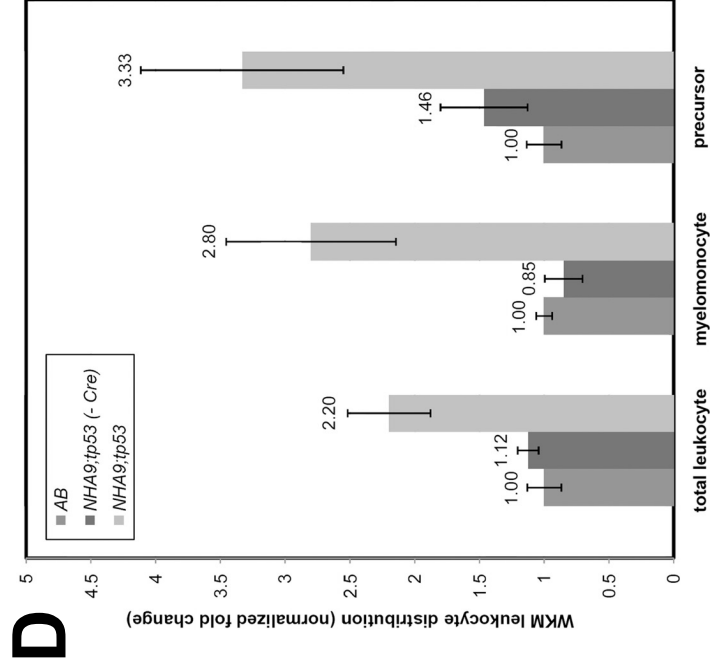
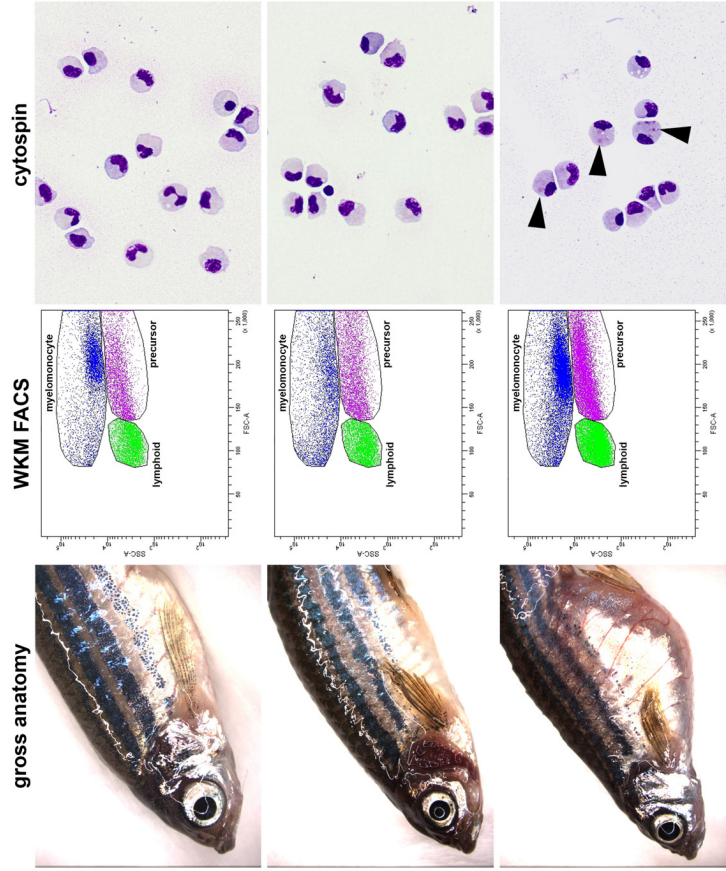
Middle panels show FACS analysis of disaggregated WKM and gating of blood cell populations by FSC and SSC.

Rightmost panels show cytopspins (100X magnification) that were collected from the ‘myelomonocyte’ gate. Cell and nucleus morphology was assessed by Wright-Giemsa stain. Representative symbols: black arrowheads = immature granulocytes with large cytoplasmic inclusions. Dot plots and cytopspins are representative of 3 independent trials.

(D) Bar graph quantification of FACS data. Raw data was normalized against *AB* wild-type and reported as mean values, error bars represent +/- SEM. *Cre*-activated, *NHA9;tp53^{M214K}* fish (n=4) display overall increased cellularity (2.2-fold vs. *AB*; 1.95-fold vs. uninjected *IGl::NHA9;tp53^{M214K}*) in all gates, and particularly in the ‘myelomonocyte’ (2.8-fold vs. *AB*; 3.3-fold vs. uninjected *IGl::NHA9;tp53^{M214K}*) and ‘precursor’ (3.3-fold vs. *AB*; 2.3-fold vs. uninjected *IGl::NHA9;tp53^{M214K}*) gates. Statistical analysis was inconclusive.

New abbreviations used: WKM = whole kidney marrow; *tp53* = *tumour protein 53*.

Acknowledgement: lab technician, Sandy Edgar, operated FACSAria™ I for panels A-C and assisted analysis in panel D; haematopathologist, Eileen McBride, analyzed Wright-Giemsa stain for panels A-C.



CHAPTER 4 *NUP98-HOXA9* ZEBRAFISH EMBRYOS DISPLAY DEFECTS IN HAEMATOPOIESIS & CELLULAR APOPTOSIS

4.1 BACKGROUND

4.1.1 Using Transgenic Zebrafish As A Tool By Focusing On Leukaemia Phenotypes in Embryos

Like the *tel-jak2a* study, expression of the human *AML1-ETO* fusion oncogene, driven by the *heat-shock protein 70* (*hsp70*) promoter also results in disruption of developmental myelopoiesis in zebrafish embryos (Yeh *et al.* 2008). Blood smears from *Tg(hsp70::AML1-ETO)* show cells with blast-like morphology. Furthermore, whole embryos show upregulation of *spi1* and downregulation of *gata1a* at 20-22 hpf, similar to the phenotype observed in *gata1a*-morphant embryos (see schematic in **Figure 4.1**). There was a differential impact on mature myeloid lineages, with increased granulocytes marked by *mpx*, but decreased monocytes marked by *lcp1*. The transforming mechanism was identified as a downregulation of *tal1/scl*, one of the master transcription factors for embryonic haematopoiesis, in posterior regions of the embryo (ICM and PBI). All phenotypes were rescued by injecting *Tg(hsp70::AML1-ETO)* embryos with either *tal1/scl* mRNA or *spi1* morpholino.

To date, the *Tg(hsp70::AML1-ETO)* line represents the most successful use of zebrafish to study the molecular biology of myeloid leukaemia. Despite the absence of an clinically-identifiable adult disease phenotype, *Tg(hsp70::AML1-ETO)* embryos have been an instrumental research tool in the identification of genetic and chemical modifiers of myeloid oncogenesis. A subset of human AML cases show deletions on chromosome 9q (del[9q]), which are specifically associated with the t(8;21) translocation yielding *AML1-ETO* (Dayyani *et al.* 2008). The effects of del(9q) result from the loss of two genes, *transducin-like enhancer of split 1* (*TLE1*) and *TLE4*, in the Notch signalling pathway. A reverse genetics approach used morpholino-knockdown of the zebrafish *TLE* homologue, *groucho3*, in *Tg(hsp70::AML1-ETO)* embryos to show an acceleration of the haemtopoietic phenotype, namely the appearance of AML blast-like cells, an increase in *mpx* expression, and a loss of circulating erythrocytes.

Taking advantage of this phenotype, Yeh *et al.* elegantly used the rescue of *gata1a* expression by TSA as a proof-of-principle springboard for a chemical modifier screen with a library of known bioactive compounds (Yeh *et al.* 2009). They identified COX2 inhibitors, such as NS-398 and Indomethacin, as novel therapeutic agents against the AML1-ETO oncoprotein. They subsequently demonstrated the critical importance of COX-prostaglandin E₂ signalling through the Wnt/ β -catenin pathway to the altered haematopoiesis phenotype in *Tg(hsp70::AML1-ETO)* fish. This same signalling axis and therapeutic strategy was also later identified in a mouse model of *Hoxa9;Meis1*-induced AML (Wang Y *et al.* 2010).

Like the disruption of haematopoiesis in *AML1-ETO* zebrafish embryos, **we hypothesized that our *NHA9* zebrafish would display defects in haematopoiesis and cellular survival.** The successful identification of robust embryonic phenotypes would allow us to use the *NHA9* zebrafish as an *in vivo* tool to investigate genetic and chemical modifiers. Indeed, *NHA9* embryos show altered haematopoiesis, with upregulated *spi1* myeloid expression at the expense of *gata1a* erythroid expression (refer back to **Figure 1.1**). Markers associated with more differentiated myeloid cells, *lcp1*, *lyz*, and *mpx* were also elevated, but to a lesser extent than *spi1*, suggesting differentiation of early myeloid progenitors may be impaired by *NHA9*. Following irradiation, *NHA9*-expressing embryos showed increased numbers of cells in G2-M transition compared to controls and absence of a normal apoptotic response, which may result from an upregulation of *B-cell lymphoma (bcl2)*. These data suggest *NHA9*-induced oncogenesis may result from a combination of defects in haematopoiesis and an aberrant response to DNA damage.

4.1.2 *NHA9* & *MEIS1*

We also hypothesized that zebrafish *meis1* will impact myeloid haematopoiesis in zebrafish embryos, and will cooperate with *NHA9* in the causation of the embryonic myeloproliferative phenotype. Co-overexpression of mouse *Meis1* with human *NHA9* in transgenic mice accelerates the onset of overt AML (*i.e.* appearance of AML blast cells and/or 25% myeloblasts in marrow), but maintains the MPN latent stage with roughly the same timing as *NHA9* alone (Kroon *et al.* 2001). Unlike the overexpression of native mouse *Hoxa9*, the expression of human *NHA9* does

upregulate mouse *Meis1* (Calvo *et al.* 2002), so this helps to explain their cooperation in mice. What is known about this relationship is that *NHA9* transformation is not inhibited by the absence of the native mouse *Hoxa9* gene (Calvo *et al.* 2002), that MEIS1 binds NHA9 at the protein level (Shen *et al.* 1999), and that the NHA9 oncoprotein either does not bind, or does not require the Pbx co-factor (Calvo *et al.* 2002). Furthermore, upregulation of human *MEIS1* may be a late-transformation event that coincides with increased proliferation of primary human CD34+ cells transformed with *NHA9* (Takeda *et al.* 2006). However, the underlying molecular mechanisms that result from cooperation between *NHA9* and *MEIS1* have gone largely unexplored. In particular, it is unknown whether *NHA9* activity can be inhibited by gene-knockdown of *MEIS1*, either in mammalian cell culture or *in vivo* mouse models. I was encouraged to find that gene-knockdown of zebrafish *meis1* in *NHA9* embryos can indeed restore wild-type levels of myeloid cells (refer to **Figure 1.1**).

Taken together, the robust embryonic defects in haematopoiesis and cell apoptosis, as well as the *meis1* findings help to characterize the *Tg(spi1::IGF::NHA9)* transgenic zebrafish line. Our *NHA9*-transgenic line thus provides a reliable tool to exploit the advantages inherent in the zebrafish for perform targeted chemical modifier and reverse genetics analyses (see **CHAPTER 5** and **CHAPTER 6**), as well as an unbiased, high-throughput modifier screen (Yeh and Munson 2010) (see **CHAPTER 8**) to identify novel genes and therapeutic agents in *NHA9*-induced AML.

4.2 EXPERIMENTAL FINDINGS

4.2.1 *NHA9* Inhibits Primitive Macrophage Differentiation And Perturbs Haematopoiesis To Promote Myeloid And Suppress Erythroid Fates

Hyperactive *HOXA9* promotes immortalization and impaired differentiation of committed myeloid precursors and HSCs *in vitro* (Calvo *et al.* 2002; Takeda *et al.* 2006; Thorsteinsdottir *et al.* 2001). We hypothesized that *NHA9*-transgenic fish would present defects in embryonic haematopoiesis, as measured by gene expression using whole-mount *in situ* hybridization (WISH). Zebrafish embryonic haematopoiesis occurs in four

waves (details in **CHAPTER 1**), and we controlled our *Cre/lox* strategy to capture the effects of *NHA9* expression during two waves of myelopoiesis.

The first wave of myelopoiesis that we investigated with our *Cre/lox* strategy was the primitive macrophages that emerge from anterior lateral plate mesoderm (ALPM) in the head region of the embryo between 12 to 24 hpf (Dobson *et al.* 2009, Le Guyader *et al.* 2008). Following heat shock at 12 hpf and WISH at 24hpf, *NHA9* (+ *Cre*) embryos displayed a 1.34 fold increase in ALPM cells expressing *spi1* compared to *AB* wild-type controls ($P<0.05$). However, other myeloid genes, *lymphocyte cytosolic protein 1* (*lcp1*) ($P=0.51$) and *lysozyme* (*lyz*) ($P=0.08$), which represent more mature myeloid markers (Hall *et al.* 2007; Le Guyader *et al.* 2008) were not increased (**Figure 4.2A**, left to right). This finding suggests that human *NHA9* may inhibit terminal differentiation of primitive macrophages in zebrafish. To our knowledge, we are the first to demonstrate this maturation phenotype as a primary function of *NHA9* expression *in vivo* (Calvo *et al.* 2002; Takeda *et al.* 2006).

The second wave of myelopoiesis that we investigated with our *Cre/lox* strategy was the emergence of dual potential erythro-myeloid progenitors (EMPs) from the posterior blood island (PBI) in the tail region of the embryo between 24 to 32 hpf (Bertrand *et al.* 2007). EMPs are the first wave of definitive haematopoiesis in the zebrafish embryo and highlight the antagonism between SPI1 and GATA1 transcription factors, which is one of dominant themes in vertebrate haematopoiesis for specifying myeloid or erythroid fate (Chou ST *et al.* 2009; Galloway *et al.* 2005; Lyons *et al.* 2002; Rhodes *et al.* 2005). Embryos were heat-shocked at 24 hpf and assessed by WISH at 28 hpf. Compared to *AB* wild-type, approximately 80% of *NHA9* (+ *Cre*) embryos displayed increased numbers of PBI cells expressing *spi1* (1.4-fold, $P<0.05$), *lcp1* (2.3-fold, $P<0.005$), *lyz* (2.8-fold, $P<0.005$), and *myeloperoxidase* (*mpx*) (1.4-fold, $P<0.05$) by WISH, with concurrent downregulation of *gata1a* (19.3-fold, $P<0.00005$) by qRT-PCR (**Figure 4.2B**, left to right) (refer to **Figure 1.1**). This suggests that EMPs in *NHA9* embryos produce more myeloid cells at the expense of erythroid cells. Upregulation of *lcp1* (1.6-fold, $P<0.0005$) and *mpx* (1.3-fold, $P<0.05$) was also seen in ALPM cells of *NHA9* embryos at 28 hpf. However, compared to cells located in the PBI, the origin of these anterior myeloid cells is less certain due to the temporal overlap of continuing

primitive haematopoiesis in the ALPM with that of definitive myeloid cells derived from EMPs. Moreover, circulation has begun at 24 hpf, thus these myeloid cells may represent residual primitive white blood cells or EMP-derived myeloid cells that have migrated anteriorly. It should be noted that the inhibited maturation phenotype seen at 24 hpf appears to be less prominent at the onset of definitive haematopoiesis in the PBI, since we observed upregulated markers of maturing myeloid cells in this region.

We considered that an increase in myeloid cells could be the result of increased cell proliferation, but were unsure of how to take measurements of the cell cycle specifically in blood cells. One could perform cell cycle analysis on isolated cells in a single cell suspension, but this is more easily done by cells that can be FACS-sorted by GFP expression. Since the Cre-activation event eliminates the *IGI* cassette, isolating cells that express *NHA9* is not easily accomplished. However, since our *Tg(spi1::IGI::NHA9)* transgenic line displays off-target expression of the transgene in CNS and musculature tissue (refer back to **Figure 3.1B** and **Figure 3.2**), we hypothesized that measurements of cell proliferation could be made in these surrogate tissues in order to study at least some of the activities of *NHA9* on cell survival.

However, we observed no overall differences (**Figure 4.3A**) between *AB* wild-type and *NHA9 (+Cre)* embryos in BrdU incorporation ($P=0.77$), which labels cells in S phase of the cell cycle, or pH3 expression ($P=0.74$), which marks cells undergoing G2-M transition. Even with Cre-activation at 18 hpf (10 hours prior to assessment), *NHA9* does not appear to contribute to acceleration of the cell cycle (**Figure 4.4**). There remained a possibility that the cell cycle may be affected only in myeloid cells. I eventually learned how to conduct cell cycle analysis in the haematopoietic compartment in whole embryos, by performing double stains for pH3 in blood cells labeled by WISH (**Figure 4.3B**, *left to right*). We confirmed that neither *spi1*-, nor *lcp1*-expressing cells displayed an increase in pH3 staining (white arrows and insets show co-localization), thus no detectable increase in cell proliferation.

4.2.2 Knockdown Of *meis1* Eliminates Myeloid Cells From The Posterior Blood Island And HSCs From The Dorsal Aorta, And Inhibits *NHA9*

Numerous studies assert a requirement for *HOXA9* and *MEIS1* in vertebrate myelopoiesis and myeloid leukaemogenesis (Azcoitia *et al.* 2005; Brun *et al.* 2004; Hisa *et al.* 2004; Izon *et al.* 1998; Kappen 2000; Ko *et al.* 2007; Lawrence *et al.* 1997; Magnusson *et al.* 2007; Shimamoto *et al.* 1999; So *et al.* 2004). Overexpression of mouse *Meis1* accelerates the onset of *NHA9*-induced leukaemia in mice, but the underlying mechanism is unknown (Kroon *et al.* 2001). I therefore decided to investigate the role of zebrafish *meis1* in the myeloproliferative phenotype of our *NHA9* embryos. Using qRT-PCR, we found that *NHA9* embryos exhibited only a mild increase in *meis1* expression (1.5 ± 0.3 -fold) (**Figure 4.5A**). However, I hypothesized that gene-knockdown of *meis1* via morpholino oligonucleotide (MO) could inhibit the myeloproliferative phenotype and restore wild-type levels of myeloid cells.

A translation-blocking MO targeted to zebrafish *meis1* has already been designed (refer back to **Table 2.2**) and is known to decrease the level of zebrafish *meis1* protein by whole-mount embryo immunofluorescence (Pillay *et al.* 2010). Wild-type and *NHA9* zebrafish embryos were injected at the one-cell stage with 1 mM *meis1* MO, and uninjected embryos served as controls. I allowed embryos to grow to 24 hpf, then performed heat-shock for 1 hour, and fixed at 28 hpf and fixed for WISH. I chose to assess the myeloproliferative phenotype through expression of *lcp1*, because it exhibited the most robust increase in unadulterated *NHA9* embryos. Compared to uninjected siblings, wild-type control embryos injected with 1 mM *meis1* MO exhibited a near-complete loss of *lcp1*-positive myeloid cells during the definitive EMP wave in the PBI tail region (**Figure 4.5B, top panels**). This is consistent with a recent study (Cvejic *et al.* 2011) that also observed loss of myeloid cells in the PBI, specifically of *lcp1*-expressing cells at 28 hpf and of Sudan Black-positive cells at 48 hpf and 2 dpf. Furthermore, Cvejic *et al.*, as well as my own preliminary investigations describe a necessity for zebrafish *meis1* in the development of HSCs in the aorta-gonad-mesonephros (AGM) region by 30 to 36 hpf. Embryos lacking *meis1* show dysregulated expression of HSC markers, *c-myb* and *runx1* (**Figure 4.6**). I also have preliminary evidence to suggest that the injection of *meis1* MO also reduces myeloproliferation in the PBI of *NHA9* embryos.

Approximately 80% of uninjected *NHA9* embryos showed the expected increase in *lcp1* expression, which is consistent with myeloproliferation. However, 70.8% of *NHA9* embryos injected with *meis1* MO show wild-type or low *lcp1* expression (**Figure 4.5B**, *bottom panels*), suggesting that the loss of *meis1* blocks *NHA9* activity.

4.2.3 *NHA9* Suppresses Cell Cycle Arrest And Apoptosis In The Presence Of DNA Damage

Decreased apoptosis and altered cell cycle regulation leading to hyperproliferation are hallmarks of oncogenesis ([Hanahan and Weinberg 2011](#)). In human AML, *NHA9* confers inferior prognosis and cellular resistance to traditional therapy, such as DNA damaging agents ([Giles et al. 2002](#)). To investigate the impact of *NHA9* in the presence of DNA damage, *NHA9* (+ *Cre*) embryos were exposed to 16 Gy IR to induce double-stranded DNA breaks ([Jette et al. 2008](#)). This level of irradiation has been shown to induce cell cycle arrest and apoptosis in zebrafish embryos ([Langenau et al. 2005b](#); [Sansam et al. 2006](#)). All embryo groups were heat-shocked at 24 hpf, select groups were irradiated at 26 hpf, and all were assessed for phenotype at 28 hpf. Similar to studies on cell proliferation, it is difficult to perform studies of apoptosis specifically in zebrafish blood cells. As before, we thus used the off-target CNS and musculature expression of the transgene in our *NHA9* embryos to facilitate these studies on apoptosis.

We first measured pH3 immunofluorescence in embryos after exposure to IR. Cells that have been stained with pH3 indicate that the G2 to M checkpoint of the cell cycle has been completed successfully. The DNA damage caused by ionizing radiation should engage this checkpoint and halt the cell cycle. *AB* wild-type embryos demonstrated a 4.2-fold reduction in pH3-labeled cells, which is consistent with cell cycle arrest. However, *NHA9* (+*Cre*) embryos only suffered a 1.6-fold decrease (relative difference of 2.6-fold, $P < 0.005$) (**Figure 4.7A**). Thus, the inability of irradiated *NHA9* embryos to suppress levels of pH3 suggests a failure of cell cycle arrest, and that *NHA9* dysregulates the cell cycle through inhibition of DNA damage checkpoints.

We next measured apoptosis in embryos after exposure to IR, using acridine orange (AO) staining. AO is a general marker of apoptosis that binds to double-stranded breaks in fragmented DNA. Irradiated control embryos, such as *AB* wild-type embryos,

Tg(hsp70::Cre) embryos, or incrossed, un-activated *IGL::NHA9* embryos displayed a wild-type pattern of AO staining, suggesting that cells were undergoing apoptosis. (**Figure 4.7B**). By contrast, irradiated *NHA9 (+ Cre)* embryos showed far fewer cells that stained with AO. This suggests that, in addition to inhibiting cell cycle arrest, *NHA9* also suppresses cellular apoptosis following IR. This loss of apoptosis can be explained by a failure of irradiated *NHA9 (+ Cre)* embryos to activate the caspase cascade, which is a conserved pathway that orchestrates cell death (Jette *et al.* 2008). Compared to *AB* wild-type embryos, *NHA9* embryos exhibit a 6.3-fold decrease in levels of the conserved marker, casp3 ($P < 0.005$) (**Figure 4.7C**). We also used microinjection of *Cre* mRNA as another way to show that the inhibition of casp3 by *NHA9* was dependent on the presence of *Cre*, and was not simply a by-product of heat-shock (**Figure 4.8, left**). As an injection control for this experiment, we injected *GFP* mRNA into *AB* wild-type embryos, and when these embryos were irradiated, they showed the expected pattern of casp3 expression. The ‘GFP’ channel (**Figure 4.8, right**) confirms a positive injection of *GFP* mRNA into *AB* embryos, and also confirms excision of the *IGL* cassette in *NHA9* embryos injected with *Cre* mRNA. Therefore, having achieved similar results with heat-shock activation of *Cre* and microinjection of *Cre* mRNA, we concluded that *NHA9* activity blocks the activation of zebrafish casp3 and thus inhibits cellular apoptosis.

Moreover, *NHA9* instigated differential expression of zebrafish *bcl2* family genes that participate in the mitochondrial apoptosis response, which is a primary outcome of DNA damage (Jette *et al.* 2008). Using qRT-PCR, *NHA9 (+ Cre)* embryos exposed to IR (designated ‘hs + IR’) exhibited normal expression of the BH3-only apoptotic activator, *bbc3/puma* (**Figure 4.7D**), suggesting that *tp53*-dependent signalling remains intact in order to activate *bbc3/puma* gene transcription (Nakano and Vousden 2001).

Furthermore, no change in expression was observed for the canonical *tp53* target gene (Sidi *et al.* 2008), *cdkn1a/p21^{waf1/cip1}*. By contrast, using WISH we observed significant upregulation of the zebrafish proto-oncogenes, *bcl2*, and *bcl2-like 1 (bcl2l1/bcl-x_L)*, in heat-shocked *NHA9 (+ Cre)* embryos (**Figure 4.7E**, black arrowheads), particularly in the haematopoietic PBI (**Figure 4.7E**, black arrows). qRT-PCR analysis confirmed that the expression levels of *bcl2* and *bcl2l1/bcl-x_L* were increased by 3.8-fold ($P < 0.00005$) and 2.1-fold ($P < 0.0005$), respectively in *NHA9 (+ Cre)* embryos. Taken together, these data

posit upregulation of *bcl2* rather than suppression of *tp53*-dependent signalling as a mechanism for *NHA9* oncogenesis *in vivo* (refer to schematic in **Figure 1.1**).

4.2.4 FACS Isolation Of Myeloid Cells Undergoing Apoptosis

We considered whether suppression of apoptosis could be observed specifically in zebrafish myeloid cells. Irradiated embryos were dissociated to a single-cell suspension and subjected to FACS analysis for GFP+ myeloid cells. Cell suspensions were supplemented with 7-AAD live cell exclusion dye, thus any cell that is undergoing apoptosis will be stained by 7-AAD. This analysis, however, suggested that myeloid cells from Cre-activated *NHA9* (+ *Cre*) embryos undergo a comparable amount of apoptosis to incrossed, un-activated '*IGL::NHA9*' embryos (**Figure 4.9**).

Despite the inability of FACS analysis to demonstrate suppression of apoptosis specifically in GFP+ myeloid cells, this assay is fraught with certain limitations, including a potentially higher radio- sensitivity of blood cells and the relatively few numbers of GFP+ myeloid cells per embryo. Furthermore, since we were able to measure apoptosis by using the off-target expression of the *NHA9* transgene in CNS and musculature tissues, our data from those trials (discussed above) makes a compelling argument for the role of *NHA9* in suppressing the response to DNA damage.

4.2.5 Modulating The Zebrafish *bcl2* Family

Our findings in zebrafish embryos suggest that inhibition of apoptosis may be mechanism that underlies *NHA9*-induced leukaemogenesis in mammals, possibly due to increased expression of the highly-conserved *BCL2* gene family. If this link could be proven conclusively, there would be a potential to use pharmacologic inhibitors of human BCL2, such as ABT-737 ([Zeitlin et al. 2008](#)), in the clinical treatment of AML patients harbouring the *NHA9* translocation. To date, unfortunately, ABT-737 and other mammalian BCL2 inhibitors do not successfully inhibit zebrafish *bcl2* proteins, for reasons unknown (Jette C, personal communication).

There has also been limited success with MO knockdown of genes in the zebrafish *bcl2* gene family. No MOs currently exist for the founding member, the *bcl2*

gene itself, and nearly all other MOs in the family (designed by the Look lab) have been translation-blocking (atg/5'UTR), often because the genes lack introns for splice-site MOs. Thus, the efficiency of knockdown cannot be known for certain in the absence of cross-reactive antibodies to detect the proteins by Western blot. Phenotypic read-outs for apoptosis function have partially aided MO design, and there exists a *bbc3/puma* that can cause embryos to become refractory to irradiation. Two MOs have been designed for zebrafish *bcl2l1/bcl-x_L*, one results in substantial apoptosis, the other does not; the actual desired or expected phenotype is debated (Jette C, personal communication).

I have tried injecting *NHA9* embryos with *bcl2l1/bcl-x_L* MO at the one-cell stage (refer back to **Table 2.2**), followed by heat-shock at 24 hpf and exposure to 16 Gy IR at 26 hpf. Embryos injected with a standard control MO (GeneTools), which is not targeted against any native RNA transcript in zebrafish, served as a control. Using AO staining as a read-out, it appeared that inhibition of zebrafish *bcl2l1/bcl-x_L* did not substantially rescue general apoptosis in *NHA9* embryos (**Figure 4.10**). In *NHA9* embryos, there was no apparent difference in the number of cells undergoing apoptosis between those injected with *bcl2l1/bcl-x_L* MO or standard control MO. Control *AB* embryos injected with standard control MO showed a regular number of apoptotic cells, which was not changed by the injection of *bcl2l1/bcl-x_L* MO. Due to the difficulties in monitoring the true efficiency of morpholino knockdown on zebrafish *bcl2l1/bcl-x_L* protein levels, this line of investigation was not further pursued.

4.3 DISCUSSION

We demonstrate novel *in vivo* findings that human *NHA9* perturbs blood cell development in zebrafish embryos leading to an abundance of early myeloid cells, and that inhibiting zebrafish *meis1* can block this activity. *NHA9* also enables zebrafish embryos to resist cytotoxic insult and inhibit cell cycle arrest and apoptosis, likely through the upregulation of zebrafish *bcl2*. Ultimately, this burgeoned myeloid population with increased survival signalling through *bcl2* in *NHA9*-transgenic fish may help to explain the development of MPN later in the animal's life (see **CHAPTER 3**).

4.3.1 Similar And Distinct Findings For *NHA9* In Fish Versus Mammals

Our study demonstrates that human *NHA9* influenced the myeloid-erythroid balance in zebrafish embryos, with an increase in myeloid precursors and a concomitant decrease in *gata1a*-expressing erythroid cells. *NHA9* may function through zebrafish *hoxa9a* and *meis1* (Calvo *et al.* 2002) or may be dominant over their native activity, ultimately impacting the downstream regulation of blood-specific transcription factors, *spi1* and *gata1a* (refer back to **Figure 1.1**). Knockdown of the zebrafish hox co-factor, *meis1*, was capable of restoring wild-type levels of myeloid cells in *NHA9* embryos, which is consistent with the ability of overexpressed mouse *Meis1* to accelerate *NHA9*-induced AML in mice. My data is first to investigate the effect of *meis1* knockdown on *NHA9* activity, and therefore provides new knowledge into this genetic collaboration as it relates to AML. However, this data is preliminary and should be repeated to confirm.

Given that *NHA9* embryos did not exhibit a significant increase of BrdU incorporation, nor enhanced staining for the mitotic marker, pH3, these findings suggest that *NHA9* primarily impacts haematopoietic differentiation in zebrafish. This phenotype is consistent with zebrafish embryos that harbour *Tg(hsp70::AML1-ETO)* (Yeh *et al.* 2009). However, our data stands in contrast to a number of mammalian *in vitro* studies that suggest *NHA9* drives cell hyperproliferation (Calvo *et al.* 2002; Kroon *et al.* 2001; Takeda *et al.* 2006). The MPN latency phase is maintained even in *NHA9;Meis1* mice, suggesting that collaborating genetic events that activate the cell cycle are essential for initiation of oncogenesis, and collaborating events that further dysregulate cellular differentiation may be important for acute transformation. These discrepancies suggest that the *in vivo* and *in vitro* effects of *NHA9* may be distinct and may highlight a requirement for collaborating events that drive the cell cycle.

4.3.2 The Role Of *meis1* And *cdx-hox* In Definitive Haematopoiesis

I have shown here that the loss of *meis1* inhibits myeloid development during the first definitive wave of zebrafish myeloid development from dual-potential EMPs in the PBI. Specifically, *meis1*-morphants exhibited a loss of *lcp1* expression in the PBI at 28 hpf. It is possible that this loss of maturing myeloid cells results from a loss of

undifferentiated EMPs, given the decrease of *gata1a* and *lmo2* markers (Bertrand *et al.* 2007) in *meis1*-morphant embryos at 24 hpf (Pillay *et al.* 2010).

Furthermore, I show that *meis1*-morphants also show a loss of *c-myb* and *runx1* expression in the mid-trunk, aorta-gonad-mesonephros (AGM) region by 30 to 36 hpf. This is consistent with a necessity of *meis1* for zebrafish HSC formation during definitive haematopoiesis, and also matches another zebrafish study showing that *meis1*-morphants dysregulate *c-myb* around 30 hpf (Cvejic *et al.* 2011). Cvejic *et al.* also found that *meis1*-morphants show loss of myeloid cells in the PBI, specifically of *lcp1*-expressing cells at 28 hpf and of Sudan Black-positive granulocytes at 48 hpf and 2 dpf. Similarly, *kgg^{tv205}* (*cdx4^{-/-}*) mutant embryos are deficient in *runx1* HSC formation, which can be rescued with *hoxa9a* mRNA (Davidson and Zon 2006). The study by Cvejic *et al.* and my preliminary findings are consistent with the requirement for *HOXA9* and *MEIS1* in vertebrate myelopoiesis (see CHAPTER 1).

4.3.3 Interplay Of *cdx-hox* And *tal1/scl* In *NHA9* Embryos

The upregulation of *spi1* and downregulation of *gata1a* in our *NHA9* line were similarly seen in the *Tg(hsp70::AML1-ETO)* zebrafish line (Yeh *et al.* 2008). An underlying mechanism for dysregulated haematopoiesis in the *AML1-ETO* fish was the downregulation of *T-cell acute lymphocytic leukaemia protein 1 / stem cell leukaemia (tal1/scl)*, one of master regulators of haematopoiesis in the posterior ICM of the zebrafish embryo. Wild-type haematopoiesis could be rescued by injecting *AML1-ETO* embryos with zebrafish *tal1/scl* mRNA. The expression of *tal1/scl* may therefore be decreased in our *NHA9* embryos. Given our MPN phenotype in adult *NHA9* fish as well, we could measure *tal1/scl* expression levels in affected animals to assess the contribution of *tal1/scl* to the establishment of clinical myeloid disease.

Zebrafish studies support the role of *tal1/scl* in the development of an early progenitor cell, termed the haemangioblast (Dooley *et al.* 2005; Juarez *et al.* 2005; Patterson *et al.* 2007). During primitive haematopoiesis, when blood cells cannot originate from multi-potent HSCs, the haemangioblast is thought to generate limited blood cell types (termed ‘haemogenic’ differentiation), such as primitive macrophages in the ALPM and primitive erythrocytes in the ICM. Haemangioblasts also produce

endothelial progeny (termed ‘angiogenic’ differentiation) (Baron 2003; Lacaud *et al.* 2001; Robertson *et al.* 1999; Orkin and Zon 2008). In this manner, blood cells and blood vessels are created simultaneously to promote continued growth of the developing animal. Since *tall/scl* is expressed in haemangioblasts, MO knockdown of *tall/scl* inhibits both myeloid development in the ALPM and erythroid development in the ICM (see schematic in **Figure 4.1**), and also undermines HSC formation during definitive haematopoiesis (Dooley *et al.* 2005; Juarez *et al.* 2005; Patterson *et al.* 2007). However, loss of *tall/scl* does not inhibit early angiogenesis in the zebrafish embryo, suggesting that *tall/scl* is more important for haemogenic differentiation. For the erythroid lineage in particular, human and zebrafish experiments show that TAL1/SCL protein is found in a multi-protein complex that controls RNA polymerase II activity at the GATA1 promoter (Bai *et al.* 2010). This helps to explain how *kgg^{tv205}* (*cdx4^{-/-}*) zebrafish embryos show a loss of *tall/scl* at 12 hpf that then leads to a loss of decrease in *gata1a* expression and, therefore, a failure of haemogenic differentiation in the ICM (Davidson and Zon 2006) (**Figure 4.1**).

Human patients harbouring *AML1-ETO* exhibit decreased expression of *MEIS1*, a member of the *CDX-HOX* transcriptional network (Lasa *et al.* 2004). This is consistent with the similar expression profiles of zebrafish *tall/scl* and *gata1a* in *AML1-ETO*-transgenic (Yeh *et al.* 2008), *meis1*-morphant (Pillay *et al.* 2010), and *cdx*-mutant embryos (Davidson and Zon 2006). However, both *cdx*-mutant and *meis1*-morphant embryos are defective in definitive waves of zebrafish haematopoiesis (Cvejic *et al.* 2011; Davidson and Zon 2006), whereas *AML1-ETO*-transgenic fish show a gain of myeloid development from the EMP wave up to 40 hpf (Yeh *et al.* 2009). Given that there is a requirement of *tall/scl* for zebrafish myeloid development (Dooley *et al.* 2005; Juarez *et al.* 2005; Patterson *et al.* 2007), and that there is a loss of *lcp1* expression in the PBI of *meis1*-morphants at 28 hpf (Cvejic *et al.* 2011), the dysregulation of *tall/scl* by *AML1-ETO* may only be important during primitive haematopoiesis, specifically for erythrocytes. Thus, the long-term regulation of zebrafish *tall/scl* by human *AML1-ETO* and its effects on myeloid development are not entirely predictable, especially once definitive haematopoiesis takes over. The dysregulation of *tall/scl* in *AML1-ETO* embryos may also be an artefact in zebrafish, given that the expression of human *SPI1* is

suppressed in human patients with *AML1-ETO* (Vangala *et al.* 2003; Zhou *et al.* 2011), whereas zebrafish *spi1* was found elevated in the *AML1-ETO* zebrafish line (Yeh *et al.* 2008). Nevertheless, it would be of interest to investigate the contribution of zebrafish *tal1/scl* to the haematopoietic phenotype in our *NHA9* embryos.

4.3.4 *NHA9* Dysregulates Cellular Homeostasis

The CNS expression in our *spi1*-directed transgenic zebrafish line provided a unique opportunity for the effects of *NHA9* on neural tissue to serve as a surrogate measure for impact on haematopoietic cells. The CNS has historically been more amenable to studies of cell cycle arrest and apoptosis in zebrafish (Berghmans *et al.* 2005; Jette *et al.* 2008; Shepard *et al.* 2005; Sidi *et al.* 2008). In treatment-related human AML, mutations in the *TP53* tumour suppressor gene are common genetic lesions that collaborate with oncogenic transformation (Pedersen-Bjergaard *et al.* 2006). Moreover, co-overexpression of mouse *Hoxa9* and *Meis1* in mammalian cell culture suppresses casp3-dependent apoptosis and confers multi-drug resistance (Wermuth and Buchberg 2005). We thus hypothesized that the human *NHA9* fusion oncogene might disrupt conserved *tp53*-dependent signalling pathways in the zebrafish. Specific blood cell measurements of cell cycle and apoptosis are difficult to perform in zebrafish, so we exploited the off-target expression of the *NHA9* transgene in CNS and musculature tissues to more easily investigate these phenomena. We found that irradiated *NHA9*-transgenic embryos failed to initiate *tp53*-dependent cell cycle arrest and apoptosis, which suggests that *NHA9* allows cells to bypass DNA damage checkpoints.

In particular, we found that *NHA9* blocked signalling cascades in the zebrafish mitochondrial apoptosis response. *NHA9* embryos showed loss of casp3 activation and dysregulation of zebrafish homologues in the conserved *B-cell leukaemia 2 (BCL2)* gene family, *bcl2*, and *bcl2l1/bcl-x_L* (Jette *et al.* 2008), but did not show evidence of dysregulation of canonical *tp53*-dependent genes, such as *bcl2 binding component 3 / p53 upregulated mediator of apoptosis (bbc3/puma)* and *cyclin-dependent kinase inhibitor 1a (cdkn1a)/p21^{waf1/cip1}*. Overexpression of *bcl2* and *bcl2l1/bcl-x_L* suppresses BH3-only genes, particularly *bbc3/puma*, which dampens the apoptotic response and is a recurrent mechanism for cellular survival in cancer, including AML (Nakano and Vousden 2001).

In particular, overexpression of *bcl2* suppresses IR-induced apoptosis in zebrafish lymphoid cells (Langenau *et al.* 2005b). These findings suggest that *NHA9* may have no direct activity on zebrafish *tp53* signalling, and that overexpression of *bcl2* may be sufficient to suppress apoptosis.

Human *BCL2* is overexpressed in a variety of human cancers and is associated with cytotoxic resistance in AML (discussed in Marcucci *et al.* 2003). Phase I trials using G3139, an antisense inhibitor of *BCL2*, achieved 30% complete remission against refractory or relapsed AML (Marcucci *et al.* 2003; Marcucci *et al.* 2005). To date, the use of approved human *BCL2* inhibitors has not been fruitful in zebrafish, and injection of MO against zebrafish *bcl2l1/bcl-x_L* did not appear to rescue general apoptosis in our *NHA9* embryos. In the future, there may be some potential for outcrossing *NHA9* fish with a transgenic line overexpressing zebrafish *bcl2* (Jette *et al.* 2008). This might help to confirm whether zebrafish *bcl2* truly modulates the embryonic and MPN phenotypes in our *NHA9* fish.

Furthermore, given that overexpression of mouse *Hoxa9* and *Meis1* suppresses cellular apoptosis *in vitro* (Wermuth and Buchberg 2005), it is possible that knockdown of zebrafish *meis1* would affect the anti-apoptotic and cell cycle arrest phenotypes observed in *NHA9* embryos. *NHA9* embryos injected with *meis1* MO could be exposed to ionizing radiation and assessed by AO staining or casp3 immunofluorescence. Cell proliferation could then be examined by BrdU incorporation (S phase) and pH3 immunofluorescence (G2-M phase transition). These experiments could then be repeated to evaluate the impact of zebrafish *meis1* overexpression on the *NHA9* phenotype.

Figure 4.1 (next page). Schematic representing the impact of the *cdx-hox* transcriptional network and *spi1-gata1a* antagonism on zebrafish primitive haematopoiesis.

A wild-type zebrafish embryo, shown near the onset (12 hpf, *left*) and conclusion (24 hpf, *right*) of primitive haematopoiesis. Embryos displayed in side profile, anterior to the left. Gene knockdowns and/or pathway modifications by pharmacological treatments (R_x) are presented for their effects on anterior-posterior morphology, the success of *tall/scl* expression (green line), and the success of haemogenic differentiation into *spi1*-expressing myeloid cells (blue line) in the ALPM or *gata1a*-expressing erythroid cells (red line) in the ICM. Angiogenic differentiation (*fli1a*) shown as pink line. In text, green check marks or red crosses represent whether haemangioblast progenitors in the ALPM and/or ICM were correctly established or whether absent. (Thickness of coloured lines denotes relative expression.) Adapted from data in Davidson *et al.* 2003; Davidson and Zon 2006; Dooley *et al.* 2005; Galloway *et al.* 2005; Juarez *et al.* 2005; Lyons *et al.* 2002; Patterson *et al.* 2007; Rhodes *et al.* 2005.

New abbreviations used: ALPM = anterior lateral plate mesoderm; *cdx* = caudal type homeobox transcription factor; *gata1a* = GATA binding factor 1 α ; ICM = intermediate cell mass; *spi1* = spleen focus forming virus (SFFV) proviral integration oncogene; *tall/scl* = T-cell acute lymphocytic leukaemia protein 1 / stem cell leukaemia; wt = wild-type.

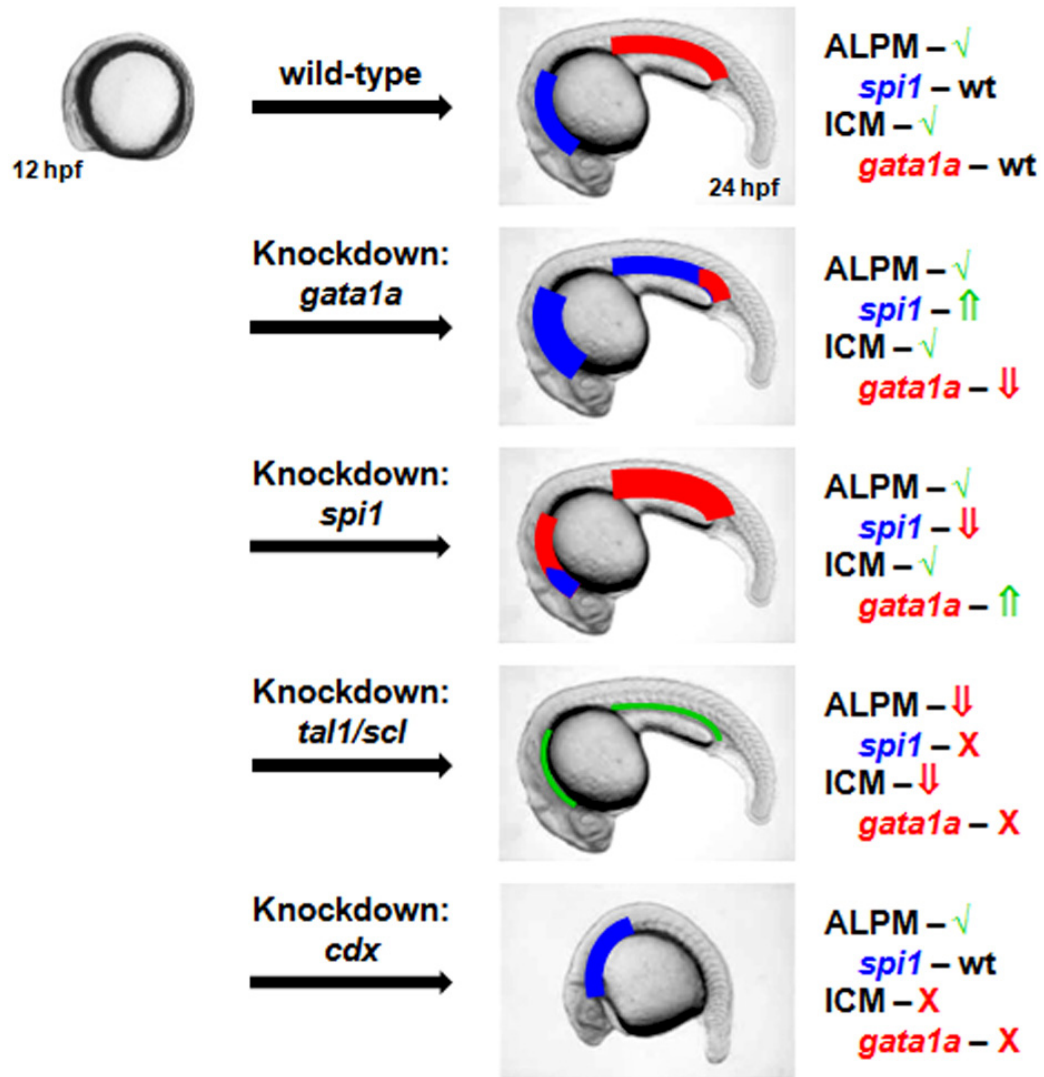


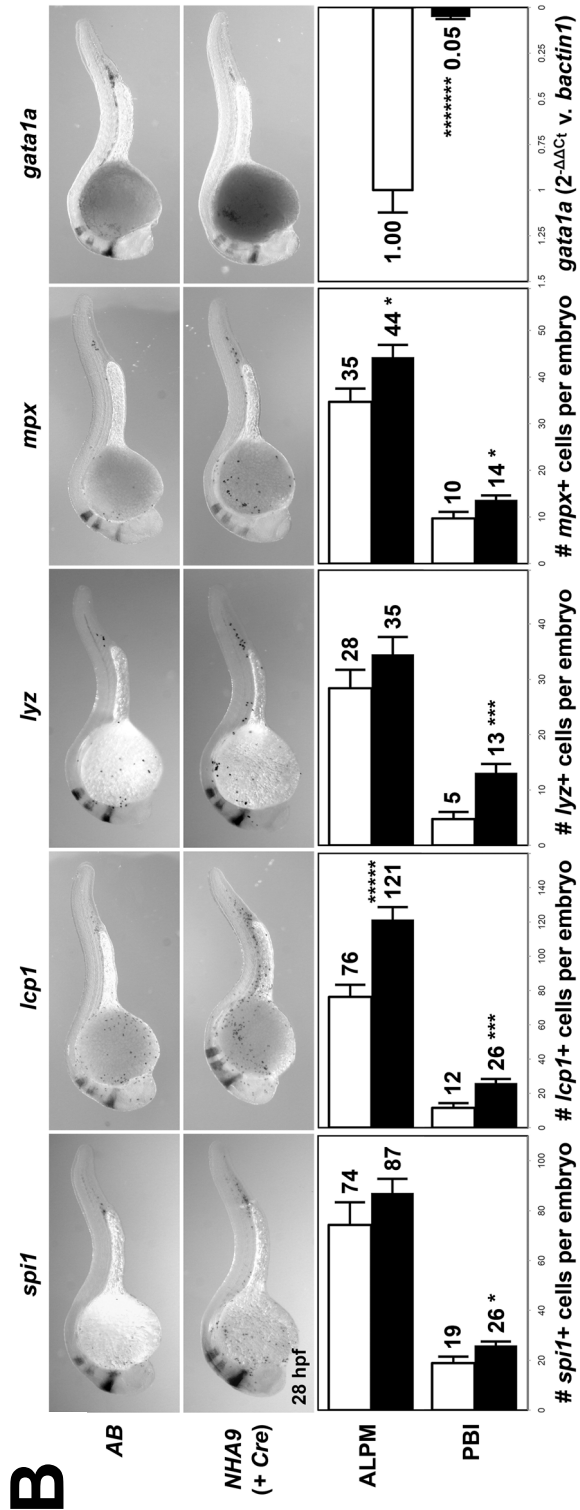
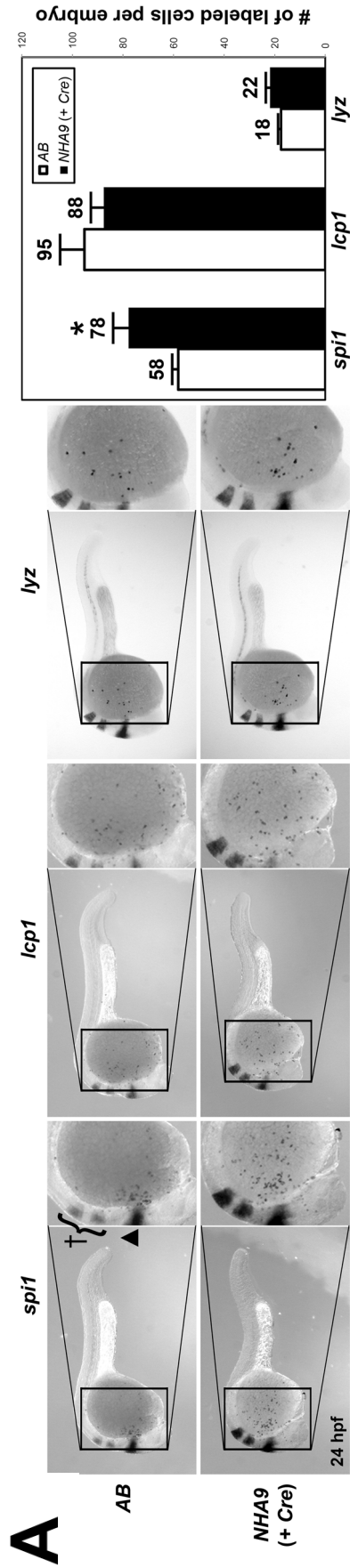
Figure 4.2 (next page). *NHA9* inhibits primitive macrophage differentiation, as well as promotes myeloid and suppresses erythroid gene expression.

Embryos displayed in side profile, anterior to the left. Bar graphs denote expression levels of indicated genes, with *AB* wild-type embryos represented by white bars and *NHA9* (+ *Cre*) embryos represented by black bars (n = the number of embryos used for quantification). For myeloid genes, expression was quantified by physically counting the number of WISH-stained cells using Image J. For erythroid genes, expression was quantified using qRT-PCR (described below). Data reported as mean values, error bars represent +/- SEM. Representative symbols for student's *t*-test results: **P*<0.05; ****P*<0.005; ******P*<0.0005; ******P*<0.00005.

(*A*) Embryos were heat-shocked at 12 hpf and assayed at 24 hpf by WISH for genes in zebrafish haematopoiesis. Insets show magnified views of ALPM in the head region of the embryos. Black punctae mark individual myeloid cells that express the indicated gene. Zebrafish genes measured are the early master myeloid gene regulator, *spi1* (*AB*, n=5; *NHA9*, n=5), and the more mature myeloid genes, *lcp1* (*AB*, n=4; *NHA9*, n=5) and *lyz* (*AB*, n=4; *NHA9*, n=5). Representative symbols mark control stains that were consistent for all embryos: ▲ = *eng2* (midbrain-hindbrain boundary); † = *egr2b/krox20* (hindbrain rhombomeres 3 and 5).

(*B*) Embryos heat-shocked at 24 hpf and assayed at 28 hpf via WISH. Zebrafish genes measured are the early master myeloid gene regulator, *spi1* (*AB*, n=7; *NHA9*, n=9), and the more mature myeloid genes, *lcp1* (*AB*, n=8; *NHA9*, n=12), *lyz* (*AB*, n=8; *NHA9*, n=10), and *mpx* (*AB*, n=13; *NHA9*, n=12), as well as the master erythroid gene regulator, *gata1a* (n=2 biological replicates, each with 45-50 embryos per genotype, qRT-PCR performed in triplicate, normalized against *AB* wild-type expression and relative to expression of housekeeping gene, *actb1* / *β-actin1*).

New abbreviations used: *egr2b* = *early growth response 2b*; EMPs = erythro-myeloid progenitors; *eng2* = *engrailed 2*; *lcp1* = *lymphocyte cytosolic protein 1*; *lyz* = *lysozyme*; *mpx* = *myeloperoxidase*; qRT-PCR = quantitative reverse transcription polymerase chain reaction; WISH = whole-mount *in situ* hybridization;



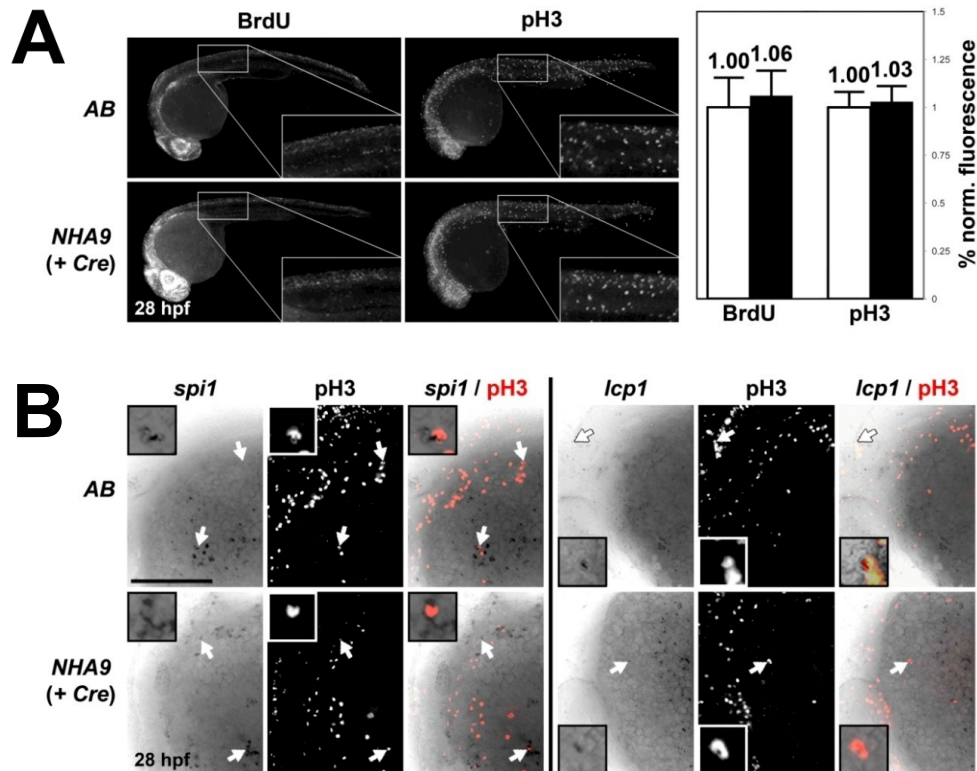


Figure 4.3. *NHA9* does not increase cellular proliferation.

Embryos heat-shocked at 24 hpf and assayed at 28 hpf. Embryos displayed in side profile, anterior to the left.

(A) Fluorescence microscopy (555 nm) to observe whole-mount embryo immunofluorescence staining for DNA synthesis, as measured by BrdU incorporation (left), or overall cellular proliferation, as measured by pH3 staining (right). White punctae mark individual cells that are positively stained for the indicated marker. Insets show magnified view of tail region used for quantification. Raw mean area fraction of fluorescence in the mid-tail region was normalized against *AB* wild-type expression and reported as mean values, error bars represent +/- SEM. *NHA9 (+ Cre)* embryos show similar BrdU ($P=0.77$; *AB*, $n=35$; *NHA9*, $n=35$) and pH3 ($P=0.74$; *AB*, $n=12$; *NHA9*, $n=14$) compared to *AB* wild-type.

(B) Cell proliferation measured specifically in myeloid cells (*AB*, $n=15$; *NHA9*, $n=15$). High-power views over the yolk sac of double stains for pH3 (red; 555 nm) in WISH-labeled cells (black; brightfield) at 28 hpf. WISH was performed for the early myeloid gene, *spi1* (left) or the more mature myeloid gene, *lcp1* (right). Insets show artificially magnified view of double-stained cells. Representative symbols; white arrow = co-localization of pH3 in blood cells. Scale bar = 200 μm .

New abbreviations used: BrdU = 5-Bromo-2-deoxyuridine; pH3 = phosphorylated histone-H3.

Acknowledgement: Honours BSc student, Märta Vigerstad, contributed BrdU stain and quantification in panel A (Michael Forrester designed experiment, supervised, assisted data analysis, and edited figure design).

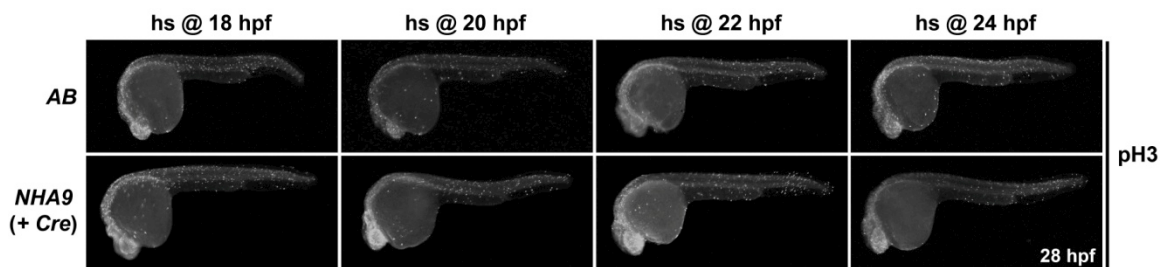


Figure 4.4. *NHA9* transgenic embryos do not exhibit hyperactive cellular proliferation.

Fluorescence microscopy (555 nm) to observe stain for pH3. Embryos heat-shocked at the indicated timepoints for Cre activation, and assayed at 28 hpf via pH3 immunofluorescence. White punctae mark individual cells that are positively stained. Embryos displayed in side profile, anterior to the left.

New abbreviations used: hs = heat-shock.

Figure 4.5 (next page). Knockdown of zebrafish *meis1* may limit *NHA9* effects on myeloid cells.

(A) RNA was extracted from wild-type and *NHA9* embryos at 28 hpf. qRT-PCR results depicted as bar graph showing level of zebrafish *meis1* expression in *NHA9* embryos (1.5 ± 0.3 -fold; n=4 biological replicates, each with 45-50 embryos per genotype, qRT-PCR performed in triplicate). Raw data was normalized against *AB* wild-type and relative to expression of housekeeping gene, *ef1a*. Values reported as mean values, error bars represent +/- SEM. Representative symbols: red and green dotted lines = lower and upper boundaries [0.5X and 1.5X expression of wild-type, respectively] for real change in expression.

(B) Embryos were either uninjected or injected at one- to four-cell stage of development with 1mM translation-blocking MO against zebrafish *meis1*. Embryos then heat-shocked at 24 hpf and stained by WISH for the expression of the myeloid gene, *lcp1*, at 28 hpf. Embryos displayed in side profile, anterior to the left, panels show magnified view of tail region only. Black punctae mark individual myeloid cells. Embryos were scored for their level of *lcp1* expression relative to wild-type, normalized to a percentage value of the total number of embryos of that genotype, and quantified in bar graph. Representative symbols: white grey bar = wild-type expression; light grey bar = low expression; dark grey bar = absent expression; black bar = high expression; n = the number of embryos used for quantification of *lcp1* expression.

Expression of *lcp1* in each embryo group is as follows:

Wild-type uninjected – 10.0% low, 90.0% wild-type;

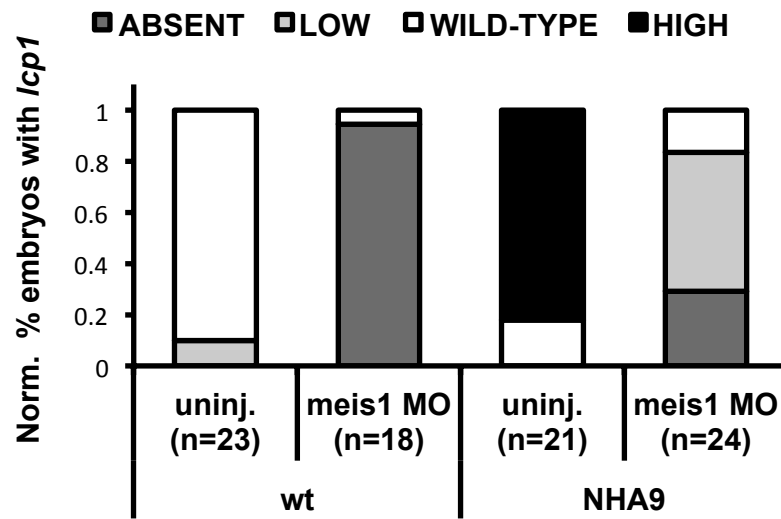
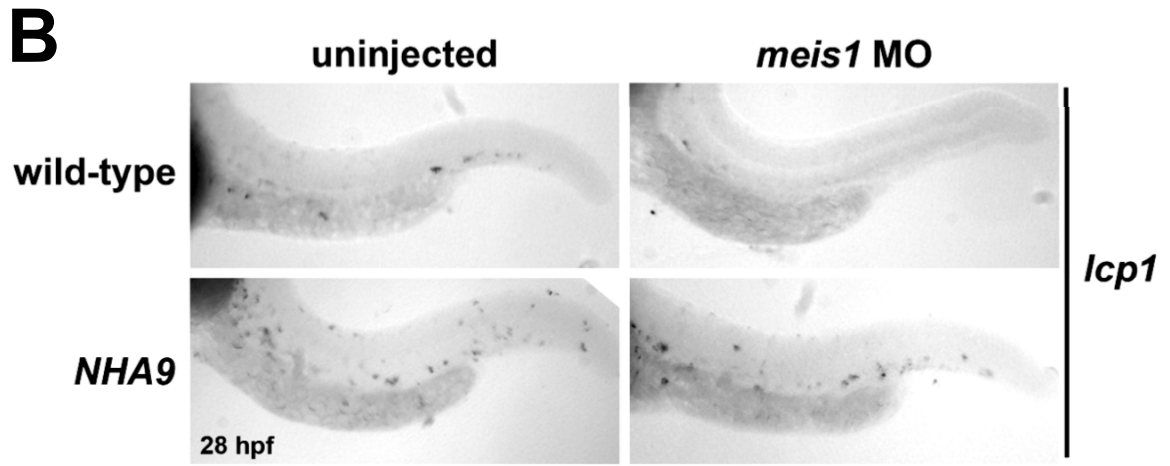
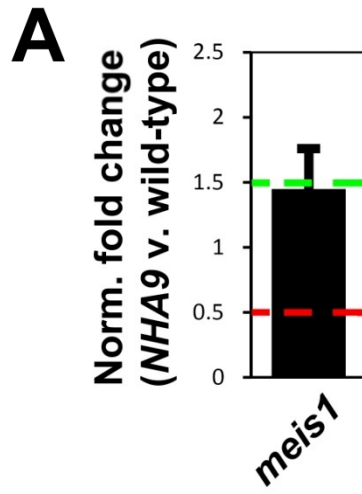
Wild-type injected with *meis1* MO – 94.5% absent, 5.5% wild-type;

***NHA9* uninjected** – 18.0% wild-type, 82.0% high;

***NHA9* injected with *meis1* MO** – 29.2% absent, 54.2% low, 16.6% wild-type.

New abbreviations used: *ef1a* = elongation factor 1 alpha; *meis1* = myeloid ecotropic integration site 1; MO = morpholino oligonucleotide.

Acknowledgement: lab technician, Andrew Coombs, assisted morpholino injection into embryos in panel B.



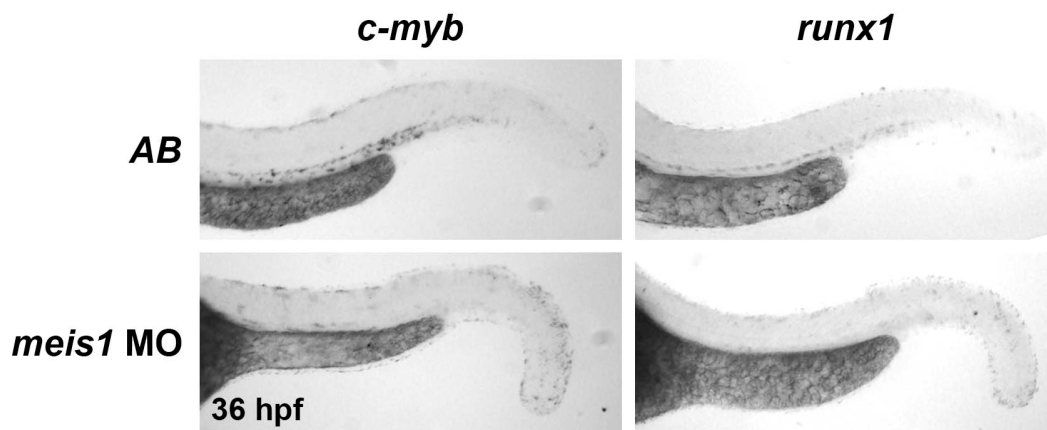


Figure 4.6. Knockdown of zebrafish *meis1* inhibits HSC development.

Embryos were either uninjected or injected with 1 mM *meis1* MO. Embryos then stained by WISH at 36 hpf. *AB* wild-type embryos show loss of *c-myb* (n=19/21) and *runx1* (n=4/6) expression in the AGM mid-trunk region. Embryos displayed in side profile, anterior to the left, panels show magnified view of tail region only.

New abbreviations used: AGM = aorta-gonad-mesonephros; *c-myb* = *v-myb myeloblastosis viral oncogene homologue (avian)*; HSC = haematopoietic stem cell; *runx1* = *runt-related transcription factor 1*.

Figure 4.7 (next page). *NHA9* suppresses *tp53*-dependent cell cycle arrest and apoptosis.

Embryos heat-shocked at 24 hpf. Selected embryos were exposed to 16 Gy IR at 26 hpf, and all assessments were performed at 28 hpf. Embryos displayed in side profile, anterior to the left. All insets show magnified view of tail region. For fluorescence microscopy, white punctae mark cells that stain positive for the indicated label. Raw mean area fraction of fluorescence in the mid-tail region of *NHA9* (+ *Cre*) embryos is normalized against *AB* wild-type and reported as mean values, error bars represent +/- SEM. Bar graphs denote *AB* with white bars, *NHA9* (+ *Cre*) with black bars. Representative symbols for student's *t*-test results: *** $P < 0.0005$; **** $P < 0.00005$; ***** $P < 0.000005$.

(A) Fluorescence microscopy (555 nm) to observe immunofluorescence for pH3. Irradiated *AB* wild-type embryos demonstrated a 4.2-fold reduction in pH3-labeled cells, whereas irradiated *NHA9* (+ *Cre*) embryos only display a 1.6-fold decrease (relative difference of 2.55-fold; *AB*, n=4; *NHA9*, n=5).

(B) Fluorescence microscopy (509 nm) to observe stain for AO. Irradiated *NHA9* (+ *Cre*) embryos show less AO staining than controls. *AB* wild-type embryos, *Tg(hsp70::Cre)* ('*Cre*'), and incrossed (*i.e.* un-activated) *NHA9* embryos ('*lGl::NHA9*') served as negative controls.

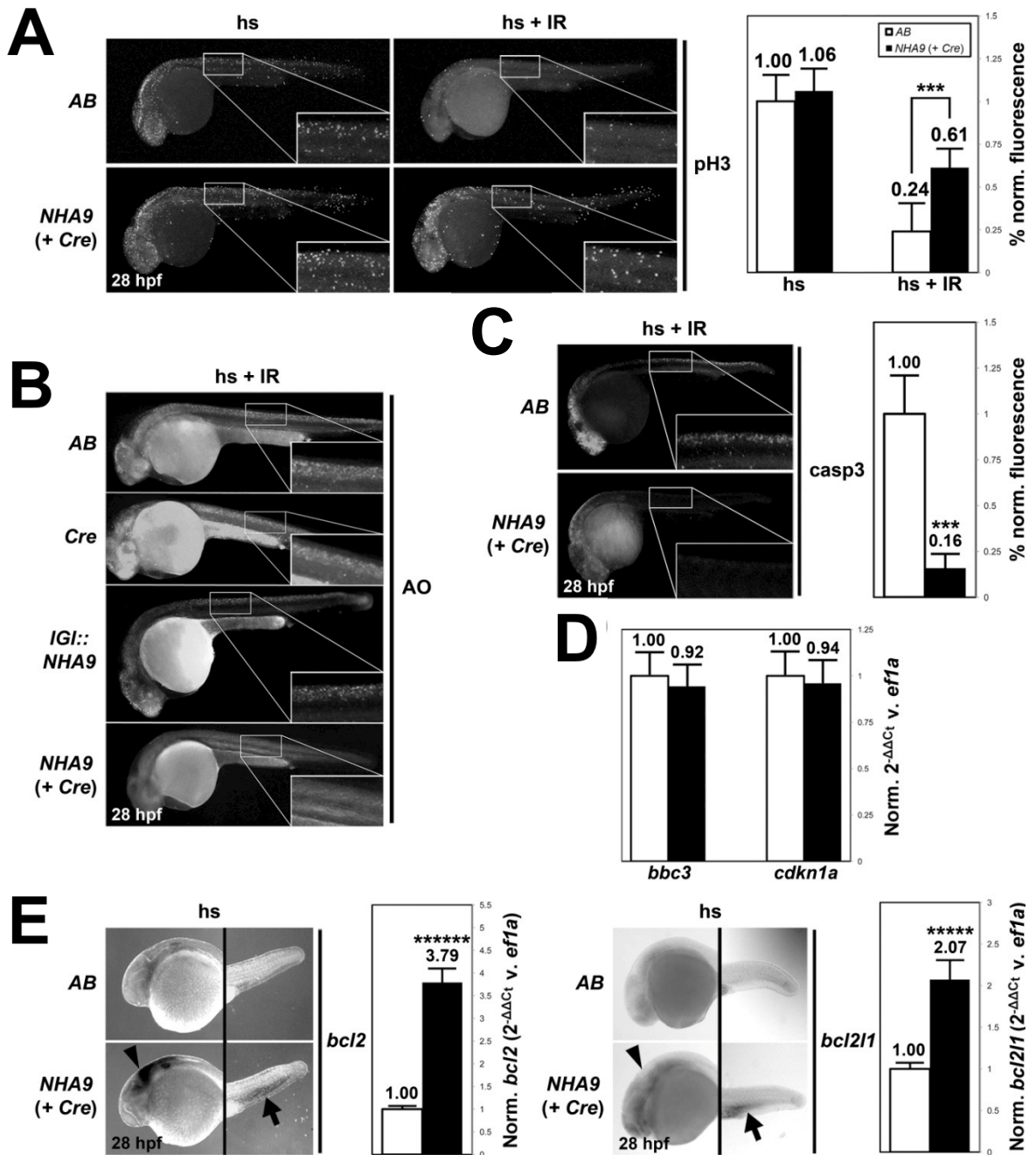
(C) Fluorescence microscopy (555 nm) to observe immunofluorescence stain for casp3. Irradiated *NHA9* (+ *Cre*) embryos display a 6.3-fold decrease in casp3 levels compared to *AB*-wild type (*AB*, n=5; *NHA9*, n=5).

(D) qRT-PCR to measure expression of zebrafish *bbc3/puma* and *cdkn1a/p21^{waf1/cip1}*. *NHA9* and *AB* wild-type embryos exhibit similar expression (0.92-fold and 0.94-fold, respectively). For qRT-PCR, RNA was extracted from wild-type and *NHA9* embryos at 28 hpf. Results depicted as bar graph showing level of indicated gene expression in *NHA9* embryos. Raw data was normalized against *AB* wild-type and relative to expression of housekeeping gene, *ef1a*. Values reported as mean values, error bars represent +/- SEM. For each gene measured by qRT-PCR, n=2 biological replicates, each with 45-50 embryos per genotype, performed in triplicate.

(E) WISH (shown in black) and qRT-PCR to measure expression of zebrafish *bcl2* and *bcl2l1/bcl-x_L*. Embryo panels show magnified view of head and tail region only. Representative symbols: black arrowhead = positive stain in head region; black arrow = positive stain in haematopoietic PBI. qRT-PCR results show increased expression in *NHA9* (+ *Cre*) embryos: *bcl2* (3.8-fold) and *bcl2l1/bcl-x_L* (2.1-fold). Methodology of qRT-PCR same as in panel D.

New abbreviations used: AO = acridine orange; casp3 = activated caspase 3; Gy = Gray; IR = ionizing radiation.

Acknowledgement: lab manager, Sahar Da'as, performed AO stain in panel B and obtained micrographs (Michael Forrester edited figure design); Honours BSc student, Ellen Boyd, performed casp3 stain in panel C, *bcl2* and *bcl2l1* stains in panel E, and obtained micrographs (Michael Forrester designed experiment, supervised, and edited figure design).



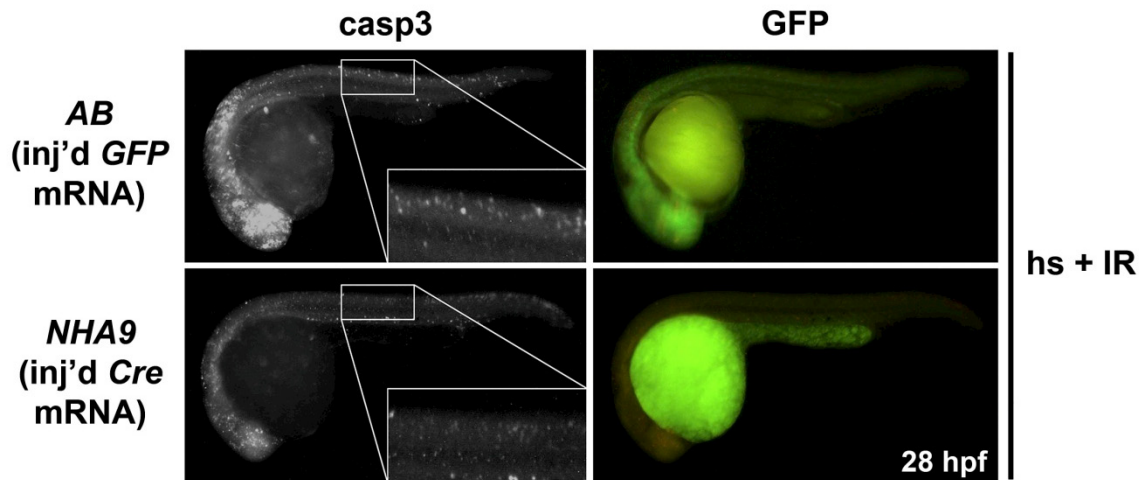


Figure 4.8. Activation of *NHA9* by microinjection of *Cre* mRNA is sufficient to achieve suppression of casp3.

Embryos at the one- to four-cell stage were injected with mRNA for either *GFP* (into *AB* wild-type) or *Cre* (into *Tg[spi1::lGl::NHA9]*). Embryos were then heat-shocked at 24hpf, exposed to 16Gy IR at 26hpf, and assayed at 28 hpf via casp3 immunofluorescence (white punctae). Embryos displayed in side profile, anterior to the left. Fluorescence microscopy used to observe casp3 expression (555 nm; *left*) or *GFP* expression (509 nm; *right*). ‘*GFP*’ panels show injection control in *AB* wild-type embryos.

Acknowledgement: Honours BSc student, Ellen Boyd, performed mRNA injection into embryos, performed casp3 stain, and obtained micrographs (Michael Forrester designed experiment, supervised, and edited figure design).

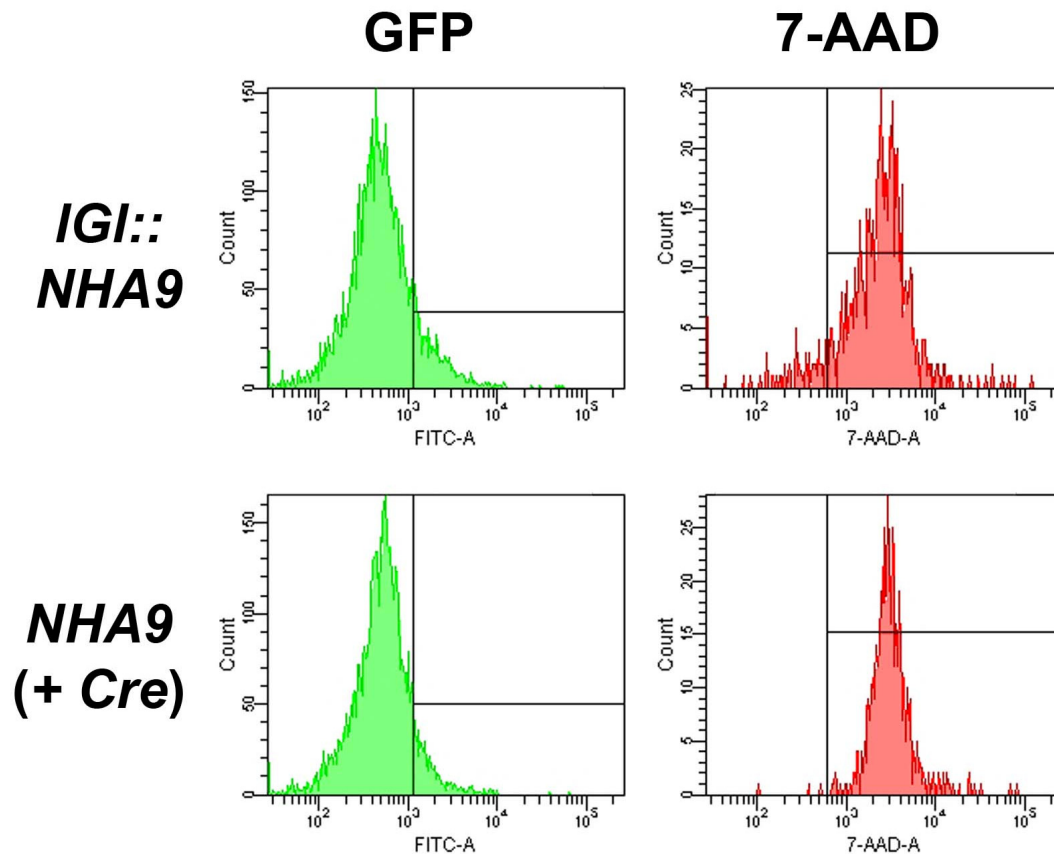


Figure 4.9. FACS analysis on GFP⁺ myeloid cells from irradiated *NHA9* embryos.

Embryos were heat-shocked at 24 hpf, exposed to 16 Gy IR at 26 hpf, and dissociated to single cell suspension for FACS analysis at 28 hpf. Cells were supplemented with 1 $\mu\text{g}/\text{mL}$ 7-AAD live cell exclusion dye. GFP⁺ myeloid cells were gated by FSC^{HI} and SSC^{HI} scatter and GFP^{HI}, and interrogated for 7-AAD^{HI} (647 nm) dead cells. Incrossed, un-activated *NHA9* embryos (*IGI::NHA9*) serve as a positive control for myeloid cells that do undergo apoptosis. Proportion of GFP^{HI}, 7-AAD^{HI} myeloid cells from *NHA9 (+ Cre)* embryos (n=2) is similar to control.

New abbreviations used: 7-AAD = 7-aminoactinomycin D; FSC = forward scatter; SSC = side scatter.

Acknowledgement: lab technician, Sandy Edgar, operated FACSAria™ I and assisted analysis.

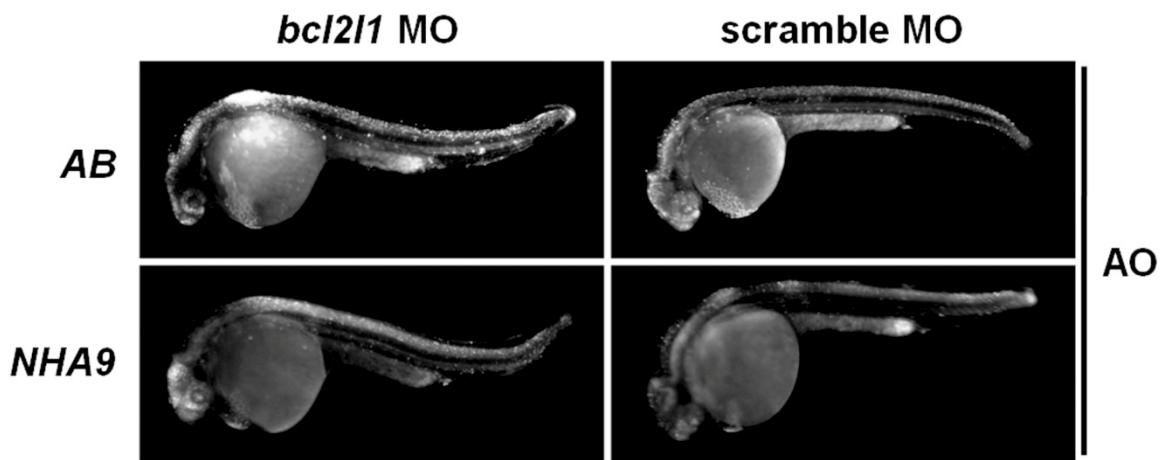


Figure 4.10. Knockdown of *bcl2l1/bcl-x_L* does not rescue apoptosis in *NHA9* transgenic embryos.

Embryos at the one- to four-cell stage were injected either with 1 mM translation-blocking MO against zebrafish *bcl2l1/bcl-x_L* or 1 mM standard control MO. Embryos were then heat-shocked at 24 hpf, exposed to 16 Gy IR at 26 hpf, and stained by AO for general apoptosis at 28 hpf. Embryos displayed in side profile, anterior to the left. Fluorescence microscopy (509 nm) used to observe AO expression.

Acknowledgement: MSc student, Tristan Dobson, performed morpholino injection into embryos.

CHAPTER 5 MICROARRAY IDENTIFIES *DNMT1* AS NOVEL GENETIC COLLABORATOR OF *NUP98-HOXA9*

5.1 BACKGROUND

5.1.1 Using Zebrafish Embryos As An *In Vivo* Tool To Study Epigenetic Mechanisms In AML

The *NUP98-HOXA9* (*NHA9*) mutation is a marker of high-risk AML in humans. AML is a genetic disease that is the result of a number of genetic lesions that dysregulate cellular differentiation (Gilliland and Tallman 2002). In humans and mice, and as we have now shown in zebrafish, *NHA9* promotes myeloid disease, and our *NHA9* zebrafish embryos show defects in haematopoiesis similar to the *AML1-ETO* fish line. Much is known about the genetic collaborators of *AML1-ETO*, but not of those that assist *NHA9*. In human AML, the *AML1-ETO* fusion oncoprotein leads to the activation of genes that the native human *RUNX1/AML1* protein might normally repress, or vice versa, and even targets novel genes (Fazi *et al.* 2007). Similarly, it is likely that the *NHA9* oncoprotein dysregulates the transcription of genes regulated by native human *HOXA9* protein. This global disruption of gene regulation is achieved, in part, due to structural changes in chromatin, where broad sections of the genome are remodelled into ‘open’ or ‘closed’ conformations (discussed in Martens *et al.* 2010 and Voss *et al.* 2009) (schematic in **Figure 5.1**). ‘Open’ chromatin is generally marked by DNA bearing methyl groups and histones bearing acetyl groups, which together keep the chromatin relaxed and accessible. The chromatin remodelling proteins involved in this activity include histone acetyltransferases (HATs) and DNA demethylases (DNA DMases). This permits direct regulation of gene expression through binding of RNA polymerase and transcription factors at promoter elements. By contrast, ‘closed’ chromatin is generally marked by methylated cytosine residues in the DNA and by histones that are methylated and unacetylated, which leads to the chromatin becoming compacted and inaccessible. The chromatin remodelling proteins involved in these activities include histone deacetylase complexes (HDACs) and DNA methyltransferases (DNMTs). This compaction broadly inhibits the expression of genes in that region of chromatin, as RNA polymerase and

transcription factors cannot bind to promoter elements. Chromatin remodelling is reversible, and the whole process is known as ‘epigenetics’.

Therefore, the oncogenic effects of *AML1-ETO* in human AML are, in part, due to a disruption of epigenetic programming, which may also be true for *NHA9*. Specifically, the *AML1-ETO* oncoprotein recruits HDACs to repress genes that are needed for terminal differentiation of blood cells (Fazi *et al.* 2007), which is a defining feature of AML. This can be pharmacologically targeted by HDAC inhibitors, such as trichostatin A (TSA), which inhibited the myeloproliferative phenotype and rescued *gata1a* erythroid expression in *Tg(hsp70::AML1-ETO)* zebrafish embryos (Yeh *et al.* 2008). This suggests that targeting epigenetic machinery may successfully inhibit certain AML oncogenes.

5.1.2 Identifying Genetic Collaborators Of *NUP98-HOXA9*

As mentioned above, the additional genetic lesions that assist *NHA9* in the transformation to AML are not well characterized. Microarray analyses in *NHA9*-transformed human cell culture have identified some gene targets, which will be discussed below. Yet the direct mechanisms of collaboration remain largely unknown, or disconnected from a therapeutic relevance, or unexplored in an *in vivo* setting. Therefore, following the success of using the *Tg(hsp70::AML1-ETO)* fish embryos as a screening tool (as discussed in CHAPTER 4), **we hypothesized that our robust *NHA9* myeloproliferation phenotype could be leveraged to identify novel collaborating genes that promote myeloid leukaemogenesis and to test therapeutic agents *in vivo*.**

In keeping with the role of epigenetics in *AML1-ETO* fish, our initial microarray analysis in *NHA9* embryos and follow-up confirmation with qRT-PCR identified upregulation of zebrafish *DNA (cytosine-5-)-methyltransferase 1 (dnmt1)*, which is another component of the epigenetic silencing machinery. I show preliminary evidence that myeloproliferation in *NHA9* embryos could be inhibited by morpholino knockdown of *dnmt1* or with pharmacologic inhibition with Decitabine (DAC; 5-aza-2'-deoxycytidine; 5-azadC), a demethylating agent used to treat human myelodysplastic syndrome (MDS) and AML. Taken together, these findings identify zebrafish *dnmt1* as a novel gene that collaborates with human *NHA9* and potentially highlight DAC as a therapeutic option for human AML patients with the *NHA9* mutation (refer back to **Figure 1.1**).

5.2 EXPERIMENTAL FINDINGS

5.2.1 Microarray Analysis Of *NHA9*-Transgenic Zebrafish Embryos

To supplement microarray analyses performed *in vitro* in human cell culture, we used our *NHA9*-transgenic zebrafish to assess global changes to gene expression *in vivo*. To maximize accuracy of our RNA comparison, Cre-activated *NHA9* embryos (the mating result of homozygous *Tg[spl1::lgl::NHA9]* fish crossed with homozygous *Tg[hsp70::Cre]* fish) were compared to un-activated *lgl::NHA9* controls (the mating result of homozygous *Tg[spl1::lgl::NHA9]* fish crossed with wild-type *AB* fish). All groups of zebrafish embryos were heat-shocked at 24 hpf, RNA extraction was performed at 28 hpf, and samples were shipped to Dr. Stephen Lewis at the Atlantic Cancer Research Institute for cDNA labeling and microarray hybridization.

5.2.2 *NHA9*-Transgenic Zebrafish Embryos Upregulate *dnmt1*

Our microarray identified *dnmt1* as the most upregulated gene in *NHA9* embryos (>7-fold) (**Figure 5.2**). *DNMT1* encodes the major maintenance DNA methyltransferase in vertebrates (Song *et al.* 2012), and its activity is one of the first steps in ‘closing’ the chromatin. Thus, *DNMT1* regulates the expression of terminal differentiation genes in various tissues via epigenetics (Anderson RM *et al.* 2009; Rai *et al.* 2006; Tittle *et al.* 2011) (**Figure 5.1**). Increased *DNMT1* expression correlates with overall lower survival in human pancreatic ductal adenocarcinoma (Zhang JJ *et al.* 2012). In AML, upregulation of *DNMT1* has been associated with loss-of-function *CCAAT/enhancer binding protein alpha (C/EBPA)* and *RUNX1* mutations in human AML. Such events lead to a repression of terminal haematopoietic differentiation (Saunthararajah *et al.* 2012), which again is a defining feature of AML. We used qRT-PCR to confirm that zebrafish *dnmt1* was upregulated by 3 ± 1 -fold in *NHA9* embryos (**Figure 5.2**). Ours is the first observation that *NHA9* activity may be linked to the vertebrate *DNMT1* gene, and therefore identifies *DNMT1* as a gene of interest for *NHA9*-induced leukaemogenesis in humans.

5.2.3 Knockdown of Zebrafish *dnmt1* Inhibits Myeloproliferation In *NHA9* Embryos

We decided to follow-up with morpholino oligonucleotide (MO) knockdown of zebrafish *dnmt1*. A translation-blocking *dnmt1* MO has already been designed (refer to **Table 2.2**) and is known to decrease the level of *dnmt1* protein by Western blot ([Rai et al. 2006](#)). A handful of studies have investigated the role of zebrafish *dnmt1* in embryonic tissue development, namely of the pancreas, liver, and eye lens ([Anderson RM et al. 2009](#); [Rai et al. 2006](#); [Tittle et al. 2011](#)). I hypothesized that knockdown of zebrafish *dnmt1* could restore wild-type levels of myeloid cells (*i.e.* block myeloproliferation) in our *NHA9* embryos. With the help of a Master's (MSc) graduate student, Adam Deveau, that I have been training, we injected *Cre* (control) and *NHA9* embryos at the one-cell stage with 0.75 mM *dnmt1* MO, and un-injected embryos served as controls. We allowed embryos to grow to 24 hpf, then performed heat-shock for 1 hour, and fixed at 30 hpf to assess myeloid expression by WISH against *lymphocyte cytosolic protein 1* (*lcp1*).

In *Cre* embryo controls, injecting *dnmt1* MO appeared to mildly decrease the whole-embryo expression of *lcp1* (**Figure 5.3**), but there is known developmental toxicity with this MO ([Rai et al. 2006](#)). We observed the expected increase of *lcp1*-expressing cells in the ALPM and PBI of activated, uninjected *NHA9* embryos compared to *Cre* controls (refer back to **Figure 4.2B**), though the percentage of embryos displaying the phenotype for these experiments was less than our previous report of 80%. Preliminary evidence suggests that injection of *dnmt1* MO results in a reversion to wild-type or low *lcp1* expression in *NHA9* embryos (**Figure 5.3**). Myeloproliferation was observed in 30.1% of uninjected *NHA9* embryos, but in none (0%) of the *NHA9* embryos injected with *dnmt1* MO.

5.2.4 Inhibiting Zebrafish *dnmt1* Enzyme Activity Blocks Myeloproliferation In *NHA9* Embryos

Conveniently, there is a known pharmacologic inhibitor of the DNMT1 enzyme, called Decitabine (DAC). DAC is a nucleoside analog of cytosine that lacks a

methylation-acceptor site, so it leads to demethylation of cellular DNA. DAC is currently used in the treatment of human AML and high-risk MDS (especially chromosome 7 anomalies, which might include the t(7;11)(p15;p15) *NHA9* translocation) (Pan *et al.* 2010). DAC has also been tested in zebrafish and an effective dose has been determined (Martin CC *et al.* 1999; Ceccaldi *et al.* 2011). As before, I hypothesized that pharmacological inhibition of zebrafish *dnmt1* enzymatic activity with DAC could block myeloproliferation in *NHA9* embryos. *Cre* (control) and *NHA9* embryos were heat-shocked for 1 hour at 24 hpf concurrently with pharmacological treatment of 75 μ M Decitabine. Treatment with 0.3% DMSO served as a vehicle control. We exposed embryos to chemicals for another 4-5 hours and then fixed embryos at 30 hpf for WISH against *lcp1*.

DAC did not appear to affect the whole-embryo expression of *lcp1* in *Cre* control embryos (**Figure 5.4**), which is consistent with previous findings that human *DNMT1* may be dispensable for normal HSC function (Trowbridge *et al.* 2012). With DMSO vehicle control, we observed the expected increase of *lcp1*-expressing cells in the ALPM and PBI of activated *NHA9* embryos compared to *Cre* controls (refer back to **Figure 4.2B**), though the percentage of embryos displaying the phenotype for these experiments (68%) was slightly less than our previous report of 80%. Preliminary data suggests that treatment with DAC results in a return to wild-type *lcp1* expression in *NHA9* embryos (4.6-fold reduction in myeloproliferation; see bar graph in **Figure 5.4**).

Taken together with the morpholino data, these findings suggest that zebrafish *dnmt1* is an important gene collaborator in *NHA9* embryos, and that targeting human DNMT1 enzyme activity with Decitabine may be a novel therapeutic option in human AML patients harbouring the *NHA9* fusion oncogene.

5.3 DISCUSSION

I performed microarray analysis on our *NHA9* zebrafish embryos and observed upregulation of *dnmt1*. Knockdown of zebrafish *dnmt1* enzyme activity with gene-blocking MO or the demethylating agent, DAC, inhibited the myeloproliferative phenotype in *NHA9* embryos. In sum, these findings suggest that zebrafish *dnmt1* is a

drugable target in our *NHA9* embryos, and that demethylating agents could be used to combat high-risk myeloid disease in human patients carrying the *NHA9* mutation.

5.3.1 Potential Mechanism For Epigenetic Dysregulation By *NHA9*

Human AML1-ETO, BCR-ABL1, MOZ-TIF2, and PML-RAR α fusion oncoproteins activate genes they might normally repress, or vice versa, and even regulate novel genes compared to their native transcription factors (Eiring *et al.* 2010; Fazi *et al.* 2007; Martens *et al.* 2010; Voss *et al.* 2009; Wang K *et al.* 2010). As was discussed in **CHAPTER 1**, *MLL*-rearrangements in mammals lead to upregulation of *HOXA9* and impact HSC differentiation possibly due to dysregulation of histone modifications (Faber *et al.* 2009; Jin *et al.* 2010; Revenko *et al.* 2010). *NHA9* oncoprotein also shows novel interactions with CREBBP and EP300 (Kasper *et al.* 1999), which together form a histone acetyltransferase (HAT) capable of opening chromatin for gene transcription (refer back to **Figure 5.1**) (Wang GG *et al.* 2007). Therefore, *NHA9* oncoprotein has unique transcriptional activity compared to the native mammalian *HOXA9* protein. In addition, human *NHA9* upregulates mouse *Meis1* expression in mice (Calvo *et al.* 2000; Calvo *et al.* 2001; Calvo *et al.* 2002), and mammalian MEIS1 proteins control the availability of histone deacetylase complexes (HDACs), CREBBP, and EP300 at HOX-regulated promoters (Choe *et al.* 2009; Kasper *et al.* 1999). Pharmacological treatment with trichostatin A (TSA), an HDAC inhibitor, rescues normal haematopoiesis in *AML1-ETO* zebrafish embryos (Serrano *et al.* 2008; Yeh *et al.* 2008), which is consistent with the recruitment of HDACs by the ETO domain of the human oncoprotein. Targeting epigenetic phenomena is gaining popularity as an alternative cancer therapy. For example, ATRA and As₂O₃ co-therapy rescues normal myeloid differentiation in human leukaemia patients carrying *PML-RARA* (Martens *et al.* 2010; Wang K *et al.* 2010). Clinical trials are also investigating the use of valproic acid, another HDAC inhibitor, in the treatment of human myeloid disease (Kuendgen *et al.* 2011).

I present the novel finding that *NHA9* embryos upregulate zebrafish *dnmt1*, which encodes a DNA methyltransferase component of the epigenetic silencing machinery that regulates blood cell differentiation. I have also found preliminary evidence that loss of zebrafish *dnmt1* enzyme activity through MO injection and pharmacologic inhibition

with Decitabine (DAC) may inhibit the *NHA9* myeloproliferative phenotype, restoring normal blood differentiation (refer back to **Figure 1.1**). These findings support the notion that epigenetics could be investigated in the context of *NHA9*-induced AML. Only one *DNMT1* homologue has been identified in zebrafish (*dnmt1*; ENSDARG00000030756, ZDB-GENE-990714-15), compared to six DNMT3 homologues (Smith TH *et al.* 2011). This increases our confidence that our microarray, MO, and DAC findings in *NHA9* zebrafish embryos would apply to human disease.

Several zebrafish studies have shown a critical role for *dnmt1* in terminal cellular differentiation in the pancreas, liver, and eye lens (Anderson RM *et al.* 2009; Chu *et al.* 2012; Rai *et al.* 2006; Tittle *et al.* 2011), thanks to its own methylating activity and its recruitment of histone methyltransferases and HDACs (**Figure 5.1**) (Guidotti *et al.* 2009). These studies used *dnmt1* null mutant lines, as well as gene-blocking morpholinos for *dnmt1* and *ubiquitin-like, containing PHD and RING finger domains, 1* (*uhrfl*). The *uhrfl* gene encodes an upstream factor that recruits *dnmt1* to DNA sites, and loss of *uhrfl* phenocopies the loss of *dnmt1* (Tittle *et al.* 2011). Zebrafish *dnmt1*^{s872} mutants show increased apoptosis of pancreatic cells and increased expression of *tp53*, *mdm2*, and *cdkn1a/p21*^{waf1/cip1} (Anderson RM *et al.* 2009). Apoptosis could be suppressed by injecting *dnmt*^{s872} mutant embryos with *tp53* gene-blocking MO. These findings suggest that, in addition to the haematopoietic phenotype in *NHA9* embryos, zebrafish *dnmt1* may also contribute to the anti-apoptotic phenotype in response to DNA damage. However, we have shown that *tp53*-signalling is likely unaffected in *NHA9* embryos, since there was no change in the expression of *bbc3/puma* and *cdkn1a/p21*^{waf1/cip1} target genes. Anderson *et al.* conjectured that zebrafish p53 is activated because genomic hypomethylation in *dnmt1*^{s872} mutants is sensed as DNA damage. Therefore, one cannot be certain upregulation of zebrafish *dnmt1* which presumably leads to genomic hypermethylation in *NHA9* embryos would prevent DNA damage responses.

A zebrafish study also demonstrated that *dnmt1* works in concert with an epigenetic co-factor, *suppressor of variegation 3-9 homologue 1a* (*suv39h1a*), a histone methyltransferase (Rai *et al.* 2006). It was proposed that zebrafish *suv39h1a* protein binds DNA that has been methylated by *dnmt1* enzyme, and that *suv39h1a* subsequently trimethylates histone H3 at lysine 9 (H3K9) to recruit histone deacetylase complexes

(HDACs). Injection of MO against zebrafish *su39h1a* phenocopied the differentiation defects seen in embryos that lack *dnmt1*, which links the methylating activity of zebrafish *dnmt1* enzyme to the broader epigenetic silencing machinery (**Figure 5.1**). This suggests that zebrafish *dnmt1-suv39h1a* epigenetic activity may regulate the haematopoietic differentiation defect in our *NHA9* embryos.

5.3.2 Targeting Epigenetic Regulation In Clinical Myeloid Disease

Single-copy deletion of mammalian *DNMT1* has little effect on normal HSC function, but loss of *DNMT1* in leukaemia-initiating cells (LICs) inhibits LIC self-renewal (Trowbridge *et al.* 2012). My findings show that inhibiting zebrafish *dnmt1* protein activity in our *NHA9* embryos can rescue normal haematopoietic differentiation, or at very least, inhibit the *NHA9* myeloproliferative phenotype. This suggests that zebrafish *dnmt1* is a drugable target in our *NHA9* embryos, and possibly also in human *NHA9*-induced myeloid disease.

Though this is the first time that the vertebrate *DNMT1* gene has been linked to human *NHA9* in the pathogenesis of myeloid disease, DAC (5-azadC) and its chemical analogue, Azacitidine (AZA; 5-azacytidine; 5-azaC) are already used as successful therapies for chronic myelomonocytic leukaemia (CMML), and high-risk MDS (especially chromosome 7 anomalies, which might include the t(7;11)(p15;p15) *NHA9* translocation) (Pan *et al.* 2010). AZA and DAC are better, less costly alternatives compared to best supportive care (BSC), which consists of red blood cell transfusions, deferoxamine, erythropoiesis-stimulating agents, platelet transfusions, and colony-stimulating factors (CSFs). Furthermore, AZA is considered to be the superior and less costly therapeutic option for MDS compared to DAC (Gidwani *et al.* 2012). Once MDS progresses to AML, however, the AZA and DAC demethylating agents may be more efficacious and less toxic when used in combination chemotherapy (Kuendgen *et al.* 2011; Maslov AY *et al.* 2012; Paul *et al.* 2010; Ryningen *et al.* 2007; Serrano *et al.* 2008). Future investigations in *NHA9* fish will explore the possibilities of combination therapies (see **CHAPTER 8**).

AZA and DAC are nucleoside analogues, and the differential clinic activities of these two agents may be due in part to prevalent nucleoside incorporation of AZA into

RNA and of DAC into DNA (Buchi *et al.* 2012). In addition to causing DNA synthesis errors, AZA and DAC target the enzymatic activity of the vertebrate DNMT1 protein. As mentioned above, upregulation of human *DNMT1* has been previously associated with loss-of-function *C/EBPA* and *RUNX1* mutations in human AML, and the activity of vertebrate DNMT1 enzyme represses terminal haematopoietic differentiation via epigenetics (Sauntharajah *et al.* 2012). Treatment with DAC restores expression of late differentiation genes, which highlight at least part of the therapeutic mechanism of AZA and DAC in human myeloid disease.

Additionally, a human cell culture study showed that both AZA and DAC decrease the levels of heterogeneous nuclear ribonucleoproteins (hnRNPs) (Buchi *et al.* 2012). Human myeloid diseases, such as those driven by *AML1-ETO* and *BCR-ABL1* (Ohshima *et al.* 2003), generally overexpress hnRNPs, which dysregulate mRNA splicing and metabolism. The human *BCR-ABL1* and *AML1-ETO* fusion oncogenes increase levels of hnRNP A2/B1 (Buchi *et al.* 2012), and studies in human gastric adenocarcinoma show that hnRNP A2/B1 colocalizes with MYC, which is a potent oncogene and shows increased activity in myeloid disease (Jing *et al.* 2011). Also, hnRNP A2/B1 interacts with hnRNP A1, which is a regulator of MYC protein translation (Martin J *et al.* 2011; Jo *et al.* 2008). Moreover, hnRNP A1 is required for normal myelopoiesis (Iervolino *et al.* 2002) and is upregulated in refractory leukaemias (Wei *et al.* 2006). *BCR-ABL1* also increases levels of hnRNP E2, which inhibits proper splicing of the mammalian *C/EBPA* transcript (Eiring *et al.* 2010). In mammals, *C/EBPA* regulates granulocyte differentiation of myeloid progenitors into neutrophils, and inactivating *C/EBPA* mutations in human AML are associated with the block in myeloid differentiation (Schwieger *et al.* 2004).

In general, mutations in several genes required for normal splicing have been identified as contributing to the pathogenesis of human MDS (Graubert *et al.* 2011; Papaemmanuil *et al.* 2011), and zebrafish have been useful tools in studying this connection. A recently-characterized zebrafish *grechetto* line harbours a mutation within the *cleavage and polyadenylation specific factor 1 (cpsf1)* gene, and shows defects in definitive myelopoiesis at 5 dpf (Bolli *et al.* 2011). Human CPSF1 protein is part of a complex of genes required for processing of the 3' untranslated region (UTR) and

addition of the poly(A) tail on a subset of pre-mRNAs. In *grechetto/cpsf1^{zdf18a12}* zebrafish mutants, the transcript encoding the snRNP70 (small nuclear ribonucleoprotein 70 [U1]) lacked a poly(A) tail (Bolli *et al.* 2011). This gene was also identified from a zebrafish screen for abnormal haematopoietic stem cell (HSC) production (Burns *et al.* 2009) and is of particular note because of its role in normal pre-mRNA splicing.

In human cell culture, both AZA and DAC decrease the cellular levels of hnRNP A2/B1 (Buchi *et al.* 2012), a binding partner of hnRNP A1. In turn, hnRNP A1 binds the 3' UTR of *E2F transcription factor 3 (E2F3)* mRNA transcripts (Eiring *et al.* 2008), which encode a chromatin assembly protein that recruits the host cell factor 1 – mixed lineage leukaemia (HCF-1 – MLL) histone methyltransferase complex to lysine 4 residues on histone H3 (H3K4) (Revenko *et al.* 2010). This is interesting because MLL protein is an upstream activator of HOXA9 protein and hnRNP activity can be suppressed by inhibiting DNMT1 enzyme. Thus, the possible link of hnRNP A1 to MLL-mediated histone methylation suggests a broad interaction network between NHA9 oncoprotein and DNMT1 enzyme (and their interacting proteins) in the regulation of key epigenetic modifications during haematopoiesis and leukaemogenesis. It is noteworthy that hnRNP activity is linked to repression of mammalian *C/EBPA* (Eiring *et al.* 2010), because downregulation of human *C/EBPA* have been observed in primary CD34+ HSCs transformed with *NHA9* (Chung *et al.* 2006). Downregulation of *C/EBPα* transcription factor is consistent with the early myelomonocytic phenotype of *NHA9*-transformed human cells and their delayed neutrophil maturation (Chung *et al.* 2006), which could reflect epigenetic reprogramming of myeloid differentiation. Enforced expression of human *C/EBPA* was able to block *NHA9*-induced proliferation in these cells.

Thus, in the pathogenesis of myeloid disease there appear to be connections between the increased activity of the DNMT1 enzyme, the curative mechanism (*i.e.* downregulating hnRNPs) of the AZA and DAC demethylating agents, the hyperactivity of hnRNPs, and the underexpression of *C/EBPA*. These connections may help to link the overexpression of zebrafish *dnmt1* in our *NHA9* embryos with the repression of human *C/EBPA* in *NHA9* human cell culture (Chung *et al.* 2006), and may also highlight an important role for epigenetic mechanisms in human *NHA9*-induced myeloid disease.

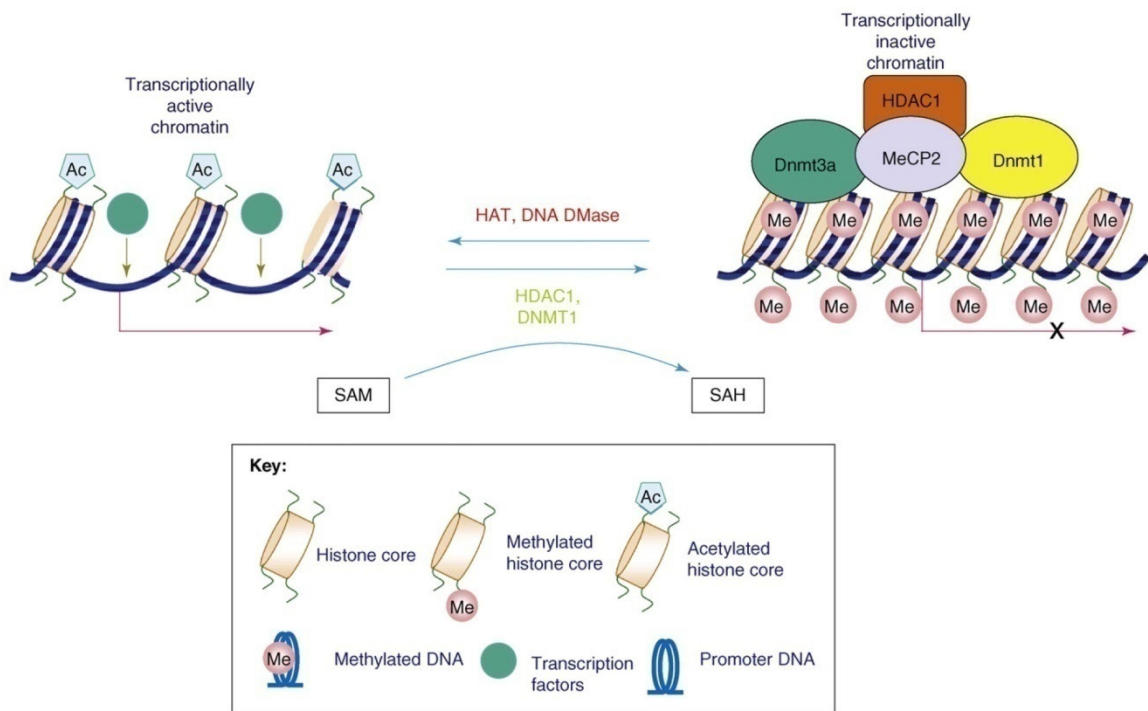


Figure 5.1. Schematic representing chromatin remodeling by DNMT1 and HDACs.

Chromatin remodeling is responsible for activation or repression of genes, such as those involved in terminal cellular differentiation. Schematic depicts the reversible interconversions that occur when promoters transition from an active (expressed) to an inactive (silenced) state. Hyperactivity of the DNMT1 and HDAC1 proteins lead to promoter methylation and histone deacetylation. This, in turn, is associated with the binding of methyl-cytosine binding proteins, such as MeCP2, DNMTs and HDAC1. The net result is the formation of a large repressor complex and a compact chromatin architecture in the vicinity of the RNA start site. The functional consequence is to block expression of the corresponding transcription unit. Adapted from [Guidotti *et al.* 2009](#).

New abbreviations used: Ac = acetyl group on histone; DNA DMase = DNA demethylase; DNMT1 = DNA (cytosine-5-)-methyltransferase 1; HAT = histone acetyltransferase; HDAC1 = histone deacetylase complex 1; Me = methyl group on DNA; MeCP2 = methyl CpG binding protein 2; SAH = S-adenosyl homocysteine; SAM = S-adenosyl methionine.

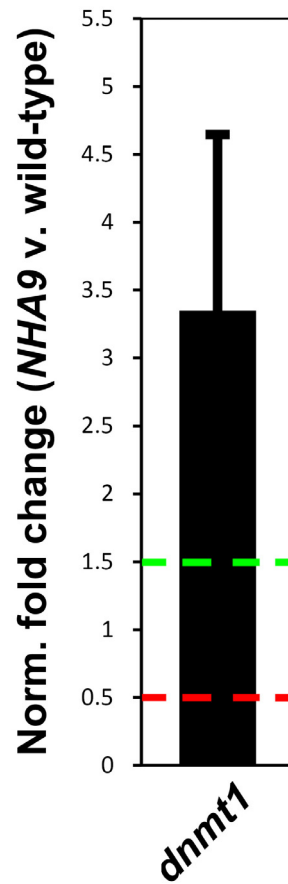


Figure 5.2. qRT-PCR from *NHA9* embryos depicting confirmation of microarray results and Wnt/ β -catenin investigations.

RNA was extracted from wild-type and *NHA9* embryos at 28 hpf. qRT-PCR results depicted as bar graph showing level of zebrafish *dnmt1* gene expression in *NHA9* embryos (3 ± 1 -fold increase; $n=3$). Raw data was normalized against *AB* wild-type and relative to expression of housekeeping gene, *ef1a* (n =the number of biological replicates, each with 45-50 embryos per genotype). Values reported as mean values, error bars represent +/- SEM. All qRT-PCR amplifications performed in triplicate. Representative symbols: red and green dotted lines = lower and upper boundaries [0.5X and 1.5X expression of wild-type, respectively] for real change in expression.

New abbreviations used: *dnmt1* = DNA (cytosine-5-)-methyltransferase 1.

Acknowledgement: Ian Chute, Daniel Leger, and Stephen Lewis at the Atlantic Cancer Research Institute performed cDNA labeling and microarray analysis, leading to the identification of *dnmt1* (Michael Forrester extracted RNA for microarray).

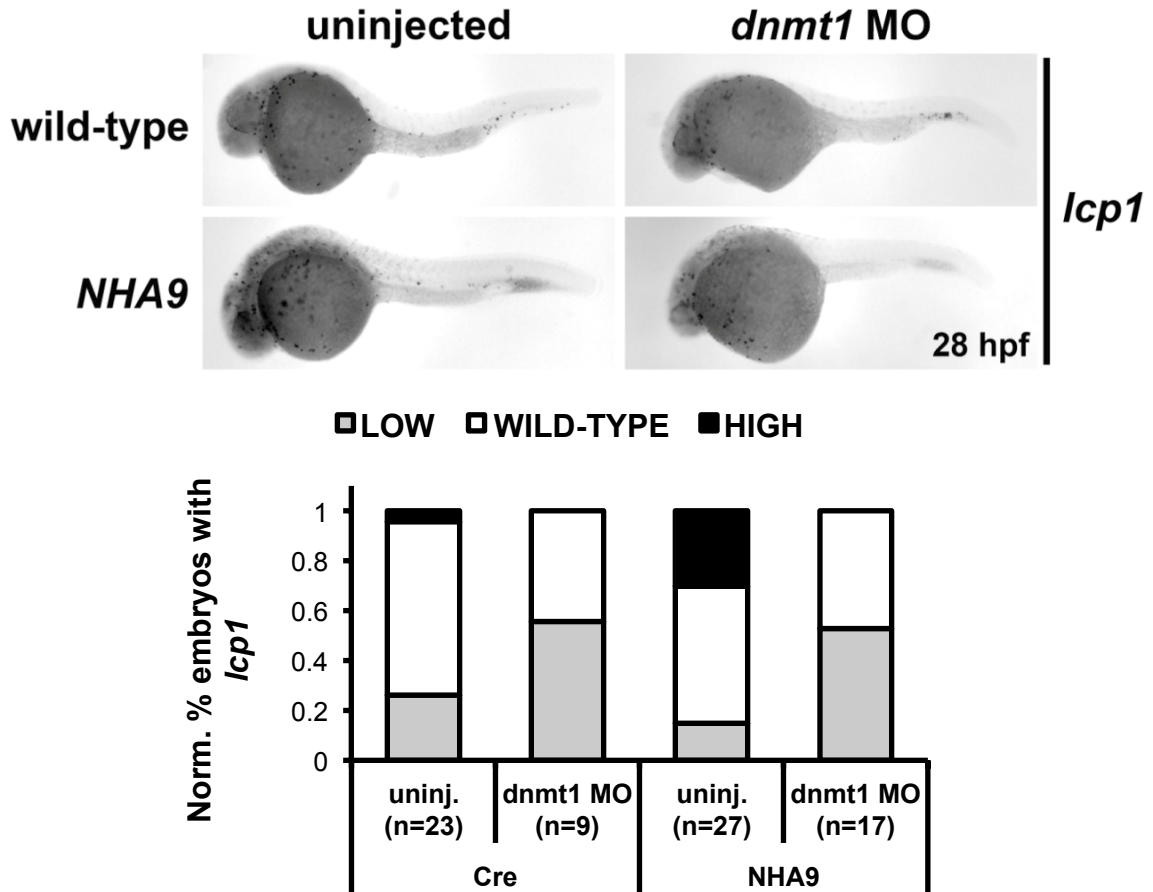


Figure 5.3. Knockdown of zebrafish *dnmt1* inhibits myeloproliferation by *NHA9*. Embryos stained by WISH for the expression of the myeloid gene, *lcp1*, at indicated timepoints. Embryos displayed in side profile, anterior to the left. Embryos were scored for their level of *lcp1* expression relative to *Cre* wild-type, normalized to a percentage value of the total number of embryos of that genotype, and quantified in bar graph. Representative symbols: white grey bar = wild-type expression; light grey bar = low expression; black bar = high expression; n = the number of embryos used for quantification of *lcp1* expression. Embryos at the one- to four-cell stage were either uninjected or injected with 0.75 mM translation-blocking *dnmt1* MO. Embryos then heat-shocked at 24 hpf and assessed at 28 hpf. Expression of *lcp1* in each embryo group is as follows:
***Cre* wild-type uninjected** – 26.0% low, 69.6% wild-type, 4.3% high;
***Cre* wild-type injected with *dnmt1* MO** – 55.6% low, 44.4% wild-type;
***NHA9* uninjected** – 14.9% low, 55.0% wild-type, 30.1% high;
***NHA9* injected with *dnmt1* MO** – 52.9% low, 47.1% wild-type.
Acknowledgement: MSc student, Adam Deveau, performed WISH stain, obtained micrographs and assisted with quantification and figure design (Michael Forrester designed experiment, supervised, performed morpholino injection of embryos, and edited analysis and figure design).

Figure 5.4 (next page). Pharmacologic inhibition of zebrafish dnmt1 enzyme activity with Decitabine inhibits myeloproliferation by *NHA9*.

Embryos stained by WISH for the expression of the myeloid gene, *lcp1*, at indicated timepoints. Embryos displayed in side profile, anterior to the left. Embryos were scored for their level of *lcp1* expression relative to *Cre* wild-type, normalized to a percentage value of the total number of embryos of that treatment group, and quantified in bar graph. Representative symbols: white grey bar = wild-type expression; black bar = high expression; n = the number of embryos used for quantification of *lcp1* expression. Embryos were treated either with 0.3% DMSO vehicle control or 75 μ M DAC, a demethylating agent and inhibitor of dnmt1. Embryos heat-shocked and treated with chemical at 24 hpf, and incubated in chemical until assessment at 30 hpf.

Expression of *lcp1* in each embryo group is as follows:

***Cre* wild-type treated with DMSO** – 82.9% wild-type, 17.1% high;

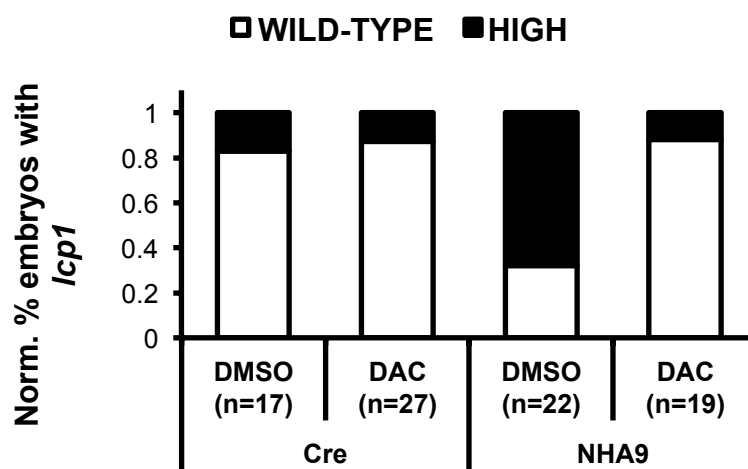
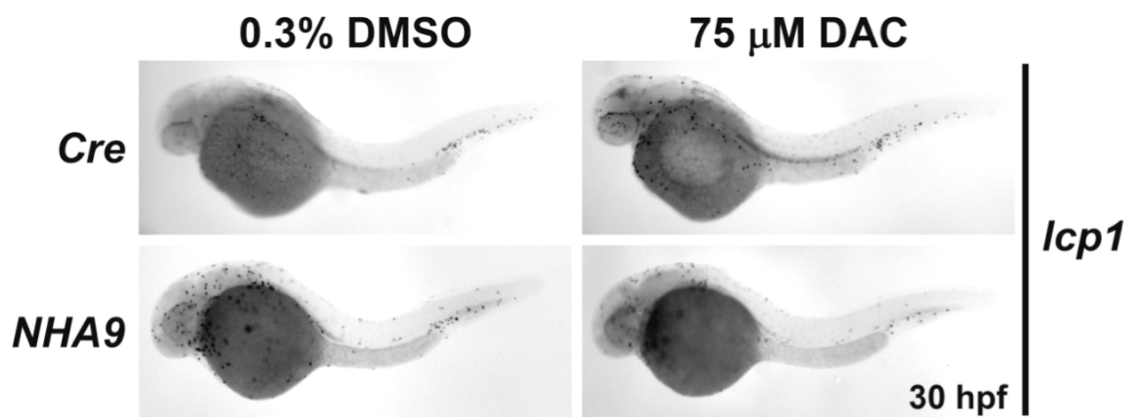
***Cre* wild-type treated with DAC** – 87.2% wild-type, 12.8% high;

***NHA9* treated with DMSO** – 32.0% wild-type, 68.0% high;

***NHA9* treated with DAC** – 88.1% wild-type; 11.9% high.

New abbreviations used: DAC = Decitabine (5-azadC); DMSO = dimethyl sulphoxide.

Acknowledgement: MSc student, Adam Deveau, performed WISH stain, obtained micrographs and assisted with quantification and figure design (Michael Forrester designed experiment, supervised, performed morpholino injection of embryos, and edited analysis and figure design).



CHAPTER 6 MANIPULATING THE *NUP98-HOXA9* MYELOPROLIFERATION PHENOTYPE BY TARGETING WNT/ β - CATENIN

6.1 BACKGROUND

6.1.1 Human *NUP98-HOXA9* Microarrays Identify Prostaglandin Signalling, Which Promotes Haematopoiesis Via Wnt/ β -catenin

Our microarray in *NUP98-HOXA9* (*NHA9*) zebrafish embryos contributes new information in addition to the microarrays already performed in human cell culture. Takeda *et al.* performed microarray analysis in *NHA9*-transformed primary human CD34+ haematopoietic stem cell culture and found upregulation of *prostaglandin-endoperoxide synthase (prostaglandin G/H synthase and cyclooxygenase) 2* (*PTGS2*). Furthermore, Ghannam *et al.* performed microarray analysis in human K562 erythroleukaemia cells that were additionally transformed with *NHA9*, and found upregulation of *PTGS1* (Ghannam *et al.* 2004). Normal K562 cells were used as a baseline for this microarray, and K562 cells on their own do not have measurable expression of human *HOXA9* mRNA (Dorsam *et al.* 2004), so the increase of *PTGS1* appears to be specific to *NHA9*. The *PTGS1* and *PTGS2* genes encode the COX1 and COX2 enzymes, leading to synthesis of the signalling molecule, prostaglandin E₂ (PGE₂). This is interesting because the COX-PGE₂ signalling axis is also upregulated in other mouse and zebrafish models of AML (Wang Y *et al.* 2010; Yeh *et al.* 2009).

As discussed in **CHAPTER 1**, two laboratories undertook chemical modifier screens in zebrafish and identified PTGS/COX inhibitors as pharmacological modifiers of haematopoietic differentiation (North *et al.* 2007; Yeh *et al.* 2009). North *et al.* subsequently showed that zebrafish PTGS/COX enzymatic activity regulates HSC formation, self-renewal, and survival (North *et al.* 2007; Goessling *et al.* 2011). Treatment of embryos with the broad-spectrum COX inhibitor, Indomethacin (Indo), led to a loss of *c-myb*- and *runx1*-expressing HSCs in the AGM haematopoietic region at 36 hpf, whereas supraphysiologic amounts of PGE₂ led to an increase in HSC formation (North *et al.* 2007). A follow-up zebrafish study showed that COX-PGE₂ signalling

ultimately drives the activity of the Wnt/ β -catenin pathway in blood cells (**Figure 6.1**), as overexpression of zebrafish *wingless-type MMTV integration site family, member 8* (*wnt8*) ligand rescued *c-myb* and *runx1* expression in embryos treated with Indo ([Goessling et al. 2009](#)). By contrast, overexpression of zebrafish *dickkopf 1b* (*dkk1b*), a negative regulator of β -catenin, eliminated normal HSC formation in zebrafish embryos and dampened the response to supraphysiologic amounts of PGE₂. These findings were subsequently corroborated in mouse cell culture. Phase III clinical trials are currently underway for 16,16-dimethyl PGE₂ (dmPGE₂), a long-acting derivative that promotes HSC regeneration, survival, and proliferation ([Lord et al. 2007](#)). Such effects could assist reconstitution of the native haematopoietic system following chemotherapy or radiation in human leukaemia patients, or bolster engraftment success in HSC transplantation therapy ([Goessling et al. 2011](#)).

Since COX-PGE₂ signalling activates Wnt/ β -catenin, and since levels of PTGS/COX enzymes appear to be elevated in human *NHA9*-induced AML, I hypothesized that this pathway would be an attractive target for investigation in our *NHA9* zebrafish. Yet there must first be a discussion of the components in the Wnt/ β -catenin pathway and the activity of this pathway in normal haematopoiesis, followed by the hyperactivity of this pathway in leukaemogenesis.

6.1.2 The Canonical Wnt/ β -catenin Pathway Promotes Self-Renewal Of Cells ('Stemness')

Activation of the Wnt pathway stabilizes intracellular β -catenin (encoded by *CTNNB1*; *catenin* [*cadherin-associated protein*], *beta 1*) (**Figure 6.1**). When Wnt ligands are absent, β -catenin is targeted for ubiquitin-mediated degradation by negative regulators, including adenomatous polyposis coli (APC), axis inhibitor (AXIN), glycogen synthase kinase 3 beta (GSK3 β), and casein kinase 1 (CK1) ([Heidel et al. 2011](#); [Reya and Clevers 2005](#)). When Wnt ligands bind to Frizzled (FZD) receptor, this activates Dishevelled (DVL), which inhibits AXIN and GSK3 β , and frees β -catenin to translocate to the nucleus. β -catenin activation is supported by the dephosphorylating activity of protein phosphatase 2A (PP2A). PGE₂ also promotes β -catenin activation through production of cyclic AMP (cAMP) by protein kinase A (PKA). At target genes, nuclear

β -catenin displaces transcriptional repressors, such as transducin-like enhancer of split (TLE/Groucho) and histone deacetylase complexes (HDACs), and drives transcription via TCF/LEF (transcription factor/lymphoid enhancer-binding factor) and cyclic AMP response element-binding (CREB)-binding protein (CREBBP). Target genes include *MYC* and *CYCLIN D1* (*CCND1*) cell cycle regulators.

In normal mammalian haematopoiesis, the Wnt/ β -catenin pathway maintains self-renewal of HSCs in the absence or suppression of differentiation cues (Kosinski *et al.* 2007). Regulators of differentiation, such as retinoic acid (RA) and colony-stimulating factors (CSFs; such as M-CSF/CSF1, GM-CSF/CSF2, G-CSF/CSF3), compete against Wnt/ β -catenin activity and promote differentiation of HSCs (Crosnier *et al.* 2006). In particular, G-CSF/CSF3 is secreted by bone marrow macrophages and endothelial cells, and it directs myeloid differentiation of HSCs and proliferation of progenitors (Beekman and Touw 2010). Similarly, RA drives differentiation in multiple organ systems (Kikuchi *et al.* 2011; Metallo *et al.* 2008; Voss *et al.* 2009), including the neutrophil lineage (de The and Chen 2010), and is important to the clinical pathogenesis and treatment of APL. Tumour cells acquire self-renewal by activating Wnt/ β -catenin, which can reprogram specialized cells to confer stem-like properties. For example, inactivation of the β -catenin negative regulator, adenomatous polyposis coli (APC) is a hallmark early transformation event in human colon cancer (Reya and Clevers 2005). With regards to leukaemia, Wnt/ β -catenin hyperactivity blocks blood cell maturation, which is a defining characteristic of AML, and this activity will be discussed in the following section.

6.1.3 AML Initiating Cells Require Wnt/ β -catenin

When Yeh *et al.* identified PTGS/COX inhibitors in their chemical modifier screen, they made this discovery by leveraging a haematopoiesis phenotype in *AML1-ETO*-transgenic zebrafish embryos (Yeh *et al.* 2008; Yeh *et al.* 2009). Soon after, this same signalling axis and therapeutic strategy was identified in the mouse model of *Hoxa9;Meis1*-induced AML (Wang Y *et al.* 2010). Indeed, it appears that the Wnt/ β -catenin pathway is hijacked by many fusion oncogenes in the development of myeloid leukaemia (Cozzio *et al.* 2003; Huntly *et al.* 2004; Jamieson *et al.* 2004; Krivtsov *et al.* 2006; Muller-Tidow *et al.* 2004; Wang Y *et al.* 2010). Activation of the Wnt/ β -catenin

pathway helps to achieve acute transformation by generating leukaemia-initiating cells (LICs), which are blocked from terminal differentiation and have the unique capacity to self-renew. LICs are at the top of the tumour cell hierarchy, with the proposed capacity to reform a tumour in the same location following therapy, or in a new location, or in a naïve healthy animal (Bonnet and Dick 1997; Dick 2005; Hope *et al.* 2003; Lapidot *et al.* 1994). In some cases, LICs are thought to be mutated HSCs (Bonnet and Dick 1997; Dick 2005; Hope *et al.* 2003; Lapidot *et al.* 1994), which already possess an active Wnt/ β -catenin pathway. This certainly appears to be true for LICs in some B-cell (Cox *et al.* 2004) and T-cell (Cox *et al.* 2007) ALL. In these cases, LICs simply retain their ability to self-renew by keeping the Wnt/ β -catenin turned on.

However, there is convincing evidence from mouse and human studies that the formation of LICs in myeloid leukaemias results from oncogene transformation of lineage-committed granulocyte-monocyte progenitors (GMPs) (**Figure 6.2**). In these cases, the LICs are not proper stem cells, but must newly acquire (or re-acquire from an earlier stage of differentiation) the ability to self-renew. Indeed, in most of the mammalian studies performed to date, the transformed GMPs maintained their differentiated phenotype but inappropriately acquired the stem-like capacity to self-renew through re-activation of the Wnt/ β -catenin pathway, whereas normal GMPs lack both self-renewal ability and Wnt/ β -catenin activity. In APL, for example, neutrophil granulocytes are lost, with an accumulation of cells at the promyelocyte stage (de The and Chen 2010). More than 90% of human APL cases (Bain 2010) exhibit the *PML-RARA* mutant transcription factor, which maintains target cells in an immature state and confers self-renewal (Martens *et al.* 2010; Voss *et al.* 2009; Wang K *et al.* 2010). The surprise is that it is the accumulated promyelocytes that are uniquely capable of initiating tumour growth (Guibal *et al.* 2009; Wojiski *et al.* 2009). Two groups demonstrated that prior to the onset of disease (*i.e.* prior to the accumulation of APL blast cells), phenotypically and morpho-logically normal promyelocytes in *PML-RARA*-transgenic mice had, in fact, acquired the capacity to self-renew and form colonies, whereas promyelocytes from wild-type animals were post-mitotic. Lineage-committed GMP cells have now been identified as LICs in a number of myeloid leukaemias, such as those driven by *MLL-AF9* (Krivtsov *et al.* 2006), *MLL-ENL* (Cozzio *et al.* 2003), and *MOZ-*

TIF2 (Huntly *et al.* 2004) human fusion oncogenes. The re-activation of the Wnt/ β -catenin pathway in GMPs appears to be important for the transforming activity of these oncogenes, including *PML-RARA* (Muller-Tidow *et al.* 2004). In CML also, the human *BCR-ABL1* mutation transforms GMPs into LICs (Huntly *et al.* 2004; Jamieson *et al.* 2004; Minami *et al.* 2008; Neering *et al.* 2007), but only after secondary mutations are acquired to activate Wnt/ β -catenin. Jamieson *et al.* used *BCR-ABL1*-transformed primary human CML cells at various stages of disease progression (chronic phase and blast crisis) to show that transformed GMPs acquired self-renewal at blast crisis, coincident with the activation of Wnt/ β -catenin. Similarly, co-overexpression of the non-fusion mouse oncogenes, *Hoxa9* and *Meis1*, confers a high penetrance of AML in mice when the Wnt/ β -catenin pathway is hyperactivated (Wang Y *et al.* 2010). Therefore, in AML pathogenesis, the re-activation of Wnt/ β -catenin in transformed GMPs appears to be a common mechanism for the formation of LICs.

6.1.4 Using *NHA9* Zebrafish Embryos To Study Wnt/ β -catenin

The specific cooperation of Wnt/ β -catenin with *NHA9*-induced disease, however, is not well characterized. **We hypothesized that myeloproliferation in *NHA9* embryos relies on, or could benefit from activation of the Wnt/ β -catenin pathway, as has been found with other fusion oncogenes in AML.** I hypothesized that we would observe abnormal gene expression for members of the zebrafish PTGS/COX-PGE₂ signalling network, which drives the activity of the Wnt/ β -catenin pathway in blood cells (Goessling *et al.* 2009; North *et al.* 2007) (Figure 6.1). I therefore expected dysregulation of any of the following zebrafish genes: the PGE₂ synthase, *ptgs1*, which was identified in a microarray analysis of human *NHA9* cell culture (Ghannam *et al.* 2004); the identified zebrafish isoforms of the COX2 enzyme, *ptgs2a* and *ptgs2b*, which were identified in a separate human *NHA9* microarray (Takeda *et al.* 2006), and were also upregulated in *AML1-ETO*-transgenic zebrafish (Yeh *et al.* 2009); and/or the zebrafish prostaglandin E receptor, subtype EP1a (*ptger1a*), which was upregulated in the mouse model of *Hoxa9;Meis1*-induced AML (Wang Y *et al.* 2010). These gene targets, however, were not identified on our microarray. By direct investigation using qRT-PCR, we did find upregulation of *ptgs2a*. It is interesting that the Wnt/ β -catenin pathway

appears to be dispensable for the self-renewal potential of adult HSCs (Wang Y *et al.* 2010), because this identifies the Wnt/ β -catenin pathway as a potential therapeutic target in human AML patients with perhaps less toxic side-effects to normal haematopoiesis. We therefore treated *NHA9* embryos with the COX inhibitor, Indo, and observed a rescue of wild-type expression for the myeloid gene, *lymphocyte cytosolic protein 1 (lcp1)*, although expression for the erythroid gene, *GATA-binding factor 1a (gata1a)*, remained suppressed. Taken together, these findings identify the Wnt/ β -catenin pathway as a possible collaborator of *NHA9* and potentially highlight Indo as a therapeutic option for human AML patients that harbour the *NHA9* mutation (refer back to **Figure 1.1**).

6.2 EXPERIMENTAL FINDINGS

6.2.1 Direct Investigation Of The Wnt/ β -catenin Pathway In *NHA9*-Transgenic Zebrafish Embryos Reveals Upregulation Of *ptgs2* Isoforms

Our *NHA9* zebrafish embryos show similar defects in haematopoietic differentiation to the *Tg(hsp70::AML1-ETO)* zebrafish line (Yeh *et al.* 2008). That group subsequently found that *AML1-ETO* upregulates the zebrafish COX-PGE₂ signalling axis (Yeh *et al.* 2009), which drives the activity of the Wnt/ β -catenin pathway in blood cells (Goessling *et al.* 2009; North *et al.* 2007) (**Figure 6.1**). The myeloproliferative effects of human *AML1-ETO* could be blocked with COX inhibitors as well as MO knockdown of zebrafish *ctnmb*, and could be accelerated with Wnt/ β -catenin stimulators (Yeh *et al.* 2009). Soon after, a mouse study used the *Hoxa9;Meis1*-induced AML model and corroborated the importance of this signalling axis and efficacy of PTGS/COX inhibition as a therapeutic strategy in mammalian myeloid disease (Wang Y *et al.* 2010).

Therefore, I hypothesized that our microarray in *NHA9* embryos would identify expression changes to zebrafish genes in the COX-PGE₂ axis. These findings would help to establish a causative link between *NHA9* and the Wnt/ β -catenin pathway in zebrafish leukaemia and would further strengthen the importance of Wnt/ β -catenin as a drugable target to inhibit multiple AML oncogenes in humans. In particular, two microarray analyses in human *NHA9* cell culture had previously identified upregulation of human *PTGS1* (Ghannam *et al.* 2004) and *PTGS2* (Takeda *et al.* 2006), encoding COX enzymes.

However, our microarray showed neither up- nor down-regulation of COX-PGE₂-related genes in *NHA9* zebrafish embryos. Despite this absence, I still proposed to explore the activity of the Wnt/ β -catenin pathway and how it may influence myeloproliferation in our *NHA9* embryos. Using qRT-PCR, I found that zebrafish *ptgs1*, the COX1 homologue, was expressed near wild-type levels (1.15 ± 0.07 -fold) (**Figure 6.3**), in contrast to the microarray study by Ghannam *et al.* 2004. This discrepancy may arise from differences between *in vitro* versus *in vivo* systems, or because the human microarray was performed on K562 leukaemia cells that were additionally transformed with *NHA9* (Ghannam *et al.* 2004). Though *EGFP*-transformed K562 cells were used as a baseline control, it cannot be ruled out that the pre-existing oncogenetic background in these cells had an impact on the expression of downstream genes. Though we observed no change in the expression of zebrafish *ptgs1* in our *NHA9* embryos, qRT-PCR did reveal a large upregulation (64 ± 6 -fold) of zebrafish *ptgs2a*, a COX2 isoform (**Figure 6.3**), consistent with the microarray study by Takeda *et al.* 2006. It is unknown why this large change to gene expression was not identified on our zebrafish microarray. Another COX2 isoform, *ptgs2b*, was also upregulated to a lesser extent (1.98 ± 0.08 -fold).

6.2.2 Inhibiting Wnt/ β -catenin In *NHA9* Embryos Blocks Myeloproliferation, But Stimulating Wnt/ β -catenin Has Unexpected Effect

Buoyed by the qRT-PCR findings, I further proposed that modifying Wnt/ β -catenin signalling would influence the activity of *NHA9* in zebrafish embryonic haematopoiesis. Extrapolating from previous studies (Wang Y *et al.* 2010; Yeh *et al.* 2009), I hypothesized that inhibiting Wnt/ β -catenin would rescue normal haematopoiesis in *NHA9* embryos. I also hypothesized that stimulating Wnt/ β -catenin would augment haematopoietic defects in *NHA9* embryos, because a hyperactive β -catenin mutation accelerated the onset of AML in mice that overexpress native *Hoxa9* and *Meis1* (Wang Y *et al.* 2010). We first used the myeloproliferative phenotype (increased *lcp1* expression) in our *NHA9*-transgenic zebrafish embryos as a phenotypic read-out. *Cre* (control) and *NHA9* embryos were heat-shocked for 1 hour at 24 hpf concurrently with pharmacological treatment. We treated embryos with 10 μ M Indo, a broad-spectrum

COX enzyme inhibitor, to decrease Wnt/ β -catenin activity. By contrast, we also treated embryos with 10 μ M dmPGE₂, a Wnt ligand, to increase Wnt/ β -catenin activity. Treatment with 0.3% DMSO served as a vehicle control. We exposed embryos to chemicals for another 4-5 hours and then fixed embryos at 30 hpf for WISH against *lcp1*.

None of the chemical treatments appeared to affect the whole-embryo expression of *lcp1* in *Cre* control embryos (**Figure 6.4**), which is consistent with previous reports (North TE, personal communication; Wang Y *et al.* 2010; Yeh *et al.* 2009). With DMSO vehicle control, we observed the expected increase of *lcp1*-expressing cells in the ALPM and PBI of activated *NHA9* embryos (78.6%) compared to *Cre* controls (refer back to **Figure 4.2B**). Treatment with Indo resulted in a near-complete return to wild-type *lcp1* expression in *NHA9* embryos, with a 3.0-fold decrease in myeloproliferation (see bar graph in **Figure 6.4**). However, we were surprised to observe that treatment with dmPGE₂ also produced a 1.8-fold decrease in the myeloproliferative phenotype, with *NHA9* embryos shifting from ‘high’ to ‘wild-type’ *lcp1* expression. This was unexpected, given our hypothesis that stimulating Wnt/ β -catenin would lead to higher levels of *lcp1*, representing accelerated myeloproliferation.

6.2.3 Inhibiting Wnt/ β -catenin In *NHA9* Embryos Does Not Rescue Erythroid Cells

We then assessed the loss of erythroid phenotype (decreased *gata1a* expression) in our *NHA9* embryos (**Figure 6.5**). Expression of *gata1a* is more easily measured at early timepoints in embryo development, so *Cre* (control) and *NHA9* embryos were heat-shocked for 1 hour at 12-14 hpf concurrently with pharmacological treatment. We exposed embryos to chemicals for another 4-5 hours and then fixed embryos at 18 hpf for WISH. None of the chemical treatments affected the expression of *gata1a* in the ICM of *Cre* control embryos, which is consistent with previous reports (Yeh *et al.* 2009). With DMSO vehicle control, we observed the expected decrease of *gata1a* expression in activated *NHA9* embryos (76.0%) compared to *Cre* controls (refer back to **Figure 4.2B**). In contrast to our findings with *lcp1* myeloproliferation, treatment with Indo resulted in only a weak rescue (1.2-fold) of wild-type *gata1a* expression in *NHA9* embryos (see bar graph in **Figure 6.5**). Treatment with dmPGE₂ did not accelerate the *NHA9* phenotype,

as we observed no greater percentage of embryos with reduced *gata1a* expression, nor a complete loss of *gata1a*.

The *lcp1* and *gata1a* findings left us uncertain about how to interpret the role of COX-PGE₂ signalling and the activation of the Wnt/β-catenin pathway in *NHA9* zebrafish embryos. I returned to qRT-PCR analysis and found a trending decrease in the expression of the zebrafish PGE₂ receptor, *ptger1a* (2.7 ± 0.6 -fold) (**Figure 6.3**). This experiment should be repeated for confirmation, but possibly suggests that treating our *NHA9* embryos with exogenous dmPGE₂ ligand would not have the expected effect of accelerating or worsening the *lcp1* or *gata1a* phenotypes. It is also possible that the large upregulation of zebrafish *ptgs2a* in *NHA9* embryos already leads to a saturation of endogenous PGE₂ levels. I also performed qRT-PCR for zebrafish *cyclin D1* (*ccnd1*), a canonical target of active Wnt/β-catenin signalling, and found only a mild upregulation of expression (1.7 ± 0.3 -fold) (**Figure 6.3**). It is possible that the design of new primers for *ccnd1* could help to identify a larger change in expression, though it should be noted that the primers used in my analysis had been used successfully in other zebrafish studies ([Duffy et al. 2005](#)).

Taken together, these findings suggest that the Wnt/β-catenin pathway may not be a major collaborator of *NHA9* in our transgenic zebrafish embryos (refer back to **Figure 1.1**). Despite the prominent anti-myeloid effect of Indo treatment on *NHA9* embryos, it is possible that this operates through a different, unknown mechanism.

6.3 DISCUSSION

I directly investigated the activity of the Wnt/β-catenin pathway in *NHA9* zebrafish embryos, and found upregulation of the zebrafish COX2 isoform, *ptgs2a*. However, interaction of *NHA9* with Wnt/β-catenin may be only partial, as inhibition with Indo seemed to restore normal myeloid, but not erythroid development, and stimulating Wnt/β-catenin did not exacerbate the myeloproliferation. In sum, I identified potential genetic collaborators and explored new therapeutic options for *NHA9*-induced myeloid leukaemogenesis. Future investigations will help to confirm these findings, and also explore the possibilities of combination therapies (see **CHAPTER 8**).

6.3.1 Reconciling Diverse Findings For Prostaglandin Signalling

We found that *NHA9* embryos overexpressed zebrafish *ptgs2a* and that myeloproliferation could be inhibited with Indo, a broad-spectrum COX inhibitor. However, stimulation of *NHA9* embryos with dmPGE₂ did not lead to the expected acceleration of myeloproliferation, and Indo treatment did not robustly rescue *gata1a*-expressing erythroid cells.

Similar to one of the *NHA9* microarray studies in human cell culture (Ghannam *et al.* 2004), K562 cells that have been additionally transformed with *AML1-ETO* show increased expression of human *PTGS2*, encoding the COX2 enzyme, and a block of K562 erythroid differentiation (Yeh *et al.* 2009). The human K562 cells could be rescued by pharmacological treatment with NS-398, a specific COX2 inhibitor, which suppressed Wnt/ β -catenin and decreased luciferase production from the TOPflash plasmid (reports TCF/LEF-dependent transcription). In *AML1-ETO* zebrafish embryos, treatment with NS-398 or Indo similarly rescued wild-type levels of *mpx* myeloid, and *gata1a* erythroid expression. Rescue was also seen upon injecting *AML1-ETO* embryos with single MOs targeted against zebrafish *ptgs1*, *ptgs2a*, *ptgs2b*, *ctnnb1*, or *ctnnb2*. By contrast, treating *AML1-ETO* embryos with supraphysiologic amounts of PGE₂, the enzymatic product of COX2, accelerated *mpx* myeloproliferation, or nullified the ability of NS-398 and Indo to rescue *gata1a* when treated concurrently. These findings place activation of the Wnt/ β -catenin pathway as a primary function of *AML1-ETO* expression *in vivo* (refer back to **Figure 6.2** for general schematic).

The inability of exogenous dmPGE₂ to accelerate *lcp1* myeloproliferation in our *NHA9* zebrafish embryos could suggest that COX-PGE₂ activation of Wnt/ β -catenin is not important in our system. Yet this appears inconsistent with the large upregulation in zebrafish *ptgs2a*, which was also observed in *NHA9*-transformed human cells (Takeda *et al.* 2006). PGE₂ positively regulates its own expression (Araki *et al.* 2003) and an excessive amount of PGE₂ in human haematopoietic cell culture actually exerts a cytostatic, and eventually apoptotic effect (North TE, personal communication). This data allows us to entertain the possibility that the level of PGE₂ is already quite saturated in our *NHA9* zebrafish embryos, which may be consistent with the observed downregulation of zebrafish *ptger1a* receptor. Our present data, however, suggests that

Wnt/ β -catenin may only partly contribute to the haematopoietic defects in *NHA9* embryos, at least in terms of COX-PGE₂ signalling.

However, before this conclusion can be made definitively, it would be instructive to treat our *NHA9* embryos with higher concentrations of Indo and dmPGE₂, as our original selection of dosages may not have been fully potent. In particular, the *gata1a* erythroid phenotype in *NHA9* embryos may be less sensitive to chemical modification, so we may yet observe a rescue to wild-type *gata1a* levels if we treated with higher doses of Indo. Also, it is possible that the apparent ‘rescue’ of wild-type *lcp1* expression in dmPGE₂-treated *NHA9* embryos may actually be an inhibition of terminal myeloid differentiation. This would be consistent with the inhibition of differentiation that we observed in the ALPM myeloid cells of *NHA9* embryos at 24 hpf (refer back to **CHAPTER 4**). Certainly, zebrafish *lcp1* may continue to mark progenitor cells through 48 hpf (Hall *et al.* 2007; Le Guyader *et al.* 2008), but it may be that pharmacological stimulation with dmPGE₂ augments the expression of zebrafish *spi1*, which marks the earliest myeloid progenitors. By focusing on the robustness of our *lcp1* phenotype, we may have missed positive contributions of the Wnt/ β -catenin pathway, which promotes ‘stemness’ and self-renewal, to the transforming activity of *NHA9*. Thus, other zebrafish myeloid markers, such as *mpx*, *lyz*, and particularly the early marker, *spi1*, should be explored in our *NHA9* embryos that have been treated with Wnt/ β -catenin modifiers. This should allow us to determine if the zebrafish Wnt/ β -catenin pathway collaborates with the human *NHA9* oncogene to block terminal differentiation of an early myeloid progenitor cell.

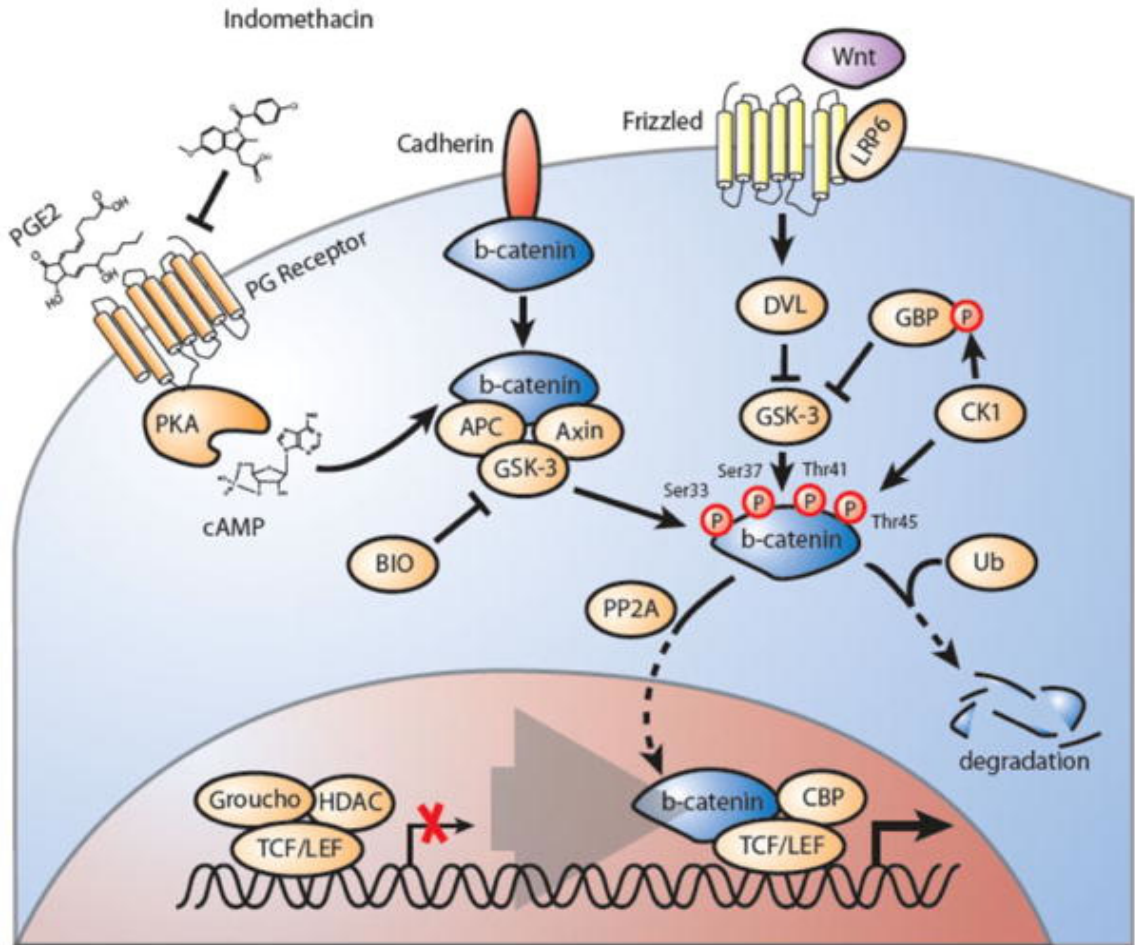


Figure 6.1. The canonical Wnt/ β -catenin signalling pathway.

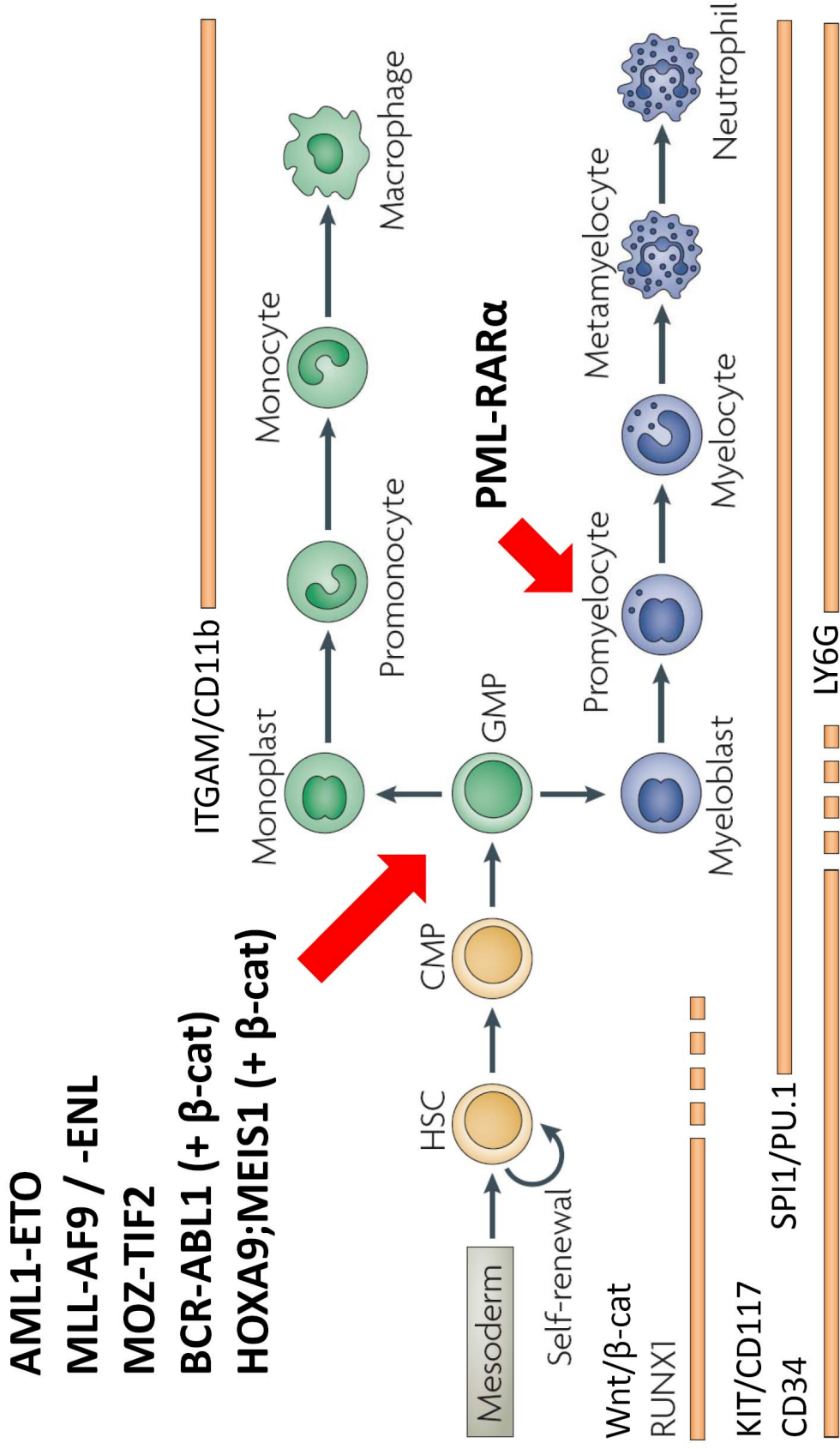
In the absence of Wnt ligands, β -catenin is in a cytosolic complex with Axin, APC, and GSK3 β , leading to phosphorylation and targeting for proteasomal degradation. Members of the TCF/LEF transcription factor family are bound in the nucleus by repressors, TLE/Groucho, and HDACs. The binding of Wnt ligands activates DVL, or binding of PGE₂ activates PKA, which frees β -catenin to translocate to the nucleus. Nuclear β -catenin binds TCF/LEF and CREBBP/CBP transcription factors to activate target genes. The COX inhibitor, Indomethacin, blocks PGE₂ synthesis, thus suppressing the pathway. Adapted from [Heidel *et al.* 2011](#).

New abbreviations used: Axin = axis inhibitor; APC = adenomatous polyposis coli; BIO = 6-bromoindirubin-30-oxime; cAMP = cyclic adenosine monophosphate; CK1 = casein kinase 1; CREBBP/CBP = cAMP response element-binding (CREB)-binding protein; DVL = Dishevelled; GBP = GSK binding protein; GSK3 β = glycogen synthase kinase 3 beta; HDAC = histone deacetylase complex; LRP6 = low-density lipoprotein receptor-related protein 6; PGE₂ = prostaglandin E₂; PKA = protein kinase A; PP2A = protein phosphatase 2A; TCF/LEF = transcription factor/lymphoid enhancer-binding factor 1; TLE/Groucho = transducin-like enhancer of split; Ub = ubiquitin.

Figure 6.2 (next page). Granulocytic and monocytic lineages, markers in myeloid differentiation, and impact of fusion oncoproteins.

Self-renewing HSCs express KIT/CD117, CD34, RUNX1 and Wnt/ β -catenin. The expression of the master regulator of myeloid development, SPI1/PU.1, pushes HSCs through a common GMP stage from which both neutrophils (marked by LY6G) and macrophages (marked by ITGAM/CD11b) delineate. Red arrows point to target cells for transformation by listed fusion oncoproteins. Note that the fusion oncoprotein, BCR-ABL1, and non-fusion oncoproteins, HOXA9;MEIS1, require a secondary mutation event that activates Wnt/ β -catenin, whereas other oncoproteins can activate Wnt/ β -catenin independently. Adapted from [Rosenbauer and Tenen 2007](#).

New abbreviations used: AML1-ETO = acute myeloid leukaemia 1—eight twenty-one; β -cat = β -catenin; BCR-ABL1 = breakpoint cluster region—v-abl Abelson murine leukaemia viral oncogene homologue 1; CMP = common myeloid progenitor; GMP = granulocyte-monocyte progenitor; HOXA9 = homeobox A9; HSC = haematopoietic stem cell; ITGAM = integrin, alpha M (complement component 3 receptor 3 subunit); KIT = v-kit Hardy-Zuckerman 4 feline sarcoma viral oncogene homologue; LY6G = lymphocyte antigen 6 complex, locus G; MEIS1 = myeloid ecotropic integration site 1; MLL-AF9 = mixed lineage leukaemia—ALL1-fused gene from chromosome 9; MLL-ENL = mixed lineage leukaemia—eleven nineteen leukaemia; MOZ-TIF2 = monocytic leukaemia zinc finger protein—transcriptional intermediary factor 2; PML-RAR α = promyelocytic leukaemia—retinoic acid receptor alpha; SPI1/PU.1 = spleen focus forming virus (SFFV) proviral integration oncogene / purine-rich (PU)-box factor 1.



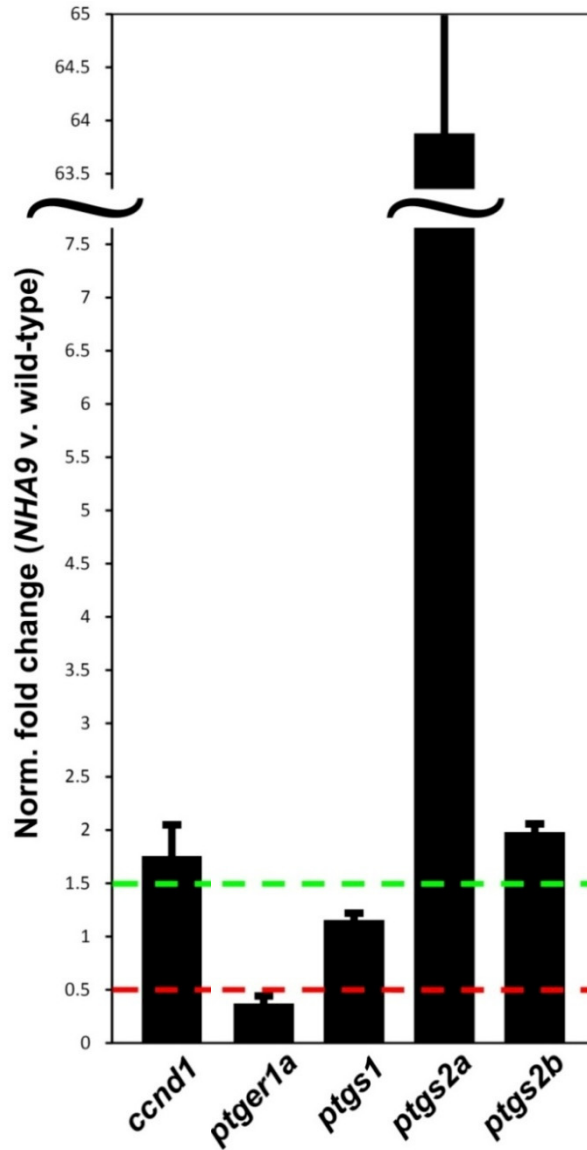


Figure 6.3. qRT-PCR from *NHA9* embryos depicting Wnt/ β -catenin investigations. RNA was extracted from wild-type and *NHA9* embryos at 28 hpf. qRT-PCR results depicted as bar graph showing level of indicated zebrafish gene expression in *NHA9* embryos. Raw data was normalized against *AB* wild-type and relative to expression of housekeeping gene, *ef1a* (n=the number of biological replicates, each with 45-50 embryos per genotype). Values reported as mean values, error bars represent +/- SEM. All qRT-PCR amplifications performed in triplicate. Representative symbols: red and green dotted lines = lower and upper boundaries [0.5X and 1.5X expression of wild-type, respectively] for real change in expression. qRT-PCR results show the following changes to gene expression in *NHA9* embryos: *ccnd1*, 1.7 ± 0.3-fold increase (n=3); *ptger1a*, 2.7 ± 0.6-fold decrease (n=2); *ptgs1*, 1.15 ± 0.07-fold wild-type-like (n=6); *ptgs2a*, 64 ± 6-fold increase (n=3); *ptgs2b*, 1.98 ± 0.08-fold increase (n=4).

Figure 6.4 (next two pages). The Wnt/ β -catenin pathway may play a limited role on the myeloproliferative phenotype in *NHA9* embryos.

Embryos were treated either with 0.3% DMSO vehicle control, 10 μ M Indo to inhibit Wnt/ β -catenin signalling, or 10 μ M dmPGE₂ to stimulate Wnt/ β -catenin signalling. Embryos heat-shocked and treated with chemical at 24 hpf, and incubated in chemical until assessment at 30 hpf. Embryos stained by WISH for the expression of the myeloid gene, *lcp1*. Embryos displayed in side profile, anterior to the left. Embryos were scored for their level of *lcp1* expression relative to *Cre* wild-type, normalized to a percentage value of the total number of embryos of that treatment group, and quantified in bar graph. Representative symbols: white grey bar = wild-type expression; black bar = high expression; n = the number of embryos used for quantification of *lcp1* expression.

Expression of *lcp1* in each embryo group is as follows:

***Cre* wild-type treated with DMSO** – 78.6% wild-type, 21.4% high;

***Cre* wild-type treated with Indo** – 86.2% wild-type, 13.8% high;

***Cre* wild-type treated with dmPGE₂** – 85.2% wild-type, 14.8% high;

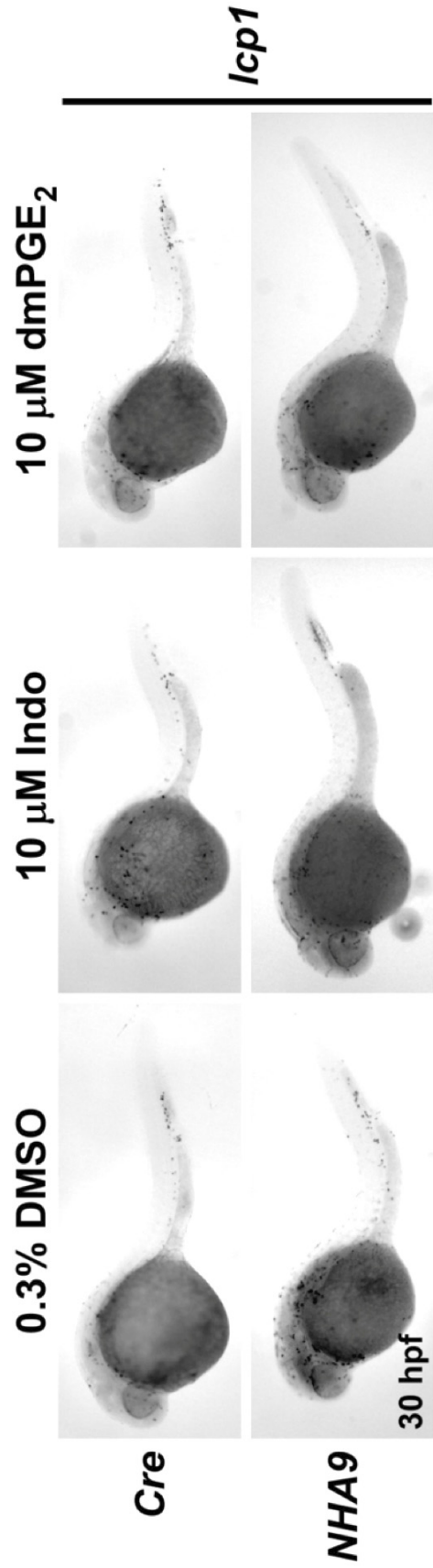
***NHA9* treated with DMSO** – 22.2% wild-type, 77.8% high;

***NHA9* treated with Indo** – 73.9% wild-type; 26.1% high;

***NHA9* treated with dmPGE₂** – 56.0% wild-type; 44.0% high.

New abbreviations used: DMSO = dimethyl sulphoxide; dmPGE₂ = 16,16-dimethyl-prostaglandin E₂; Indo = Indomethacin.

Acknowledgement: MSc student, Adam Deveau, assisted drug treatment, performed WISH stain, obtained micrographs, and assisted quantification and figure design (Michael Forrester designed experiment, supervised, and edited analysis and figure design).



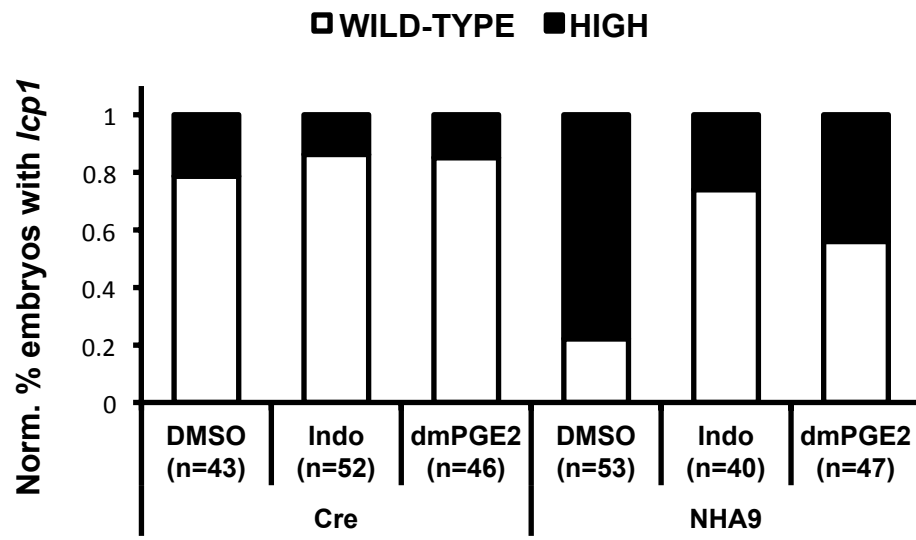


Figure 6.5 (next page). Inhibition of the Wnt/ β -catenin pathway weakly rescues erythroid development in *NHA9* embryos.

Embryos were treated either with 0.3% DMSO vehicle control, 10 μ M Indo to inhibit Wnt/ β -catenin, or 10 μ M dmPGE₂ to stimulate Wnt/ β -catenin. Embryos heat-shocked and treated with chemical at 12 hpf, and incubated in chemical until assessment at 18 hpf. Embryos stained by WISH for the expression of the erythroid gene, *gatala*. Embryos displayed in side profile, anterior to the left. Embryos were scored for their level of *gatala* expression relative to *Cre* wild-type, normalized to a percentage value of the total number of embryos of that treatment group, and quantified in bar graph. Representative symbols: white grey bar = wild-type expression; light grey bar = low expression; n = the number of embryos used for quantification of *gatala* expression.

Expression of *gatala* in each embryo group is as follows:

***Cre* wild-type treated with DMSO** – 14.3% low, 85.7% wild-type;

***Cre* wild-type treated with Indo** – 15.4% low, 84.6% wild-type;

***Cre* wild-type treated with dmPGE₂** – 8.3% low, 91.7% wild-type;

***NHA9* treated with DMSO** – 76.0% low, 24.0% wild-type;

***NHA9* treated with Indo** – 63.0% low; 37.0% wild-type;

***NHA9* treated with dmPGE₂** – 84.0% low; 16.0% wild-type.

Acknowledgement: MSc student, Adam Deveau, assisted drug treatment, performed WISH stain, obtained micrographs, and assisted quantification and figure design (Michael Forrester designed experiment, supervised, and edited analysis and figure design).

CHAPTER 7 *IN VIVO* ANTI-LEUKAEMIA ACTIVITY OF NOVEL PRODIGIOSENES IN A ZEBRAFISH XENOGRAFT MODEL

7.1 BACKGROUND

7.1.1 A Pressing Need For Novel Anti-Leukaemia Agents

As discussed in **CHAPTER 1**, myeloid leukaemias represent a heterogeneous group of diseases that are in need of novel therapeutic agents ([Marcucci *et al.* 2011](#); [Roboz 2011](#)). AML remains fatal for 40% of patients, both due to refractory disease and toxicity from traditional therapeutic agents ([Roboz 2011](#)). Some experts believe that AML treatment has reached a ‘plateau’ in efficacy ([Lowenberg *et al.* 2011](#)) and several high-profile clinical trials in paediatric centres over the past decade have been unable to significantly improve overall survival of patients ([Woods 2006](#)). Certainly, an enriched understanding of the underlying molecular mechanisms that contribute to disease is critical to aid the design of targeted therapies in the long-term (see **CHAPTER 4**, and **CHAPTER 5**). However, the current need for new drugs is pressing, particularly ones that affect unique cellular processes and that may avoid overlapping toxicities with current chemotherapies, such as Cytarabine (arabinofuranosyl cytidine, Ara-C), and anthracyclins ([Attar *et al.* 2008](#); [Walter *et al.* 2010](#)).

7.1.2 A Zebrafish Xenotransplantation Model To Investigate Genetics And Drug Responses Of Human Myeloid Leukaemia Cells

Overall, compared to the lymphoid tumours, animal models of myeloid leukaemia are relatively less penetrant with disease rates ranging from 25% ([Le *et al.* 2007](#)) to <1% ([Zhuravleva *et al.* 2008](#)). The use of other haematopoietic promoters may facilitate more faithful models of human myeloid disease in zebrafish. In particular, dissection of the zebrafish *runx1* promoter has provided new insights into the regulation of this gene in zebrafish but may also prove to be a better driver of oncogene induced malignant myeloid disease ([Lam *et al.* 2010](#)). Tissue culture assays and animal models have been instrumental in determining key key molecular pathways in cancer and novel drug

development. However, *in vitro* assays lack the critical context of the tumour micro-environment, while mouse xenografts are cost-prohibitive and require extensive engraftment time. Therefore, one potential complimentary strategy is xenotransplantation of human or mouse myeloid leukaemia cells into zebrafish.

By contrast, the use of zebrafish facilitates scalability, where large numbers of rapidly-developing, externally-fertilized, transparent embryos can be used to screen compounds in a high-throughput manner. There has been a great deal of recent interest in developing methodologies for xenotransplantation of human or mouse cancer cells into zebrafish and applying this approach to screening molecular mechanisms and therapeutic options in myeloid disease. By using embryos at 48 hours post fertilization (hpf), xenograft rejection is minimized, by virtue of their lack of an adaptive immune system during the first week of life (Lam SH *et al.* 2004). Incubation of xenografted embryos at 35°C enables growth of injected human cell lines in a fully-constituted, 3D, *in vivo* micro-environment, without compromising zebrafish embryogenesis (Corkery *et al.* 2011; Lee *et al.* 2005). The development of the *casper* mutant fish line that permanently maintains transparency into adulthood (White *et al.* 2008) has provided another valuable tool for longitudinal observation of malignant cell populations.

A number of anatomic sites in the 48 hpf embryo have been trialled for xenografting, such as the hindbrain ventricle (Haldi *et al.* 2006), liver (Marques IJ *et al.* 2009), posterior cardinal vein (Pruvot *et al.* 2011), and Duct of Cuvier (Nicoli *et al.* 2007) (some of these sites can be observed in **Figure 1.5**). Some groups have also tested human cancer cell injections into early embryos between 3.5 to 4.5 hpf (Lee *et al.* 2005), and even 25 to 35 dpf juvenile zebrafish (Stoletov *et al.* 2007). Other groups have chosen the yolk sac for the site of injection (Haldi *et al.* 2006; Marques IJ *et al.* 2009), and this is what our group had previously chosen for our leukaemia xenotransplantation pilot study (Corkery *et al.* 2011). Our reasons for choosing the yolk sac as an injection site, as well as other pitfalls of zebrafish xenotransplantation will be discussed further below.

Two groups, including ours, have exploited xenotransplantation for the study of myeloid leukaemias (Corkery *et al.* 2011; Pruvot *et al.* 2011). Both groups demonstrated successful engraftment and proliferation of CM-DiI fluorescently labelled K562 erythroleukaemia and NB4 acute promyelocytic leukaemia (APL) human cell lines

following yolk sac injection in 48 hpf zebrafish embryos. Moreover, response to targeted therapy with imatinib mesylate in human K562 cells harbouring the BCR-ABL1 oncoprotein or with all-*trans* retinoic acid (ATRA), a targeted inhibitor of the PML-RAR α oncoprotein found in human NB4 cells was observed with the addition of these compounds to the water of xenografted embryos. Pruvot *et al.*, observed a reduction in the number of xenografted K562 cells upon exposure to imatinib and a dose-dependent teratogenic effect and death of NB4 cell xenografted embryos treated with ATRA. Our group has developed a robust *ex vivo* cell proliferation assay to quantify cell numbers over time following xenotransplantation (**Figure 7.1**). Using this assay, we demonstrated that engrafted cells specifically responded to known targeted therapeutic agents, resulting in decreased cell numbers but no embryonic toxicity. Specifically, xenografted K562 cells are inhibited by imatinib, and xenografted NB4 cells are inhibited by ATRA. Importantly, when therapeutic agents were swapped and applied against the opposite cell type, leukaemia cells continued to proliferate demonstrating that human cancer cells can be specifically targeted in a zebrafish xenotransplantation model.

Given the pressing need for new anti-leukaemia agents with less toxicity ([Attar *et al.* 2008](#); [Walter *et al.* 2010](#)), these studies open the door for using the zebrafish xenotransplantation platform to rapidly assess the efficacy of novel compounds on the proliferation of human leukaemia cells *in vivo*. Xenotransplantation could also enable screens of currently-available anti-cancer agents for off-label, *in vivo* activity against human leukaemia cells.

7.1.3 Prodigiosin & Its Derivatives Have Anti-Cancer Activity

Prodigiosin (**1**) (**Figure 7.2, left**) is the parent member of a family of tripyrrolic natural products, isolated from *Serratia*, *Streptomyces*, and *Bacillus* strains of bacteria. Prodigiosin possesses potent immunosuppressive, antimicrobial and cytotoxic properties ([Manderville 2001](#); [Montaner and Perez-Tomas 2003](#); [Furstner and Grabowski 2001](#)). Coley's Toxin ([Rook 1992](#)), consisting of bacterial extracts including *Serratia Marcescens* that contain Prodigiosin (**1**) and was successfully used as an anti-cancer agent before its withdrawal by the FDA due to high systemic toxicity ([Perez-Tomas *et al.* 2003](#)). The anti-cancer activity of Prodigiosin (**1**) is thought to result from transport of

H⁺/Cl⁻ ions over phospholipid membranes (Furstner and Grabowski 2001; Sato *et al.* 1998; Seganish and Davis 2005) and copper-induced double-strand DNA cleavage (Furstner and Grabowski 2001; Melvin *et al.* 1999; Melvin *et al.* 2001; Melvin *et al.* 2002a; Melvin *et al.* 2002b; Park *et al.* 2003).

Prodigiosin (**1**) is cytotoxic to various human cancer cell lines, for example haematopoietic (Montaner *et al.* 2000), colon (Montaner and Perez-Tomas 2001), and gastric (Diaz-Ruiz *et al.* 2001) cancer cell lines. Early *in vitro* studies showed Prodigiosin (**1**) to be exceptionally potent against P388 leukaemia (Boger and Patel 1988), alongside significant activity against other cancerous cell lines. Removal of the methoxy substituent (**2**) resulted in greatly diminished cytotoxicity and removal of all substituents (**3**) led to equal or further reduced activity (**Figure 7.2, right**). This trend in activity was studied further by D'Alessio and co-workers (D'Alessio and Rossi 1996; D'Alessio *et al.* 2000; Rizzo *et al.* 1999), who found that adding alkoxy substituents of increasing size led to a step-wise reduction in activity and cytotoxicity, which ultimately could improve selectivity.

Other studies of note focused on the modes of action involved in Prodigiosin-induced apoptosis. Cell lines examined include Jurkat-T cells (Ramoneda and Perez-Tomas 2002; Montaner and Perez-Tomas 2002a; Montaner and Perez-Tomas 2002b; Perez-Tomas *et al.* 2003), HL60 leukaemia cells (Melvin *et al.* 2002a; Melvin *et al.* 2002b) and B-cell chronic lymphocytic leukaemia (B-CLL) cells (Campas *et al.* 2003). Prodigiosin induced apoptosis of B-CLL cells through caspase activation, which was the first report showing that Prodigiosin induces apoptosis in human primary cancer cells (Campas *et al.* 2003).

Dr. Alison Thompson in the Department of Chemistry at Dalhousie University researches the chemistry of pyrrolic compounds, and her lab has great expertise in the synthesis and tailored modifications of important pyrroles. The Thompson lab has created new derivatives of the Prodigiosin tripyrrole, which are called prodigiosenes, and these novel compounds have shown anti-cancer activity against leukaemia cell lines *in vitro*, which includes K562 erythroleukaemia cells, which harbour the human *BCR-ABL1* fusion oncogene found in CML (Gale and Canaani 1984). We engaged in a collaborative study with the Thompson lab to test the *in vivo* anti-leukaemia activity of prodigiosenes.

To do this, we exploited the enhanced imaging capabilities of the zebrafish embryo to serve as a xenotransplantation platform for the injection of human leukaemia cells. **We hypothesized that a xenotransplantation model in zebrafish embryos could help to characterize novel chemotherapeutic agents that have efficacy against myeloid leukaemia.**

In a brief departure from my studies on *NHA9* transgenic zebrafish, we injected K562 leukaemia cells into zebrafish embryos and treated them with prodigiosenes. I found that prodigiosenes inhibited the proliferation of K562 cells to an equal or greater extent than current therapeutics, and that some of these new compounds were modified to give less toxic side effects to embryos. Given the high toxicity of their parent compound, these modified prodigiosenes may be an effective alternative and may ultimately prove to have less toxicity if selected for clinical trials in human leukaemia patients.

7.2 EXPERIMENTAL FINDINGS

7.2.1 Synthesis Of C-Ring Modified Prodigiosenes

To date, most structure-activity relationship studies of prodigiosenes have focused on the A-ring (**3**) with some success in retention of the anti-proliferative behaviour of the parent compound (**1**). As mentioned above, the lab of Dr. Alison Thompson performs synthesis and tailored modifications of important pyrroles, and is engaged in many projects using synthesized derivatives of natural Prodigiosin, called prodigiosenes. Their work concerns structural modification of the C-ring (**3**), an area that was previously under-developed. In particular, they created four novel C-ring modified prodigiosenes (designated **8a-d**).

7.2.2 C-Ring Modified Prodigiosenes **8a-d Show Novel Anti-Leukaemia Activity *In Vitro***

All four novel prodigiosenes were selected for screening by the National Cancer Institute (NCI) against their panel of 60 human cell lines, derived from nine cancer cell types. The averaged results of these *in vitro* screens are shown in **Table 7.1**, alongside

those previously determined for Prodigiosin (**1**) (Regourd *et al.* 2007). With the exception of **8d**, all compounds showed sufficient anti-cancer activity to warrant further study. Prodigiosene **8b** was selected by the NCI for additional toxicity studies, which found that **8b** caused no deaths in mice at 50 mg/kg, versus acute system toxicity at 4 mg/kg for Prodigiosin (**1**, NCI data). Of further interest, during the original 60-line screen prodigiosenes **8a-d** displayed enhanced activity against leukaemia cell lines compared to lines representing the other eight types of cancer included in the NCI panel (Figure 7.3). Indeed, compounds **8a-d** uniformly lead to cell death against the leukaemia cell lines: note the negative growth percentages across the leukaemia cell lines *versus* negative and positive growth of cells across all of the other cancer types. This preferential activity was not observed for any of the previous C-ring modified prodigiosenes that have been synthesized by the Thompson lab.

7.2.3 *In Vivo* Anti-Leukaemia Activity Of Novel C-Ring Modified Prodigiosenes **8a-d** In A Zebrafish Xenograft Model

We were approached by the Thompson lab to investigate the effects of these prodigiosenes in an animal model, namely the zebrafish. To validate their *in vitro* studies, we investigated the efficacy of the novel prodigiosenes against leukaemia cell survival *in vivo* using a novel zebrafish xenotransplantation platform. We recently pioneered this strategy for the study of anti-leukaemia agents in a live animal model. We used mutant *casper* fish, which lack all pigment and are thus ideal for longitudinal tracking of fluorescently-labelled cells *in vivo* (White *et al.* 2008). CM-DiI-labelled K562 human leukaemia cells (~50 cells) were micro-injected directly into the yolk sac of *casper* (*roy orbison*^{-/-}; *nacre*^{-/-}) embryos at 48 hours of life (Corkery *et al.* 2011).

K562 cells were chosen because they harbour the t(9;22)(q34;q11) translocation termed the Philadelphia chromosome, which results in the the pathognomonic *BCR-ABL1* fusion gene found in human chronic myelogenous leukaemia (CML) (Gale and Canaani 1984). The human BCR-ABL1 oncoprotein can be successfully targeted by tyrosine kinase inhibitors, including the prototypic imatinib mesylate (IM; Gleevec®) (Hughes *et al.* 2010). Our lab previously performed a proof-of-principle study with xenografted K562 cells in zebrafish embryos, showing that leukaemia cell proliferation could be

inhibited upon treatment of with IM (Corkery *et al.* 2011). Corkey *et al.* developed a cell quantification assay to evaluate drug responses, where xenografted embryos are dissociated to a single cell suspension at 24 and 72 hours post-injection followed by analysis of fluorescence to measure the average average number of cells per embryo. This assay demonstrated that xenografted K562 cells specifically responded to IM, resulting in decreased cell numbers but no toxicity to the fish embryo. By contrast, the xenografted K562 cells proliferated normally when embryos were treated with ATRA, the targeted inhibitor for PML-RAR α oncoprotein. Thus, using the K562 leukaemia cell line and IM treatment provided a positive control to evaluate the efficacy of our prodigiosenes.

Successful xenotransplantation into zebrafish was determined by the presence of a fluorescent mass at the injection site 24 hours post injection (hpi) (**Figure 7.4**). We then sought to determine whether synthetic prodigiosenes **8a-d** could inhibit growth of the leukaemia cells. Injected embryos were divided into six groups: two controls, and one each with addition of a prodigiosene (**8**) to the water. The optimal dose (50% of maximum tolerated dose [MTD]) was determined by conducting toxicity curves using 48-hour zebrafish embryos treated for 72 hours. Prodigiosenes **8c** (2 μ M) and **8d** (3 μ M) were better tolerated than **8a** (0.2 μ M) and **8b** (0.2 μ M). In fact, a truly lethal dose of **8c** and **8d** could not be determined, so the MTD was defined as the dose at which embryo swimming activity began to decline.

Engrafted embryos were followed using live cell microscopy (**Figure 7.4**) and living embryos were imaged every 24 hours to monitor cell numbers and migration. We observed that K562 cells engrafted in vehicle and drug treated fish either exhibited proliferation and extensive migration throughout the fish (*i.e.* proliferative), a single stable mass of cells (*i.e.* cytostatic), or visible regression of tumour mass (*i.e.* cytotoxic) over time. We classified embryos into these three categories, on the basis of our scoring.

Embryos treated with 0.3% dimethyl sulphoxide (DMSO) organic solvent served as negative control, showing abundant K562 cell proliferation and entry of cells into circulation (**Figure 7.5A**). Embryos treated with 20 μ M IM served as a positive control, demonstrating no cell proliferation or migration (**Figure 7.5B**). By comparison, prodigiosenes (**8a-d**) inhibited K562 cell activity to a similar or greater degree than IM,

preventing proliferation and migration of the leukaemia cells (**Figure 7.5C-F**). The effects of prodigiosenes appeared to be graduated (**Figure 7.5G** shows scoring table): **8a** was predominantly cytostatic (**Figure 7.5C**), while **8b** (**Figure 7.5D**) and **8d** (**Figure 7.5F**) were moderately cytotoxic. Activity of compound **8c** was of particular note, being strongly cytotoxic (**Figure 7.5E**). Migration of K562 cells was sometimes observed in embryos treated with prodigiosenes, independent of apparent cytostatic activity of the compound. This suggests that prodigiosenes do not affect cell migration. Migration of K562 cells in fish with clear cytotoxic effects and tumour regression were rarely seen.

7.2.4 Difficulties Quantifying Anti-Leukaemia Effects Of Prodigiosenes

We attempted to use the *ex vivo* cell proliferation assay to quantify the effects of prodigiosenes **8a-d** on the proliferation of xenotransplanted K562 cells. However, measuring the fluorescence of Cm-DiI proved unsuccessful, due to the intensity of background fluorescence from the aromatic prodigiosenes.

We therefore attempted a modified *ex vivo* proliferation assay, based on immunofluorescence (IF) directed to human cell surface proteins. We first tried IF against CD34 (cluster of differentiation marker 34), which should be highly expressed in CML ([Marques DS *et al.* 2010](#)), but our stock of K562 cells showed no positive staining and this may sometimes be a function of length of time spent in cell culture (Liwski R, personal communication). High-throughput FACS analysis using a panel of fluorophore-conjugated antibodies identified CD33 and CD45 (the human leukocyte antigen; [Wittamer *et al.* 2011](#)) as markers for subpopulations of our K562 culture, but we were warned that even these were not robust cell markers (Liwski R, personal communication). Indeed, even double IF directed against both of these markers could not raise the cell-specific signal above the level of background fluorescence from prodigiosenes.

7.2.5 Attempts To Assess Activity Of Prodigiosenes on *NHA9*-Transgenic Embryos

Given that Prodigiosin (**1**) and prodigiosenes **8a-d** have similar ability to induce copper-mediated DNA cleavage, ([Melvin *et al.* 2001](#)) and that native Prodigiosin induced

apoptosis of B-CLL cells through caspase activation (Campas *et al.* 2003), we hypothesized that treatment with prodigiosenes could overcome the apoptosis defect in *NHA9*-transgenic embryos, specifically through the activation of caspase 3 (casp3).

I treated groups of *NHA9*-transgenic embryos with prodigiosene both prior to, and immediately following heat-shock at 24 hpf, followed by exposure to 16 Gy ionizing radiation (IR) at 26 hpf and fixation for casp3 immunostaining at 28 hpf. *NHA9*-transgenic embryos exposed to IR only served as a control, as well as similar treatments with *Cre*-transgenic embryos. I elected to trial this procedure using 2 μ M **8c**, given its relatively mild toxicity and qualitative potency against K562 cells.

Preliminary results, however, remain inconclusive, mostly due to inefficient immunostaining of casp3 for unknown reasons (possibly human error), even in *Cre* control embryos. Yet, as before, even in embryos where casp3 staining was regular, the background fluorescence from prodigiosene may prove problematic for quantifying treatment effects. Some *Cre* control embryos exposed to IR only (“IR + DMSO”) showed the expected casp3 pattern, indicative of cells undergoing apoptosis (**Figure 7.6, left**). *Cre* embryos that were exposed to both IR and 2 μ M **8c** prodigiosene (“IR + **8c**”) exhibited a high level of background fluorescence, which would hinder measurements for specific casp3 staining (**Figure 7.6, right**). It may be recommended to employ immunohistochemistry (IHC) techniques, such as terminal deoxynucleotidyl transferase dUTP nick end labeling (TUNEL), or even simply using chromogenic detection of casp3 rather than IF.

7.3 DISCUSSION

Native Prodigiosin (**1**) has potential efficacy as an anti-cancer agent but high toxicities preclude its clinical use. The Thompson lab has designed four prodigiosenes bearing pendant alkyl ester groups on the C-ring. These novel compounds exhibited novel selectivity for leukaemia cells *in vitro* that I helped to corroborate *in vivo* using the zebrafish xenotransplantation model. Initial results are promising, with all compounds demonstrating anti-proliferation of K562 leukaemia cells and, in some cases, exhibiting less toxic side effects to the zebrafish embryos. This work extends the use of zebrafish xenografts to determine the *in vivo* sensitivity of human cancer cells to novel drugs (see

CHAPTER 8). It also suggests that tailoring prodigiosenes may ultimately represent novel therapeutics for human leukaemia with improved anti-cancer potency and reduced toxicity compared to the parent compound, Prodigiosin.

7.3.1 Potential Pitfalls Of Zebrafish Xenotransplantation

As mentioned above, several anatomical locations in the zebrafish embryo have been tested for xenotransplantation. Our group decided on the yolk sac for several reasons: this injection site is more easily accessed compared to others, especially the thinly-visible Duct of Cuvier; there is minimal risk of damage to the embryo (thus leading to increased survival post-injection); similarly, there is minimal disruption to embryogenesis; and finally, we wanted to minimize any passive entry of human cancer cells into the zebrafish circulation. This last factor was important to us, because we wanted to standardize the ‘starting point’ (or the ‘starting environment’) for the human cancer cells in all embryos, in order to take accurate measurements of human cell proliferation. Circulating human cancer cells could potentially be exposed to multiple microenvironments; a human cell found near the eye could possibly encounter very different proliferative or anti-proliferative factors compared to a human cell found near the heart. We decided that this variety of microenvironments would be difficult to control for in our cell counting assay. Thus, we chose injection into the yolk sac as a standardized environment, and any of our injected embryos that displayed human cancer cells within the zebrafish circulation at 24 hpi were discarded from further analysis.

However, injection of human cancer cells into the yolk sac carries a potential disadvantage to cellular proliferation, as zebrafish studies have shown that neutrophils help developing tumours to grow. An early indicator of tumour proliferation is the production of hydrogen peroxide (H_2O_2). H_2O_2 is a reactive oxygen species (ROS) that is produced in both tumour cells and healthy neighbouring cells by dual oxidase (DUOX), a member of the NADPH oxidase (NOX) family of enzymes. The result of ROS production is the recruitment of neutrophils to the tumour region, and zebrafish models of epithelial carcinoma suggest that these visitations by neutrophils help the tumour cells to proliferate (Feng Y *et al.* 2010). Specifically, gene knockdown of zebrafish *duox* in either tumour cells or neighbouring cells results in less ROS production, less neutrophil

recruitment, and less tumour growth. For our studies with human cancer cells injected into the zebrafish yolk sac, there are no neighbouring cells in the region to help with the production of H₂O₂. More importantly, there is much less opportunity for circulating neutrophils, which migrate over top of the yolk sac, to visit these human cancer cells in the yolk interior. Overall, these considerations suggest that human cancer cells injected into the yolk sac might be limited in their ability to proliferate. If true, this would certainly interfere with our ability to use our zebrafish xenotransplantation to fully characterize the activity of anti-cancer agents.

Finally, the current set-up of our *ex vivo* cell counting assay relies on measurements of non-specific fluorescence from Cm-DiI-labelled cells. As my study on prodigiosenes illustrates, a pitfall in this approach is that any chemical compounds exhibiting red autofluorescence make it very difficult to discern individual cells (or to distinguish human cells from zebrafish cells), which interferes with measurements of cell proliferation. These difficulties have also been observed for doxorubicin (Corkery D, personal communication), which exhibits a low level of autofluorescence in the red channel. Using IF directed against human cell surface proteins could be an effective solution to autofluorescent compounds, providing that the intensity of IF signal rises above the level of background fluorescence. Unfortunately, this proved difficult to perform with my prodigiosene study, given that we could not find a robust marker for the human K562 leukaemia cells. We are currently investigating a qRT-PCR based approach to measure the effects of prodigiosenes on K562 cell proliferation. Xenotransplant embryos will be dissociated to a single-cell suspension, RNA will be extracted, and we will measure the levels of human *BCR-ABL1* mRNA transcripts against a standard curve of K562 cell numbers, similar to how residual CML disease is monitored clinically in human leukaemia patients (Emig *et al.* 1999; Jones *et al.* 2003). This may allow us to accurately pinpoint the number of human K562 leukaemia cells that are extracted from each treatment group of xenotransplant zebrafish embryos.

Table 7.1. Mean *in vitro* activity^a of Prodigiosin (**1**) and prodigiosenes **8a-d** over 60 cancer cell lines.

Entry	Compound	Log ₁₀ mean GI ₅₀	Log ₁₀ mean TGI	Log ₁₀ mean LC ₅₀
1	1	-7.85	-5.68	-6.65
2	8a	-6.24	-5.44	-4.59
3	8b	-6.70	-5.71	-4.81
4	8c	-6.27	-5.27	-4.52
5	8d	-5.45	-4.82	-4.29

^a <http://dtp.nci.nih.gov/branches/btb/ivclsp.html>; average of two repeat screens.

Acknowledgement: Deborah Smithen performed experiment, analysed data, and created table.

New abbreviations used: GI₅₀ = 50% growth inhibition (concentration); LC₅₀ = 50% lethal concentration; TGI = total growth inhibition.

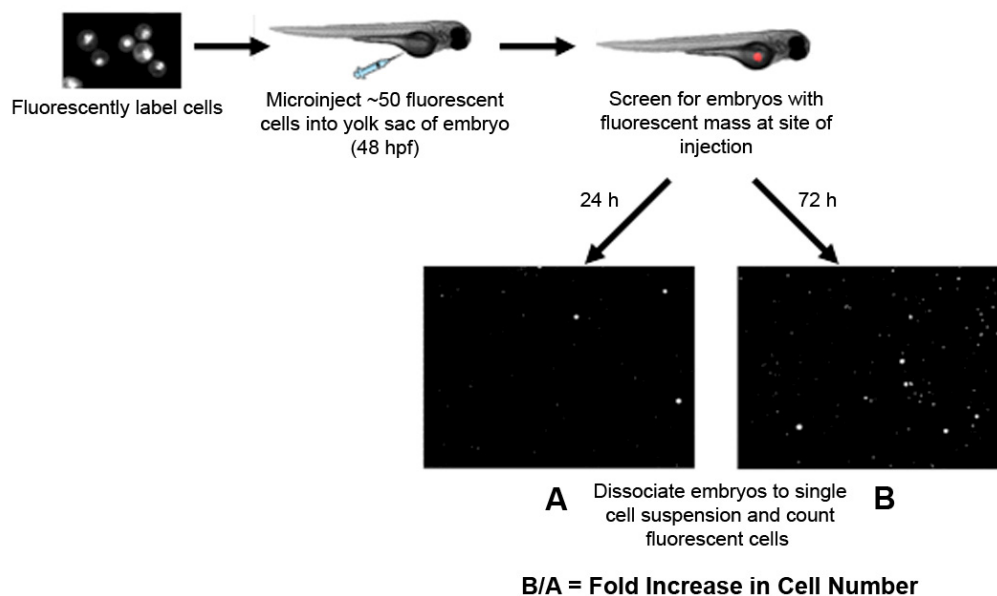
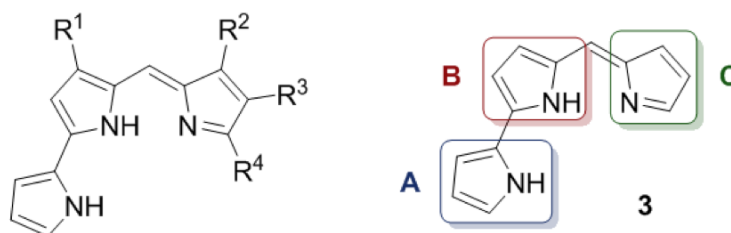


Figure 7.1. Schematic of *in vivo* cell proliferation assay in xenotransplanted zebrafish embryos.

Human leukaemia cells are fluorescently labelled with a cell tracking dye. Approximately 25–50 fluorescently labelled cells are microinjected into the yolk sac of 48 hpf *casper* embryos. Embryos are screened using fluorescent microscopy for the presence of a fluorescent mass at the site of injection. Positive embryos are divided into two groups: one is maintained at 35°C for 24 hours, and the other is maintained until the time point of interest with or without drug exposure. At the end of each time point embryos are enzymatically dissociated to a single cell suspension and the number of fluorescent cells in the suspension is counted using a semi-automated macro in ImageJ. The number of fluorescent cells present at the later time point divided by the number of fluorescent cells at 24 hours represents the fold increase in cell number. Adapted from [Corkery *et al.* 2011](#).



- 1: Prodigiosin;** $R^1 = \text{OMe}$;
 $R^2 = \text{H}$; $R^3 = (\text{CH}_2)_4\text{CH}_3$; $R^4 = \text{CH}_3$
2: $R^1 = R^2 = \text{H}$; $R^3 = (\text{CH}_2)_4\text{CH}_3$; $R^4 = \text{CH}_3$

Figure 7.2. Prodigiosin (1), analogue (2) and prodigiosene core structure (3).

Organic structure of Prodigiosin, and labelling of ring groups.
Acknowledgement: Deborah Smithen created diagram.

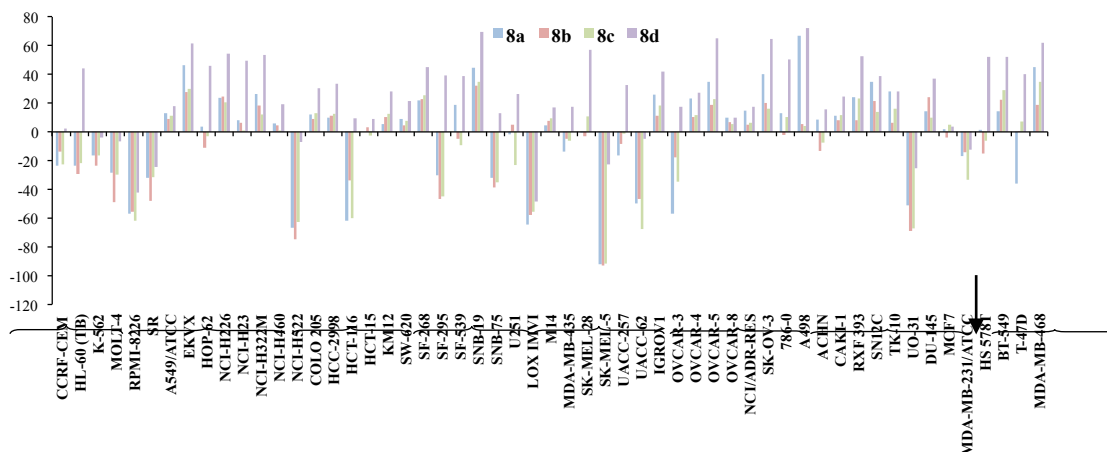


Figure 7.3. Novel anti-leukaemia activity of C-ring modified prodigiosenes.

In vitro activity^a of prodigiosenes **8a-d**, at 10 μ M concentration, tested against 60 human cancer cell lines representing 9 different cancer types in the NIH/NCI Developmental Therapeutics Program.

(^a <http://dtp.nci.nih.gov/branches/btb/ivclsp.html>; average of two repeat screens.)

Acknowledgement: Deborah Smithen performed experiment, analysed data, and created graph.



Figure 7.4. Baseline activity (24 hpi) of xenotransplanted K562 leukaemia cells in zebrafish embryo.

Brightfield (*left*) and 555 nm fluorescent (*right*) images of *casper* zebrafish embryo at 24 hpi following injection of K562 human leukaemia cells at 48 hpf. Embryo displayed in side profile, anterior to the left. Scale bar = 1 mm, intervals = 250 μ m.

New abbreviations used: hpi = hours post injection.

Acknowledgement: Dale Corkery injected embryos with leukaemia cells.

Figure 7.5 (next two pages). Anti-leukaemia activity of prodigiosenes 8a-d *in vivo* against K562 human leukaemia cells injected into *casper* zebrafish.

Embryos injected at 48 hpf with K562 human leukaemia cells. K562 cell numbers and spreading were monitored through live cell microscopy every 24 hours up to 96 hpi. Brightfield (*left*) and 555 nm fluorescent (*right*) images of *casper* zebrafish embryo at indicated timepoints. Embryo displayed in side profile, anterior to the left.

(*A-F*) Embryos were treated with (*A*) 0.3% DMSO (negative control); (*B*) 20 μ M IM (positive control) (Corkery *et al.* 2011); (*C*) 0.2 μ M **8a**; (*D*) 0.2 μ M **8b**; (*E*) 2 μ M **8c**; and (*F*) 3 μ M **8d**. Drugs added directly to water at 50% maximum tolerated dose [MTD]. Embryos began treatment with chemical at 24 hpi, and were incubated in chemical until end of assessment.

Representative symbols: autofluorescence of prodigiosenes in the zebrafish liver [*] and swim bladder [**]; white arrows indicate leukaemia cells.

(*G*) Bar graph summarizing *in vivo* activity of prodigiosenes. The effects of treatments on K562 activity were scored relative to DMSO control, then normalized to a percentage value of the total number of embryos of that treatment group. Representative symbols: white grey bar = “proliferative”; light grey bar = “cytostatic”; black bar = “cytotoxic”; n = number of embryos used for analysis.

Values of K562 cell proliferation in each embryo group is as follows:

DMSO – 76.9% proliferative, 23.1% cytostatic;

IM – 8.3% proliferative, 83.4% cytostatic; 8.3% cytotoxic;

8a – 30.8% proliferative, 53.8% cytostatic; 15.4% cytotoxic;

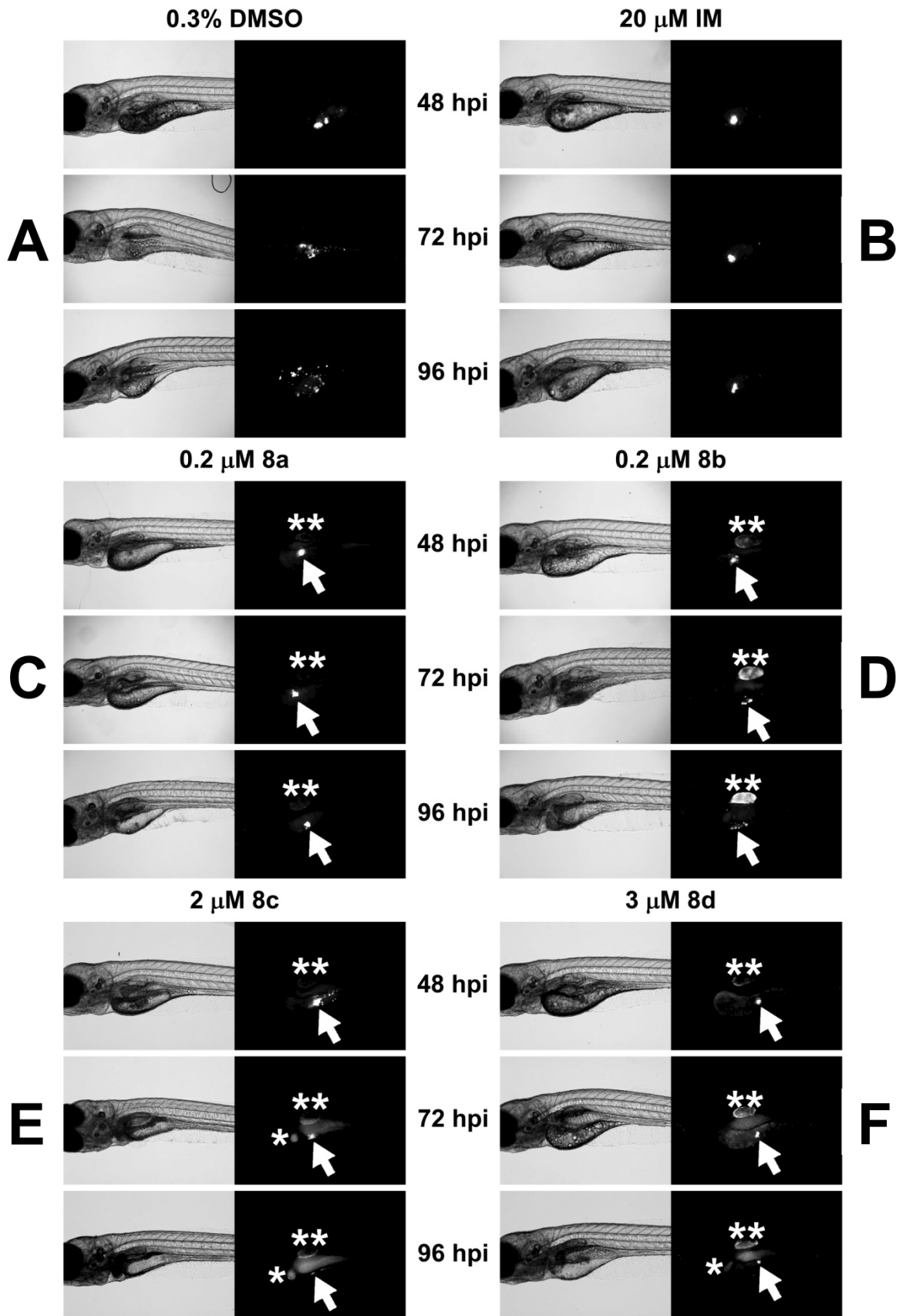
8b – 21.4% proliferative, 35.7% cytostatic; 42.9% cytotoxic;

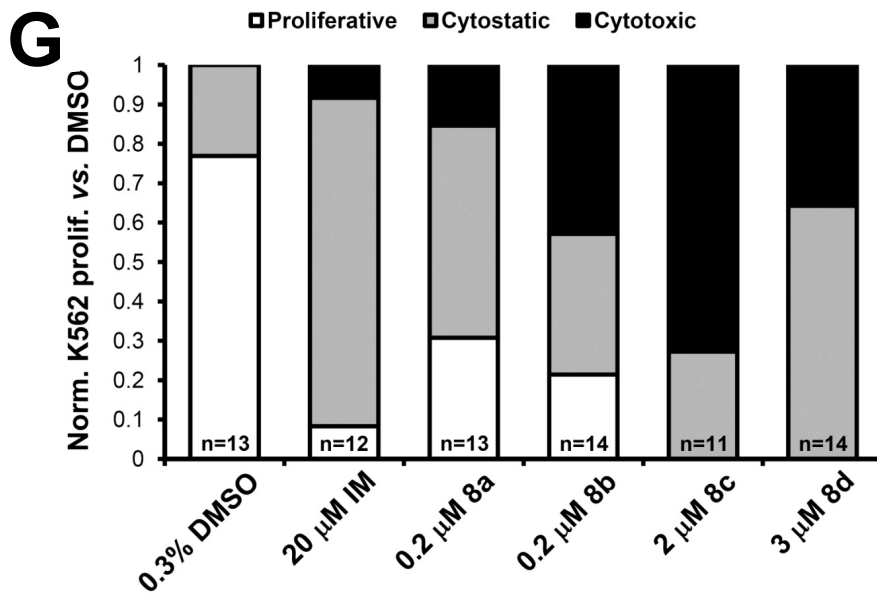
8c – 27.3% cytostatic; 72.7% cytotoxic;

8d – 64.3% cytostatic; 35.7% cytotoxic.

New abbreviations used: IM = imatinib mesylate.

Acknowledgement: Dale Corkery injected embryos with leukaemia cells.





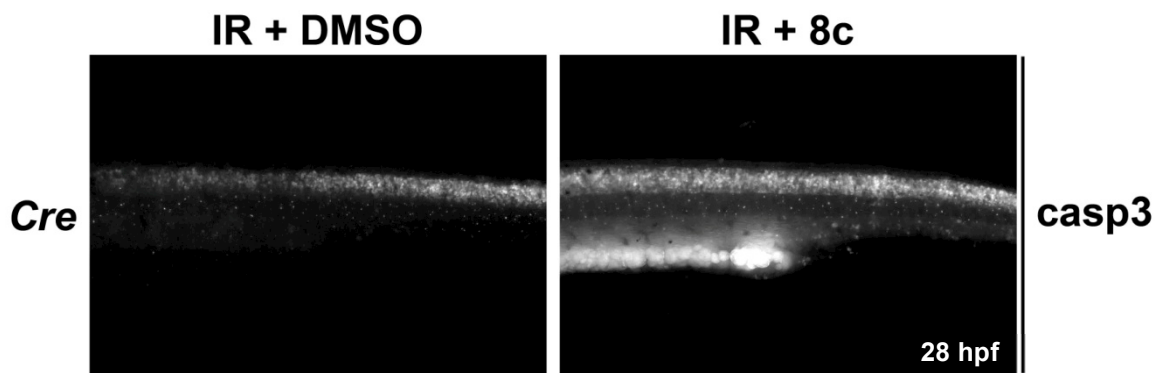


Figure 7.6. Comparison of casp3 immunofluorescence in *Cre* embryos treated with IR only versus IR + prodigiosene.

Embryos were treated with 16 Gy IR at 26 hpf and treated with either DMSO ("IR + DMSO"; *left*) or with 2 μ M **8c** ("IR + 8c"; *right*). Embryos were incubated in chemical and stained for immunofluorescence of casp3 at 28 hpf. Embryo displayed in side profile, anterior to the left, panels show magnified view of tail region only. Fluorescence microscopy (555 nm) used to observe casp3 expression.

CHAPTER 8 CONCLUSIONS & RECOMMENDATIONS FOR STUDYING FUTURE PHENOTYPES & MODIFIERS

8.1 SUMMARY OF FINDINGS

My accomplishments thus far have been to generate and characterize a transgenic zebrafish model of high risk *NHA9*-induced myeloid disease. *NHA9*-transgenic animals exhibit MPN disease between 19 to 23 months of life, but do not progress to overt AML (*i.e.* appearance of AML blast cells and/or 25% myeloblasts in marrow). We also gained mechanistic insights using *NHA9* embryos. Following DNA damage, *NHA9* embryos suppressed cell cycle arrest and apoptosis, possibly due to upregulation of *bcl2*. Our chief interest was that *NHA9* embryos showed altered haematopoiesis, with increased *spi1* myeloid cells at the expense of *gata1a* erythroid cells. This “myeloproliferation” phenotype appeared to be inhibited upon gene knockdown of the HOX co-factor, *meis1*, which is known to collaborate with *NHA9*. I also identified novel genetic collaborators and we are pursuing experiments that confirm the interaction between *NHA9* and the DNA methylating activity of *dnmt1*, and to determine the true impact of hyperactivity in the Wnt/ β -catenin signalling pathway. Our transgenic zebrafish tool provides unique opportunities for better understanding the genetic and molecular interactions underlying myeloid leukaemogenesis and in the identification of new agents that can be used to improve disease outcome. Future investigations with the *NHA9*-transgenic zebrafish line will exploit the advantages inherent in the zebrafish model for performing a chemical modifier screen to identify potential therapeutic compounds targeted for high risk AML (Yeh *et al.* 2009). These findings will provide further insight into disease pathogenesis and reveal promising new agents and future drugable targets in this aggressive disease.

8.2 *NHA9* & MYELOID DISEASE

8.2.1 Challenges To Modelling Myeloid Disease In Transgenic Zebrafish

The MPN disease in our *NHA9*-transgenic zebrafish displayed long latency and no progression to overt myeloid leukaemia. Long latency was also observed in the *NHA9*

mouse models, but this eventually progressed to overt AML (Iwasaki M *et al.* 2005; Kroon *et al.* 2001). Unfortunately, the zebrafish may be unable to recapitulate all aspects of a mammalian disease. For example, the lack of ‘true’ bone marrow microenvironment in zebrafish may limit the availability of certain cell signalling ligands that are known to be important to haematopoiesis and leukaemogenesis in mammals. For example, the bone-remodeling cells, osteoblasts and osteoclasts, are major producers of osteopontin, which is an extracellular matrix (ECM) component of mammalian bone marrow that binds the CD44 cell surface receptor on HSCs (Weber *et al.* 1996). Osteopontin signalling regulates HSC numbers both in a positive and negative manner. It can promote the expression of G-CSF, a molecule that reduces HSCs by driving myeloid differentiation (reviewed in Scadden 2006). However, osteopontin signalling can also lead to the secretion of PGE₂ (Stamp *et al.* 2004), which activates the Wnt/ β -catenin pathway to increase HSC proliferation and survival (North *et al.* 2007; Goessling *et al.* 2011). In mammalian leukaemogenesis, CML cells enter the bone marrow by inappropriately expressing the osteopontin receptor, CD44 (Krause *et al.* 2006), which is normally only found on HSCs. Therefore, even though HSCs in the adult zebrafish do develop in a special ‘kidney marrow’, it is unknown whether this microenvironment is fully analogous in its expression of similar (or compensatory) ligands, such as osteopontin. Additionally, the zebrafish homologues of certain key regulatory proteins have yet to be identified, such as the GTP-binding protein, CDKN2A/ ARF, which is important for TP53-dependent cell cycle arrest and apoptosis in mammals (Look AT, personal communication). However, our *NHA9* fish, as well as the *AML1-ETO* fish (Yeh *et al.* 2009) have shown that leveraging robust embryonic phenotypes can be advantageous towards identifying novel gene collaborators and therapeutic agents. Thus, despite possibilities that zebrafish models of AML may not fully recapitulate the mammalian disease, they surely will continue to contribute to AML research.

The latency and low penetrance of overt AML in our *NHA9* line has also been seen in other zebrafish models of this disease. The problem may lie in part with the lack of available myeloid-targeted promoters that are active in early blood cells. Even with the advantages of the *spi1* promoter used in several studies – and even with both the myeloid and more ubiquitous expression in our own *NHA9*-transgenic line (see

CHAPTER 3) – the expression of zebrafish *spi1* is normally downregulated during terminal myeloid differentiation, and is active in only ~2% of adult haematopoietic kidney marrow cells (Hsu *et al.* 2004). This could account for the low incidence of AML in *Tg(spi1::MOZ-TIF2-EGFP)* fish (Zhuravleva *et al.* 2008) and the lack of progression to overt AML in *Tg(spi1::FLAG-tel-jak2a)* fish (Onnebo *et al.* 2005), *Tg(hsp70::AML1-ETO)* fish (Yeh *et al.* 2008), and now our *Tg(spi1::lgl::NHA9)* fish.

At the start of this project, our choice of zebrafish promoter was limited by lack of available blood-targeted promoters, in general, and early myeloid-targeted promoters, in particular. However, low incidence of oncogenesis is not uncommon in models using other promoters, including *Tg(rag2::EGFP-Myc)*-induced T cell acute lymphoblastic leukaemia (T-ALL) (5% incidence) (Langenau *et al.* 2003), *Tg(actb1::EGFP-TEL-AML1)*-induced pre-B-ALL (5% incidence) (Sabaawy *et al.* 2006). Furthermore, targeted promoters have also proven troublesome in other models of fish leukaemia. Sabaawy *et al.* showed that only expression of the *TEL-AML1* fusion oncogene from ubiquitous zebrafish *actb1* and *Xenopus* elongation factor 1 (*Xef1*) promoters, but not from the early lymphoid-targeted *rag2* promoter could produce pre-B-ALL in transgenic zebrafish (Sabaawy *et al.* 2006). Thus, promoters that are active earlier in zebrafish blood development may be more robust at driving leukaemic transformation, but they may carry the caveat of off-target effects. This was seen in *Tg(actb1::lgl::K-RAS^{G12D})* fish, where MPN was one of a spectrum of disease phenotypes, including rhabdomyosarcoma, intestinal hyperplasia, and zMPNST (Le *et al.* 2007). However, in mice, the use of lineage-restricted myeloid promoters (*i.e.* *cathepsin G* [*CTSG*] [Guibal *et al.* 2009; Iwasaki M *et al.* 2005; Wojiski *et al.* 2009], *S100 calcium binding protein A8/migration inhibitory factor-related protein 8* [*S100A8/MRP8*] [Guibal *et al.* 2009]) has not limited the success of oncogenic transformation. This may stem from the tendency of many AML fusion oncogenes to transform a committed myeloid progenitor cell into the leukaemia-initiating cell (LIC) (as discussed in **CHAPTER 6**). In the zebrafish, the use of more lineage-restricted myeloid promoters (*i.e.* *lyz*, *mpx*, *mpeg*, *csflr*) have flourished in the field of leukocyte trafficking (Elks *et al.* 2011; Ellett *et al.* 2011; Gray *et al.* 2011; Hall *et al.* 2007), so these may ultimately provide alternative tools for future fish models of myeloid leukaemogenesis.

Potency of the oncogenic signal is another hurdle to successfully modelling leukaemia in fish. For example, *Tg(spi1::FLAG-tel-jak2a)* fish (Onnebo *et al.* 2005) as well as early models of *Tg(rag2::EGFP-Myc)* fish (Langenau *et al.* 2003) display such severe embryonic abnormalities that animals do not survive to breeding age, and so embryos must be re-injected for every study. Cre/lox-inducible strategies can be helpful to establish germline transmission of the oncogene, but historically the most reliable method to control Cre activity was to use the zebrafish *hsp70* promoter, which is known to have leaky expression (Feng H *et al.* 2007; Langenau *et al.* 2005a; Le *et al.* 2007), which we have also observed in our floxed *NHA9* model (Forrester *et al.* 2011). Direct use of the *hsp70* promoter to drive oncogene expression has proven fruitful in the study of *AML1-ETO*, but the absence of an adult phenotype may reflect the transience of promoter activity following heat-shock activation. Tamoxifen-inducible Cre (Cre-ERT2) can dramatically improve upon the leaky expression in the original *Tg(hsp70:Cre)* animals (Hans *et al.* 2011; Mosimann *et al.* 2011). Hans *et al.* show that, even at temperature ranges of 37 to 42°C, recombination events can be blocked completely in *Tg(hsp70:Cre-ERT2)* animals if tamoxifen is not applied following heat-shock.

Other intriguing developments include the mosaic expression of transgenes, in which a stable transgenic line is not produced, but rather experiments are performed on the F0 generation fish that was directly injected with the transgenes (Chen EY and Langenau 2011; Langenau *et al.* 2008). Such strategies can permit a rapid and detailed analysis of the effect on oncoprotein expression in individual cells. A recent study of zebrafish T-ALL found that mosaic expression of Notch oncoprotein expanded a population of pre-malignant thymocytes, but could not promote the formation of LICs (Blackburn *et al.* 2012). Such studies can facilitate rapid analysis into the specific contributions of single (or combinations of) oncogenes to disease development, without the need for establishing a germline transgenic model.

Finally, clinical myeloid disease has been achieved in only three zebrafish models to date, including ours (Forrester *et al.* 2011; Le *et al.* 2007; Zhuravleva *et al.* 2008), including ours. Of these models, overt AML has been identified only once (Zhuravleva *et al.* 2008), and was a rare event (<1% incidence) that has not yet been reported again since its initial discovery. This suggests that the acquisition of mutations within

collaborating proto-oncogenes and/or inactivations of tumour suppressor genes may occur less readily in the short life expectancy of the zebrafish. Alternatively, the acquisition of disease-promoting co-operating mutations may be masked by increased genetic redundancy that has resulted from widespread duplication of the teleost genome (Amores *et al.* 1998). However, the zebrafish is well suited to test specific interactions between collaborating oncogenes due to its high fecundity and thus capacity to generate large numbers of animal with a range of genotypes, as recently demonstrated in neuroblastoma (Zhu *et al.* 2012). Collaborating mutations may thus be necessary to achieve acute transformation to AML in the zebrafish

With regards to tumour suppressor genes, the clinical relevance of such models is apparent from the Targeting Induced Local Lesions in Genomes (TILLing)-derived *tp53* mutant animals (Berghmans *et al.* 2005; Parant *et al.* 2010; Sidi *et al.* 2008). However, given the absence of knockout technology mediated by homologous recombination, it has been difficult to achieve targeted, heritable gene knockdown in zebrafish. The last few years has seen major technical advances in this regard, such as zinc finger nuclease (ZFN)-induced cleavage and repair resulting in gene knockouts (Doyon *et al.* 2008; Meng *et al.* 2008). Zebrafish laboratories worldwide can now utilize an oligomerized pool engineering (OPEN) system for *in vitro* and *in silico* identification and validation of potential gene targeting ZFNs (Maeder *et al.* 2008; Maeder *et al.* 2009), sometimes using bioinformatics alone (Sander *et al.* 2011b). Most recently, evidence has shown that plant-derived transcriptional activator like nucleases (TALENs) function even more faithfully in the zebrafish system to target the enzymatic cleavage component of the FOK1 endonuclease to within a few bases of the desired double stranded DNA break (Huang *et al.* 2011; Sander *et al.* 2011a). We anticipate the optimization of homologous recombination methodologies to finally permit conditional knockin models of disease.

We were encouraged that our zebrafish model of *NHA9*-induced disease matched the mouse model (Kroon *et al.* 2001), both with a similar time-frame of onset and the initial presentation of MPN. With regards to collaborating oncogenes, transgenic fish harbouring multiple oncogenes has been a successful strategy in zebrafish ALL (Feng H *et al.* 2010). Thus future strategies to assess the contribution of collaborating mutations could be targeted at overexpression strategies of two, three or four genes. In the next

section, I discuss strategies to stably overexpress the mouse-derived HOX co-factor, *Meis1*, which accelerated the onset of AML in *NHA9* mice (Kroon *et al.* 2001), as well as the *Xenopus*-derived, hyperactive β -catenin mutation (Wang Y *et al.* 2010), which accelerated the onset of AML in *Hoxa9;Meis1* mice.

8.2.2 Future Directions – New Transgenic Tools

The Berman lab has substantial experience with the Gateway® cloning system (Invitrogen). This system permits rapid and efficient generation of constructs through recombinant-based cloning of promoters, target genes, and 3' fluorescent molecular tags with a *Tol2* transposable element in a single reaction (Kwan *et al.* 2007, Villefranc *et al.* 2007). During the tenure of my PhD project, I prepared several new gene expression tools that are ready for injection into zebrafish embryos to establish germline transgenic lines, or for preparation of various mRNA of interest.

The lack of overt AML (*i.e.* appearance of AML blast cells and/or 25% myeloblasts in marrow) in our *NHA9* adult fish likely highlights a requirement for additional genetic lesions that promote acute transformation. Thus, I engineered transgenic vectors for mouse *Meis1* and the *Xenopus*-derived, hyperactive β -catenin(S/T \rightarrow A) mutation (genetically referred to as “*ctnnb1-b**”) in order to look at their effects on disease progression in adult *NHA9* fish. The β -catenin(S/T \rightarrow A) mutant protein is resistant to phosphorylation, so it cannot be targeted for degradation by APC and GSK3 β negative regulators. The frog *ctnnb1-b** mutation was functional in mice (Wang Y *et al.* 2010), so it is likely to work in zebrafish.

Given the success of *Tg(hsp70::AML1-ETO)* fish, I decided to link my genes to the *heat shock protein 70* (*hsp70*) promoter. I designed two transgenic constructs: pTol2-*Tg(hsp70::Meis1::2A-mCherry)* and pTol2-*Tg(hsp70::ctnnb1-b*::2A-mCherry)*. The mCherry red fluorescent protein distinguishes expression of these transgenes from the GFP already present in our *NHA9* line. A schematic for generating these new germline transgenics is shown in **Figure 8.1** (figure depicts frog *ctnnb1-b**, but will be identical for mouse *Meis1*). We will inject construct into approximately 500 Cre-activated *NHA9* embryos at the one-cell stage. Germline transmission will be approximately 30-50%, thanks to the efficiency of the *Tol2* transposon. Once injected, F0 fish will be reared to

sexual maturity (3 to 4 months post-fertilization) and backcrossed to Cre-activated *NHA9* fish. The F1 offspring will be screened by heat-shock at 24-48 hpf for the presence of red fluorescence and confirmed by genomic PCR for frog *ctnnb1-b** (or mouse *Meis1*) on single embryos to identify germline F1 embryos and their F0 founder parent. F1 fish will be incrossed to generate F2 fish that will be homozygous for both Cre-activated *NHA9* and frog *ctnnb1-b** (or mouse *Meis1*) constructs (25% of F2 offspring), displaying red fluorescence. Cre-activated *NHA9;ctnnb1-b** (or *NHA9;Meis1*) transgenic embryos will be heat-shocked at 24 hpf and subjected to similar embryonic WISH, apoptosis and cell cycle assays as we have already performed. For controls, we will use non-heat shocked transgenics that will express the pre-activated NHA9 protein, but not the frog β -catenin(S/T \rightarrow A) (or mouse *Meis1*) protein.

A proportion of fish will be reared to adulthood. Animals with decreased activity or appearing ill will be sacrificed. A subset of well-appearing fish will also be sacrificed at 3, 6, and 12 months and examined for gross or histopathological involvement of peripheral blood, kidney marrow, and spleen to evaluate if co-expression of hyperactive frog β -catenin(S/T \rightarrow A) (or mouse *Meis1*) results in progression of *NHA9*-induced disease to frank leukaemia. As with the *MOZ-TIF2* fish line (Zhuravleva *et al.* 2008), we will also perform FACS on kidney to compare with fish expressing human *NHA9* alone to assess whether co-expression of frog *ctnnb1-b** (or mouse *Meis1*) leads to differences in blood cell number and differentiation, such as an increase of immature myeloid cells.

For short-term experiments, I have also generated pCS2+ gene expression plasmids for human *NHA9*, mouse *Hoxa9*, mouse *Meis1*, and frog *ctnnb1-b**. These will enable synthesis of mRNA for transient overexpression in zebrafish embryos.

8.3 NHA9 & MEIS1

8.3.1 Future Directions – Modulating *meis1* In *NHA9* Embryos

It is known that *NHA9* transforming activity is not inhibited in mutant mice lacking *Hoxa9* (Calvo *et al.* 2002), that mammalian MEIS1 binds NHA9 at the protein level (Shen *et al.* 1999), and that NHA9 oncoprotein either does not bind, or does not require the Pbx co-factor (Calvo *et al.* 2002). It has been previously unknown whether

NHA9 can be inhibited by knockdown of MEIS1 protein. My preliminary evidence pertaining to *NHA9* zebrafish embryos injected with *meis1* MO suggests that the loss of zebrafish *meis1* can indeed limit myeloproliferation in these animals (see **CHAPTER 4**). This suggests that *meis1* is most likely required for the oncogenic activity of *NHA9*.

This does not necessarily reflect that *NHA9* upregulates zebrafish *meis1* gene expression, as qRT-PCR analysis in *NHA9* embryos found only a mild increase of fish *meis1* compared to wild-type. However, colleagues and I have shown that a threshold level of *meis1* protein is required for zebrafish haematopoiesis (Pillay *et al.* 2010), and this is likely to be most important to *NHA9* pathogenesis. Furthermore, studies in *NHA9*-transformed primary human cell culture suggest that upregulation of human *MEIS1* may be a late-transformation event that coincides with increased cellular proliferation (Takeda *et al.* 2006). Therefore, the absence of hyperproliferation in our *NHA9* embryos may be consistent with the borderline increase of zebrafish *meis1* expression.

These findings are important because of the co-upregulation of *HOXA9* and *MEIS1* in human AML (Golub *et al.* 1999), as well as the contributions of *MEIS1* to leukaemogenesis by *HOXA9* and *NHA9* (Choe *et al.* 2009). Injection of zebrafish *meis1* MO into *NHA9* embryos should be repeated for confirmation of the myeloid phenotype, and to assess whether *gata1a* erythroid expression can be rescued. The next step to establishing a mechanistic cooperation of zebrafish *meis1* with *NHA9* would be to evaluate the impact of *meis1* overexpression, either on its own or co-overexpression with zebrafish *hoxa9a*. Gateway® (Invitrogen) pCS2 expression vectors for zebrafish *meis1* and mouse *Meis1* are available in the Berman lab, which can be used to synthesize mRNA for injection into *NHA9* embryos. WISH assays will determine if co-overexpression of *NHA9* and zebrafish *meis1* (or mouse *Meis1*) exacerbates the *lcp1* and *gata1a* phenotypes. Mouse *Meis1* previously demonstrated cooperation with human *NHA9* to produce AML in mice (Iwasaki M *et al.* 2005; Kroon *et al.* 2001), thus we anticipate no complications overexpressing mouse *Meis1* in our *NHA9* zebrafish.

8.3.2 Future Directions – Microarray Analyses For *NHA9* & *meis1*

We will endeavour to characterize direct gene targets of *NHA9* and fish *meis1* (or mouse *Meis1*) combined activity. The gene expression profiles for (a) *NHA9* embryos

(the ‘control’ embryos) will be compared with the ‘experimental’ embryos: (b) *NHA9 + meis1* (using mRNA) and (c) *NHA9 – meis1* (using MO). Compared to wild-type embryos and embryos with *NHA9* alone, embryos with *NHA9 + meis1* will demonstrate an ‘overexpressed’ gene expression profile, highlighting which genes have been affected by the addition of *meis1*. Embryos with *NHA9 – meis1* will display an ‘underexpressed’ gene expression profile, highlighting which genes have been affected by the removal of *meis1*. We anticipate that the overlap of *meis1* ‘overexpressed’ and ‘underexpressed’ expression profiles will identify a small subset of genes that are directly targeted in the zebrafish by *NHA9* and *meis1* together. Furthermore, these gene expression signatures can be compared both to the results of a prior microarray conducted on *NHA9*-transduced primary human HSCs (Chung *et al.* 2006; Ghannam *et al.* 2004; Takeda *et al.* 2006) and (following REB approval) two of each adult and paediatric patients with AML harbouring the *NHA9* translocation to evaluate which zebrafish signature is most representative of the human cancer signature. Ethics proposals to use primary tissue samples are expected to be time-consuming, although my supervisor, Dr. Jason Berman, will be able to facilitate access as a clinician and Vice Chair of the Myeloid Biology Subcommittee of the Children’s Oncology Group (COG). Other expected limitations include: the redundancy in the zebrafish genome (Amores *et al.* 1998), which could mask some changes to gene expression; the zebrafish genome is less annotated compared to mammals and there are less nucleotide ‘spots’ on a zebrafish microarray chip (Lewis S, personal communication), which means that not all possible homologous genes can be measured with current technology; and rigorous analytical tools will be required to compare the gene expression signatures obtained from multiple experimental conditions, which means that some important changes to gene expression could be screened out.

8.4 *NHA9* & *DNMT1*

8.4.1 Future Directions – Zebrafish *dnmt1* In *NHA9* Embryos

As discussed in **CHAPTER 5**, my preliminary findings suggest that *NHA9* drives leukaemogenesis, at least in part, through the epigenetic activity of zebrafish *dnmt1* enzyme. We should confirm the collaboration of zebrafish *dnmt1* with *NHA9* by

measuring the rescue of *gata1a* erythroid expression following *dnmt1* MO injection or DAC treatment. Following this, upstream and downstream factors in the *dnmt1* pathway and the broader epigenetic network need to be considered to fully investigate this link.

DNMT1 methylates cytosine residues in DNA, so we would expect *NHA9* embryos to show hypermethylation due to the increased expression of zebrafish *dnmt1*. This could be confirmed using a bisulphite sequencing adaptation to a methylation assay that has been previously used to track *dnmt1* enzyme activity in zebrafish (Anderson RM *et al.* 2009). In brief, genomic DNA would be isolated from at least 10 embryos and treated with bisulphite to convert unmethylated cytosines to uracils (methylated cytosines resist conversion). PCR-based sequencing could then be targeted against the consensus *DANA* sequence, a short interspersed nuclear element (SINE) that comprises ~10% of the zebrafish genome and that is methylated by *dnmt1* (Izsvak *et al.* 1996). In *dnmt1*^{s872} mutant embryos that lack *dnmt1* enzyme activity, the *DANA* sequence was hypomethylated (Anderson RM *et al.* 2009), so it would exhibit more uracil conversion compared to wild-type. Thus, we would expect that the increased *dnmt1* enzyme activity in *NHA9* embryos would hypermethylate the *DANA* sequence, which would exhibit less uracil conversion compared to wild-type.

Injections of mRNA and MO into *NHA9* embryos permit further study of *dnmt1* and other epigenetic factors. Rai *et al.* have produced expression vectors for a catalytically-inactive human *DNMT1*^{C1226S} mutation, and the homologous mutation in zebrafish, *dnmt1*^{C1109S} (Rai *et al.* 2006). Injection of these mutant mRNAs might competitively inhibit the native zebrafish *dnmt1* and thus reduce the myeloproliferation in *NHA9* embryos. By contrast, injecting *NHA9* embryos with mRNAs for the wild-type forms of human *DNMT1* or zebrafish *dnmt1* would be expected to further accelerate the myeloproliferative phenotype. Zebrafish MOs are available for the upstream factor, *uhrfl*, which recruits *dnmt1* to DNA sites (Chu *et al.* 2012; Tittle *et al.* 2011). MOs are also available for the epigenetic co-factor, *suv39h1a*, a histone methyltransferase that works in tandem with *dnmt1* to regulate terminal differentiation (Rai *et al.* 2006). Injection of *NHA9* embryos with *uhrfl* or *suv39h1a* MO may corroborate our experiments with *dnmt1* MO. By contrast, injection of *uhrfl* or *suv39h1a* mRNA might further augment zebrafish *dnmt1* activity and accelerate myeloproliferation. Cross-

reactive antibodies are also available for zebrafish *dnmt1* and *uhrf1* proteins, so Western blots could be used to monitor the efficiency of MO and mRNA injections.

Chemical modifications of zebrafish *dnmt1* activity in *NHA9* embryos could potentially be a rich area of investigation. Given our preliminary success with Decitabine (DAC; 5-azadC), the next logical step would be to assess inhibition of *NHA9* with a closely-related DNMT1 inhibitor, Azacitidine (AZA; 5-azaC). AZA, is only slightly more toxic to zebrafish embryos than DAC (maximum tolerated dose [MTD] for AZA = 75 μ M, compared to MTD for DAC = 100 μ M) (Martin CC *et al.* 1999; Ceccaldi *et al.* 2011). DAC and AZA are nucleoside analogues, so part of their therapeutic action is incorporation into cellular nucleic acids leading to genotoxic stress, but they also bind to free-floating DNMT1 enzyme. It is interesting, however, that DAC treatment cannot rescue human leukaemia cells that lack DNMT3A and DNMT3B proteins (Patel *et al.* 2010), which are *de novo* DNA methyltransferases that work in concert with DNMT1 to regulate histone deacetylation complexes (HDACs) and ultimately epigenetic silencing (refer back to **Figure 5.1**). This suggests that DAC (5-azadC) must first incorporate into DNA and interact with *de novo* methyltransferases before it can effectively target DNMT1. Thus, it may not always be effective to use DAC or AZA to treat MDS and AML that overexpress *DNMT1*, because *DNMT3* family genes can also be under-expressed or mutated to inactive forms (Gowher *et al.* 2006; Shah *et al.* 2011). DAC treatment appeared to be effective in our *NHA9* zebrafish embryos, but investigating the expression of the *DNMT3* homologues may nevertheless be warranted. In zebrafish, there are six genes that comprise the *dnmt3* family: consensus is that *dnmt6* primarily accounts for *dnmt3a* enzyme activity (*dnmt8* as alternate), and *dnmt4* accounts for *dnmt3b* enzyme activity (*dnmt3*, 5, 7 as alternates) (Smith TH *et al.* 2011). Using qRT-PCR on *NHA9* embryos, I propose measuring expression of zebrafish *dnmt4* and *dnmt6*. Injecting MOs for these genes into *NHA9* embryos would be an interesting experiment, but the results cannot be entirely anticipated due to potential gene redundancy.

Importantly, DAC treatment restores expression of late differentiation genes, but alone may be insufficient to cure myeloid disease when used as monotherapy (Sauntharajah *et al.* 2012). There is also a risk that DAC treatment is itself carcinogenic, as genome-wide DNA hypomethylation can lead to genomic instability,

chromosome rearrangements, and secondary tumours in animals (Maslov AY *et al.* 2012). This cautions against the indiscriminate use of demethylating agents, and affirms the value in searching for effective combination chemotherapy regimens. *NHA9* embryos could serve as tools for the design of such combination therapies. Based on discussions in **CHAPTER 5**, myeloid disease is associated with hyperactivity of hnRNPs (Wei *et al.* 2006), and treating human leukaemia cells with DAC or AZA downregulates hnRNPA2/B1 expression (Buchi *et al.* 2012). Extending farther, hyperactivity of hnRNPs leads to the suppression of protein phosphatase 2A (PP2A), and the rescue of PP2A function in human CML cells triggers proteasome degradation of the human BCR-ABL1 oncoprotein, leading to cell-cycle arrest and apoptosis (Perrotti and Neviani 2007). Using qRT-PCR, if zebrafish *hnrnp*, particularly *hnrnpa1*, is shown to be upregulated in *NHA9* embryos, this would suggest that DAC (or AZA) treatment could synergize with pharmacologic agonists of PP2A (e.g., forskolin and FTY720) (Barresi *et al.* 2000; Kotani *et al.* 2010).

Furthermore, the sequential link between DNA methylation and histone deacetylation (Guidotti *et al.* 2009) (refer to **Figure 5.1**) suggests that DAC treatment of our *NHA9* embryos could be combined with HDAC inhibitors, such as TSA (Yeh *et al.* 2008) or VPA (Farooq *et al.* 2008). A handful of studies suggest that the combination of a demethylating agent and an HDAC inhibitor better promotes epigenetic ‘normalcy’ than either compound alone, and that such a combination could effectively combat epigenetic dysregulation in myeloid disease (Kuendgen *et al.* 2011; Ning *et al.* 2012; Paul *et al.* 2010; Rynningen *et al.* 2007; Serrano *et al.* 2008).

8.5 NHA9 & WNT/ β -CATENIN

8.5.1 Wnt/ β -Catenin Regulates The *CDX-HOX* Network

In mammals, *TCF3* encodes a Wnt/ β -catenin repressor (Solberg *et al.* 2012), and injection of a *Xenopus*-derived dominant-negative *pcf3* constitutively inhibited Wnt/ β -catenin pathway signalling in zebrafish and disturbed dorsal-ventral patterning (Sumoy *et al.* 1999). Zebrafish studies show that *pcf711a* and *pcf711b* (which are described as having ‘TCF3 activity’) associate with HDACs and repress the Wnt/ β -catenin pathway. It is

interesting that the zebrafish *pcf71l* genes were identified as negative regulators of Wnt/ β -catenin in the context of regulating *cdx4* expression (Ro and Dawid 2011), because this links Wnt/ β -catenin to the *cdx-hox* network and therefore to haematopoiesis.

Furthermore, injection of *wnt3a/wnt8a* MO or *dickkopf 1b (dkk1b)* mRNA both led to decreased *gata1a* erythroid expression at the 8-somite stage. These are phenocopies of *kugleig (kkg^{tv205c}; cdx4^{-/-})* mutant zebrafish, and is consistent with studies that show a role for Wnt/ β -catenin in regulating mouse *Cdx4* (Lengerke et al. 2008). The CDX-HOX transcriptional network is implicated in AML pathogenesis (Bansal et al. 2006; Davidson et al. 2003; Davidson and Zon 2006; Frohling et al. 2007; Koo et al. 2010; Magnusson et al. 2007), and *NHA9* represents a mutated component of this pathway. Therefore, *NHA9* and Wnt/ β -catenin may very well collaborate in dysregulating zebrafish *cdx-hox* activity.

8.5.2 Future Directions – Zebrafish Wnt/ β -catenin In *NHA9* Embryos

My experimental findings suggest that the Wnt/ β -catenin pathway may play a complex, or limited role in *NHA9*-induced leukaemogenesis. Treating *NHA9* embryos with higher concentrations of Indo and dmPGE₂ should be top priority to better determine if our experiments to date have under- or over-estimated the impact of Wnt/ β -catenin on the activity of *NHA9*. Upstream and downstream factors in the pathway also need to be considered. In particular, strategies are needed to definitively activate β -catenin, such as inhibiting the negative regulators that are downstream of the ligands and receptors.

Cross-reactive antibodies are available for the transcriptionally active, hypophosphorylated form of β -catenin (Wang Y et al. 2010), so Western blot could confirm whether *NHA9* truly activates the Wnt/ β -catenin pathway. As discussed above, the Wnt/ β -catenin pathway regulates the expression of *cdx4* (Ro and Dawid 2011). Thus, the *kugleig (kkg^{tv205c}; cdx4^{-/-})* (Davidson et al. 2003) mutant line, which is available in the Berman laboratory, could be used to assess whether *NHA9* and Wnt/ β -catenin are upstream or downstream of (or in a feedback loop with) zebrafish *cdx4*.

TCF4 and LEF1 proteins are the transcription factors activated downstream of canonical Wnt/ β -catenin signalling. Definitive hyperactivation of the Wnt/ β -catenin pathway in zebrafish could be achieved with mRNA for the *wnt8a* upstream ligand

(Goessling *et al.* 2009) or the *lefl* downstream transcription factor (Gamba *et al.* 2010). Alternatively, MOs against any of the well-known negative regulators (*axin1*, *dkk1b*, *gsk3b*), or the *tcf7l1a* and *tcf7l1b* transcriptional repressors (Ro and Dawid 2011) may suffice. We also acquired the *Xenopus*-derived, hyperactive β -catenin(S/T \rightarrow A) mutation from Dr. Scott Armstrong's laboratory, which was used to promote *Hoxa9;Meis1*-induced mouse AML (Wang Y *et al.* 2010). We have already placed frog *ctnnb1-b** cDNA into Gateway® (Invitrogen) middle entry clones to generate mRNA, though a tolerated injection dose that permits normal embryo development up to 28 hpf has been difficult to determine. Inhibiting the Wnt/ β -catenin pathway in *NHA9* embryos with mRNA and MO would corroborate findings from the Indo treatments. Injecting zebrafish with *wnt3a/wnt8a* MO or *dkk1b* mRNA phenocopy the decrease in *gata1a* erythroid expression that is seen in *kkg^{tr205c}* embryos (Ro and Dawid 2011). These reagents would be of great interest to test in our *NHA9* embryos.

Given our success with Indo treatments, the next logical step would be to test a specific COX2 inhibitor, such as NS-398 (Yeh *et al.* 2009). This would help to determine whether zebrafish COX-PGE₂ signalling truly works to activate the Wnt/ β -catenin in the presence of *NHA9*. As discussed above, PGE₂ levels may be saturated in our *NHA9* embryos, and this may be the result of the large overexpression of zebrafish *ptgs2a*. If true, then specific inhibition of zebrafish COX2 with NS-398 may better inhibit *NHA9* and restore wild-type haematopoiesis. We could also explore alternative Wnt/ β -catenin stimulants, such as treating *NHA9* embryos with 6-bromoindirubin-3'-oxime (BIO), a specific GSK3 β inhibitor (refer back to **Figure 6.1**) (Yeh *et al.* 2009).

Finally, as discussed above for *meis1*, we will evaluate the impact of *NHA9* and fish Wnt/ β -catenin on global gene expression using microarray. Identifying the target genes of Wnt/ β -catenin signalling will allow us to further understand how LICs are created in myeloid leukaemia. We will compare gene expression profiles for (a) *NHA9* 'control' embryos against 'experimental' embryos: (b) *NHA9* + agonist (+ β -catenin) to generate an 'overexpressed' genetic profile; (c) *NHA9* + antagonist ($-$ β -catenin) to generate an 'underexpressed' genetic profile. The most efficient chemical modifiers will be identified in the aforementioned studies. We anticipate that the overlap of 'overexpressed' and 'underexpressed' expression profiles will identify a subset of genes

that will have a high probability of being direct downstream targets of β -catenin in the presence of *NHA9*. Expected limitations are the same as discussed for *meis1* above.

8.6 A POSSIBLE ROLE FOR RETINOIC ACID IN *NHA9* EMBRYOS

8.6.1 Retinoic Acid Signalling & *hox*-Independent Activity of *cdx*

The role of retinoic acid (RA) in the *NHA9* myeloproliferation phenotype could also be considered. Retinoic acid (RA) is a secreted morphogen that promotes cell differentiation in embryogenesis (Niederreither and Dolle 2008). Similar to the interplay of Wnt/ β -catenin with the zebrafish *cdx-hox* network, recent work in zebrafish has shown that *cdx4* is in a regulatory loop with RA to regulate haematopoiesis (Bansal *et al.* 2006; de Jong *et al.* 2010). Supraphysiologic amounts of RA cause a posteriorizing phenotype with anterior truncation of embryos (Xu *et al.* 2009). A gain in RA signalling inhibits myelopoiesis (decreased *spi1*) in the zebrafish ALPM (Liang *et al.* 2012) as well as erythropoiesis (decreased *gata1a*) in the zebrafish ICM by limiting the expression of the haemangioblast markers, *tall/scl* and *lmo2* (de Jong *et al.* 2010). It is likely that RA reprograms haemangioblast differentiation towards angiogenic fates, given the gain in expression of the vascular marker, *fli1a* (Figure 8.2).

By contrast, pharmacologic inhibition of RA activity – using either an aldehyde dehydrogenase inhibitor (4-diethylamino-benzaldehyde; DEAB), or a pan-RA receptor (RAR) antagonist (AGN193109) – led to a gain of ALPM myeloid development, similar to *gata1a*-morphants (Galloway *et al.* 2005; Rhodes *et al.* 2005). Increased expression of *spi1* (Ma *et al.* 2010), *lcp1*, and *mpx* (Liang *et al.* 2012) was linked to posterior extensions of *tall/scl* and *lmo2* expression in the ALPM (Ma *et al.* 2010). DEAB treatment also led to anterior extensions of *gata1a* expression in the ICM (de Jong *et al.* 2010), similar to the phenotype in *spi1*-morphant embryos (Rhodes *et al.* 2005). These findings appear to be inconsistent with SPI1-GATA1 antagonism, but taken together they suggest that RA broadly limits haemangioblast formation during primitive haematopoiesis. Suppressing RA permits a broad increase in the expression of zebrafish *tall/scl*, forming new haemangioblasts that generate both *spi1* myeloid cells from the expanded ALPM as well as *gata1a* erythroid cells from the expanded ICM (Figure 8.2).

Mouse studies show that RA activates the *Cdx-Hox* network (Bansal *et al.* 2006), and zebrafish studies show that *cdx4* activity subsequently represses *retinaldehyde dehydrogenase 2 (raldh2)* (de Jong *et al.* 2010). The zebrafish *cdx4-raldh2* regulatory loop suppresses RA biosynthesis in the posterior regions of the embryo, suggesting that the loss of haematopoiesis (decreased *tal1/scl* and *gata1a* expression) in *kkg^{fv205} (cdx4^{-/-})* mutant embryos results from ectopic RA signalling. Indeed, treatment with DEAB rescued the normal *gata1a* expression pattern in *kkg^{fv205}* mutant embryos (de Jong *et al.* 2010) (**Figure 8.2**). Thus, when *cdx4* is absent, zebrafish *tal/scl* is deactivated on two fronts: it cannot be activated by *cdx-hox* and is repressed by hyper-active RA from *raldh2*. This helps to explain why injection of *hoxa9a* mRNA into *cdx*-mutant embryos only partially rescues the expression *tal1/scl* and *gata1a* (Davidson and Zon 2006).

8.6.2 Future Directions – Possible Interplay of Wnt/ β -Catenin And Retinoic Acid In *NHA9* Embryos

RA drives progenitor proliferation and differentiation in multiple systems, including embryonic segment identity (de Jong *et al.* 2010; Liang *et al.* 2012; Voss *et al.* 2009; Xu *et al.* 2009), epithelial differentiation (Metallo *et al.* 2008), and wound healing by cardiomyocytes (Kikuchi *et al.* 2011). Though RA inhibits haemangioblast formation and haemogenic differentiation during zebrafish primitive haematopoiesis (de Jong *et al.* 2010; Liang *et al.* 2012), RA in mammals is critical for differentiation of the neutrophil lineage (de The and Chen 2010), and supraphysiologic amounts of all-*trans* RA (ATRA) targets LICs for differentiation in the clinical treatment of APL. In normal haematopoiesis, the Wnt/ β -catenin pathway maintains self-renewal of HSCs in the absence or suppression of differentiation cues (Kosinski *et al.* 2007). Regulators of differentiation, such as RA and colony-stimulating factors (CSFs), compete against Wnt/ β -catenin activity and promote differentiation of HSCs (Crosnier *et al.* 2006). In human blood cell culture, inhibition of RA signalling by pharmacological treatment with DEAB promotes the expansion of the self-renewing HSC population, which could be reversed by co-treatment with supraphysiologic doses of ATRA (Chute *et al.* 2006).

Zebrafish *spadetail (spt^{b104})* mutants have further highlighted the convergence and competition between Wnt/ β -catenin and RA in the regulation of mesoderm differentiation

and haematopoiesis. The *spt*^{b104} line carries a null mutation in zebrafish *T-box gene 16* (*tbx16*), and embryos show a loss of haemangioblasts and of *c/ebpa* and *gata1a* expression in the ICM (Mueller RL *et al.* 2010). Microarray analysis on *spt*^{b104} zebrafish embryos showed upregulation of the *wnt8a* ligand and the canonical *frizzled 10* (*fzd10*) receptor, as well as downregulation of RA synthesizing enzymes, *aldehyde dehydrogenase family 1, member A2* (*aldh1a2*) and *retinol dehydrogenase 1-like* (*rdh1l*). These findings suggest that mesoderm cells in *spt*^{b104} embryos fail to differentiate in the absence of RA, as Wnt/ β -cat continues to promote self-renewal. It is interesting that *hoxa11a* is also a downstream target of *tbx16* in zebrafish, as this possibly links the RA and Wnt/ β -catenin pathways back to the *cdx-hox* network. In *NHA9* embryos, one could analyze the expression of genes in the RA biosynthetic pathway, to determine if they are downregulated. Treatment of *NHA9* embryos with ATRA could also be investigated as a therapeutic option to inhibit myeloproliferation.

8.7 FUTURE DIRECTIONS – A SYNTHESIS OF DNMT1, WNT/ β -CATENIN, CDX-HOX, AND RA

There is convincing evidence in mammalian models that oncogene transformation of lineage-committed GMPs is a common mechanism for the generation of LICs in myeloid leukaemia, provided that the Wnt/ β -cat pathway is activated for the acquisition of self-renewal (discussed in CHAPTER 6, and also refer to Figure 6.2). This suggests that targeting Wnt/ β -cat could be a successful therapeutic strategy in the treatment of AML (Wang Y *et al.* 2010; Yeh *et al.* 2009). However, it is possible that targeting the Wnt/ β -catenin pathway for inhibition in human AML may not be entirely effective, or at least not as monotherapy. A recent study showed that knockdown of human *CTNNB* using a short hairpin RNA (shRNA) lentiviral approach reduced the *in vivo* engraftment potential for mouse xenotransplantations of the HL60 human leukaemia cell line (Gandillet *et al.* 2011) and of *MLL-ENL*-transformed mouse bone marrow (Yeung *et al.* 2010), but not of primary human AML cells (Gandillet *et al.* 2011). This led Gandillet *et al.* to speculate that not all AML cells are ‘addicted’ to the Wnt/ β -catenin pathway, despite its upregulation by many fusion oncogenes.

Yet knockdown of human *CTNNB* did reduce the number of colony-forming unit (CFU) blast cells in the primary human AML samples (Gandillet *et al.* 2011), including samples harbouring *MLL*-rearrangements (Yeung *et al.* 2010). Furthermore, *CTNNB*-knockdown did significantly improve the differentiation response of human HL60 cells following ATRA treatment (Gandillet *et al.* 2011), suggesting that inhibition of Wnt/ β -catenin and RA may be a successful strategy for combination chemotherapy. Both RA (de Jong *et al.* 2010) and Wnt/ β -catenin (Ro and Dawid 2011; Lengerke *et al.* 2008) regulate the expression of zebrafish *cdx4*. Furthermore, both Wnt/ β -catenin (Wang Y *et al.* 2010) and mammalian *CDX4* (Koo *et al.* 2010) could be considered for drug targeting, because they are dispensable for adult HSC function in mice, but their loss in LICs (including *MLL*-rearranged cells) inhibits self-renewal and blocks leukaemogenesis.

Mammalian *DNMT1* is also dispensable in normal haematopoiesis, but required in LICs (Trowbridge *et al.* 2012). Moreover, a recent zebrafish study has linked RA and Wnt/ β -catenin signalling to the regulation of DNA methylation (Rai *et al.* 2010). This group showed that APC, a negative regulator of β -catenin, controls RA biosynthesis via zebrafish *rdh11*, which subsequently regulates methylation and demethylation machinery. Similarly, in human colorectal cancer cells, reactivation of APC reduced expression of human *DNMT1* (Campbell and Szyf 2003). Finally, the human *AML1-ETO* oncoprotein recruits DNMT1 and other epigenetic silencing machinery to repress the RA pathway, and pharmacological treatment of human *AML1-ETO* cells with AZA synergizes with ATRA to achieve terminal differentiation (Fazi *et al.* 2007). We could therefore leverage the myeloproliferative phenotype in our *NHA9* zebrafish embryos for testing new combination chemotherapy regimens, in relation to RA signalling, the canonical Wnt/ β -catenin pathway, the *cdx-hox* transcriptional network, and *dnmt1* activity.

8.8 FUTURE INVESTIGATIONS WITH XENOTRANSPLANTATION

One of the greatest promises for the future of the zebrafish model is its ability to make a significant contribution to the field of myeloid leukaemogenesis by identifying novel therapeutic compounds through chemical screens targeting developmental or early larval phenotypes (see below). The ability to undertake larger scale screening projects is

being enhanced by the application of this platform to xenografted cells as well as recent advances in automated image acquisition and analysis capabilities (Peravali *et al.* 2011).

Xenotransplantation could also enable screens of currently-available anti-cancer agents for off-label, *in vivo* activity against human leukaemia cells. More recently, as has been demonstrated for some gastrointestinal tumours (Marques IJ *et al.* 2009), our lab has undertaken studies using primary leukaemia patient-derived bone marrow (Balci TB, Corkery DP, Dellaire G, Berman JN, unpublished results). Our lab has seen similar robust engraftment, proliferation, and circulation of primary leukaemia samples and confirmed this process to be an active process, requiring functional living cells, as fixed control cells remained in the yolk. Other groups have further demonstrated differential engraftment of human leukaemias subpopulations, with engraftment of CD34+ putative leukaemia stem cells but not from CD34- cells, indicating that zebrafish models may reflect the biology of disease in a similar way to mice and enable studies on LICs (Bonnet and Dick 1997; Pruvot *et al.* 2011; Wang JC *et al.* 1998). In parallel, with other tools, such as the development of syngeneic fish lines (*CGI*) (Smith AC *et al.* 2010) and the *casper* mutant fish line that permanently maintains transparency into adulthood (White *et al.* 2008), xenotransplantation will enable the zebrafish to explore questions of LIC frequency, clonogenicity and the ability to serially transplant disease.

There is a complexity of genetic lesions in AML, a poor understanding of the underlying molecular biology, and a heterogeneity of treatment response (<60% overall cure rate). Zebrafish xenotransplant models could ultimately be used in real-time analysis of primary human patient biopsies – including high-risk AML cells with upregulated *HOXA9* expression, and even AML cells that harbour *NHA9* – as a diagnostic tool to predict effective therapeutic regimen. They may also inform subsequent mouse studies of promising novel agents, ultimately leading to Phase I clinical trials.

8.9 NHA9-TRANSGENIC ZEBRAFISH PRESENT AN ATTRACTIVE *IN VIVO* MODEL FOR HIGH-THROUGHPUT DRUG DISCOVERY IN MYELOID DISEASE

NHA9 expression signifies a poor prognosis when found expressed in *de novo* or treatment-related AML or MDS in humans (Chou WC *et al.* 2009; Hatano *et al.* 1999;

Moore MA *et al.* 2007). Current therapeutic strategies including intensive chemotherapy and stem cell transplantation have not improved the cure rate in *NHA9*-induced AML (Chou WC *et al.* 2009). Despite a discouraging overall survival rate of less than 60% for human AML, targeted therapeutics have shown great success against subtypes of myeloid disease with reduced toxicity (reviewed in John AM *et al.* 2004), such as imatinib mesylate (IM; Gleevec®) for use against *BCR-ABL1*-induced CML. In particular, AML is characterized by a block in myeloid differentiation, and many of the fusion oncoproteins that we have discussed tend to repress genes that are required for differentiation. Targeted agents that break these blockades may be ideal candidates for future ‘differentiation therapies’. For example, treatment of *PML-RARA*-induced APL with all-*trans* retinoic acid (ATRA), a differentiation molecule that discourages self-renewal, rescues the proper maturation of granulocytic myeloid cells (Martens *et al.* 2010; Wang K *et al.* 2010). In this thesis, I have also shown that the haematopoietic defects in *NHA9* zebrafish embryos can be blocked by DAC, which relieves epigenetic repression of differentiation, as well as Indo, which inhibits the Wnt/ β -catenin self-renewal pathway. DAC and Indo may represent potential ‘differentiation therapies’ against *NHA9* in humans. Aiming for more of these discoveries in *NHA9*-induced AML would be of particular benefit to high-risk patients.

Of all vertebrate model organisms, the zebrafish has the unique capacity to support high-throughput screens *in vivo* using embryos. With evidence of both an MPN-like disease in adult fish and a developmental haematopoietic phenotype in embryos, our *NHA9* model provides an excellent opportunity to initiate an annotated bioactive compound screen. We will search for agents that restore normal levels of red blood cells (measured by *in situ* for *gata1a*) in *NHA9* zebrafish embryos. The rescue of *gata1a* as a “gain of function” read-out was a successful strategy in the screen performed on *Tg(hsp70:: AML1-ETO)* zebrafish (Yeh *et al.* 2009), and will increase specificity for a positive result. These phenotypes in *NHA9* embryos are robust and reproducible in 80% of embryos – necessary features for a phenotype to be reliably evaluated in a chemical screen. We would hypothesize that PTGS/COX enzyme inhibitors will be identified in the drug screen, which has been previously shown in other models (Wang Y *et al.* 2010; Yeh *et al.* 2009) and would be consistent with our own experiments using Indomethacin.

The purpose of performing this screen is that we may also identify drugs that target new genetic pathways, which may be unique to *NHA9*-induced leukaemia.

Zebrafish chemical screening strategies have been well-outlined (Hong 2009; Yeh *et al.* 2009). We will use the gain of wild type *gata1a* expression by WISH in 18 hpf *NHA9* embryos as a phenotypic readout (**Figure 8.3**), with WISH for *lcp1* expression at 28 hpf as a confirmatory assay for promising compounds. *NHA9* embryos at 12-14 hpf will be arrayed in a 96-well plate with 5-6 embryos per well. Compounds will be transferred from library to embryo plates at final concentration of 10-30 μ M by multi-pipettor or manual pin-transfer using a multiblott replicator (V&P Scientific, San Diego). Embryos will be heat-shocked and remain incubated in compound at 28.5°C for 4-5 hours of exposure. At 18 hpf, embryos will be fixed for WISH against *gata1a* for the primary screen, and against *lcp1* for the secondary screen.

Evidence of both restored erythroid and myeloid cell numbers to wild type levels will suggest a compound with potentially targeted specificity in *NHA9*-induced myeloid disease. We will employ known bioactive compounds from Sigma-Lopac 1280 and Biomol ICCB (Enzo) libraries, with representative compounds from promising drug families, such as tyrosine kinase inhibitors, anti-apoptotic agents, channel modulators, and prostaglandin agonists. Many of these compounds represent previously approved Federal Drug Agency (FDA)/Health Canada drugs, which will enable the rapid translation of promising ‘hits’ to Phase I clinical trials as a re-purposed therapy. Thus, in employing these particular libraries, we have the opportunity to discover truly new prospective agents, as well as potentially new applications for known medications. In addition, my supervisor, Dr. Jason Berman is a member of the Myeloid Committee of the COG, which makes him well-positioned to assist in forming the appropriate team to follow up the development of any molecules with promise for use in a clinical setting. The Biomol ICCB library is already in place in our lab, and we plan to obtain the Sigma-Lopac library in the near future.

Once chemical ‘hits’ have been determined, their identity will be confirmed by mass spectrometry against individual compounds purchased from Sigma or Enzo. A successful ‘hit’ identified in embryos expressing *NHA9* alone could subsequently be tested on embryos expressing *NHA9* + collaborating zebrafish genes and pathways

(*meis1*, *dnmt1*, Wnt/ β -catenin) to evaluate whether this compound retains efficacy or could synergize with other therapeutic agents, such as DAC. Identified compounds could also be tested in xenotransplantation studies, using *NHA9*-transformed human or mouse cells (cultured or primary) injected into *casper* embryos to assess drug efficacy against mammalian cells. Finally, microarray analysis will be conducted on embryos following exposure to this compound to assess whether the zebrafish leukaemic gene expression signature can be restored to a wild-type signature found in unaltered *AB* or *Cre* (wild type) embryos.

Based on precedence, we foresee identifying 2 or 3 promising chemical ‘hits’ from these initial smaller libraries, that demonstrate restored *gata1a* expression in *NHA9* embryos. These “hits” may not succeed at the validation stage. However, the use of well-annotated libraries, as well as the future potential to perform screens on much larger chemical libraries should increase the chances of finding a *bona fide* drug with therapeutic implications for *NHA9*-induced AML in human patients.

8.10 CLOSING REMARKS

The zebrafish embryo has contributed significantly to our understanding of the developmental biology of haematopoiesis and myelopoiesis over the past decade. The exponential rise in our ability to dissect the biology of myeloid cells in this small vertebrate will no doubt fuel further insights and broaden the scope for current models of myeloid leukaemias. One of the greatest promises for the future of the zebrafish model in myeloid research is the leveraging of embryonic or early larval phenotypes for the identification of genetic and chemical modifiers. These can be undertaken using deliberate, targeted hypotheses (reverse genetics/chemistry), or unbiased, high-throughput screens (forward genetics/chemistry). The growing recognition and acceptance of the zebrafish for studying myeloid biology will enable it to secure a place among other model systems including mouse and cell culture, as a component in a pipeline of preclinical tools to better interrogate molecular pathways and rapidly identify novel therapies with conserved effects across organisms likely to impact outcome for patients with myeloid diseases.

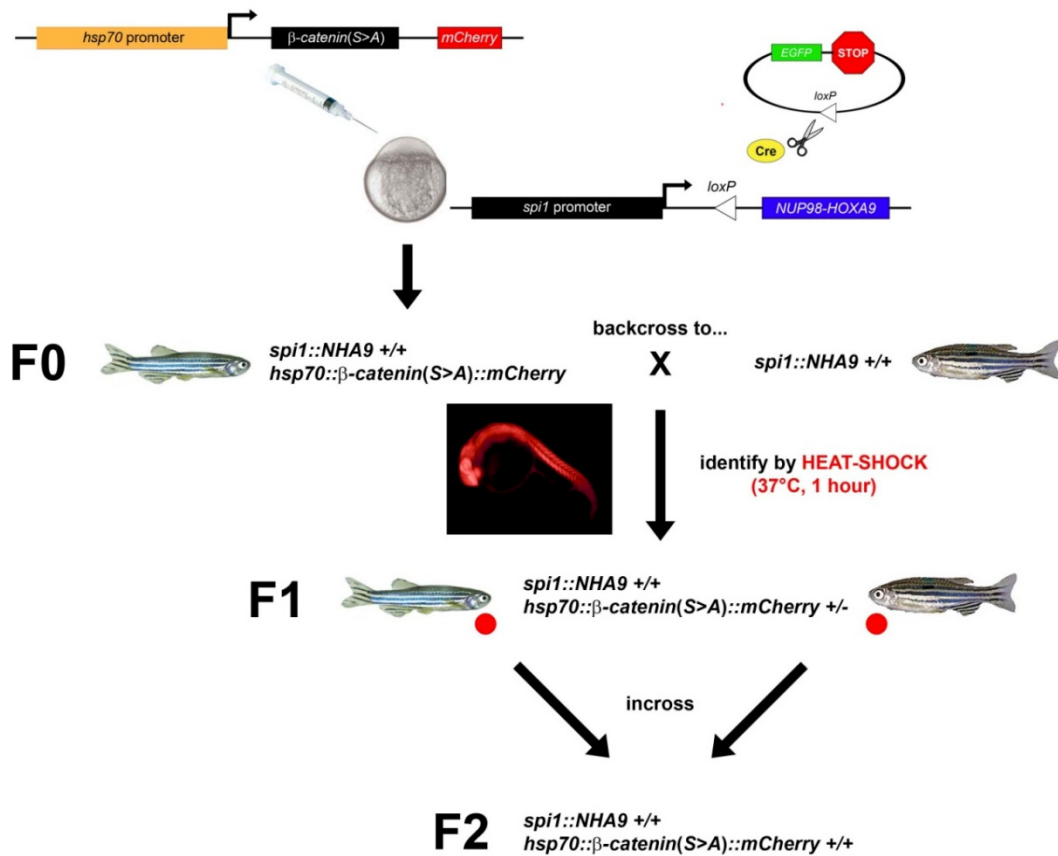


Figure 8.1. Mating strategy to obtain *NHA9* + β -catenin(S/T→A) zebrafish.

The *hsp70::ctnnb1-b*::mCherry* Gateway® transgenic construct will be injected *NHA9* embryos at the one-cell stage. Injected F0 fish will be reared to sexual maturity and backcrossed to homozygous (+/+) *NHA9* fish. F1 offspring will be screened by heat-shock for the presence of red fluorescence (red dot) to identify germline transmission and a founder parent. F1 offspring will be homozygous for *NHA9* and heterozygous (+/-) for β -catenin(S/T→A). Red-fluorescent F1 fish will be incrossed to generate F2 fish that will be homozygous for both *NHA9* and *ctnnb1-b** constructs. A similar strategy will be used to obtain double-transgenic *NHA9+Meis1* zebrafish.

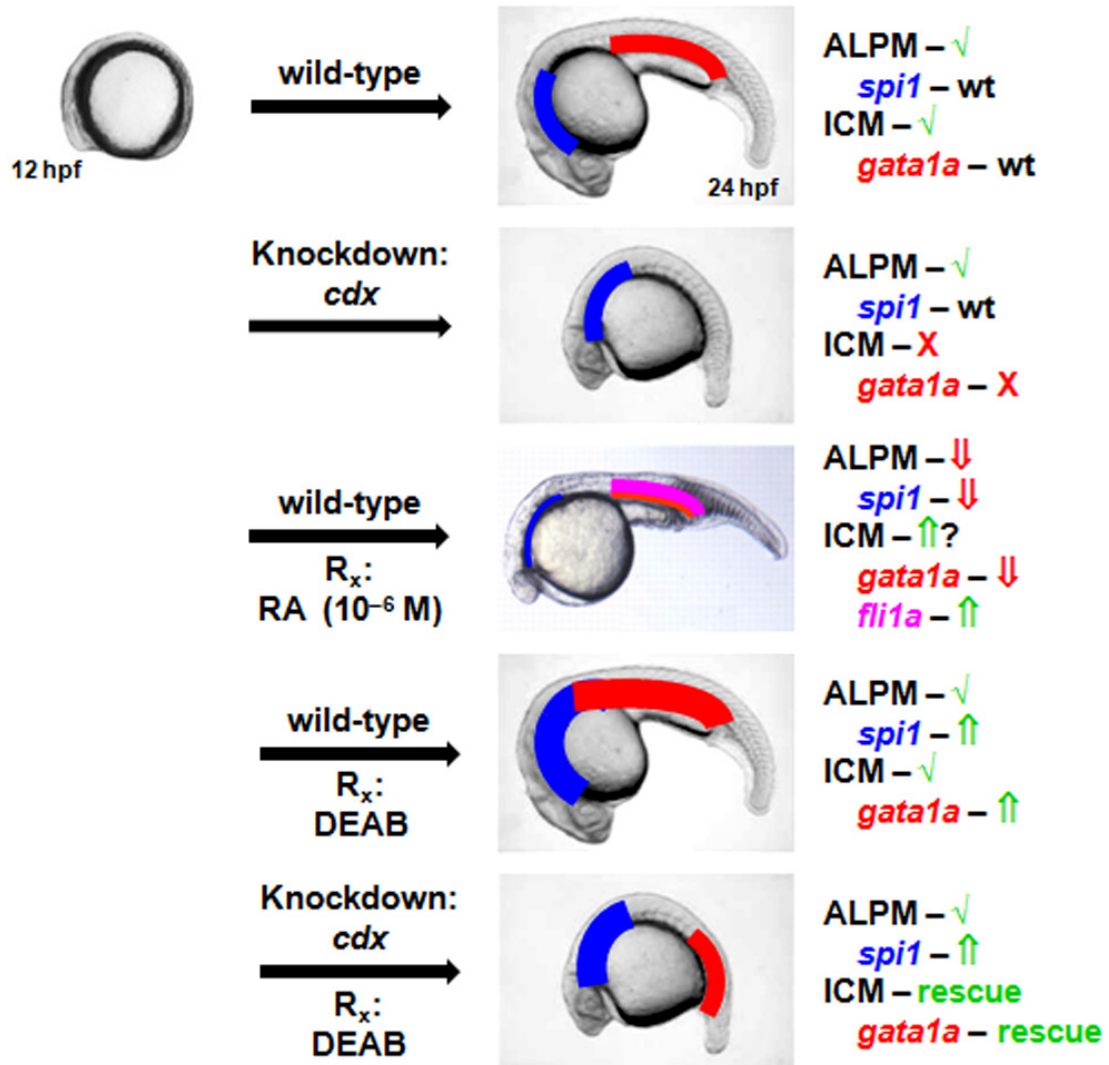


Figure 8.2. Schematic representing the impact of the *cdx4-raldh2* regulatory loop on zebrafish primitive haematopoiesis.

A wild-type zebrafish embryo, shown near the onset (12 hpf, *left*) and conclusion (24 hpf, *right*) of primitive haematopoiesis. Embryos oriented anterior to the left. Gene knockdowns and/or pathway modifications by pharmacological treatments (R_x) are presented for their effects on anterior-posterior morphology, and the success of haemogenic differentiation into *spi1*-expressing myeloid cells (blue line) in the ALPM or *gata1a*-expressing erythroid cells (red line) in the ICM. Angiogenic differentiation (*flil1a*) shown as pink line. In text, green check marks or red crosses represent whether *tal1/scl*-expressing haemangioblast progenitors in the ALPM and/or ICM were correctly established or whether absent. (Thickness of coloured lines denotes relative expression. Adapted from data in Davidson *et al.* 2003; Davidson and Zon 2006; de Jong *et al.* 2010; Liang *et al.* 2012. **New abbreviations used:** RA = retinoic acid; DEAB = 4-diethylamino-benzaldehyde.

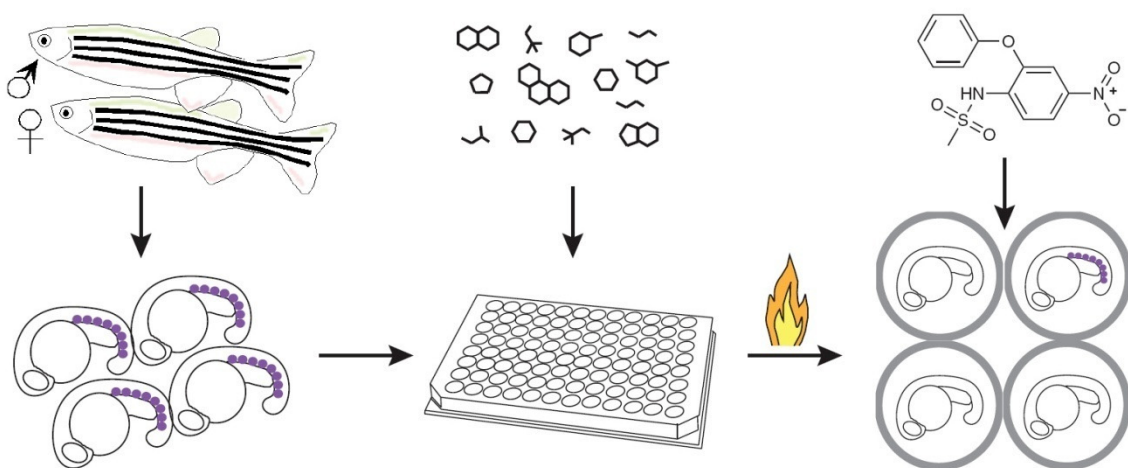


Figure 8.3. Screening for drugs that block *NHA9*.

Embryos are bathed in a panel of drugs at 12-14 hpf, then heat-shocked to activate *NHA9*. Embryos are incubated in drugs until 18 hpf when red cells are assessed by *in situ* for *gata1a* (purple dots). *NHA9* normally inhibits red cell development, but a few drugs may block *NHA9* and rescue normal levels of *gata1a*. Adapted from [Yeh et al. 2009](#).

BIBLIOGRAPHY

- AB/Ambion. (2001) User Bulletin #2 ABI PRISM 7700 Sequence Detection System.
- AB/Ambion. (2005) Real-Time PCR System Chemistry Guide.
- Abramovich C, Pineault N, Ohta H, Humphries RK. (2005) Hox genes: from leukemia to hematopoietic stem cell expansion. *Ann N Y Acad Sci.* **1044**: 109-16.
- Abu-Shaar M, Ryoo HD, Mann RS. (1999) Control of the nuclear localization of Extradenticle by competing nuclear import and export signals. *Genes Dev.* **13**(8): 935-45.
- Ahuja HG, Popplewell L, Tcheurekdjian L, Slovak ML. (2001) NUP98 gene rearrangements and the clonal evolution of chronic myelogenous leukemia. *Genes Chromosomes Cancer.* **30**(4): 410-5.
- Amatruda JF, Zon LI. (1999) Dissecting hematopoiesis and disease using the zebrafish. *Dev Biol.* **216**(1): 1-15.
- Amores A, Force A, Yan YL *et al.* (1998) Zebrafish hox clusters and vertebrate genome evolution. *Science.* **282**(5394): 1711-4.
- Amsterdam A, Sadler KC, Lai K *et al.* (2004) Many ribosomal protein genes are cancer genes in zebrafish. *PLoS Biol.* **2**(5): E139.
- Anderson KL, Smith KA, Pio F, Torbett BE, Maki RA. (1998) Neutrophils deficient in PU.1 do not terminally differentiate or become functionally competent. *Blood.* **92**(5): 1576-85.
- Anderson RM, Bosch JA, Goll MG *et al.* (2009) Loss of Dnmt1 catalytic activity reveals multiple roles for DNA methylation during pancreas development and regeneration. *Dev Biol.* **334**(1): 213-23.
- Araki Y, Okamura S, Hussain SP *et al.* (2003) Regulation of cyclooxygenase-2 expression by the Wnt and ras pathways. *Cancer Res.* **63**(3): 728-34.
- Attar EC, De Angelo DJ, Supko JG *et al.* (2008) Phase I and pharmacokinetic study of bortezomib in combination with idarubicin and cytarabine in patients with acute myelogenous leukemia. *Clin Cancer Res.* **14**(5): 1446-54.
- Azcoitia V, Aracil M, Martinez-A C, Torres M. (2005) The homeodomain protein Meis1 is essential for definitive hematopoiesis and vascular patterning in the mouse embryo. *Dev Biol.* **280**(2): 307-20.

- Bahary N, Zon LI. (1998) Use of the zebrafish (*Danio rerio*) to define hematopoiesis. *Stem Cells*. **16 Suppl 2**: 67-78.
- Bai X, Kim J, Yang Z *et al.* (2010) TIF1gamma controls erythroid cell fate by regulating transcription elongation. *Cell*. **142**(1): 133-43.
- Bain BJ. (2010) *Leukaemia Diagnosis - 4th Ed.* Wiley-Blackwell, Hoboken, NJ, USA.
- Balla KM, Lugo-Villarino G, Spitsbergen JM *et al.* (2010) Eosinophils in the zebrafish: prospective isolation, characterization, and eosinophilia induction by helminth determinants. *Blood*. **116**(19): 3944-54.
- Bansal D, Scholl C, Frohling S *et al.* (2006) Cdx4 dysregulates *Hox* gene expression and generates acute myeloid leukemia alone and in cooperation with Meis1a in a murine model. *Proc Natl Acad Sci U S A*. **103**(45): 16924-9.
- Baron MH. (2003) Embryonic origins of mammalian hematopoiesis. *Exp Hematol*. **31**(12): 1160-9.
- Barresi MJ, Stickney HL, Devoto SH. (2000) The zebrafish slow-muscle-omitted gene product is required for Hedgehog signal transduction and the development of slow muscle identity. *Development*. **127**(10): 2189-99.
- Baumann R, Dragon S. (2005) Erythropoiesis and red cell function in vertebrate embryos. *Eur J Clin Invest*. **35 Suppl 3**: 2-12.
- Beekman R, Touw IP. (2010) G-CSF and its receptor in myeloid malignancy. *Blood*. **115**(25): 5131-6.
- Bei L, Lu Y, Eklund EA. (2005) HOXA9 activates transcription of the gene encoding gp91Phox during myeloid differentiation. *J Biol Chem*. **280**(13): 12359-70.
- Bennett CM, Kanki JP, Rhodes J *et al.* (2001) Myelopoiesis in the zebrafish, *Danio rerio*. *Blood*. **98**(3): 643-51.
- Berghmans S, Murphey RD, Wienholds E *et al.* (2005) Tp53 Mutant Zebrafish Develop Malignant Peripheral Nerve Sheath Tumors. *Proc Natl Acad Sci U S A*. **102**(2): 407-12.
- Berman J, Hsu K, Look AT. (2003) Zebrafish as a model organism for blood diseases. *Br J Haematol*. **123**(4): 568-76.
- Berman JN, Kanki JP, Look AT. (2005) Zebrafish as a model for myelopoiesis during embryogenesis. *Exp Hematol*. **33**(9): 997-1006.

- Bertrand JY, Jalil A, Klaine M, Jung S, Cumano A, Godin I. (2005) Three pathways to mature macrophages in the early mouse yolk sac. *Blood*. **106**(9): 3004-11.
- Bertrand JY, Kim AD, Violette EP, Stachura DL, Cisson JL, Traver D. (2007) Definitive hematopoiesis initiates through a committed erythromyeloid progenitor in the zebrafish embryo. *Development*. **134**(23): 4147-56.
- Bertrand JY, Kim AD, Teng S, Traver D. (2008) CD41+ cmyb+ precursors colonize the zebrafish pronephros by a novel migration route to initiate adult hematopoiesis. *Development*. **135**(10): 1853-62.
- Bertrand JY, Chi NC, Santoso B, Teng S, Stainier DY, Traver D. (2010) Haematopoietic stem cells derive directly from aortic endothelium during development. *Nature*. **464**(7285): 108-11.
- Bjornsson JM, Larsson N, Brun AC *et al.* (2003) Reduced proliferative capacity of hematopoietic stem cells deficient in Hoxb3 and Hoxb4. *Mol Cell Biol*. **23**(11): 3872-83.
- Blackburn JS, Liu S, Raiser DM *et al.* (2012) Notch signalling expands a pre-malignant pool of T-cell acute lymphoblastic leukemia clones without affecting leukemia-propagating cell frequency. *Leukemia*.
- Boger DL, Patel M. (1988) Total synthesis of prodigiosin, prodigiosene, and desmethoxyprodigiosin: Diels-Alder reactions of heterocyclic azadienes and development of an effective palladium(II)-promoted 2,2'-bipyrrrole coupling procedure. *J Org Chem*. **53**(7): 1405-15.
- Boisset JC, van Cappellen W, Andrieu-Soler C, Galjart N, Dzierzak E, Robin C. (2010) In vivo imaging of haematopoietic cells emerging from the mouse aortic endothelium. *Nature*. **464**(7285): 116-20.
- Bolli N, Payne EM, Rhodes J *et al.* (2011) cpsfl is required for definitive HSC survival in zebrafish. *Blood*. **117**(15): 3996-4007.
- Bonnet D, Dick JE. (1997) Human acute myeloid leukemia is organized as a hierarchy that originates from a primitive hematopoietic cell. *Nat Med*. **3**(7): 730-7.
- Borrow J, Shearman AM, Stanton VP, Jr *et al.* (1996) The t(7;11)(p15;p15) translocation in acute myeloid leukaemia fuses the genes for nucleoporin NUP98 and class I homeoprotein HOXA9. *Nat Genet*. **12**(2): 159-67.
- Brun AC, Bjornsson JM, Magnusson M *et al.* (2004) Hoxb4-deficient mice undergo normal hematopoietic development but exhibit a mild proliferation defect in hematopoietic stem cells. *Blood*. **103**(11): 4126-33.

- Buchi F, Spinelli E, Masala E *et al.* (2012) Proteomic analysis identifies differentially expressed proteins in AML1/ETO acute myeloid leukemia cells treated with DNMT inhibitors azacitidine and decitabine. *Leuk Res.* **36**(5): 607-18.
- Burns CE, Galloway JL, Smith AC *et al.* (2009) A genetic screen in zebrafish defines a hierarchical network of pathways required for hematopoietic stem cell emergence. *Blood.* **113**(23): 5776-82.
- Calvo KR, Sykes DB, Pasillas M, Kamps MP. (2000) Hoxa9 immortalizes a granulocyte-macrophage colony-stimulating factor-dependent promyelocyte capable of biphenotypic differentiation to neutrophils or macrophages, independent of enforced meis expression. *Mol Cell Biol.* **20**(9): 3274-85.
- Calvo KR, Knoepfler PS, Sykes DB, Pasillas MP, Kamps MP. (2001) Meis1a suppresses differentiation by G-CSF and promotes proliferation by SCF: potential mechanisms of cooperativity with Hoxa9 in myeloid leukemia. *Proc Natl Acad Sci U S A.* **98**(23): 13120-5.
- Calvo KR, Sykes DB, Pasillas MP, Kamps MP. (2002) Nup98-HoxA9 immortalizes myeloid progenitors, enforces expression of Hoxa9, Hoxa7 and Meis1, and alters cytokine-specific responses in a manner similar to that induced by retroviral co-expression of Hoxa9 and Meis1. *Oncogene.* **21**(27): 4247-56.
- Campas C, Dalmau M, Montaner B *et al.* (2003) Prodigiosin induces apoptosis of B and T cells from B-cell chronic lymphocytic leukemia. *Leukemia.* **17**(4): 746-50.
- Campbell PM, Szyf M. (2003) Human DNA methyltransferase gene DNMT1 is regulated by the APC pathway. *Carcinogenesis.* **24**(1): 17-24.
- Ceccaldi A, Rajavelu A, Champion C *et al.* (2011) C5-DNA methyltransferase inhibitors: from screening to effects on zebrafish embryo development. *Chembiochem.* **12**(9): 1337-45.
- Chang CP, Shen WF, Rozenfeld S, Lawrence HJ, Largman C, Cleary ML. (1995) Pbx proteins display hexapeptide-dependent cooperative DNA binding with a subset of Hox proteins. *Genes Dev.* **9**(6): 663-74.
- Chang CP, Jacobs Y, Nakamura T, Jenkins NA, Copeland NG, Cleary ML. (1997) Meis proteins are major in vivo DNA binding partners for wild-type but not chimeric Pbx proteins. *Mol Cell Biol.* **17**(10): 5679-87.
- Chen EY, Langenau DM. (2011) Zebrafish models of rhabdomyosarcoma. *Methods Cell Biol.* **105**: 383-402.

- Choe SK, Lu P, Nakamura M, Lee J, Sagerstrom CG. (2009) Meis cofactors control HDAC and CBP accessibility at Hox-regulated promoters during zebrafish embryogenesis. *Dev Cell*. **17**(4): 561-7.
- Chou ST, Khandros E, Bailey LC *et al.* (2009) Graded repression of PU.1/Sfpi1 gene transcription by GATA factors regulates hematopoietic cell fate. *Blood*. **114**(5): 983-94.
- Chou WC, Chen CY, Hou HA *et al.* (2009) Acute myeloid leukemia bearing t(7;11)(p15;p15) is a distinct cytogenetic entity with poor outcome and a distinct mutation profile: comparative analysis of 493 adult patients. *Leukemia*. **23**(7): 1303-10.
- Choudhry P, Joshi D, Funke B, Trede N. (2011) Alcama mediates Edn1 signalling during zebrafish cartilage morphogenesis. *Dev Biol*. **349**(2): 483-93.
- Chu J, Loughlin EA, Gaur NA *et al.* (2012) UHRF1 phosphorylation by cyclin A2/cyclin-dependent kinase 2 is required for zebrafish embryogenesis. *Mol Biol Cell*. **23**(1): 59-70.
- Chung KY, Morrone G, Schuringa JJ *et al.* (2006) Enforced expression of NUP98-HOXA9 in human CD34(+) cells enhances stem cell proliferation. *Cancer Res*. **66**(24): 11781-91.
- Chute JP, Muramoto GG, Whitesides J *et al.* (2006) Inhibition of aldehyde dehydrogenase and retinoid signalling induces the expansion of human hematopoietic stem cells. *Proc Natl Acad Sci U S A*. **103**(31): 11707-12.
- Cook WD, McCaw BJ, Herring C *et al.* (2004) PU.1 is a suppressor of myeloid leukemia, inactivated in mice by gene deletion and mutation of its DNA binding domain. *Blood*. **104**(12): 3437-44.
- Corkery DP, Delleire G, Berman JN. (2011) Leukaemia xenotransplantation in zebrafish-chemotherapy response assay in vivo. *Br J Haematol*. **153**(6): 786-9.
- Covassin LD, Siekmann AF, Kacergis MC *et al.* (2009) A genetic screen for vascular mutants in zebrafish reveals dynamic roles for Vegf/Plcg1 signalling during artery development. *Dev Biol*. **329**(2): 212-26.
- Cox CV, Evely RS, Oakhill A, Pamphilon DH, Goulden NJ, Blair A. (2004) Characterization of acute lymphoblastic leukemia progenitor cells. *Blood*. **104**(9): 2919-25.
- Cox CV, Martin HM, Kearns PR, Virgo P, Evely RS, Blair A. (2007) Characterization of a progenitor cell population in childhood T-cell acute lymphoblastic leukemia. *Blood*. **109**(2): 674-82.

- Cozzio A, Passegue E, Ayton PM, Karsunky H, Cleary ML, Weissman IL. (2003) Similar MLL-associated leukemias arising from self-renewing stem cells and short-lived myeloid progenitors. *Genes Dev.* **17**(24): 3029-35.
- Crosnier C, Stamatakis D, Lewis J. (2006) Organizing cell renewal in the intestine: stem cells, signals and combinatorial control. *Nat Rev Genet.* **7**(5): 349-59.
- Cvejic A, Serbanovic-Canic J, Stemple DL, Ouwehand WH. (2011) The role of meis1 in primitive and definitive hematopoiesis during zebrafish development. *Haematologica.* **96**(2): 190-8.
- Da'as S, Teh EM, Dobson JT *et al.* (2011) Zebrafish mast cells possess an FcγRI-like receptor and participate in innate and adaptive immune responses. *Dev Comp Immunol.* **35**(1): 125-34.
- Da'as SI, Coombs AJ, Balci TB, Grondin CA, Ferrando AA, Berman JN. (2012) The zebrafish reveals dependence of the mast cell lineage on Notch signalling in vivo. *Blood.* **119**(15): 3585-94.
- D'Alessio R, Rossi A. (1996) Short Synthesis of Undecylprodigiosine. A New Route to 2,2'-Bipyrrrolyl- pyrromethene Systems. *Synlett.* 513-4.
- D'Alessio R, Bargiotti A, Carlini O *et al.* (2000) Synthesis and immunosuppressive activity of novel prodigiosin derivatives. *J Med Chem.* **43**(13): 2557-65.
- Das BC, McCartin K, Liu TC, Peterson RT, Evans T. (2010) A forward chemical screen in zebrafish identifies a retinoic acid derivative with receptor specificity. *PLoS One.* **5**(4): e10004.
- Dash AB, Williams IR, Kutok JL *et al.* (2002) A murine model of CML blast crisis induced by cooperation between BCR/ABL and NUP98/HOXA9. *Proc Natl Acad Sci U S A.* **99**(11): 7622-7.
- Davidson AJ, Ernst P, Wang Y *et al.* (2003) Cdx4 Mutants Fail to Specify Blood Progenitors and can be Rescued by Multiple Hox Genes. *Nature.* **425**(6955): 300-6.
- Davidson AJ, Zon LI. (2006) The caudal-related homeobox genes *cdx1a* and *cdx4* act redundantly to regulate hox gene expression and the formation of putative hematopoietic stem cells during zebrafish embryogenesis. *Dev Biol.* **292**(2): 506-18.
- Dayyani F, Wang J, Yeh JR *et al.* (2008) Loss of TLE1 and TLE4 from the del(9q) commonly deleted region in AML cooperates with AML1-ETO to affect myeloid cell proliferation and survival. *Blood.* **111**(8): 4338-47.
- de Jong JL, Davidson AJ, Wang Y *et al.* (2010) Interaction of retinoic acid and *scl* controls primitive blood development. *Blood.*

- de The H, Chen Z. (2010) Acute promyelocytic leukaemia: novel insights into the mechanisms of cure. *Nat Rev Cancer*. **10**(11): 775-83.
- den Hartigh J, Brandenburg HC, Vermeij P. (1989) Stability of azacitidine in lactated Ringer's injection frozen in polypropylene syringes. *Am J Hosp Pharm*. **46**(12): 2500-5.
- Detrich HW,3rd, Westerfield M, Zon LI. (1999) Overview of the Zebrafish system. *Methods Cell Biol*. **59**: 3-10.
- Di Rosa P, Villaescusa JC, Longobardi E *et al.* (2007) The homeodomain transcription factor Prep1 (pKnox1) is required for hematopoietic stem and progenitor cell activity. *Dev Biol*. **311**(2): 324-34.
- Diaz-Ruiz C, Montaner B, Perez-Tomas R. (2001) Prodigiosin induces cell death and morphological changes indicative of apoptosis in gastric cancer cell line HGT-1. *Histol Histopathol*. **16**(2): 415-21.
- Dick JE. (2005) Acute myeloid leukemia stem cells. *Ann N Y Acad Sci*. **1044**: 1-5.
- DiMartino JF, Selleri L, Traver D *et al.* (2001) The Hox cofactor and proto-oncogene Pbx1 is required for maintenance of definitive hematopoiesis in the fetal liver. *Blood*. **98**(3): 618-26.
- Dobson JT, Seibert J, Teh EM *et al.* (2008) Carboxypeptidase A5 identifies a novel mast cell lineage in the zebrafish providing new insight into mast cell fate determination. *Blood*. **112**(7): 2969-72.
- Dobson JT, Da'as S, McBride ER, Berman JN. (2009) Fluorescence-activated cell sorting (FACS) of whole mount in situ hybridization (WISH) labelled haematopoietic cell populations in the zebrafish. *Br J Haematol*. **144**(5): 732-5.
- Donovan A, Brownlie A, Zhou Y *et al.* (2000) Positional cloning of zebrafish ferroportin-1 identifies a conserved vertebrate iron exporter. *Nature*. **403**(6771): 776-81.
- Dooley KA, Davidson AJ, Zon LI. (2005) Zebrafish scl functions independently in hematopoietic and endothelial development. *Dev Biol*. **277**(2): 522-36.
- Dorak MT. (2006) *Real-time PCR*. Taylor & Francis Group, New York, NY, USA.
- Dorsam ST, Ferrell CM, Dorsam GP *et al.* (2004) The transcriptome of the leukemogenic homeoprotein HOXA9 in human hematopoietic cells. *Blood*. **103**(5): 1676-84.
- Doyon Y, McCammon JM, Miller JC *et al.* (2008) Heritable targeted gene disruption in zebrafish using designed zinc-finger nucleases. *Nat Biotechnol*. **26**(6): 702-8.

- Du L, Xu J, Li X *et al.* (2011) Rumba and Haus3 are essential factors for the maintenance of hematopoietic stem/progenitor cells during zebrafish hematopoiesis. *Development*. **138**(4): 619-29.
- Dudley AT, Tabin CJ. (2000) Constructive antagonism in limb development. *Curr Opin Genet Dev*. **10**(4): 387-92.
- Duffy KT, McAleer MF, Davidson WR *et al.* (2005) Coordinate control of cell cycle regulatory genes in zebrafish development tested by cyclin D1 knockdown with morpholino phosphorodiamidates and hydroxypropyl-phosphono peptide nucleic acids. *Nucleic Acids Res*. **33**(15): 4914-21.
- Duriez A, Vigneron JH, Zenier HA, May I, Demore BM. (2011) Stability of azacitidine suspensions. *Ann Pharmacother*. **45**(4): 546.
- Ebner A, Cabernard C, Affolter M, Merabet S. (2005) Recognition of distinct target sites by a unique Labial/Extradenticle/Homothorax complex. *Development*. **132**(7): 1591-600.
- Edling CE, Hallberg B. (2007) c-Kit--a hematopoietic cell essential receptor tyrosine kinase. *Int J Biochem Cell Biol*. **39**(11): 1995-8.
- Eiring AM, Neviani P, Santhanam R *et al.* (2008) Identification of novel posttranscriptional targets of the BCR/ABL oncoprotein by ribonomics: requirement of E2F3 for BCR/ABL leukemogenesis. *Blood*. **111**(2): 816-28.
- Eiring AM, Harb JG, Neviani P *et al.* (2010) miR-328 functions as an RNA decoy to modulate hnRNP E2 regulation of mRNA translation in leukemic blasts. *Cell*. **140**(5): 652-65.
- Eklund EA. (2007) The role of HOX genes in malignant myeloid disease. *Curr Opin Hematol*. **14**(2): 85-9.
- Elks PM, van Eeden FJ, Dixon G *et al.* (2011) Activation of hypoxia-inducible factor-1alpha (Hif-1alpha) delays inflammation resolution by reducing neutrophil apoptosis and reverse migration in a zebrafish inflammation model. *Blood*. **118**(3): 712-22.
- Ellett F, Pase L, Hayman JW, Andrianopoulos A, Lieschke GJ. (2011) Mpeg1 Promoter Transgenes Direct Macrophage-Lineage Expression in Zebrafish. *Blood*. **117**(4): e49-56.
- Emig M, Saussele S, Wittor H *et al.* (1999) Accurate and rapid analysis of residual disease in patients with CML using specific fluorescent hybridization probes for real time quantitative RT-PCR. *Leukemia*. **13**(11): 1825-32.

- Eramo A, Pallini R, Lotti F *et al.* (2005) Inhibition of DNA methylation sensitizes glioblastoma for tumor necrosis factor-related apoptosis-inducing ligand-mediated destruction. *Cancer Res.* **65**(24): 11469-77.
- Erickson T, Scholpp S, Brand M, Moens CB, Waskiewicz AJ. (2007) Pbx proteins cooperate with Engrailed to pattern the midbrain-hindbrain and diencephalic-mesencephalic boundaries. *Dev Biol.* **301**(2): 504-17.
- Faber J, Krivtsov AV, Stubbs MC *et al.* (2009) HOXA9 is required for survival in human MLL-rearranged acute leukemias. *Blood.* **113**(11): 2375-85.
- Fanning SR, Sekeres MA, Theil K. (2009) Acute Myelogenous Leukemia. in *Disease Management Project - Hematology & Oncology*. Cleveland Clinic Center for Continuing Education.
- Farooq M, Sulochana KN, Pan X *et al.* (2008) Histone deacetylase 3 (hdac3) is specifically required for liver development in zebrafish. *Dev Biol.* **317**(1): 336-53.
- Fazi F, Zardo G, Gelmetti V *et al.* (2007) Heterochromatic gene repression of the retinoic acid pathway in acute myeloid leukemia. *Blood.* **109**(10): 4432-40.
- Feitsma H, Cuppen E. (2008) Zebrafish as a cancer model. *Mol Cancer Res.* **6**(5):685-94.
- Feng H, Langenau DM, Madge JA *et al.* (2007) Heat-shock induction of T-cell lymphoma/leukaemia in conditional Cre/lox-regulated transgenic zebrafish. *Br J Haematol.* **138**(2): 169-75.
- Feng H, Stachura DL, White RM *et al.* (2010) T-lymphoblastic lymphoma cells express high levels of BCL2, S1P1, and ICAM1, leading to a blockade of tumor cell intravasation. *Cancer Cell.* **18**(4): 353-66.
- Feng Y, Santoriello C, Mione M, Hurlstone A, Martin P. (2010) Live imaging of innate immune cell sensing of transformed cells in zebrafish larvae: parallels between tumor initiation and wound inflammation. *PLoS Biol.* **8**(12):e1000562.
- Forrester AM, Grabher C, McBride ER *et al.* (2011) NUP98-HOXA9-transgenic zebrafish develop a myeloproliferative neoplasm and provide new insight into mechanisms of myeloid leukaemogenesis. *Br J Haematol.* **155**(2): 167-81.
- Forrester AM, Berman JN, Payne EM. (2012) Myelopoiesis and myeloid leukaemogenesis in the zebrafish. *Adv Hematol.* **2012**: 358518. Epub 2012 Jul 20.
- Frazer JK, Meeker ND, Rudner L *et al.* (2009) Heritable T-cell malignancy models established in a zebrafish phenotypic screen. *Leukemia.* **23**(10): 1825-35.

- French CR, Erickson T, Callander D *et al.* (2007) Pbx homeodomain proteins pattern both the zebrafish retina and tectum. *BMC Dev Biol.* **7**: 85.
- Frohling S, Scholl C, Bansal D, Huntly BJ. (2007) HOX gene regulation in acute myeloid leukemia: CDX marks the spot? *Cell Cycle.* **6**(18): 2241-5.
- Fung TK, Chung MI, Liang R, Leung AY. (2010) Role of a novel zebrafish nup98 during embryonic development. *Exp Hematol.* **38**(11): 1014,1021.e1-2.
- Furstner A, Grabowski EJ. (2001) Studies on DNA cleavage by cytotoxic pyrrole alkaloids reveal the distinctly different behavior of roseophilin and prodigiosin derivatives. *Chembiochem.* **2**(9): 706-9.
- Furstner A. (2003) Chemistry and biology of roseophilin and the prodigiosin alkaloids: a survey of the last 2500 years. *Angew Chem Int Ed Engl.* **42**(31): 3582-603.
- Gale RP, Canaani E. (1984) An 8-kilobase abl RNA transcript in chronic myelogenous leukemia. *Proc Natl Acad Sci U S A.* **81**(18): 5648-52.
- Galloway JL, Wingert RA, Thisse C, Thisse B, Zon LI. (2005) Loss of gata1 but not gata2 converts erythropoiesis to myelopoiesis in zebrafish embryos. *Dev Cell.* **8**(1): 109-16.
- Gamba L, Cubedo N, Lutfalla G, Ghysen A, Dambly-Chaudiere C. (2010) Lef1 controls patterning and proliferation in the posterior lateral line system of zebrafish. *Dev Dyn.* **239**(12): 3163-71.
- Gandillet A, Park S, Lassailly F *et al.* (2011) Heterogeneous sensitivity of human acute myeloid leukemia to beta-catenin down-modulation. *Leukemia.* **25**(5): 770-80.
- Ghannam G, Takeda A, Camarata T, Moore MA, Viale A, Yaseen NR. (2004) The oncogene Nup98-HOXA9 induces gene transcription in myeloid cells. *J Biol Chem.* **279**(2): 866-75.
- Gidwani R, Khan ZM, Fenaux P, Beach CL, Pashos CL. (2012) A cost-effectiveness analysis of using azacitidine vs. decitabine in treating patients with myelodysplastic syndromes. *J Med Econ.* **15**(1): 145-54.
- Giles FJ, Keating A, Goldstone AH, Avivi I, Willman CL, Kantarjian HM. (2002) Acute myeloid leukemia. *Hematology Am Soc Hematol Educ Program.* : 73-110.
- Gilliland DG, Tallman MS. (2002) Focus on acute leukemias. *Cancer Cell.* **1**(5): 417-20.
- Goessling W, North TE, Loewer S *et al.* (2009) Genetic interaction of PGE2 and Wnt signalling regulates developmental specification of stem cells and regeneration. *Cell.* **136**(6): 1136-47.

- Goessling W, Allen RS, Guan X *et al.* (2011) Prostaglandin E2 enhances human cord blood stem cell xenotransplants and shows long-term safety in preclinical nonhuman primate transplant models. *Cell Stem Cell.* **8**(4): 445-58.
- Goina E, Skoko N, Pagani F. (2008) Binding of DAZAP1 and hnRNPA1/A2 to an exonic splicing silencer in a natural BRCA1 exon 18 mutant. *Mol Cell Biol.* **28**(11): 3850-60.
- Golemovic M, Sucic M, Zadro R *et al.* (2006) IgH and TCRgamma gene rearrangements, cyclin A1 and HOXA9 gene expression in biphenotypic acute leukemias. *Leuk Res.* **30**(2): 211-21.
- Golub TR, Slonim DK, Tamayo P *et al.* (1999) Molecular classification of cancer: class discovery and class prediction by gene expression monitoring. *Science.* **286**(5439): 531-7.
- Gowher H, Loutchanwoot P, Vorobjeva O *et al.* (2006) Mutational analysis of the catalytic domain of the murine Dnmt3a DNA-(cytosine C5)-methyltransferase. *J Mol Biol.* **357**(3): 928-41.
- Grabher C, Joly JS, Wittbrodt J. (2004) Highly efficient zebrafish transgenesis mediated by the meganuclease I-SceI. *Methods Cell Biol.* **77**: 381-401.
- Graubert TA, Shen D, Ding L *et al.* (2011) Recurrent mutations in the U2AF1 splicing factor in myelodysplastic syndromes. *Nat Genet.* **44**(1): 53-7.
- Gray C, Loynes CA, Whyte MK, Crossman DC, Renshaw SA, Chico TJ. (2011) Simultaneous intravital imaging of macrophage and neutrophil behaviour during inflammation using a novel transgenic zebrafish. *Thromb Haemost.* **105**(5): 811-9.
- Gregory M, Jagadeeswaran P. (2002) Selective labeling of zebrafish thrombocytes: quantitation of thrombocyte function and detection during development. *Blood Cells Mol Dis.* **28**(3): 418-27.
- Griffis ER, Craige B, Dimaano C, Ullman KS, Powers MA. (2004) Distinct functional domains within nucleoporins Nup153 and Nup98 mediate transcription-dependent mobility. *Mol Biol Cell.* **15**(4): 1991-2002.
- Grimwade D, Walker H, Oliver F *et al.* (1998) The importance of diagnostic cytogenetics on outcome in AML: analysis of 1,612 patients entered into the MRC AML 10 trial. The Medical Research Council Adult and Children's Leukaemia Working Parties. *Blood.* **92**(7): 2322-33.
- Growney JD, Shigematsu H, Li Z *et al.* (2005) Loss of Runx1 perturbs adult hematopoiesis and is associated with a myeloproliferative phenotype. *Blood.* **106**(2): 494-504.

- Grunwald DJ, Eisen JS. (2002) Headwaters of the zebrafish -- emergence of a new model vertebrate. *Nat Rev Genet.* **3**(9): 717-24.
- Guibal FC, Alberich-Jorda M, Hirai H *et al.* (2009) Identification of a myeloid committed progenitor as the cancer-initiating cell in acute promyelocytic leukemia. *Blood.* **114**(27): 5415-25.
- Guidotti A, Dong E, Kundakovic M, Satta R, Grayson DR, Costa E. (2009) Characterization of the action of antipsychotic subtypes on valproate-induced chromatin remodeling. *Trends Pharmacol Sci.* **30**(2): 55-60.
- Haldi M, Ton C, Seng WL, McGrath P. (2006) Human melanoma cells transplanted into zebrafish proliferate, migrate, produce melanin, form masses and stimulate angiogenesis in zebrafish. *Angiogenesis.* **9**(3): 139-51.
- Hall C, Flores MV, Storm T, Crosier K, Crosier P. (2007) The zebrafish lysozyme C promoter drives myeloid-specific expression in transgenic fish. *BMC Dev Biol.* **7**: 42.
- Hall C, Flores MV, Chien A, Davidson A, Crosier K, Crosier P. (2009) Transgenic zebrafish reporter lines reveal conserved Toll-like receptor signalling potential in embryonic myeloid leukocytes and adult immune cell lineages. *J Leukoc Biol.* **85**(5): 751-65.
- Hanahan D, Weinberg RA. (2011) Hallmarks of cancer: the next generation. *Cell.* **144**(5): 646-74.
- Hans S, Freudenreich D, Geffarth M, Kaslin J, Machate A, Brand M. (2011) Generation of a non-leaky heat shock-inducible Cre line for conditional Cre/lox strategies in zebrafish. *Dev Dyn.* **240**(1): 108-15.
- Hatano Y, Miura I, Nakamura T, Yamazaki Y, Takahashi N, Miura AB. (1999) Molecular heterogeneity of the NUP98/HOXA9 fusion transcript in myelodysplastic syndromes associated with t(7;11)(p15;p15). *Br J Haematol.* **107**(3): 600-4.
- Heidel FH, Mar BG, Armstrong SA. (2011) Self-renewal related signalling in myeloid leukemia stem cells. *Int J Hematol.* **94**(2): 109-17.
- Heinrichs S, Berman JN, Ortiz TM *et al.* (2005) CD34+ cell selection is required to assess HOXA9 expression levels in patients with myelodysplastic syndrome. *Br J Haematol.* **130**(1): 83-6.
- Herbomel P, Thisse B, Thisse C. (1999) Ontogeny and behaviour of early macrophages in the zebrafish embryo. *Development.* **126**(17): 3735-45.
- Herbomel P, Levraud JP. (2005) Imaging early macrophage differentiation, migration, and behaviors in live zebrafish embryos. *Methods Mol Med.* **105**: 199-214.

- Hisa T, Spence SE, Rachel RA *et al.* (2004) Hematopoietic, angiogenic and eye defects in Meis1 mutant animals. *EMBO J.* **23**(2): 450-9.
- Hong CC. (2009) Large-scale small-molecule screen using zebrafish embryos. *Methods Mol Biol.* **486**: 43-55.
- Hope KJ, Jin L, Dick JE. (2003) Human acute myeloid leukemia stem cells. *Arch Med Res.* **34**(6): 507-14.
- Hove JR, Koster RW, Forouhar AS, Acevedo-Bolton G, Fraser SE, Gharib M. (2003) Intracardiac fluid forces are an essential epigenetic factor for embryonic cardiogenesis. *Nature.* **421**(6919): 172-7.
- Hsu K, Traver D, Kutok JL *et al.* (2004) The pu.1 promoter drives myeloid gene expression in zebrafish. *Blood.* **104**(5): 1291-7.
- Huang P, Xiao A, Zhou M, Zhu Z, Lin S, Zhang B. (2011) Heritable gene targeting in zebrafish using customized TALENs. *Nat Biotechnol.* **29**(8): 699-700.
- Hughes TP, Hochhaus A, Branford S *et al.* (2010) Long-term prognostic significance of early molecular response to imatinib in newly diagnosed chronic myeloid leukemia: an analysis from the International Randomized Study of Interferon and STI571 (IRIS). *Blood.* **116**(19): 3758-65.
- Hume DA. (2006) The mononuclear phagocyte system. *Curr Opin Immunol.* **18**(1):49-53.
- Huntly BJ, Shigematsu H, Deguchi K *et al.* (2004) MOZ-TIF2, but not BCR-ABL, confers properties of leukemic stem cells to committed murine hematopoietic progenitors. *Cancer Cell.* **6**(6): 587-96.
- Iervolino A, Santilli G, Trotta R *et al.* (2002) hnRNP A1 nucleocytoplasmic shuttling activity is required for normal myelopoiesis and BCR/ABL leukemogenesis. *Mol Cell Biol.* **22**(7): 2255-66.
- Iwasaki H, Mizuno S, Wells RA, Cantor AB, Watanabe S, Akashi K. (2003) GATA-1 converts lymphoid and myelomonocytic progenitors into the megakaryocyte/erythrocyte lineages. *Immunity.* **19**(3): 451-62.
- Iwasaki M, Kuwata T, Yamazaki Y *et al.* (2005) Identification of cooperative genes for NUP98-HOXA9 in myeloid leukemogenesis using a mouse model. *Blood.* **105**(2): 784-93.
- Izon DJ, Rozenfeld S, Fong ST, Komuves L, Largman C, Lawrence HJ. (1998) Loss of function of the homeobox gene Hoxa-9 perturbs early T-cell development and induces apoptosis in primitive thymocytes. *Blood.* **92**(2): 383-93.

- Izsvak Z, Ivics Z, Garcia-Estefania D, Fahrenkrug SC, Hackett PB. (1996) DANA elements: a family of composite, tRNA-derived short interspersed DNA elements associated with mutational activities in zebrafish (*Danio rerio*). *Proc Natl Acad Sci U S A.* **93**(3): 1077-81.
- Jamieson CH, Ailles LE, Dylla SJ *et al.* (2004) Granulocyte-macrophage progenitors as candidate leukemic stem cells in blast-crisis CML. *N Engl J Med.* **351**(7): 657-67.
- Jaw TJ, You LR, Knoepfler PS *et al.* (2000) Direct interaction of two homeoproteins, homothorax and extradenticle, is essential for EXD nuclear localization and function. *Mech Dev.* **91**(1-2): 279-91.
- Jette CA, Flanagan AM, Ryan J *et al.* (2008) BIM and other BCL-2 family proteins exhibit cross-species conservation of function between zebrafish and mammals. *Cell Death Differ.* **15**(6): 1063-72.
- Jin S, Zhao H, Yi Y, Nakata Y, Kalota A, Gewirtz AM. (2010) c-Myb binds MLL through menin in human leukemia cells and is an important driver of MLL-associated leukemogenesis. *J Clin Invest.* **120**(2): 593-606.
- Jing GJ, Xu DH, Shi SL *et al.* (2011) Aberrant expression and localization of hnRNP-A2/B1 is a common event in human gastric adenocarcinoma. *J Gastroenterol Hepatol.* **26**(1): 108-15.
- Jo OD, Martin J, Bernath A, Masri J, Lichtenstein A, Gera J. (2008) Heterogeneous nuclear ribonucleoprotein A1 regulates cyclin D1 and c-myc internal ribosome entry site function through Akt signalling. *J Biol Chem.* **283**(34): 23274-87.
- John AM, Thomas NS, Mufti GJ, Padua RA. (2004) Targeted therapies in myeloid leukemia. *Semin Cancer Biol.* **14**(1): 41-62.
- Jones CD, Yeung C, Zehnder JL. (2003) Comprehensive validation of a real-time quantitative bcr-abl assay for clinical laboratory use. *Am J Clin Pathol.* **120**(1): 42-8.
- Juarez MA, Su F, Chun S, Kiel MJ, Lyons SE. (2005) Distinct roles for SCL in erythroid specification and maturation in zebrafish. *J Biol Chem.* **280**(50): 41636-44.
- Kalen M, Wallgard E, Asker N *et al.* (2009) Combination of reverse and chemical genetic screens reveals angiogenesis inhibitors and targets. *Chem Biol.* **16**(4): 432-41.
- Kappen C. (2000) Disruption of the homeobox gene Hoxb-6 in mice results in increased numbers of early erythrocyte progenitors. *Am J Hematol.* **65**(2): 111-8.
- Kasper LH, Brindle PK, Schnabel CA, Pritchard CE, Cleary ML, van Deursen JM. (1999) CREB binding protein interacts with nucleoporin-specific FG repeats that

- activate transcription and mediate NUP98-HOXA9 oncogenicity. *Mol Cell Biol.* **19**(1): 764-76.
- Kawagoe H, Humphries RK, Blair A, Sutherland HJ, Hogge DE. (1999) Expression of HOX genes, HOX cofactors, and MLL in phenotypically and functionally defined subpopulations of leukemic and normal human hematopoietic cells. *Leukemia.* **13**(5): 687-98.
- Kikuchi K, Holdway JE, Major RJ *et al.* (2011) Retinoic Acid production by endocardium and epicardium is an injury response essential for zebrafish heart regeneration. *Dev Cell.* **20**(3): 397-404.
- Kimmel CB, Ballard WW, Kimmel SR, Ullmann B, Schilling TF. (1995) Stages of embryonic development of the zebrafish. *Dev Dyn.* **203**(3): 253-310.
- Kissa K, Herbomel P. (2010) Blood stem cells emerge from aortic endothelium by a novel type of cell transition. *Nature.* **464**(7285): 112-5.
- Knoepfler PS, Lu Q, Kamps MP. (1996) Pbx-1 Hox heterodimers bind DNA on inseparable half-sites that permit intrinsic DNA binding specificity of the Hox partner at nucleotides 3' to a TAAT motif. *Nucleic Acids Res.* **24**(12): 2288-94.
- Ko KH, Lam QL, Zhang M *et al.* (2007) Hoxb3 deficiency impairs B lymphopoiesis in mouse bone marrow. *Exp Hematol.* **35**(3): 465-75.
- Kokel D, Bryan J, Laggner C *et al.* (2010) Rapid behavior-based identification of neuroactive small molecules in the zebrafish. *Nat Chem Biol.* **6**(3): 231-7.
- Koo S, Huntly B, Wang Y *et al.* (2010) Cdx4 is dispensable for murine adult hematopoietic stem cells but promotes MLL-AF9-mediated leukemogenesis. *Haematologica.*
- Kosinski C, Li VS, Chan AS *et al.* (2007) Gene expression patterns of human colon tops and basal crypts and BMP antagonists as intestinal stem cell niche factors. *Proc Natl Acad Sci U S A.* **104**(39): 15418-23.
- Kotani T, Iemura S, Natsume T, Kawakami K, Yamashita M. (2010) Mys protein regulates protein kinase A activity by interacting with regulatory type Ialpha subunit during vertebrate development. *J Biol Chem.* **285**(7): 5106-16.
- Krause DS, Lazarides K, von Andrian UH, Van Etten RA. (2006) Requirement for CD44 in homing and engraftment of BCR-ABL-expressing leukemic stem cells. *Nat Med.* **12**(10): 1175-1180.
- Krivtsov AV, Twomey D, Feng Z *et al.* (2006) Transformation from committed progenitor to leukaemia stem cell initiated by MLL-AF9. *Nature.* **442**(7104): 818-22.

- Kroon E, Kros J, Thorsteinsdottir U, Baban S, Buchberg AM, Sauvageau G. (1998) Hoxa9 transforms primary bone marrow cells through specific collaboration with Meis1a but not Pbx1b. *EMBO J.* **17**(13): 3714-25.
- Kroon E, Thorsteinsdottir U, Mayotte N, Nakamura T, Sauvageau G. (2001) NUP98-HOXA9 expression in hemopoietic stem cells induces chronic and acute myeloid leukemias in mice. *EMBO J.* **20**(3): 350-61.
- Kuendgen A, Bug G, Ottmann OG *et al.* (2011) Treatment of poor-risk myelodysplastic syndromes and acute myeloid leukemia with a combination of 5-azacytidine and valproic acid. *Clin Epigenetics.* **2**(2): 389-99.
- Kwan KM, Fujimoto E, Grabher C *et al.* (2007) The Tol2kit: a multisite gateway-based construction kit for Tol2 transposon transgenesis constructs. *Dev Dyn.* **236**(11): 3088-99.
- Lacaud G, Robertson S, Palis J, Kennedy M, Keller G. (2001) Regulation of hemangioblast development. *Ann N Y Acad Sci.* **938**: 96,107; discussion 108.
- Lam EY, Chau JY, Kalev-Zylinska ML *et al.* (2009) Zebrafish runx1 promoter-EGFP transgenics mark discrete sites of definitive blood progenitors. *Blood.* **113**(6): 1241-9.
- Lam EY, Hall CJ, Crosier PS, Crosier KE, Flores MV. (2010) Live imaging of Runx1 expression in the dorsal aorta tracks the emergence of blood progenitors from endothelial cells. *Blood.* **116**(6): 909-14.
- Lam SH, Chua HL, Gong Z, Lam TJ, Sin YM. (2004) Development and maturation of the immune system in zebrafish, *Danio rerio*: a gene expression profiling, in situ hybridization and immunological study. *Dev Comp Immunol.* **28**(1): 9-28.
- Langenau DM, Traver D, Ferrando AA *et al.* (2003) Myc-induced T cell leukemia in transgenic zebrafish. *Science.* **299**(5608): 887-90.
- Langenau DM, Feng H, Berghmans S, Kanki JP, Kutok JL, Look AT. (2005a) Cre/lox-regulated transgenic zebrafish model with conditional myc-induced T cell acute lymphoblastic leukemia. *Proc Natl Acad Sci U S A.* **102**(17): 6068-73.
- Langenau DM, Jette C, Berghmans S *et al.* (2005b) Suppression of apoptosis by bcl-2 overexpression in lymphoid cells of transgenic zebrafish. *Blood.* **105**(8): 3278-85.
- Langenau DM, Keefe MD, Storer NY *et al.* (2007) Effects of RAS on the genesis of embryonal rhabdomyosarcoma. *Genes Dev.* **21**(11): 1382-95.

- Langenau DM, Keefe MD, Storer NY *et al.* (2008) Co-injection strategies to modify radiation sensitivity and tumor initiation in transgenic Zebrafish. *Oncogene*. **27**(30): 4242-8.
- Lapidot T, Sirard C, Vormoor J *et al.* (1994) A cell initiating human acute myeloid leukaemia after transplantation into SCID mice. *Nature*. **367**(6464): 645-8.
- Lasa A, Carnicer MJ, Aventin A *et al.* (2004) MEIS 1 expression is downregulated through promoter hypermethylation in AML1-ETO acute myeloid leukemias. *Leukemia*. **18**(7): 1231-7.
- Lawrence HJ, Helgason CD, Sauvageau G *et al.* (1997) Mice bearing a targeted interruption of the homeobox gene HOXA9 have defects in myeloid, erythroid, and lymphoid hematopoiesis. *Blood*. **89**(6): 1922-30.
- Lawrence HJ, Rozenfeld S, Cruz C *et al.* (1999) Frequent co-expression of HOXA9 and MEIS1 homeobox genes in human myeloid leukemias. *Leukemia*. **13**(12): 1993-9.
- Lawrence HJ, Christensen J, Fong S *et al.* (2005) Loss of expression of the Hoxa-9 homeobox gene impairs the proliferation and repopulating ability of hematopoietic stem cells. *Blood*. **106**(12): 3988-94.
- Le Guyader D, Redd MJ, Colucci-Guyon E *et al.* (2008) Origins and unconventional behavior of neutrophils in developing zebrafish. *Blood*. **111**(1): 132-41.
- Le X, Langenau DM, Keefe MD, Kutok JL, Neuberg DS, Zon LI. (2007) Heat shock-inducible Cre/Lox approaches to induce diverse types of tumors and hyperplasia in transgenic zebrafish. *Proc Natl Acad Sci U S A*. **104**(22): 9410-5.
- Leacock SW, Basse AN, Chandler GL, Kirk AM, Rakheja D, Amatruda JF. (2012) A zebrafish transgenic model of Ewing's sarcoma reveals conserved mediators of EWS-FLI1 tumorigenesis. *Dis Model Mech*. **5**(1): 95-106.
- Lee LM, Seftor EA, Bonde G, Cornell RA, Hendrix MJ. (2005) The fate of human malignant melanoma cells transplanted into zebrafish embryos: assessment of migration and cell division in the absence of tumor formation. *Dev Dyn*. **233**(4): 1560-70.
- Lengerke C, Schmitt S, Bowman TV *et al.* (2008) BMP and Wnt specify hematopoietic fate by activation of the *Cdx-Hox* pathway. *Cell Stem Cell*. **2**(1): 72-82.
- Lewis RS, Stephenson SE, Ward AC. (2006) Constitutive activation of zebrafish Stat5 expands hematopoietic cell populations in vivo. *Exp Hematol*. **34**(2): 179-87.
- Liang D, Jia W, Li J, Li K, Zhao Q. (2012) Retinoic acid signalling plays a restrictive role in zebrafish primitive myelopoiesis. *PLoS One*. **7**(2): e30865.

- Lieschke GJ, Oates AC, Crowhurst MO, Ward AC, Layton JE. (2001) Morphologic and functional characterization of granulocytes and macrophages in embryonic and adult zebrafish. *Blood*. **98**(10): 3087-96.
- Liu F, Wen Z. (2002) Cloning and expression pattern of the lysozyme C gene in zebrafish. *Mech Dev*. **113**(1): 69-72.
- Liu S, Leach SD. (2011) Zebrafish models for cancer. *Annu Rev Pathol*. **6**: 71-93.
- Liu TX, Howlett NG, Deng M *et al.* (2003) Knockdown of zebrafish Fancd2 causes developmental abnormalities via p53-dependent apoptosis. *Dev Cell*. **5**(6): 903-14.
- Longobardi E, Blasi F. (2003) Overexpression of PREP-1 in F9 teratocarcinoma cells leads to a functionally relevant increase of PBX-2 by preventing its degradation. *J Biol Chem*. **278**(40): 39235-41.
- Lord AM, North TE, Zon LI. (2007) Prostaglandin E2: making more of your marrow. *Cell Cycle*. **6**(24): 3054-7.
- Lowenberg B, Pabst T, Vellenga E *et al.* (2011) Cytarabine dose for acute myeloid leukemia. *N Engl J Med*. **364**(11): 1027-36.
- Lyons SE, Lawson ND, Lei L, Bennett PE, Weinstein BM, Liu PP. (2002) A nonsense mutation in zebrafish gata1 causes the bloodless phenotype in vlad tepes. *Proc Natl Acad Sci U S A*. **99**(8): 5454-9.
- Ma AC, Ward AC, Liang R, Leung AY. (2007) The role of jak2a in zebrafish hematopoiesis. *Blood*. **110**(6): 1824-30.
- Ma AC, Fan A, Ward AC *et al.* (2009) A novel zebrafish jak2a(V581F) model shared features of human JAK2(V617F) polycythemia vera. *Exp Hematol*. **37**(12): 1379,1386.e4.
- Ma AC, Chung MI, Liang R, Leung AY. (2010) A DEAB-sensitive aldehyde dehydrogenase regulates hematopoietic stem and progenitor cells development during primitive hematopoiesis in zebrafish embryos. *Leukemia*. **24**(12): 2090-9.
- Maeder ML, Thibodeau-Beganny S, Osiak A *et al.* (2008) Rapid "open-source" engineering of customized zinc-finger nucleases for highly efficient gene modification. *Mol Cell*. **31**(2): 294-301.
- Maeder ML, Thibodeau-Beganny S, Sander JD, Voytas DF, Joung JK. (2009) Oligomerized pool engineering (OPEN): an 'open-source' protocol for making customized zinc-finger arrays. *Nat Protoc*. **4**(10): 1471-501.

- Magnusson M, Brun AC, Lawrence HJ, Karlsson S. (2007) Hoxa9/hoxb3/hoxb4 compound null mice display severe hematopoietic defects. *Exp Hematol.* **35**(9): 1421-8.
- Manderville RA. (2001) Synthesis, proton-affinity and anti-cancer properties of the prodigiosin-group natural products. *Curr Med Chem Anticancer Agents.* **1**(2): 195-218.
- Mann RS, Lelli KM, Joshi R. (2009) Hox specificity unique roles for cofactors and collaborators. *Curr Top Dev Biol.* **88**: 63-101.
- Marcucci G, Byrd JC, Dai G *et al.* (2003) Phase 1 and pharmacodynamic studies of G3139, a Bcl-2 antisense oligonucleotide, in combination with chemotherapy in refractory or relapsed acute leukemia. *Blood.* **101**(2): 425-32.
- Marcucci G, Stock W, Dai G *et al.* (2005) Phase I study of oblimersen sodium, an antisense to Bcl-2, in untreated older patients with acute myeloid leukemia: pharmacokinetics, pharmacodynamics, and clinical activity. *J Clin Oncol.* **23**(15): 3404-11.
- Marcucci G, Haferlach T, Dohner H. (2011) Molecular genetics of adult acute myeloid leukemia: prognostic and therapeutic implications. *J Clin Oncol.* **29**(5): 475-86.
- Marques DS, Sandrini JZ, Boyle RT, Marins LF, Trindade GS. (2010) Relationships between multidrug resistance (MDR) and stem cell markers in human chronic myeloid leukemia cell lines. *Leuk Res.* **34**(6): 757-62.
- Marques IJ, Weiss FU, Vlecken DH *et al.* (2009) Metastatic behaviour of primary human tumours in a zebrafish xenotransplantation model. *BMC Cancer.* **9**: 128.
- Martens JH, Brinkman AB, Simmer F *et al.* (2010) PML-RARalpha/RXR Alters the Epigenetic Landscape in Acute Promyelocytic Leukemia. *Cancer Cell.* **17**(2):173-85.
- Martin CC, Laforest L, Akimenko MA, Ekker M. (1999) A role for DNA methylation in gastrulation and somite patterning. *Dev Biol.* **206**(2): 189-205.
- Martin J, Masri J, Cloninger C *et al.* (2011) Phosphomimetic substitution of heterogeneous nuclear ribonucleoprotein A1 at serine 199 abolishes AKT-dependent internal ribosome entry site-transacting factor (ITAF) function via effects on strand annealing and results in mammalian target of rapamycin complex 1 (mTORC1) inhibitor sensitivity. *J Biol Chem.* **286**(18): 16402-13.
- Maslov AY, Lee M, Gundry M *et al.* (2012) 5-Aza-2'-deoxycytidine-induced genome rearrangements are mediated by DNMT1. *Oncogene.* Feb 20 [Epub ahead of print].

- Mathias JR, Dodd ME, Walters KB, Yoo SK, Ranheim EA, Huttenlocher A. (2009) Characterization of zebrafish larval inflammatory macrophages. *Dev Comp Immunol.* **33**(11): 1212-7.
- Maves L, Waskiewicz AJ, Paul B *et al.* (2007) Pbx homeodomain proteins direct Myod activity to promote fast-muscle differentiation. *Development.* **134**(18): 3371-82.
- Mayotte N, Roy DC, Yao J, Kroon E, Sauvageau G. (2002) Oncogenic interaction between BCR-ABL and NUP98-HOXA9 demonstrated by the use of an in vitro purging culture system. *Blood.* **100**(12): 4177-84.
- McCurley AT, Callard GV. (2008) Characterization of housekeeping genes in zebrafish: male-female differences and effects of tissue type, developmental stage and chemical treatment. *BMC Mol Biol.* **9**: 102.
- McKercher SR, Torbett BE, Anderson KL *et al.* (1996) Targeted disruption of the PU.1 gene results in multiple hematopoietic abnormalities. *EMBO J.* **15**(20): 5647-58.
- McNulty CL, Peres JN, Bardine N, van den Akker WM, Durston AJ. (2005) Knockdown of the complete Hox paralogous group 1 leads to dramatic hindbrain and neural crest defects. *Development.* **132**(12): 2861-71.
- Melvin MS, Ferguson DC, Lindquist N, Manderville RA. (1999) DNA Binding by 4-Methoxypyrrolic Natural Products. Preference for Intercalation at AT Sites by Tambjamine E and Prodigiosin. *J Org Chem.* **64**(18): 6861-9.
- Melvin MS, Wooton KE, Rich CC *et al.* (2001) Copper-nuclease efficiency correlates with cytotoxicity for the 4-methoxypyrrolic natural products. *J Inorg Biochem.* **87**(3): 129-35.
- Melvin MS, Tomlinson JT, Park G *et al.* (2002a) Influence of the a-ring on proton affinity and anticancer properties of the prodigiosins. *Chem Res Toxicol.* **15**(5): 734-41.
- Melvin MS, Calcutt MW, Nofle RE, Manderville RA. (2002b) Influence of the a-ring on the redox and nuclease properties of the prodigiosins: importance of the bipyrrrole moiety in oxidative DNA cleavage. *Chem Res Toxicol.* **15**(5): 742-8.
- Meng X, Noyes MB, Zhu LJ, Lawson ND, Wolfe SA. (2008) Targeted gene inactivation in zebrafish using engineered zinc-finger nucleases. *Nat Biotechnol.* **26**(6): 695-701.
- Mercader N, Leonardo E, Azpiazu N *et al.* (1999) Conserved regulation of proximodistal limb axis development by Meis1/Hth. *Nature.* **402**(6760): 425-9.

- Metallo CM, Ji L, de Pablo JJ, Palecek SP. (2008) Retinoic acid and bone morphogenetic protein signalling synergize to efficiently direct epithelial differentiation of human embryonic stem cells. *Stem Cells*. **26**(2): 372-80.
- Minami Y, Stuart SA, Ikawa T *et al.* (2008) BCR-ABL-transformed GMP as myeloid leukemic stem cells. *Proc Natl Acad Sci U S A*. **105**(46): 17967-72.
- Minehata K, Kawahara A, Suzuki T. (2008) Meis1 Regulates the Development of Endothelial Cells in Zebrafish. *Biochem Biophys Res Commun*. **374**(4): 647-52.
- Moellering RE, Cornejo M, Davis TN *et al.* (2009) Direct inhibition of the NOTCH transcription factor complex. *Nature*. **462**(7270): 182-8.
- Moens CB, Selleri L. (2006) Hox cofactors in vertebrate development. *Dev Biol*. **291**(2): 193-206.
- Molina G, Vogt A, Bakan A *et al.* (2009) Zebrafish chemical screening reveals an inhibitor of Dusp6 that expands cardiac cell lineages. *Nat Chem Biol*. **5**(9): 680-7.
- Montaner B, Navarro S, Pique M *et al.* (2000) Prodigiosin from the supernatant of *Serratia marcescens* induces apoptosis in haematopoietic cancer cell lines. *Br J Pharmacol*. **131**(3): 585-93.
- Montaner B, Perez-Tomas R. (2001) Prodigiosin-induced apoptosis in human colon cancer cells. *Life Sci*. **68**(17): 2025-36.
- Montaner B, Perez-Tomas R. (2002a) Prodigiosin induces caspase-9 and caspase-8 activation and cytochrome C release in Jurkat T cells. *Ann N Y Acad Sci*. **973**: 246-9.
- Montaner B, Perez-Tomas R. (2002b) The cytotoxic prodigiosin induces phosphorylation of p38-MAPK but not of SAPK/JNK. *Toxicol Lett*. **129**(1-2): 93-8.
- Montaner B, Perez-Tomas R. (2003) The prodigiosins: a new family of anticancer drugs. *Curr Cancer Drug Targets*. **3**(1): 57-65.
- Monteiro R, Pouget C, Patient R. (2011) The gata1/pu.1 lineage fate paradigm varies between blood populations and is modulated by tif1gamma. *EMBO J*. **30**(6): 1093-103.
- Moore MA, Chung KY, Plasilova M *et al.* (2007) NUP98 dysregulation in myeloid leukemogenesis. *Ann N Y Acad Sci*. **1106**: 114-42.
- Mosimann C, Kaufman CK, Li P, Pugach EK, Tamplin OJ, Zon LI. (2011) Ubiquitous transgene expression and Cre-based recombination driven by the ubiquitin promoter in zebrafish. *Development*. **138**(1): 169-77.

- Mueller BU, Pabst T, Fos J *et al.* (2006) ATRA resolves the differentiation block in t(15;17) acute myeloid leukemia by restoring PU.1 expression. *Blood*. **107**(8): 3330-8.
- Mueller RL, Huang C, Ho RK. (2010) Spatio-temporal regulation of Wnt and retinoic acid signalling by tbx16/spadetail during zebrafish mesoderm differentiation. *BMC Genomics*. **11**: 492.
- Muller-Tidow C, Steffen B, Cauvet T *et al.* (2004) Translocation products in acute myeloid leukemia activate the Wnt signalling pathway in hematopoietic cells. *Mol Cell Biol*. **24**(7): 2890-904.
- Murayama E, Kissa K, Zapata A *et al.* (2006) Tracing hematopoietic precursor migration to successive hematopoietic organs during zebrafish development. *Immunity*. **25**(6): 963-75.
- Murphey RD, Stern HM, Straub CT, Zon LI. (2006) A chemical genetic screen for cell cycle inhibitors in zebrafish embryos. *Chem Biol Drug Des*. **68**(4): 213-9.
- Nakamura T, Largaespada DA, Shaughnessy JD, Jr, Jenkins NA, Copeland NG. (1996a) Cooperative activation of Hoxa and Pbx1-related genes in murine myeloid leukaemias. *Nat Genet*. **12**(2): 149-53.
- Nakamura T, Largaespada DA, Lee MP *et al.* (1996b) Fusion of the nucleoporin gene NUP98 to HOXA9 by the chromosome translocation t(7;11)(p15;p15) in human myeloid leukaemia. *Nat Genet*. **12**(2): 154-8.
- Nakano K, Vousden KH. (2001) PUMA, a novel proapoptotic gene, is induced by p53. *Mol Cell*. **7**(3): 683-94.
- Neering SJ, Bushnell T, Sozer S *et al.* (2007) Leukemia stem cells in a genetically defined murine model of blast-crisis CML. *Blood*. **110**(7): 2578-85.
- Nerlov C, Querfurth E, Kulesa H, Graf T. (2000) GATA-1 interacts with the myeloid PU.1 transcription factor and represses PU.1-dependent transcription. *Blood*. **95**(8): 2543-51.
- Nicoli S, Ribatti D, Cotelli F, Presta M. (2007) Mammalian tumor xenografts induce neovascularization in zebrafish embryos. *Cancer Res*. **67**(7): 2927-31.
- Niederreither K, Dolle P. (2008) Retinoic acid in development: towards an integrated view. *Nat Rev Genet*. **9**(7): 541-53.
- Ning SF, Li QY, Liang MM *et al.* (2012) Methylation characteristics and developmental potential of Guangxi Bama minipig (*Sus scrofa domestica*) cloned embryos from donor cells treated with trichostatin A and 5-aza-2'-deoxycytidine. *Zygote*. : 1-9.

- North TE, Goessling W, Walkley CR *et al.* (2007) Prostaglandin E2 regulates vertebrate haematopoietic stem cell homeostasis. *Nature*. **447**(7147): 1007-11.
- Ohshima K, Karube K, Hamasaki M *et al.* (2003) Differential chemokine, chemokine receptor and cytokine expression in Epstein-Barr virus-associated lymphoproliferative diseases. *Leuk Lymphoma*. **44**(8): 1367-78.
- Onnebo SM, Condrón MM, McPhee DO, Lieschke GJ, Ward AC. (2005) Hematopoietic perturbation in zebrafish expressing a tel-jak2a fusion. *Exp Hematol*. **33**(2):182-8.
- Orkin SH, Zon LI. (2008) Hematopoiesis: an evolving paradigm for stem cell biology. *Cell*. **132**(4): 631-44.
- Pan F, Peng S, Fleurence R, Linnehan JE, Knopf K, Kim E. (2010) Economic analysis of decitabine versus best supportive care in the treatment of intermediate- and high-risk myelodysplastic syndromes from a US payer perspective. *Clin Ther*. **32**(14): 2444-56.
- Papaemmanuil E, Cazzola M, Boulton J *et al.* (2011) Somatic SF3B1 mutation in myelodysplasia with ring sideroblasts. *N Engl J Med*. **365**(15): 1384-95.
- Parant JM, George SA, Holden JA, Yost HJ. (2010) Genetic modeling of Li-Fraumeni syndrome in zebrafish. *Dis Model Mech*. **3**(1-2): 45-56.
- Park G, Tomlinson JT, Melvin MS, Wright MW, Day CS, Manderville RA. (2003) Zinc and copper complexes of prodigiosin: implications for copper-mediated double-strand DNA cleavage. *Org Lett*. **5**(2): 113-6.
- Passegue E, Weisman IL. (2005) Leukemic stem cells: where do they come from? *Stem Cell Rev*. **1**(3): 181-8.
- Pastor T, Pagani F. (2011) Interaction of hnRNPA1/A2 and DAZAP1 with an Alu-derived intronic splicing enhancer regulates ATM aberrant splicing. *PLoS One*. **6**(8): e23349.
- Patel K, Dickson J, Din S, Macleod K, Jodrell D, Ramsahoye B. (2010) Targeting of 5-aza-2'-deoxycytidine residues by chromatin-associated DNMT1 induces proteasomal degradation of the free enzyme. *Nucleic Acids Res*. **38**(13): 4313-24.
- Patterson LJ, Gering M, Eckfeldt CE *et al.* (2007) The transcription factors Scl and Lmo2 act together during development of the hemangioblast in zebrafish. *Blood*. **109**(6): 2389-98.
- Patton EE, Widlund HR, Kutok JL *et al.* (2005) BRAF mutations are sufficient to promote nevi formation and cooperate with p53 in the genesis of melanoma. *Curr Biol*. **15**(3): 249-54.

- Paul TA, Bies J, Small D, Wolff L. (2010) Signatures of polycomb repression and reduced H3K4 trimethylation are associated with p15INK4b DNA methylation in AML. *Blood*. **115**(15): 3098-108.
- Pedersen-Bjergaard J, Christiansen DH, Desta F, Andersen MK. (2006) Alternative genetic pathways and cooperating genetic abnormalities in the pathogenesis of therapy-related myelodysplasia and acute myeloid leukemia. *Leukemia*. **20**(11): 1943-9.
- Peravali R, Gehrig J, Giselbrecht S *et al.* (2011) Automated feature detection and imaging for high-resolution screening of zebrafish embryos. *BioTechniques*. **50**(5): 319-24.
- Perez-Tomas R, Montaner B, Llagostera E, Soto-Cerrato V. (2003) Prodigiosins, proapoptotic drugs with anticancer properties. *Biochem Pharmacol*. **66**(8): 1447-52.
- Perrotti D, Neviani P. (2007) From mRNA metabolism to cancer therapy: chronic myelogenous leukemia shows the way. *Clin Cancer Res*. **13**(6): 1638-42.
- Peterson RT, Shaw SY, Peterson TA *et al.* (2004) Chemical suppression of a genetic mutation in a zebrafish model of aortic coarctation. *Nat Biotechnol*. **22**(5): 595-9.
- Pevny L, Simon MC, Robertson E *et al.* (1991) Erythroid differentiation in chimaeric mice blocked by a targeted mutation in the gene for transcription factor GATA-1. *Nature*. **349**(6306): 257-60.
- Pillay LM, Forrester AM, Erickson T, Berman JN, Waskiewicz AJ. (2010) The Hox cofactors Meis1 and Pbx act upstream of gata1 to regulate primitive hematopoiesis. *Dev Biol*. **340**(2): 306-17.
- Pineault N, Buske C, Feuring-Buske M *et al.* (2003) Induction of acute myeloid leukemia in mice by the human leukemia-specific fusion gene NUP98-HOXD13 in concert with Meis1. *Blood*. **101**(11): 4529-38.
- Popperl H, Rikhof H, Chang H, Haffter P, Kimmel CB, Moens CB. (2000) Lazarus is a Novel Pbx Gene that Globally Mediates Hox Gene Function in Zebrafish. *Mol Cell*. **6**(2): 255-67.
- Provost E, Rhee J, Leach SD. (2007) Viral 2A peptides allow expression of multiple proteins from a single ORF in transgenic zebrafish embryos. *Genesis*. **45**(10): 625-9.
- Pruvot B, Jacquelin A, Droin N *et al.* (2011) Leukemic cell xenograft in zebrafish embryo for investigating drug efficacy. *Haematologica*. **96**(4): 612-6.

- Rai K, Nadauld LD, Chidester S *et al.* (2006) Zebrafish Dnmt1 and Suv39h1 regulate organ-specific terminal differentiation during development. *Mol Cell Biol.* **26**(19): 7077-85.
- Rai K, Sarkar S, Broadbent TJ *et al.* (2010) DNA demethylase activity maintains intestinal cells in an undifferentiated state following loss of APC. *Cell.* **142**(6): 930-42.
- Ramoneda BM, Perez-Tomas R. (2002) Activation of protein kinase C for protection of cells against apoptosis induced by the immunosuppressor prodigiosin. *Biochem Pharmacol.* **63**(3): 463-9.
- Ransom DG, Haffter P, Odenthal J *et al.* (1996) Characterization of zebrafish mutants with defects in embryonic hematopoiesis. *Development.* **123**: 311-9.
- Ransom DG, Bahary N, Niss K *et al.* (2004) The zebrafish moonshine gene encodes transcriptional intermediary factor 1gamma, an essential regulator of hematopoiesis. *PLoS Biol.* **2**(8): E237.
- Rawlings JS, Rosler KM, Harrison DA. (2004) The JAK/STAT signalling pathway. *J Cell Sci.* **117**(Pt 8): 1281-3.
- Regourd J, Ali AA, Thompson A. (2007) Synthesis and anti-cancer activity of C-ring-functionalized prodigiosin analogues. *J Med Chem.* **50**(7): 1528-36.
- Rekhtman N, Radparvar F, Evans T, Skoultchi AI. (1999) Direct interaction of hematopoietic transcription factors PU.1 and GATA-1: functional antagonism in erythroid cells. *Genes Dev.* **13**(11): 1398-411.
- Renshaw SA, Loynes CA, Trushell DM, Elworthy S, Ingham PW, Whyte MK. (2006) A transgenic zebrafish model of neutrophilic inflammation. *Blood.* **108**(13): 3976-8.
- Revenko AS, Kalashnikova EV, Gemo AT, Zou JX, Chen HW. (2010) Chromatin loading of E2F-MLL complex by cancer-associated coregulator ANCCA via reading a specific histone mark. *Mol Cell Biol.* **30**(22): 5260-72.
- Reya T, Clevers H. (2005) Wnt signalling in stem cells and cancer. *Nature.* **434**(7035): 843-50.
- Rhodes J, Hagen A, Hsu K *et al.* (2005) Interplay of pu.1 and gata1 determines myeloid-erythroid progenitor cell fate in zebrafish. *Dev Cell.* **8**(1): 97-108.
- Rieckhof GE, Casares F, Ryoo HD, Abu-Shaar M, Mann RS. (1997) Nuclear translocation of extradenticle requires homothorax, which encodes an extradenticle-related homeodomain protein. *Cell.* **91**(2): 171-83.

- Rizzo V, Morelli A, Pinciroli V, Sciangula D, D'Alessio R. (1999) Equilibrium and kinetics of rotamer interconversion in immunosuppressant prodigiosin derivatives in solution. *J Pharm Sci.* **88**(1): 73-8.
- Ro H, Dawid IB. (2011) Modulation of Tcf3 repressor complex composition regulates cdx4 expression in zebrafish. *EMBO J.* **30**(14): 2894-907.
- Robertson S, Kennedy M, Keller G. (1999) Hematopoietic commitment during embryogenesis. *Ann N Y Acad Sci.* **872**: 9,15; discussion 15-6.
- Roboz GJ. (2011) Novel approaches to the treatment of acute myeloid leukemia. *Hematology Am Soc Hematol Educ Program.* **2011**: 43-50.
- Roche J, Zeng C, Baron A *et al.* (2004) Hox expression in AML identifies a distinct subset of patients with intermediate cytogenetics. *Leukemia.* **18**(6): 1059-63.
- Rojo I, de Ilarduya OM, Estonba A, Pardo MA. (2007) Innate immune gene expression in individual zebrafish after *Listonella anguillarum* inoculation. *Fish Shellfish Immunol.* **23**(6): 1285-93.
- Rook G. (1992) Tumours and Coley's toxins. *Nature.* **357**(6379): 545.
- Rosenbauer F, Tenen DG. (2007) Transcription factors in myeloid development: balancing differentiation with transformation. *Nat Rev Immunol.* **7**(2): 105-17.
- Rozen S, Skaletsky H. (2000) Primer3 on the WWW for general users and for biologist programmers. *Methods Mol Biol.* **132**: 365-86.
- Rudner LA, Brown KH, Dobrinski KP *et al.* (2011) Shared acquired genomic changes in zebrafish and human T-ALL. *Oncogene.* **30**(41): 4289-96.
- Ryningen A, Stapnes C, Bruserud O. (2007) Clonogenic acute myelogenous leukemia cells are heterogeneous with regard to regulation of differentiation and effect of epigenetic pharmacological targeting. *Leuk Res.* **31**(9): 1303-13.
- Sabaawy HE, Azuma M, Embree LJ, Tsai HJ, Starost MF, Hickstein DD. (2006) TEL-AML1 transgenic zebrafish model of precursor B cell acute lymphoblastic leukemia. *Proc Natl Acad Sci U S A.* **103**(41): 15166-71.
- Sachidanandan C, Yeh JR, Peterson QP, Peterson RT. (2008) Identification of a novel retinoid by small molecule screening with zebrafish embryos. *PLoS One.* **3**(4): e1947.
- Sander JD, Cade L, Khayter C *et al.* (2011a) Targeted gene disruption in somatic zebrafish cells using engineered TALENs. *Nat Biotechnol.* **29**(8): 697-8.

- Sander JD, Dahlborg EJ, Goodwin MJ *et al.* (2011b) Selection-free zinc-finger-nuclease engineering by context-dependent assembly (CoDA). *Nat Methods*. **8**(1): 67-9.
- Sansam CL, Shepard JL, Lai K *et al.* (2006) DTL/CDT2 is essential for both CDT1 regulation and the early G2/M checkpoint. *Genes Dev*. **20**(22): 3117-29.
- Sarno JL, Kliman HJ, Taylor HS. (2005) HOXA10, Pbx2, and Meis1 protein expression in the human endometrium: formation of multimeric complexes on HOXA10 target genes. *J Clin Endocrinol Metab*. **90**(1): 522-8.
- Sato T, Konno H, Tanaka Y *et al.* (1998) Prodigiosins as a new group of H⁺/Cl⁻ symporters that uncouple proton translocators. *J Biol Chem*. **273**(34): 21455-62.
- Sauntharajah Y, Triozzi P, Rini B *et al.* (2012) p53-Independent, normal stem cell sparing epigenetic differentiation therapy for myeloid and other malignancies. *Semin Oncol*. **39**(1): 97-108.
- Scadden DT. (2006) The stem-cell niche as an entity of action. *Nature*. **441**(7097): 1075-1079.
- Scandura JM, Boccuni P, Cammenga J, Nimer SD. (2002) Transcription factor fusions in acute leukemia: variations on a theme. *Oncogene*. **21**(21): 3422-44.
- Schwieger M, Lohler J, Fischer M, Herwig U, Tenen DG, Stocking C. (2004) A dominant-negative mutant of C/EBPalpha, associated with acute myeloid leukemias, inhibits differentiation of myeloid and erythroid progenitors of man but not mouse. *Blood*. **103**(7): 2744-52.
- Scott EW, Simon MC, Anastasi J, Singh H. (1994) Requirement of transcription factor PU.1 in the development of multiple hematopoietic lineages. *Science*. **265**(5178): 1573-7.
- Seganish JL, Davis JT. (2005) Prodigiosin is a chloride carrier that can function as an anion exchanger. *Chem Commun (Camb)*. **(46)**(46): 5781-3.
- Seiter K, Harris JE. (2011) "Acute Myeloid Leukemia Staging". Medscape. May 20, 2011. <http://emedicine.medscape.com/article/2006750-overview>
- Serrano E, Carnicer MJ, Lasa A *et al.* (2008) Epigenetic-based treatments emphasize the biologic differences of core-binding factor acute myeloid leukemias. *Leuk Res*. **32**(6): 944-53.
- Shah MY, Licht JD. (2011) DNMT3A mutations in acute myeloid leukemia. *Nat Genet*. **43**(4): 289-90.

- Shanmugam K, Green NC, Rambaldi I, Saragovi HU, Featherstone MS. (1999) PBX and MEIS as non-DNA-binding partners in trimeric complexes with HOX proteins. *Mol Cell Biol.* **19**(11): 7577-88.
- Shen WF, Rozenfeld S, Kwong A, Kom ves LG, Lawrence HJ, Largman C. (1999) HOXA9 forms triple complexes with PBX2 and MEIS1 in myeloid cells. *Mol Cell Biol.* **19**(4): 3051-61.
- Shepard JL, Stern HM, Pfaff KL, Amatruda JF. (2004) Analysis of the cell cycle in zebrafish embryos. *Methods Cell Biol.* **76**: 109-25.
- Shepard JL, Amatruda JF, Stern HM *et al.* (2005) A zebrafish bmyb mutation causes genome instability and increased cancer susceptibility. *Proc Natl Acad Sci U S A.* **102**(37): 13194-9.
- Shimamoto T, Tang Y, Naot Y *et al.* (1999) Hematopoietic progenitor cell abnormalities in Hoxc-8 null mutant mice. *J Exp Zool.* **283**(2): 186-93.
- Shimizu T, Bae YK, Hibi M. (2006) Cdx-Hox code controls competence for responding to Fgfs and RA in zebrafish neural tissue. *Development.* **133**(23):4709-19.
- Shivdasani RA, Mayer EL, Orkin SH. (1995) Absence of blood formation in mice lacking the T-cell leukaemia oncoprotein tal-1/SCL. *Nature.* **373**(6513): 432-4.
- Shivdasani RA, Fujiwara Y, McDevitt MA, Orkin SH. (1997) A lineage-selective knockout establishes the critical role of transcription factor GATA-1 in megakaryocyte growth and platelet development. *EMBO J.* **16**(13): 3965-73.
- Sidi S, Sanda T, Kennedy RD *et al.* (2008) Chk1 suppresses a caspase-2 apoptotic response to DNA damage that bypasses p53, Bcl-2, and caspase-3. *Cell.* **133**(5):864-77.
- Simoos FC, Peterkin T, Patient R. (2011) Fgf differentially controls cross-antagonism between cardiac and haemangioblast regulators. *Development.* **138**(15): 3235-45.
- Slape C, Aplan PD. (2004) The role of NUP98 gene fusions in hematologic malignancy. *Leuk Lymphoma.* **45**(7): 1341-50.
- Smith AC, Raimondi AR, Salthouse CD *et al.* (2010) High-throughput cell transplantation establishes that tumor-initiating cells are abundant in zebrafish T-cell acute lymphoblastic leukemia. *Blood.* **115**(16): 3296-303.
- Smith TH, Collins TM, McGowan RA. (2011) Expression of the dnmt3 genes in zebrafish development: similarity to Dnmt3a and Dnmt3b. *Dev Genes Evol.* **220**(11-12): 347-53.

- So CW, Karsunky H, Wong P, Weissman IL, Cleary ML. (2004) Leukemic transformation of hematopoietic progenitors by MLL-GAS7 in the absence of Hoxa7 or Hoxa9. *Blood*. **103**(8): 3192-9.
- Solberg N, Machon O, Machonova O, Krauss S. (2012) Mouse Tcf3 represses canonical Wnt signalling by either competing for beta-catenin binding or through occupation of DNA-binding sites. *Mol Cell Biochem*. **365**(1-2): 53-63.
- Song J, Teplova M, Ishibe-Murakami S, Patel DJ. (2012) Structure-based mechanistic insights into DNMT1-mediated maintenance DNA methylation. *Science*. **335**(6069): 709-12.
- Stachura DL, Svoboda O, Lau RP *et al.* (2011) Clonal analysis of hematopoietic progenitor cells in the zebrafish. *Blood*. **118**(5): 1274-82.
- Stainier DY, Weinstein BM, Detrich HW, 3rd, Zon LI, Fishman MC. (1995) Cloche, an early acting zebrafish gene, is required by both the endothelial and hematopoietic lineages. *Development*. **121**(10): 3141-50.
- Stamp LK, Cleland LG, James MJ. (2004) Upregulation of synoviocyte COX-2 through interactions with T lymphocytes: role of interleukin 17 and tumor necrosis factor-alpha. *J Rheumatol*. **31**(7): 1246-1254.
- Stevens KE, Mann RS. (2007) A balance between two nuclear localization sequences and a nuclear export sequence governs extradenticle subcellular localization. *Genetics*. **175**(4): 1625-36.
- Stoletov K, Montel V, Lester RD, Gonias SL, Klemke R. (2007) High-resolution imaging of the dynamic tumor cell vascular interface in transparent zebrafish. *Proc Natl Acad Sci U S A*. **104**(44):17406-11.
- Stopka T, Amanatullah DF, Papetti M, Skoultchi AI. (2005) PU.1 inhibits the erythroid program by binding to GATA-1 on DNA and creating a repressive chromatin structure. *EMBO J*. **24**(21): 3712-23.
- Streisinger G, Walker C, Dower N, Knauber D, Singer F. (1981) Production of clones of homozygous diploid zebra fish (*Brachydanio rerio*). *Nature*. **291**(5813): 293-6.
- Sumoy L, Kiefer J, Kimelman D. (1999) Conservation of intracellular Wnt signalling components in dorsal-ventral axis formation in zebrafish. *Dev Genes Evol*. **209**(1): 48-58.
- Takeda A, Goolsby C, Yaseen NR. (2006) NUP98-HOXA9 induces long-term proliferation and blocks differentiation of primary human CD34+ hematopoietic cells. *Cancer Res*. **66**(13): 6628-37.

- Tang R, Dodd A, Lai D, McNabb WC, Love DR. (2007) Validation of zebrafish (*Danio rerio*) reference genes for quantitative real-time RT-PCR normalization. *Acta Biochim Biophys Sin (Shanghai)*. **39**(5): 384-90.
- Thorsteinsdottir U, Kroon E, Jerome L, Blasi F, Sauvageau G. (2001) Defining roles for HOX and MEIS1 genes in induction of acute myeloid leukemia. *Mol Cell Biol*. **21**(1): 224-34.
- Thorsteinsdottir U, Mamo A, Kroon E *et al.* (2002) Overexpression of the myeloid leukemia-associated Hoxa9 gene in bone marrow cells induces stem cell expansion. *Blood*. **99**(1): 121-9.
- Tittle RK, Sze R, Ng A *et al.* (2011) Uhrf1 and Dnmt1 are required for development and maintenance of the zebrafish lens. *Dev Biol*. **350**(1): 50-63.
- Traver D, Paw BH, Poss KD, Penberthy WT, Lin S, Zon LI. (2003) Transplantation and in vivo imaging of multilineage engraftment in zebrafish bloodless mutants. *Nat Immunol*. **4**(12): 1238-46.
- Trowbridge JJ, Sinha AU, Zhu N, Li M, Armstrong SA, Orkin SH. (2012) Haploinsufficiency of Dnmt1 impairs leukemia stem cell function through derepression of bivalent chromatin domains. *Genes Dev*. **26**(4): 344-9.
- Vangala RK, Heiss-Neumann MS, Rangatia JS *et al.* (2003) The myeloid master regulator transcription factor PU.1 is inactivated by AML1-ETO in t(8;21) myeloid leukemia. *Blood*. **101**(1): 270-7.
- Villefranc JA, Amigo J, Lawson ND. (2007) Gateway compatible vectors for analysis of gene function in the zebrafish. *Dev Dyn*. **236**(11): 3077-87.
- Vogelstein B, Kinzler KW. (2004) Cancer genes and the pathways they control. *Nat Med*. **10**(8): 789-99.
- Voss AK, Collin C, Dixon MP, Thomas T. (2009) Moz and retinoic acid coordinately regulate H3K9 acetylation, Hox gene expression, and segment identity. *Dev Cell*. **17**(5): 674-86.
- Walter RB, Appelbaum FR, Tallman MS, Weiss NS, Larson RA, Estey EH. (2010) Shortcomings in the clinical evaluation of new drugs: acute myeloid leukemia as paradigm. *Blood*. **116**(14): 2420-8.
- Wang JC, Lapidot T, Cashman JD *et al.* (1998) High level engraftment of NOD/SCID mice by primitive normal and leukemic hematopoietic cells from patients with chronic myeloid leukemia in chronic phase. *Blood*. **91**(7): 2406-14.

- Wang GG, Cai L, Pasillas MP, Kamps MP. (2007) NUP98-NSD1 links H3K36 methylation to Hox-A gene activation and leukaemogenesis. *Nat Cell Biol.* **9**(7): 804-12.
- Wang K, Wang P, Shi J *et al.* (2010) PML/RARalpha targets promoter regions containing PU.1 consensus and RARE half sites in acute promyelocytic leukemia. *Cancer Cell.* **17**(2): 186-97.
- Wang QF, Wu G, Mi S *et al.* (2011) MLL fusion proteins preferentially regulate a subset of wild-type MLL target genes in leukemic genome. *Blood.* **117**(25): 6895-905.
- Wang Y, Krivtsov AV, Sinha AU *et al.* (2010) The Wnt/beta-catenin pathway is required for the development of leukemia stem cells in AML. *Science.* **327**(5973): 1650-3.
- Ward AC, McPhee DO, Condrón MM *et al.* (2003) The zebrafish *spi1* promoter drives myeloid-specific expression in stable transgenic fish. *Blood.* **102**(9): 3238-40.
- Warga RM, Kane DA, Ho RK. (2009) Fate mapping embryonic blood in zebrafish: multi- and unipotential lineages are segregated at gastrulation. *Dev Cell.* **16**(5): 744-55.
- Warren AJ, Colledge WH, Carlton MB, Evans MJ, Smith AJ, Rabbitts TH. (1994) The oncogenic cysteine-rich LIM domain protein *rbtn2* is essential for erythroid development. *Cell.* **78**(1): 45-57.
- Waskiewicz AJ, Rikhof HA, Hernandez RE, Moens CB. (2001) Zebrafish *Meis* functions to stabilize *Pbx* proteins and regulate hindbrain patterning. *Development.* **128**(21): 4139-51.
- Waskiewicz AJ, Rikhof HA, Moens CB. (2002) Eliminating zebrafish *pbx* proteins reveals a hindbrain ground state. *Dev Cell.* **3**(5): 723-33.
- Weber GF, Ashkar S, Glimcher MJ, Cantor H. (1996) Receptor-ligand interaction between CD44 and osteopontin (*Eta-1*). *Science.* **271**(5248):509-512.
- Wei Q, Li Y, Chen L *et al.* (2006) Genes differentially expressed in responsive and refractory acute leukemia. *Front Biosci.* **11**: 977-82.
- Weinstein BM, Schier AF, Abdelilah S *et al.* (1996) Hematopoietic mutations in the zebrafish. *Development.* **123**: 303-9.
- Wermuth PJ, Buchberg AM. (2005) *Meis1*-mediated apoptosis is caspase dependent and can be suppressed by coexpression of *HoxA9* in murine and human cell lines. *Blood.* **105**(3): 1222-30.
- Westerfield M. (2000) *The Zebrafish Book. A guide for the laboratory use of zebrafish (Danio rerio).* 4th ed. University of Oregon Press, Eugene, OR, USA.

- White RM, Sessa A, Burke C *et al.* (2008) Transparent adult zebrafish as a tool for in vivo transplantation analysis. *Cell Stem Cell.* **2**(2): 183-9.
- Wittamer V, Bertrand JY, Gutschow PW, Traver D. (2011) Characterization of the mononuclear phagocyte system in zebrafish. *Blood.* **117**(26): 7126-35.
- Wojiski S, Guibal FC, Kindler T *et al.* (2009) PML-RARalpha initiates leukemia by conferring properties of self-renewal to committed promyelocytic progenitors. *Leukemia.* **23**(8): 1462-71.
- Woods WG. (2006) Curing childhood acute myeloid leukemia (AML) at the half-way point: promises to keep and miles to go before we sleep. *Pediatr Blood Cancer.* **46**(5): 565-9.
- Xu F, Li K, Tian M *et al.* (2009) N-CoR is required for patterning the anterior-posterior axis of zebrafish hindbrain by actively repressing retinoid signalling. *Mech Dev.* **126**(10): 771-80.
- Yang HW, Kutok JL, Lee NH *et al.* (2004) Targeted expression of human MYCN selectively causes pancreatic neuroendocrine tumors in transgenic zebrafish. *Cancer Res.* **64**(20): 7256-62.
- Yeh JR, Munson KM, Chao YL, Peterson QP, Macrae CA, Peterson RT. (2008) AML1-ETO reprograms hematopoietic cell fate by downregulating scl expression. *Development.* **135**(2): 401-10.
- Yeh JR, Munson KM, Elagib KE, Goldfarb AN, Sweetser DA, Peterson RT. (2009) Discovering chemical modifiers of oncogene-regulated hematopoietic differentiation. *Nat Chem Biol.* **5**(4): 236-43.
- Yeh JR, Munson KM. (2010) Zebrafish small molecule screen in reprogramming/cell fate modulation. *Methods Mol Biol.* **636**: 317-27.
- Yeung J, Esposito MT, Gandillet A *et al.* (2010) beta-Catenin mediates the establishment and drug resistance of MLL leukemic stem cells. *Cancer Cell.* **18**(6): 606-18.
- Zeitlin BD, Zeitlin IJ, Nor JE. (2008) Expanding circle of inhibition: small-molecule inhibitors of Bcl-2 as anticancer cell and antiangiogenic agents. *J Clin Oncol.* **26**(25): 4180-8.
- Zhang DE, Hohaus S, Voso MT *et al.* (1996) Function of PU.1 (Spi-1), C/EBP, and AML1 in early myelopoiesis: regulation of multiple myeloid CSF receptor promoters. *Curr Top Microbiol Immunol.* **211**: 137-47.

- Zhang JJ, Zhu Y, Zhu Y *et al.* (2012) Association of increased DNA methyltransferase expression with carcinogenesis and poor prognosis in pancreatic ductal adenocarcinoma. *Clin Transl Oncol.* **14**(2): 116-24.
- Zhang P, Behre G, Pan J *et al.* (1999) Negative cross-talk between hematopoietic regulators: GATA proteins repress PU.1. *Proc Natl Acad Sci U S A.* **96**(15): 8705-10.
- Zhang P, Zhang X, Iwama A *et al.* (2000) PU.1 inhibits GATA-1 function and erythroid differentiation by blocking GATA-1 DNA binding. *Blood.* **96**(8): 2641-8.
- Zhou J, Li B, Wu J *et al.* (2011) Essential Role for PU.1 in MEIS1 Activation and MLL Fusion Leukemia, *ASH Annual Meeting Abstracts.* **118**(21): 3466.
- Zhu S, Lee JS, Guo F *et al.* (2012) Activated ALK collaborates with MYCN in neuroblastoma pathogenesis. *Cancer Cell.* **21**(3): 362-73.
- Zhuravleva J, Paggetti J, Martin L *et al.* (2008) MOZ/TIF2-induced acute myeloid leukaemia in transgenic fish. *Br J Haematol.* **143**(3): 378-82.

APPENDIX A COPYRIGHT AND PERMISSIONS – DEVELOPMENTAL BIOLOGY (ELSEVIER)

ELSEVIER Home Products User Resources About Us Support & Contact Elsevier Websites

Search [Advanced Product Search](#)

▲ For Authors

Journal authors' home

- Why publish with Elsevier
- Resource center
- Guide to publishing with Elsevier
- Funding body agreements/policies
- Authors' rights
- Track your accepted article
- FAQ

Book authors' home

Permissions

- ▶ Products
- ▶ Support & contact
- ▶ About Elsevier
- ▶ User Resources

Authors' Rights

Copyright

Intellectual property, in particular, copyright (rights in editorial content), trademarks (rights in brands for services or journals), and database rights (rights in compilations of information), form the foundation of Elsevier's publishing services and communications businesses. Elsevier embraces the opportunities the digital environment offers for communication and access, while at the same time recognizing the new risks that this environment poses: the ease with which unauthorized copies can be made and distributed worldwide.

Our Objective

We aim to manage digital rights and brands amidst the structural changes that the "information society" represents, while at the same time recognizing the shared goals we have with our customers and authors. These include providing the widest possible distribution of scientific and medical content and services in a financially sustainable business model.

Elsevier wants to ensure a proper balance between the scholarly rights which authors retain (or are granted/transferred back in some cases) and the rights granted to Elsevier that are necessary to support our mix of business models. We routinely analyze and modify our policies to ensure we are responding to authors' needs and concerns, and the concerns generally of the research and scholarly communities.

[What rights do you retain as a journal author?](#)
[*Commercial purposes and systematic distribution](#)
[When Elsevier changes its journal usage policies, are those changes also retroactive?](#)
[How do I obtain a Journal Publishing Agreement?](#)
[Why does Elsevier request transfer of copyright?](#)
[Can you provide me with a PDF file of my article?](#)
[Authors' Responsibilities](#)
[Obtaining permissions](#)


What rights do you retain as a journal author?

As a journal author, you retain rights for a large number of author uses, including use by your employing institute or company. These rights are retained and permitted without the need to obtain specific permission from Elsevier. These include:

- the right to make copies (print or electronic) of the journal article for your own personal use, including for your own classroom teaching use;
- the right to make copies and distribute copies (including via e-mail) of the journal article to research colleagues, for personal use by such colleagues for scholarly purposes*;
- the right to post a pre-print version of the journal article on Internet web sites including electronic pre-print servers, and to retain indefinitely such version on such servers or sites for scholarly purposes* (with some exceptions such as The Lancet and Cell Press. See also our information on electronic preprints for a more detailed discussion on these points)*;
- the right to post a revised personal version of the text of the final journal article (to reflect changes made in the peer review process) on your personal or institutional web site or server for scholarly purposes*, incorporating the complete citation and with a link to the Digital Object Identifier (DOI) of the article (but not in subject-oriented or centralized repositories or institutional repositories with mandates for systematic postings unless there is a specific agreement with the publisher- see www.elsevier.com/fundingbody agreements for further information]);
- the right to present the journal article at a meeting or conference and to distribute copies of such paper or article to the delegates attending the meeting;
- for your employer, if the journal article is a 'work for hire', made within the scope of the author's employment, the right to use all or part of the information in (any version of) the journal article for other intra-company use (e.g. training);
 - patent and trademark rights and rights to any process or procedure described in the journal article;
 - the right to include the journal article, in full or in part, in a thesis or dissertation;
 - the right to use the journal article or any part thereof in a printed compilation of your works, such as collected writings or lecture notes (subsequent to publication of the article in the journal); and
 - the right to prepare other derivative works, to extend the journal article into book-length form, or to otherwise re-use portions or excerpts in other works, with full acknowledgement of its original publication in the journal.

228


APPENDIX B COPYRIGHT AND PERMISSIONS – ADVANCES IN HEMATOLOGY (HINDAWI PUBLISHING CORPORATION)



Hindawi Publishing Corporation

Go

Home Journals About Us



Browse Menu

- Journals by Subject
- Journals by Title

Information Menu

- Abstracting and Indexing
- Hindawi in the Press
- Institutional Memberships
- Press Releases
- Resources and Tools
- Subscription Information

Open Access

Open Access is a publishing model that provides immediate, worldwide, barrier-free access to the full text of research articles without requiring a subscription to the journal in which these articles are published.

In this model, the publication costs are usually covered by the author's institution or research funds. These Open Access charges replace subscription charges and allow the publishers to make the published material freely available to all interested online readers. At the same time, authors who publish in Open Access journals retain the copyright of their article.

Other than their cost-recovery model, Open Access journals are no different from traditional subscription-based journals; they undergo the same peer-review and quality control as any other scholarly journal. Moreover, Open Access allows for maximum visibility, uptake and use of the published material.

**APPENDIX C COPYRIGHT AND PERMISSIONS – BRITISH
JOURNAL OF HAEMATOLOGY (WILEY-BLACKWELL)**

HOME / MEDICINE, NURSING & DENTISTRY / HEMATOLOGY / GENERAL HEMATOLOGY /



bjh

British Journal of Haematology

Journal Menu

- Journal Home
- Aims & Scope
- Author Guidelines
- Editorial Contacts
- View content online
- Association / Society

Sales and Services

- Subscribe / Renew
- Recommend to Library
- Customer Services
- Permissions
- Reprints/Offprints
- Advertising
- Supplements

British Journal of Haematology

The Official Journal of the British Society for Haematology

Edited by:

Finbarr E. Cotter and Deborah Rund

Print ISSN: 0007-1048

Online ISSN: 1365-2141

Frequency: Twenty-four issues a year

Current Volume: 152 / 2011

ISI Journal Citation Reports® Ranking: 2009: Hematology: 13 / 61

Impact Factor: 4.597

Permissions and Copyright Information

Top ▲

***PLEASE NOTE: If the links highlighted here do not take you to those web sites, please copy and paste address in your browser.**

Permission to reproduce Wiley journal Content:

Effective immediately, requests to reproduce material from John Wiley & Sons journal content are being handled through the Rightslink® online service. Wiley no longer accepts requests or forms for Wiley journal content sent via email, fax or mail.

Simply follow the steps below to obtain permission via the Rightslink® system:

- Locate the article you wish to reproduce on Wiley Online Library (<http://onlinelibrary.wiley.com>)
- Navigate to the abstract page.
- Click on the 'Request Permissions' link, under the 'ARTICLE TOOLS' menu
- Follow the online instructions and select your requirements from the drop down options and click on 'quick price' to get a quote
- Create a RightsLink® account to complete your transaction (and pay, where applicable)
- Read and accept our Terms & Conditions and Download your license
- For any technical queries please contact customercare@copyright.com
- For further information and to view a Rightslink® demo please visit www.wiley.com and select Rights& Permissions.

AUTHORS - If you wish to reuse your own article (or an amended version of it) in a new publication of which you are the author, editor or co-editor, prior permission is not required (with the usual acknowledgements). However, a formal grant of license can be downloaded free of charge from Rightslink if required.

Photocopying

Teaching institutions with a current paid subscription to the journal may make multiple copies for teaching purposes without charge, provided such copies are not resold or copied. In all other cases, permission should be obtained from a reproduction rights organisation (see below) or directly from Rightslink®.

Copyright Licensing Agency

Institutions based in the UK with a valid photocopying and/or digital license with the Copyright Licensing Agency may copy excerpts from Wiley and Wiley Blackwell books and journals under the terms of their license. For further information go to CLA.

APPENDIX D ETHICS APPROVAL



UNIVERSITY COMMITTEE ON LABORATORY ANIMALS

Protocol Number: 11-129

Investigator: Jason Berman

Expiry Date: Dec 1, 2012

Category/Level: D

Title of Study: Molecular Interrogation / Small Molecule Screen of NUP98-HOXA8 Induced AML in the Zebrafish

Species: zebrafish

Leslie Lord
Secretary – University Committee on Laboratory Animals
Dalhousie University
1390 LeMarchant St. Halifax, N.S. 902-494-1270 leslie.lord@dal.ca

WEBSITE: <http://animaethics.dal.ca>

IMPORTANT FUNDING INFORMATION:

Incompliance with granting agency and Dalhousie University policy, the Office of Research Services in not permitted to release funding instalments into research accounts until documentiaton of all necessary approvals are submitted to Research Services (ie. Human ethics, animal ethics, biohazard and radiation permits).